Promotors: Prof. dr. ir. Koen Dewettinck
Prof. dr. ir. Frédéric Depypere

Laboratory of Food Technology and Engineering
Department of Food Safety and Food Quality
Ghent University

Dean: Prof. dr. ir Guido Van Huylenbroeck

Rector: Prof. dr. Paul Van Cauwenberghe

UNIVERSITEIT GENT

FACULTY OF BIOSCIENCE ENGINEERING

Academic year 2012-2013

TUNING FUNCTIONALITY OF WAXY STARCH/XANTHAN GUM SYSTEMS BY VARYING PROCESSING CONDITIONS

by

ir. Bart Heyman

Promotors: Prof. dr. ir. Koen Dewettinck & Prof. dr. ir. Frédéric Depypere

Thesis submitted in fulfillment of the requirements for the degree of Doctor (PhD) in the Applied Biological Sciences

Dutch translation of the title:

Sturen van de functionaliteit van waxy zetmeel/xanthaan systemen door wijziging van de procesomstandigheden

For citation:
HEYMAN, B. (2013). Tuning functionality of waxy starch/xanthan gum systems by varying processing conditions. PhD thesis, Ghent University, Belgium, 173p.

ISBN-number**:** 978-90-5989-649-9

DANKWOORD

Tijdens de uitvoering van mijn masterthesis, kwam ik al snel tot de vaststelling dat levensmiddelenonderzoek wel ‘my cup of tea’ is, zoals ze bij ons in Ninove zeggen. Ik hoefde dan ook geen tweemaal na te denken toen professor Dewettinck voorstelde om een doctoraat in zijn labo te starten. Dit betekende het begin van zes woelige, maar leerrijke jaren. De oorspronkelijk geplande samenwerking met Tate & Lyle kon niet doorgaan, en zo belandde ik op het Flanders’ FOOD project rond stabiliteit van sauzen. Niet alleen zorgde dit onderzoek ervoor dat ik tot op vandaag tegen wil en dank geassocieerd wordt met de ‘béchamelsaus’, het mondde ook uit in een nieuw, fundementeler onderzoeksvoorstel. Door het BOF werd een beurs toegekend voor een doctoraat rond het thema “functionaliteit van xanthaan/zetmeel combinaties”, hetgeen uiteindelijk geleid heeft tot deze thesis. Binnen een labo waar het toch voornamelijk draait om chocolade en andere vetgebaseerde systemen, vormde het zeker een uitdaging op dergelijk thema te werken. Dit doctoraat is dan ook tot stand gekomen door de hulp en steun van verschillende mensen. Het is dan ook niet meer dan gepast om hen hier even in de bloemetjes te zetten.

Vooreerst wil ik mijn promotors professor Koen Dewettinck en professor Frédéric Depypere bedanken. Koen, vanaf de eerste vergadering bij Tate & Lyle voelde ik mij gesterkt door een groot vertrouwen en dat is gedurende de voorbije 6 jaren onveranderd gebleven, bij welke tegenslag dan ook. Naast de motivatietankbeurten, kon ik altijd binnenspringen voor een wetenschappelijke of andere gedachtewisseling, in het bijzonder tijdens het laatste jaar van dit doctoraat. Daarenboven heb ik van je geleerd hoe je een wetenschappelijk idee, probleemstelling of resultaat op een duidelijke manier aan de man kan brengen. Frédéric, bij mijn beginjaren binnen FTE heb je me uitstekend geholpen om mijn onderzoek op de rails te zetten. Daarnaast zorgde ook jij voor steun en motivatie wanneer nodig. Je overstap naar Barry-Callebaut kwam er plots maar niet geheel onverwacht, toch kon ik nog steeds op je rekenen voor een kritische en niets-missende blik op de onderzoeksresultaten, de artikels en deze thesis.

I would also like to express my gratitude to the members of the examination committee for enthusiastically proofreading this manuscript and adding valuable comments: Dr. Catherine Loisel, Prof. Christophe Courtin, Prof. Paul Van der Meeren, Prof. Ashok Patel. and Prof. Marc Van Meirvenne.

Een extra woordje van dank voor Prof. Van der Meeren (Particle and Interfacial Technology Group, PAINT) is zeker gepast. Paul, onze besprekingen hebben in een belangrijke mate bijgedragen tot dit werk. Op wetenschappelijk vlak heb ik zonder twijfel enorm veel van je opgestoken. Steeds was je bereid om mijn onderzoek kritisch, maar altijd constructief onder de loep te nemen. Uit dezelfde onderzoeksgroep wil ik ook Dr. Pieter Saveyn (intussen ex-PAINT) en Quenten Denon bedanken voor goeie raad en assistentie bij respectievelijk pulsed-NMR en Mastersizer.

Ook de samenwerking met Winnok De Vos (Cell Systems & Cellular Imaging, Ugent) voor het confocale werk was telkens zeer aangenaam. Het heeft maanden gevergd om de juiste bereidingswijze van de stalen te optimaliseren, maar ons geduld werd beloond met een paar mooie resultaten. Filip Van Bockstaele (Hogent) wil ik bedanken voor de hulp bij de PCA en de het nalezen van hoofdstuk 4. De grondstoffen en nuttig advies werden voorzien door Rudy Wouters (Beneo-Remy), Bea Willemse-Klaassen (Avebe) en wijlen Johan L'Ecluse en Dirk Vindevogel (Cargill).

Doctoreren betekent ook: zoeken naar gepaste analysetechnieken. Verschillende methodes werden getest, maar hebben helaas dit doctoraat niet gehaald. Reden te meer om de mensen die me bijstonden bij dit 'onverzilverde' werk, langs deze weg te danken voor hun inspanningen: Prof. Luce Vander Elst (Université de Mons) met 17O-relaxatie, Dr. Bart Lucas (Laboratory of General Biochemistry & Physical Pharmacy, Ugent) met zetasizer. Masterstudenten Michael Verlinden en Dieter De Hertogh hebben bij de start van dit doctoraat belangrijk verkennend werk verricht en me op die manier geholpen de juiste onderzoekslijnen af te bakenen.

Despite several staff-changes, the atmosphere in the FTE-group has always been exceptionally good. Therefore I would like to thank all former and current members for the wonderful times we had. Some of them even deserve some extra words. Ashok, as a full-blooded researcher, you will undoubtedly inspire the current and future PhD-students. I have always enjoyed our talks in the lab, in particular your passion and enthusiasm for the development of innovative foodstructures. De laborantes hebben me de voorbije jaren uitstekend bijgestaan: Marleen en Corine voor het werk met de Unimix, Beatrijs voor het labellen van de xanthaan en de hulp bij de opvolgingsexperimenten. Met jullie samenwerken was niet enkel zeer aangenaam, ik kon er bovendien steeds op vertrouwen dat alles tot in de puntjes werd uitgevoerd! Mr. Benny is zowat het Zwitsers zakmes van het labo: geschikt om welke klus dan ook te klaren, al duurt het soms wat om hem te vinden als je hem nodig hebt. Bestellingen, herstellingen, analyses, practica, kantklossen en bloemschikken: Benny weet het allemaal probleemloos te combineren. Benny, FTE zou er een pak anders uitzien zonder jou! Ook Paul Provijn, King of Administration, hielp me vele malen m'n weg te zoeken in het labyrint van de Ugent-bureaucratie.

Stefanie, binnen een jaartje is het jouw beurt om te verdedigen en hoewel ik er een hekel aan had als iemand dit tegen mezelf zei: ik ben ervan overtuigd dat de afronding van je doctoraat vlekkeloos zal verlopen. Veel succes met de laatste tests in Japan! Kim, het assistentschap combineren met een complex doctoraatsthema is niet evident, maar als er iemand is die deze taak aankan, ben jij het wel! 'Ancienne' Nathalie, zorgt voor sfeer en decibels, omdat ze nu eenmaal altijd goedgezind is! Eveline, intussen al 2 jaar ex-collega, maar bovenal gedurende vier jaar een ideale bureaugenote, bedankt voor de fantastische wetenschappelijke, minder wetenschappelijke en veel minder wetenschappelijke babbels. Claudia, op mijn allereerste werkdag werd je mij toegewezen als thesisstudente. Ondanks je West-Vlaamse roots, beheerste je het Nederlands al vrij goed en bovendien bleek al snel wat voor harde werker je bent. Ik heb intussen met jou 5 jaar een bureau gedeeld, en ik kon me geen betere overbuur wensen. Ik sta nog elke dag versteld van je ijver en constante behulpzaamheid. Ik kan je alleen maar het beste toewensen op elk gebied! Davy, als thesisbegeleider zorgde je ervoor dat ik de smaak voor onderzoek te pakken kreeg. Zonder jou had ik dus waarschijnlijk nooit beslist om een doctoraat te starten. In de jaren die daarop volgden, werd alleen maar duidelijk hoe belangrijk je bent voor de goede werking en de goede sfeer van het labo. Veel succes met je nieuwe project! Bijpraten zullen we wel regelmatig doen bij een pizza prostituto!

Mijn vrienden zorgden voor de broodnodige ontspanningsmomenten, en enkelen onder hen verdienen daarom een eervolle vermelding in dit doctoraat. Tom en Thijs: we bewandelen al sinds de humaniora hetzelfde traject, daarom alleen al moest dit doctoraat er zeker en vast komen! Benjamin en Bastiaan, Glorious Bastards en vaste leden van quizploeg Camping Casablanca, hielpen me steevast de zinnen te verzetten. Datzelfde geldt trouwens ook voor ontdekkingsreizigster Katrijn.

Schoonmoeder Bea stond vaak paraat met bemoedigende woorden. Mijn ouders kan ik in een paar zinnen onmogelijk voldoende danken voor de fantastische opvoeding, de onvoorwaardelijke steun en de kansen die ze mij hebben gegeven. Hun bijdrage tot dit doctoraat is hoedanook veel groter en belangrijker dan ze zelf ooit zullen toegeven!

Tot slot wil ik Lientje in de bloemetjes zetten. Omdat ik onder de doctoraatsstress niet altijd de gemakkelijkste was. Omdat je heel veel taken op je nam, waar ik me geen zorgen over hoefde te maken. Omdat je Andréhazesgewijs in mij gelooft. Omdat je mij gelukkig maakt en laat inzien wat echt belangrijk is in het leven.

TABLE OF CONTENTS

Table of Contents

LIST OF SYMBOLS AND ABBREVIATIONS

$\|G^*\|$	complex modulus
A	parameter empirical modeling T_2 evolution
a_0	parameter empirical modeling apparent viscosities gum free pastes
a_g	parameter empirical modeling apparent viscosities gum containing pastes
B	parameter empirical modeling T_2 evolution
B_0	external magnetic field
b_0	parameter empirical modeling apparent viscosities gum free pastes
b_g	parameter empirical modeling apparent viscosities gum containing pastes
c	starch concentration
C	parameter empirical modeling T_2 evolution
c*	critical overlap concentration
c**	entanglement concentration
c_0	parameter empirical modeling apparent viscosities gum free pastes
c_a	concentration bordering the anisotropic region
c_{cp}	close-packing concentration
c_D	third critical xanthan concentration
c_g	parameter empirical modeling apparent viscosities gum containing pastes
c_i	concentration bordering the isotropic region
CPMG	Carr-Purcell-Meiboom-Gill
D(0.1)	diameter of 10th percentile of the volume-weighted particle size distribution
D[3,0]	volume equivalent mean diameter of heated starch granule
D[4,3]	volume-weighted mean diameter of heated starch granule
D_0[3,0]	volume equivalent mean diameter of raw starch granule
DSC	differential scanning calorimetry
G'	storage or elastic modulus
G"	loss or viscous modulus
H	heated xanthan solutions
K	constant relating the polymer concentration to the number of exchangeable protons
k	consistency index
k_{gel}	proton exchange rate
m_w	solvent mass
n	flow behavior index
PC	principal component
PCA	principal components analysis
PSD	particle size distribution
RVA	rapid visco-analyzer

T_2	spin-spin or transverse relaxation time
T_{20}	Extrapolated T_2 relaxation time at start preservation experiments
$T_{2\text{bulk water}}$	T_2 relaxation time of the bulk water
$T_{2\text{gel}}$	intrinsic relaxation time of protons in exchangeable sites
$T_{2\text{measured}}$	measured T_2 relaxation time
T_c	gelatinization conclusion temperature
T_m	xanthan conformational transition temperature
T_o	gelatinization onset temperature
T_p	gelatinization peak temperature
UH	unheated xanthan solutions
X	Xanthan gum (abbreviation used in tables)
XRD	X-ray diffraction
ΔH	gelatinization enthalpy
ΔH_{tot}	total gelatinization enthalpy
ΔH_{ungel}	gelatinization enthalpy of the ungelatinized starch fraction
Φ	swollen starch volume fraction
δ	starch density
δ	phase angle
δ_w	solvent density
γ	gyromagnetic constant
$\dot{\gamma}$	shear rate
$\dot{\gamma}_c$	characteristic shear rate for shear thickening
η	apparent viscosity
η_0	zero rate viscosity
η_{20}	apparent viscosity at 20°C
η_{85}	apparent viscosity at 85°C
ω	precessional frequency spin nucleus
σ_0	yield stress
σ_s	shear stress
τ	pulse spacing CPMG-sequence

SUMMARY

Starches and gums or non-starch hydrocolloids are very often combined in foods. These functional ingredients provide a desirable texture and mouthfeel to products like dairy or soy desserts and drinks, sauces in ready-to-eat meals, salad dressings, table-top sauces and their light derivatives. Furthermore, they improve the physicochemical stability of the products through their emulsion-stabilizing and water-holding capacities. As a consequence of their commercial popularity, starch/gum combinations are extensively studied. However, scientific literature contains many contradictory observations regarding their gelatinization and pasting behavior, their synergistic interactions and their rheological properties in general. Most of these differences can be attributed to the widely differing nature of the starch and gum varieties that are studied.

This dissertation focused specifically on waxy starch/xanthan systems. A detailed overview of the available literature regarding both xanthan gum and starch functionality is presented in chapter 1. Xanthan gum is an anionic polysaccharide, produced by fermentation of *Xanthomonas campestris.* In the presence of salt and at low temperatures, xanthan molecules in solution adopt an ordered helical conformation. Upon heating, a reversible conformational transition to a random coil structure takes place. Waxy starches contain almost no amylose and therefore they lack the strong gelling properties of normal starches, which makes them suitable for applications that require a more fluid-like behavior. However, the native varieties are sensitive towards elevated temperatures and shearing conditions, which cause granules to break up. For this reason chemically modified waxy starches are very frequently encountered in foodstuffs. Mainly driven by a negative consumer perception, ingredient producers are continuously looking for native alternatives for these chemically treated starches. This thesis was rather approached from the point of view of the food manufacturer and aimed at evaluating the effects of varying production conditions (salt content, applied concentrations, shearing, heating temperatures) on the functionality development of waxy starch/xanthan systems. The addition of gums to native starch systems, may overcome or compensate their shortcomings. Particularly regarding xanthan gum, some direct effects on the swelling and degradation behavior of starch granules have been reported in literature. A better practical understanding could assist in a more sensible use of these additives and should help to tune their functionality by altering the processing conditions. This could lead to an improved performance in products like dressings, soups and sauces.

In the second chapter, the effects of xanthan gum on the pasting behavior and flow properties of various types of waxy starches (potato, rice, native and modified maize) were studied. This setup aimed at deriving more generalized conclusions. Special attention was given to the effects of the conformational transition of xanthan gum. Although there was no significant effect on the gelatinization behavior of the starches, the occurrence of a conformational change induced a marked viscosity reduction during pasting. However, the effect of this transition was not directly noticeable in the flow behavior of the pastes after cooling, where the ordered conformation is restored. The flow behavior of the mixed pastes during pasting, but also after cooling, strongly depended on the specific type of starch that was combined with the gum. For modified maize and rice starch there was a marked effect of xanthan gum. Conversely, its relative influence was much smaller for potato and native maize starch systems. These differences were attributed to variations in swelling power and more importantly, variations in degradation behavior. As opposed to modified maize and rice starch used here, potato and native maize starch exhibited a significant degree of breakdown during the pasting step at 85°C. It was stated that the rheological properties for the latter systems were primarily governed by the amylopectin present in the continuous phase. Further, it was concluded that granule integrity is a prerequisite for optimal xanthan functionality.

The fragile nature of native waxy maize and potato starches is clearly their main technological disadvantage. In chapter 3, it was attempted to preserve the granule structure during preparation, by imposing lower heating temperatures. It was demonstrated that when native waxy starches (maize or potato) are pasted at temperatures slightly higher than the gelatinization onset temperature, their swelling can be more controlled, but a limited fraction of the starch will remain ungelatinized. Under these conditions, granule disruption could be limited and a higher shear rate was even beneficial towards complete viscosity development, probably by weakening the intermolecular bonds in the granules and thus facilitating their water uptake. The heating temperature therefore proved to be a critical process parameter. When the temperature is too low, swelling will be incomplete and at more elevated temperatures, granule disruption will become more predominant. It was also suggested that in the latter case, the presence of xanthan gum can help to partly diminish the breakdown.

The mild temperature processing of fragile waxy starches proved to be beneficial towards preserving their granular integrity. However, it was not known to which extent the microstructure of mildly heated (70 or 72°C) pastes changed during preservation and how

this was affected by xanthan gum. Therefore, chapter 4 was devoted to the physicochemical stability of these systems. The pastes heated to 70°C were structurally stable throughout the storage period of 8 weeks. Limited changes were attributed to shrinking of the granules and intensified granule associations. The addition of xanthan gum did not induce a higher stability, however, due to its direct contribution to the structural features of the systems, changes occurring in the starch fraction were partly masked. When the pastes were heated to a slightly more elevated temperature (72°C), a higher fraction of the granules was broken down. This rendered the structures to be more unstable and a slow but significant gelation was observed for all systems. This behavior was attributed to the association and crystallization of amylopectin molecules which are present in both the continuous phase and the granules. Under these circumstances, xanthan gum was found to enhance the gelation process. A phase separation between both polymers (amylopectin and xanthan) in the continuous phase, which favors intermolecular association, was proposed as an underlying mechanism.

Chapter 5 focused on the influence of guar and xanthan gum on the shear induced breakdown of waxy maize starch granules. The use of slow heating rates and low heating temperatures allowed to restrict thermal breakdown. The effects of different shearing conditions (no shear, 50 s^{-1} and 150 s^{-1}) during pasting were compared to elucidate the influence of the gums on granule swelling and breakdown. At the concentrations studied here, both gums did not induce marked differences in granule swelling. However, granule degradation was clearly affected by their presence. The ability of xanthan to inhibit granule disruption was reaffirmed, and guar gum appeared not to have this property. As a consequence, marked differences in particle size distributions, as well as rheological properties were observed between guar and xanthan containing systems. It was stated that both gums can enhance the rheological properties of these systems, but guar gum rather masks the shortcomings of the starch, whereas xanthan gum can actively improve the performance of the granules by better preserving their structure. It was proposed that xanthan gum exhibits a unique property, which modifies the impact between the granules during pasting. In this perspective, the ability of xanthan gum to associate with the starch granule surface, which is claimed by some authors, was investigated. Confocal micrographs demonstrated that this effect takes place at low salt concentrations. However, its role in the granule stabilizing effects appears unlikely. Therefore it was suggested that during pasting, xanthan gum reduces the impact between the granules by the formation of a shear-induced anisotropic organization in the continuous phase.

Their different effects on granule degradation (and possibly swelling) complicate the comparison between guar and xanthan gum regarding their direct rheological effect on waxy starch systems. Therefore, the final chapter (6) focused on cross-linked starch systems in which granule degradation effects are limited. The effects of both gums were evaluated at different (swollen) starch volume fractions. First of all, it was demonstrated that the effects of gums on the flow behavior strongly depended on the starch content. At low starch volume fractions, the viscosity was primarily determined by the continuous gum phase. At higher starch volume fractions, the flow properties were governed by granule-granule interactions, hereby reducing the relative contribution of the gums. The effect of guar gum on the viscosity was purely additive over the studied concentration range. Conversely, xanthan gum exhibited the unique property of facilitating the flow in concentrated starch dispersions. Consequently, these results favored the aforementioned hypothesis of anisotropic arrangement of xanthan in the continuous phase, which is promoted at higher (effective) polymer concentrations. This specific effect of xanthan gum was observed at low temperatures as well as at elevated temperatures and occurs in both the ordered and the disordered conformation.

Small deformation rheology demonstrated that already at relatively low starch volume fractions, a network of interacting granules is formed. Under these circumstances the network is further strengthened by a coexisting network of interacting gum molecules. In this regard, xanthan gum proved to be more effective due to its capacity of forming weak gel entangled networks. As the starch fraction increases, the concentrated continuous gum phase partly hinders granule interactions, thus enhancing the viscous character of the resulting pastes.

It could be concluded that throughout this dissertation some valuable insights regarding waxy starch/xanthan functionality was gained. In particular, it has become clear that lowering the processing temperature of native waxy starches to the gelatinization temperature range greatly improves their structural preservation. Furthermore, the rheological properties of native waxy starch systems can be tuned indirectly (granule protection) and indirectly (exclusion effects) by the incorporation of xanthan gum. Some aspects presented in this work remain unclear and deserve a separate study. More specifically the phase behavior of amylopectin/xanthan and the precise effects of xanthan anisotropy on the flow behavior of (starch) dispersions. Although an important step has been made, this work primarily counts as an incentive, and further research is required to reach commercial applicability. In this light, other types of starch and/or the use of different holding times could further help to mimic the behavior of chemically modified starches.

SAMENVATTING

Zetmelen worden in levensmiddelformuleringen zeer vaak gecombineerd met niet-zetmeel hydrocolloïden of gommen. De combinatie van deze functionele ingrediënten zorgt voor de gewenste sensorische eigenschappen (textuur, mondgevoel) in producten zoals zuivel- of soja-gebaseerde desserten en drankjes, sauzen in kant-en-klare maaltijden, dressings, hartige geëmulgeerde sauzen en hun light-varianten. Als emulsie-stabilisator en waterbinder verbeteren ze bovendien de fysicochemische stabiliteit van deze producten.

De focus van dit doctoraat lag op het sturen van de functionaliteit van waxy zetmeel/xanthaan systemen. In hoofdstuk 1 wordt de bestaande wetenschappelijke literatuur aangaande zetmeel en xanthaangom functionaliteit samengevat. Xanthaangom is een anionisch polysaccharide dat wordt geproduceerd door fermentatie van de bacterie *Xanthomonas campestris*. In de aanwezigheid van zout en bij lage temperaturen nemen de xanthaanmoleculen een geordende helicale structuur aan. Bij verhitten kan een conformatiewijziging plaatsvinden, waarbij de molecule transformeert naar een random coil. Waxy zetmelen bevatten geen amylose en vertonen daardoor veel minder sterke gelerende eigenschappen, wat interessant kan zijn voor toepassingen waar een zekere graad van vloeibaarheid gewenst is. Jammer genoeg zijn de natieve varianten zeer zwak, en erg gevoelig voor verhoogde temperaturen en afschuifkrachten, waarbij de granules opbreken. Om deze reden worden waxy zetmelen vaak chemisch verknoopt om hun gebruik in industriële toepassingen mogelijk te maken. Omwille van een eerder negatieve perceptie bij de consument, is er echter een stijgende vraag naar meer natuurlijke alternatieven voor chemisch gemodificeerde zetmelen. Voor vele ingrediëntleveranciers vormt deze zoektocht dan ook een hele uitdaging. In het kader van deze problematiek, worden de bestaande productieprocessen van afgewerkte levensmiddelen minder op de korrel genomen. Daarom werd in deze thesis onderzocht hoe de functionaliteit van natieve zetmelen gestuurd (liefst verbeterd) worden door aanpassing van de procesomstandigheden (zoutdosering, gehanteerde concentraties, afschuifomstandigheden, temperaturen) en door de toevoeging van xanthaangom. Gommen worden momenteel voornamelijk gecombineerd met (gemodificeerde) zetmelen om de eigenschappen van het afgewerkte product te verbeteren. Het wordt echter ook gesuggereerd dat hun aanwezigheid de intrinsieke eigenschappen van natief zetmeel kan verbeteren. In het bijzonder voor xanthaangom zijn verschillende effecten op het zwelling- en degradatiegedrag van de granulen beschreven. Een beter inzicht in de

effecten van de aanwezigheid van xanthaangom en het variëren van de procescondities kan immers leiden tot een rationeler gebruik van deze componenten.

In het tweede hoofdstuk werden de effecten van xanthaan gom op het pastinggedrag en de vloei-eigenschappen van verschillende waxy zetmeelsystemen (aardappel, rijst, natief en gemodificeerd mais) bestudeerd. Bijzondere aandacht werd geschonken aan de invloed van de xanthaantransitie. Hoewel er geen siginificant effect was op het gelatinisatiegedrag van de zetmelen, ging de conformatietransitie tijdens pasting gepaard met een duidelijke viscositeitsreductie. Daarentegen was dit effect niet merkbaar in het vloeigedrag van de gekoelde dispersies. De reologische eigenschappen van de zetmeel/xanthaan combinaties bleken sterk afhankelijk van het gebruikte type zetmeel. Het vloeigedrag van de systemen met gemodificeerd maiszetmeel of rijstzetmeel, werd sterk beïnvloed door xanthaan, zowel tijdens de pastingstap als na de koeling. De effecten waren daarentegen veel minder uitgesproken in het geval van aardappel of natief maiszetmeel. Deze verschillen werden voornamelijk toegeschreven aan verschillen in het degradatiegedrag van de verscheidene types. In tegenstelling tot gemodificeerd mais- en rijstzetmeel, bleek een verhittingsstap tot 85°C zeer destructief voor natief mais- en aardappelzetmeel. Er werd dan ook besloten dat een hoge graad van granule-integriteit een voorwaarde is voor optimale xanthaanfunctionaliteit.

In hoofdstuk 3 werd getracht om de granulestructuur van zwakke zetmeeltypes (mais en aardappel) beter te bewaren door tijdens de verhittingsstap lagere temperaturen op te leggen. Zo werd aangetoond dat wanneer natieve zetmelen verwerkt worden bij temperaturen net boven de gelatinizatie onset, hun swelling beter gecontroleerd kan worden. Een fractie van het zetmeel zal hierdoor echter onverstijfseld blijven. De disruptie van de granules kon onder deze omstandigheden beperkt worden en een verhoogde afschuifsnelheid leidde zelfs tot een betere viscositeitsopbouw. De maximale verhittingstemperatuur blijkt daarom een kritische procesparameter. Wanneer de temperatuur te laag is, zal de zwelling te onvolledig blijven, bij hogere temperaturen, zullen er dan weer te veel granules opbreken. Voornamelijk in dit laatste geval, kan xanthaangom gedeeltelijk deze destructieve effecten beperken.

De milde temperatuursbehandeling van zwakke zetmeeltypes is nuttig gebleken met oog op de bewaring van de granulestructuur. Het is echter niet duidelijk in welke mate de microstructuur wijzigt bij bewaring gedurende meerdere weken, en welke rol de aanwezigheid van xanthaan hierin kan spelen. In hoofdstuk 4 de fysicochemische stabiliteit dan ook onder de loepe genomen. Wanneer dispersies van natief waxy maiszetmeel verhit werden tot 70°C, konden de systemen beschreven worden als een zwak netwerk van geaggregeerde gezwollen, grotendeels intacte granules. Structureel vonden er slechts beperkte veranderingen plaats gedurende de bewaringstermijn van 8 weken. Deze werden toegeschreven aan het krimpen van de granules en/of een toename in de mate van granule-aggregatie. Wanneer xanthaan aanwezig was, resulteerde dit niet in een hogere stabiliteit, maar door zijn directe bijdrage in de structurele eigenschappen van het systeem, konden wijzigingen in het zetmeel gedeeltelijk gemaskeerd worden. Wanneer de systemen echter verhit werden tot een iets hogere temperatuur (72°C), is een groter aantal granules stukgekookt, wat leidt tot een hogere instabiliteit, en een trage maar duidelijke gelering trad op tijdens bewaring. Dit gedrag werd toegeschreven aan de associatie en herkristallisatie van de amylopectine molecules die aanwezig zijn in zowel de granules als in de continue fase. Onder deze omstandigheden bleek xanthaangom het geleringsproces zelfs te versterken. Een fasescheiding tussen beide polymeren in de continue fase, waardoor de effectieve amylopectinconcentratie lokaal toeneemt, werd voorgesteld als onderliggend mechanisme.

In hoofdstuk 5 werd onderzocht welke rol xanthaan en guar gom kunnen spelen in de granuleafbraak ten gevolge van opgelegde afschuifkrachten. Het gebruik van lage opwarmsnelheden en lage maximale temperaturen, lieten toe dat thermische disintegratie beperkt bleef. De bestudeerde systemen werden bereid bij verschillende vervormingssnelheden. Bij de beschouwde concentraties veroorzaakten beide gommen geen significante effecten op de granulezwelling. Degradatie kon daarentegen wel worden beïnvloed. The resultaten bevestigden de beschermende rol van xanthaan, terwijl guar gom niet over deze eigenschap bleek te beschikken. Dit leidde tot merkbare verschillen in granulegrootte verdeling en het reologisch gedrag van de gekoelde dispersies, waarbij guar eerder de tekortkomingen van het zetmeel maskeert, terwijl xanthaangom ook actief de granules beschermt. Er werd gesteld dat xanthaangom een unieke eigenschap vertoont die ervoor zorgt dat de impact tussen de granules wordt gewijzigd tijdens pasting. In deze context werd onderzocht of xanthaangom kan associeren met het granuleoppervlak, zoals wordt beweerd door andere onderzoekers. Confocale beelden toonden aan dat dit effect wel degelijk plaatsvindt bij lage zoutgehaltes. Het effect hiervan op de granulestabilisatie lijkt echter onwaarschijnlijk. Een meer waarschijnlijke verklaring kan gevonden worden in de vorming van een door afschuiving geïnduceerde anisotropie van de xanthaanmoleculen in de continue fase. Deze sterke moleculaire alignering, gidst mogelijks de granules in een vlot vloeipatroon, en beschermt op deze manier hun structuur.

Omwille van hun uiteenlopende effecten op granule degradatie (en mogelijks zwelling), is het moeilijk om de directe reologische effecten van guar en xanthaan in kaart te brengen. Daarom werd in het laatste hoofdstuk gebruik gemaakt van chemisch verknoopte zetmelen die veel minder gemakkelijk opbreken. De effecten van beide gommen werden geëvalueerd bij verschillende zetmeel volumefracties. Ten eerste werd duidelijk dat de specifieke effecten van de gommen afhankelijk waren van het zetmeelgehalte. Bij lage concentraties, werd de viscositeit gedomineerd door de continue gomfase. Wanneer meer zetmeel aanwezig is, wordt het vloeigedrag bepaald door granule-granule interacties met, relatief gezien, een beperktere bijdrage van de gomfractie. Het effect van guar was additief over het gehele concentratiebereik. Xanthaangom daarentegen faciliteerde de vloei van de meer geconcentreerde dispersies (verlaagt de viscositeit). Deze resultaten ondersteunden dan ook de voornoemde hypothese van anisotropie van de xanthaanmoleculen. Dit specifieke effect werd bovendien geobserveerd bij zowel hoge als lage temperaturen en vindt plaats voor de helicale én de random coil conformatie.

Met behulp van dynamische reologie werd aangetoond dat reeds bij relatief lage zetmeelvolumes een netwerk van geassocieerde granules gevormd wordt. Bij dergelijke systemen kan het netwerk verder versterkt worden door een nevennetwerk gevormd door interagerende gom-moleculen. Xanthaan bleek effectiever dan guar betreffende dit aspect omwille van zijn capaciteit om zwakke gelnetwerken te vormen. Wanneer het zetmeelgehalte toeneemt, verhindert de geconcentreerde gomfase gedeeltelijk de granule interacties, hetgeen leidt tot een meer viskeus karakter van de dispersies.

Dit doctoraat leverde waardevolle inzichten op wat betreft waxy zetmeel/xanthaan functionaliteit. In het bijzonder blijkt dat het hanteren van procestemperaturen in de buurt van het gelatinisatiebereik, het granulebehoud van de natieve zetmelen substantieel verbetert. Verder werd duidelijk dat de reologische eigenschappen van deze zetmeelsystemen direct (door exclusie-effecten) maar ook indirect (granule bescherming) kunnen gestuurd worden door de toevoeging van xanthaangom. De bevindingen uit deze thesis kunnen op hun beurt het startpunt vormen voor nieuwe onderzoekspistes. In het bijzonder dient het fase-gedrag van amylopectine en xanthaangom verder in kaart gebracht te worden, alsook de invloed van de anisotropische organisatie van xanthaangom op het vloeigedrag van zetmeeldispersies. Wat de praktische toepasbaarheid van de resultaten betreft, kan er gesteld worden dat een verdere uitdieping vereist is (bijvoorbeeld vergelijken van andere types zetmeel, variatie van de isotherme tijden) om het gedrag van chemisch gemodificeerde zetmelen nog beter te benaderen.

OUTLINE OF THE RESEARCH

OUTLINE OF THE RESEARCH

Combinations of starches and non-starch hydrocolloids or gums are used abundantly in the food industry. The aim of this dissertation was to gain a generalized understanding of waxy starch/waxy systems and more specifically to study how their functionality (primarily their rheological properties) can be tuned by variation of the processing conditions.

Traditionally, the pasting properties of starch systems are derived at a fixed temperature-time-shear combination by means of Brabender amylographs or rapid visco-analyzers. For this work, the starch pasting cell was used for the preparation and analysis of the samples. This rheometer geometry allowed the variation of accurately controlled processing conditions (temperature, shear rate, heating and cooling rates) for the preparation of the starch pastes, while continuously monitoring the viscosity. The resulting pastes were further analyzed by several other techniques (rheology, laser light scattering and confocal scanning laser microscopy). In this way, the microstructural analyses could be directly related with the pasting behavior, as they were performed on the same samples. Throughout the setup, each chapter builds further on a particular aspect of a preceding one (Figure 1).

In the first chapter, an overview of the literature regarding xanthan, starch and starch/gum functionality is presented. The second chapter focuses on the influence of xanthan on the pasting and flow properties of various waxy starches. In particular, the effects of the xanthan conformational transition were studied. For this setup, waxy starches of different botanical origin were assessed in order to obtain more generalized conclusions. From a practical point of view, the intention was to help clarifying some of the discrepancies found in literature. Starch and gum concentrations were chosen within ranges typically used in food systems.

Waxy maize and potato starches disintegrate very easily at elevated temperatures, hereby losing most of their functionality. Therefore, chapter 3 focused on the functionality development of the starch/xanthan systems, when processed at temperatures within the gelatinization range. In chapter 4, the physicochemical stability of these systems was evaluated over a preservation period of 8 weeks. High amounts of sample were required, for this preservation study, therefore the samples were prepared by means of a lab-scale unimix system.

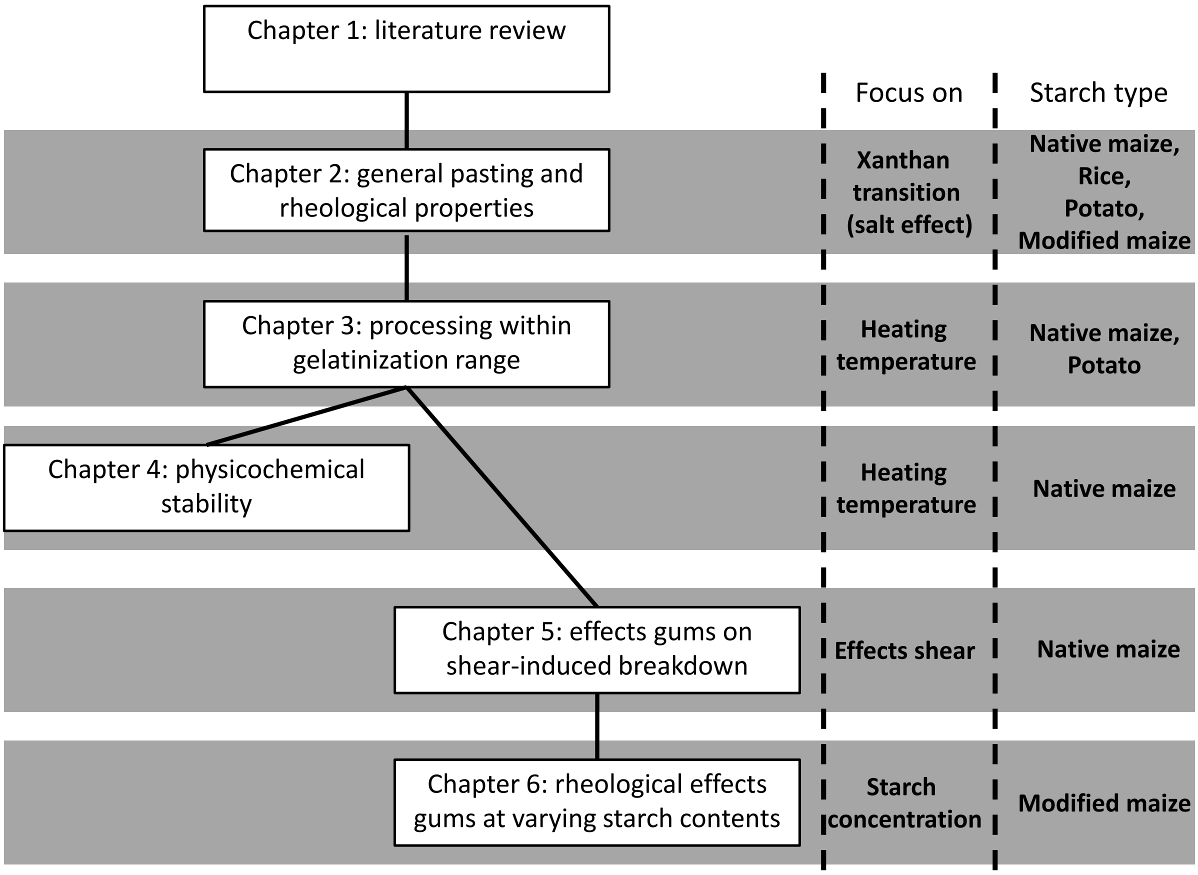

Figure 1: Outline of the research

Gums in general, and xanthan gum in particular, can tune the rheological properties of starch pastes in different ways. A direct contribution logically results from their presence in the bulk phase. However, when heated together, gums can influence the swelling and degradation of granules, which in turn affects the behavior or the mixed system. The intention of chapter 5 and chapter 6 was to gain a more fundamental insight in the direct and indirect effects of xanthan gum on waxy starch systems. Therefore, the experimental setups in both chapters were designed in such a manner that part of the possible effects are excluded in order to facilitate the interpretation. For both chapters, the specific effects caused by xanthan gum were derived by comparison with gum free and guar gum containing systems. The latter allowed to designate whether another high molecular weight polysaccharide is capable of inducing the same phenomena as xanthan gum.

Firstly (chapter 5), the effects of guar and xanthan gum on the shear induced breakdown of native waxy maize starch granules were studied. The use of slow heating rates and low heating temperatures allowed to restrict thermal breakdown. The effects of different shearing conditions (no shear, 50 s^{-1} and 150 s^{-1}) were compared to elucidate the underlying mechanisms.

Their different effects on granule degradation (and possibly swelling) complicate the comparison between guar and xanthan gum. If indirect effects of gums can be excluded, a more fundamental insight in their direct rheological effects could be developed. Therefore, the final chapter (6) focused on systems containing chemically cross-linked starch in which granule degradation effects are limited.

1. LITERATURE REVIEW

1.1. XANTHAN GUM

1.1.1. INTRODUCTION

Xanthan gum is an extracellular polysaccharide produced by fermentation of *Xanthomonas campestris*. This high molecular weight biopolymer is soluble in cold water and exhibits unique rheological properties. Part of its commercial success can be attributed to its ability to withstand elevated temperatures and to an excellent stability across a wide pH range. The most important industrial applications are viscosity modification and stabilization of food (sauces and dressings, baked goods, beverages, desserts and ice creams) and personal care products (lotions, creams and body washes) (Imeson, 2010). Xanthan is also used in drilling fluids for enhanced oil recovery and to attain drag reduction in piping (Wyatt & Liberatore, 2009).

Xanthan consists of a cellulosic backbone (1,4-linked β-D-glucose residues) having a trisaccharide side chain attached to O-3 of alternate D-glucosyl residues. The side chains are (3→1)-α-linked D-mannopyranose, (4→1)-β-D-mannopyranose and (2→1)-β-D-glucuronic acid, which account for the anionic properties of xanthan gum (Figure 1-1). Molecular weights of xanthan gum are usually in the order of 10^6 g/mol (Born *et al.*, 2005).

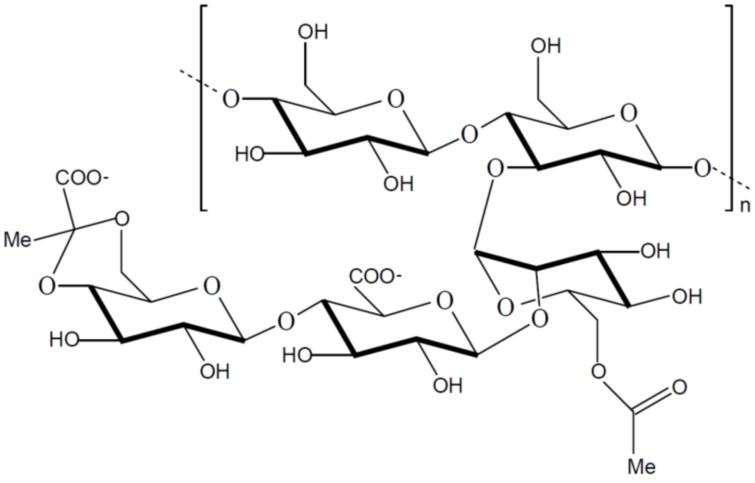

Figure 1-1: Repeating unit in the structure of xanthan gum (Hamman, 2010)

About 40 percent of the terminal mannose residues are 4,6-pyruvated and the inner mannose is mostly 6-acetylated, both depending on which strain of *Xanthomonas campestris* the xanthan is isolated from (Born *et al.*, 2010; Chaplin, 2009; Katzbauer, 1998). Variations in processing procedures and conditions may also lead to differing degrees of acetyl substitution and pyruvic acetal substitution (Bresolin *et al.*, 1998; Wyatt & Liberatore, 2010).

1.1.2. PRODUCTION

Xanthan gum is produced by aerobic fermentation of *Xanthomonas campestris*. A small amount of the strain is activated in a small reactor containing a nutrient medium. After growth, this culture can be used to inoculate successive fermenters, which are used for the actual xanthan synthesis. Industrial production is usually performed by a batch-wise submersed fermentation. Throughout the fermentation process, pH, aeration, temperature and agitation are monitored and controlled. At temperatures between 30 and 33°C the highest polymer yield is attained. During fermentation, the broth acidifies, but in industrial processes the pH is kept between 7 and 8, which is ideal for production. Oxygen is provided by agitation of the fermentation broth. Because the viscosity changes during the process, fermentor and agitator design are of utmost importance. Growth substrate is also introduced into the system. Glucose is the most commonly used carbon source, and ammonium salts or amino acids are used as nitrogen source. The polymer production is promoted by a high ratio of carbon to nitrogen in the medium (Born *et al.*, 2005). The production process is schematically represented in Figure 1-2.

During the exponential growth phase, xanthan synthesis is maximal, but production continues during the succeeding stationary phase. In the different growth phases, xanthan molecules with different molecular weight and different degree of substitution are produced. Hence, the microstructural composition of the resulting batch is quite polydisperse. The quantity of polymer increases until about 30h after inoculation, when a steady state is reached with termination of bacterial growth and polymer production. At this point, the fermentation is stopped (Born *et al.*, 2005).

Post-fermentation treatments account for up to 50% of the total production costs. First, a pasteurization is performed to kill the bacteria. Subsequently, the whole fermentation broth is precipitated with isopropyl alcohol or ethanol. The obtained coagulum is isolated by solid-liquid separation, rinsed with alcohol, pressed and dried. Finally, the xanthan is ground, resulting in a white or cream-colored powder with particle sizes ranging from 80 to 250 µm. The final product contains about 85% pure xanthan gum, 5% biomass and 10% moisture. A filtration step sometimes precedes precipitation. This step serves to remove cell debris and yields clarified xanthan, which is used for transparent applications (Born *et al.*, 2005).

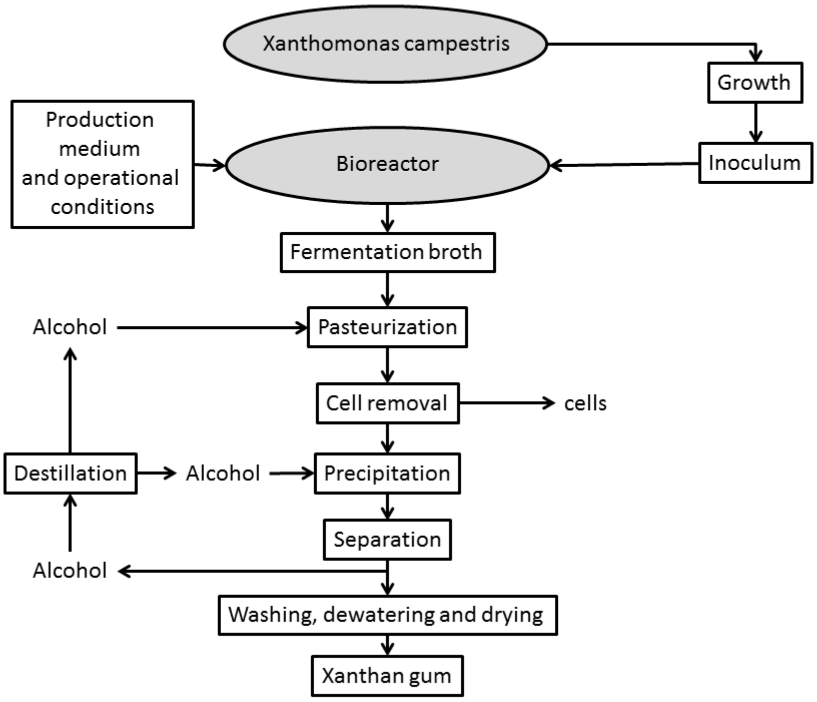

Figure 1-2: Schematic representation of the xanthan gum production process (adapted from Garcia-Ochoa *et al.* (2000))

1.1.3. XANTHAN CONFORMATIONS

At room temperature and in the presence of salt, xanthan adopts an ordered helical conformation, single or double stranded, depending on the thermal history of the sample (Laneuville *et al.*, 2013). The side chains are folded-down and associated with the backbone by non-covalent interactions. The helix is stabilized by hydrogen bonds, electrostatic interaction and steric effects, thus resulting in a semi-flexible rod-like structure (Meyer *et al.*, 1993; Rodd *et al.*, 2000). Generally, a distinction is made between two different ordered states: native and renatured. The native form is the conformation under which xanthan appears in the unpasteurized fermentation broth. Renatured xanthan is obtained after heating (above the transition temperature, see 1.1.3.1) and subsequent cooling of native or already renatured xanthan. The distinction between the native and renatured conformation is important since commercially available xanthan gum is often heat treated and thus sold under its renatured form (Choppe *et al.*, 2010). The details of its ordered conformations, as well as the number of chains involved have been discussed by many authors but still remain controversial. Most authors consider native xanthan as a helically paired dimer (Sato *et al.*, 1984). However, the absence of a molecular weight reduction upon thermal denaturation has convinced other researchers that native xanthan exists as a monomer folded back to itself in a hairpin like fashion, thus generating the double helical structure (Milas & Rinaudo, 1986).

1.1.3.1. Denaturation

Upon heating, the ordered secondary structure undergoes a conformational transition to a disordered structure, where the side chains project away from the backbone. The structure of the disordered conformation can be described as a broken or imperfect helix (Wyatt & Liberatore, 2009). The characteristic transition temperature T_m is dependent on the ionic strength of the solution (Muller *et al.*, 1986; Rochefort & Middleman, 1987), the acetyl and pyruvate acetal contents (Smith *et al.*, 1981) and the concentration of the polymer (Milas *et al.*, 1995). A higher ionic strength induces a higher transition temperature (Figure 1-3).

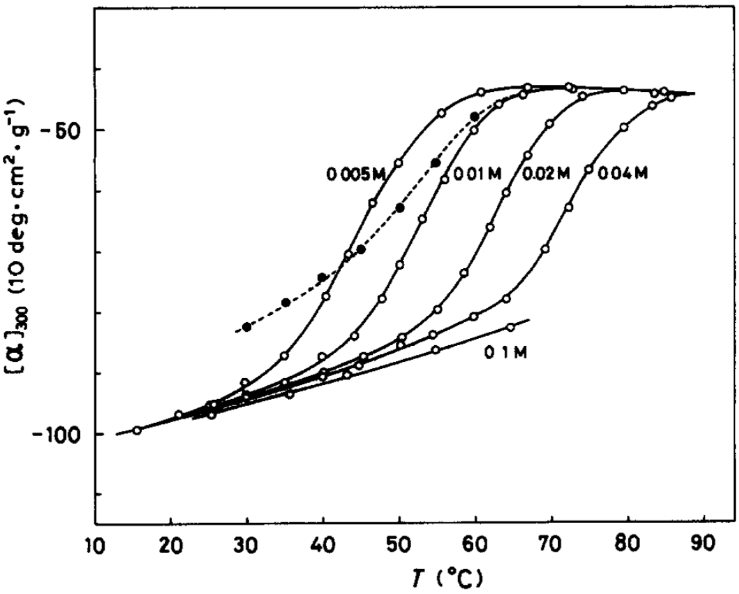

Figure 1-3: Xanthan conformational transition during heating at different NaCl concentrations as measured by optical rotation (dotted line is the result of successive lowering of the temperature for the solution with 0.01M NaCl) (Liu *et al.*, 1987)

In dilute xanthan solutions, T_m rises from near room temperature in the absence of salts to slightly above the boiling point of water at a NaCl concentration of 0.1M. In concentrated solutions the ionic character of the polymer contributes to the ionic strength and further increases T_m (Lee & Brant, 2002c). Remarkably, the pH-dependence of the xanthan transition is studied far less frequently than the effect of NaCl. Holzwarth (1976) found that lowering the pH from neutral to acidic, causes an increase in transition temperature. Conversely, an alkaline environment results in a faster denaturation (Bejenariu *et al.*, 2010). It should be noted that the thermal interconversion of the ordered and disordered forms occurs over a temperature range of 10°C or more and the limits of this range depend on the specific property that is monitored (Lee & Brant, 2002c).

Whether or not the molecules dissociate into monomers or remain associated during denaturation, appears to depend on the heating conditions. It is stated that this might explain some of the contradictions found in literature (Born *et al.*, 2010; Capron *et al.*, 1997). Several authors have suggested that the denaturation process of the double helical conformation is a two-step process and follows an extension-dissociation path. According to Muller & Lecourtier (1988) the lateral chains unfold in the first stage, resulting in a more extended and more flexible double helical structure. Others demonstrated that the double helix melts down from both ends to produce a dimerized expanded coil (Capron *et al.*, 1997; Liu *et al.*, 1987). The ends of the chain can dissociate where short portions of ordered double strands in the middle remains associated, forming an X-like molecule. At this step the molecular weight does not change but the molecule has a smaller persistence length. The second step is an intermolecular process and occurs under more severe conditions (i.e. salinities < 10^{-5} M) or exposure to temperatures above T_m for longer periods of time (Kawakami *et al.*, 1990). Under such conditions the molecular weight is roughly halved indicating a complete dissociation of aggregates and double helices into single-stranded chains. Furthermore, the degree of dissociation was also suggested to depend on the concentration used. In dilute concentrations (0.1 wt%), double stranded xanthan can dissociate into two single chains, but at a higher concentration of molecules (1-2 wt%), they can only partly dissociate due to steric effects (Capron *et al.*, 1998b; Matsuda *et al.*, 2009).

1.1.3.2. Renaturation

When cooling denatured xanthan to temperatures below T_m, renatured xanthan is formed (a temperature hysteresis is generally observed). The reassembly of chains generates an architecture which differs from the original one and depends on the ionic strength and whether the heat treatment was performed on dilute or concentrated solutions. In dilute solutions (< 0.1%), when the xanthan dimers have been fully dissociated, each dissociated single chain forms the anti-parallel double helical structure folded in a hairpin-like fashion during cooling (Capron *et al.*, 1997; Matsuda *et al.*, 2009). When more concentrated xanthan solutions are renatured, a highly entangled structure is formed in which intermolecular interactions are very prevalent (Capron *et al.*, 1998c; Kawakami *et al.*, 1990; Matsuda *et al.*, 2009; Oviatt & Brant, 1993). In the renaturation process, the denatured xanthan dimers aggregate linearly by the mismatched pairing (Matsuda *et al.*, 2009). This mechanism is depicted in Figure 1-4. These interactions most likely share the characteristics of those stabilizing the ordered xanthan structure before thermal denaturation (Sereno *et al.*, 2007). The extent of intermolecular association depends on the molecular weight distribution, the method of sample preparation and in particular on the thermal history of the sample. Sonication and molecular weight fractionation of the double helical material produce samples with more highly perfected helical order, containing fewer segments available for network formation (Lee & Brant, 2002a). The conformational changes and reassociations that take place during heating and recooling steps are illustrated in Figure 1-4.

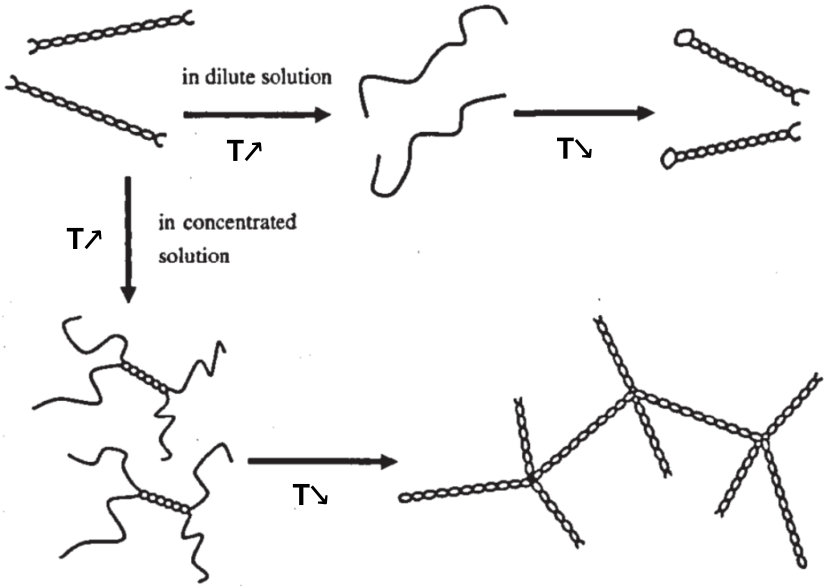

Figure 1-4: Denaturation and renaturation processes occurring in xanthan solutions (Matsuda *et al.*, 2009)

The presence of NaCl affects the reorganization of the xanthan gum structure on cooling from above T_m. For dilute systems, Camesano & Wilkinson (2001) observed that the presence of salt was required for complete intramolecular renaturation. Similarly, it was observed that for more concentrated solutions, molecular aggregation was favored in the presence of salts (Capron *et al.*, 1998a; Kawakami *et al.*, 1990; Matsuda *et al.*, 2009; Rochefort & Middleman, 1987). In dilute as well as more concentrated solutions, inter- or intramolecular associations are restricted at low salt contents, due to electrostatic repulsion between the anionic charges on the polymer. When salts are added, intermolecular associations can more easily take place due to shielding of this repulsion (Sereno *et al.*, 2007).

1.1.4. *RHEOLOGY OF XANTHAN SOLUTIONS*

Like many other polymer systems, xanthan solutions exhibit a newtonian plateau at low shear rates where the viscosity is independent of the applied shear rate. As the shear rate is increased, the viscosity is markedly reduced. Compared to other polysaccharides, the shear-thinning behavior of xanthan gum is much more extreme (Figure 1-5). These high viscosities at low shear rates and very low viscosities at high shear are typical for xanthan gum. Therefore, its addition to foodstuffs imparts texture and mouthfeel while guaranteeing easy mixing, pumping and pouring during production (Imeson, 2010).

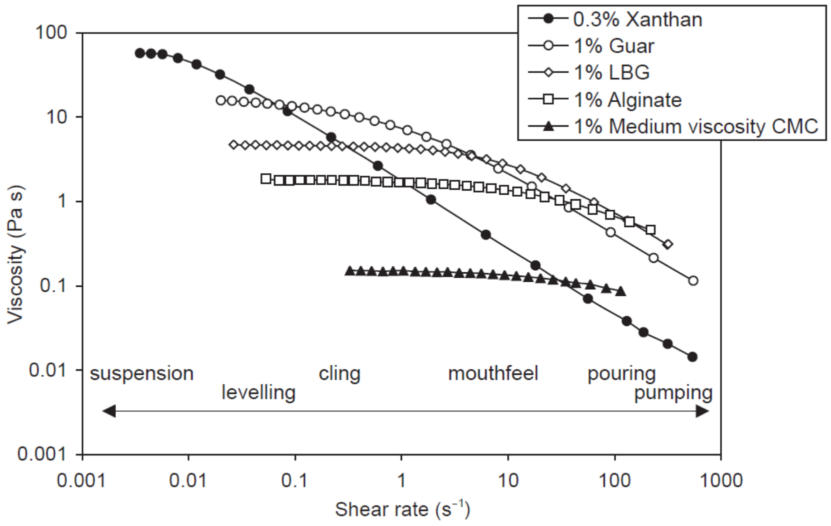

Figure 1-5: Flow behavior of xanthan gum solutions compared with other polysaccharides (Imeson, 2010)

1.1.4.1. Rheology scaling of polymeric solutions

Based on their rheological behavior, critical concentrations are often derived for polymer solutions. Mostly two characteristic concentrations, c* and c**, are observed, bordering regions with differing rheological behavior: a dilute region, an intermediate (or semidilute unentangled) region and an entangled region. Generally, these concentrations are derived by plotting the rheological characteristic (zero shear rate viscosity η_0, characteristic relaxation time τ) in a log-log plot versus the polymer concentration (Wyatt & Liberatore, 2009). The critical overlap concentration c*, marks the onset of molecular overlap: individual molecules begin to physically interact in the quiescent state (Rodd *et al.*, 2000). Starting at the entanglement concentration c**, viscosity increases more rapidly as a function of polymer content. From this point, polymers engage in intermolecular associations. A schematic overview of these different concentration regimes is depicted in Figure 1-6.

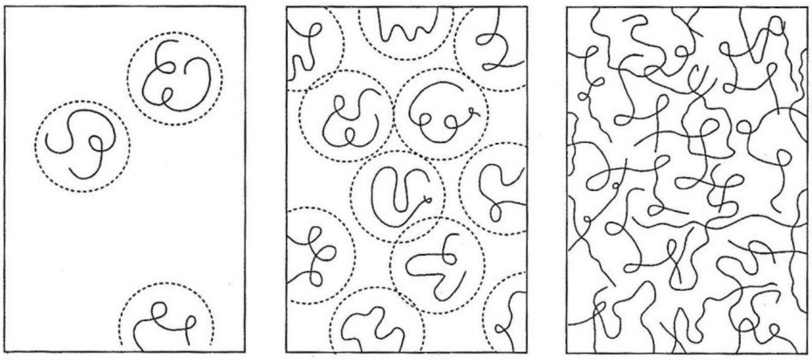

Figure 1-6: Concentration regimes in polymeric solutions: dilute (Left), overlapping (Middle) and entangled (Right) (Walstra, 2003)

1.1.4.2. Concentration dependence of xanthan rheology

When studying the concentration-dependent rheological behavior of xanthan gum, many discrepancies are encountered. Evidently, there is a strong effect of the molecular weight distribution and the acetyl and pyruvate substitution of the sample used. Even more important are the preparation conditions. Particularly in more concentrated solutions, the rheological properties of the studied solutions are strongly dependent on the thermal history as well as the ionic content (Meyer *et al.*, 1993).

There is some general agreement that at concentrations below 0.01-0.03 (w/v)% (c*), xanthan solutions can be described as dilute (Cuvelier & Launay, 1986; Southwick *et al.*, 1981; Wyatt & Liberatore, 2009). In this concentration range, the slope of the log η_0-log concentration plot equals about 1.2. These solutions behave as Newtonian fluids and the elastic modulus tends to zero. Above this overlap concentration (but below c**), intermolecular interactions become important and the viscosity increases more sharply with concentration ($\eta_0 \sim C^2$). The solutions exhibit typical semidilute, weak elastic behavior, where the moduli are strongly frequency dependent and crossover between G' and G" appears.

Although the specific interpretations may vary, a second critical concentration c**, is reported above which the rheological properties of the xanthan solutions markedly change. In most cases, this occurs at concentrations around 0.1-0.2% (Cuvelier & Launay, 1986; Meyer *et al.*, 1993; Rochefort & Middleman, 1987; Southwick *et al.*, 1981; Wyatt & Liberatore, 2009). Milas *et al.* (1990) and Wyatt & Liberatore (2009) describe these solutions as entangled solutions without specific interactions, hence denominating c** as 'entanglement concentration'. Cuvelier & Launay (1986) remarked that the viscosity increases more sharply (η_0 ~ C^4) than observed for purely physical entanglements. Furthermore, small deformation rheology of these systems demonstrates gellike behavior, where G' is higher than G" over a very wide frequency range and both moduli are weakly affected by the frequency. Therefore, the presence of a transient network induced by specific attractive interactions is considered to be more likely (Richardson & Rossmurphy, 1987; Rochefort & Middleman, 1987). The network is formed at relatively low concentrations, but with increasing concentrations, the elasticity and thus the number of interacting chain segments levels off (Choppe *et al.*, 2010; Cuvelier & Launay, 1986). It was suggested that this behavior could be explained by junction zones consisting of parallel-packed chain segments, which could also account for the strongly shear thinning properties of xanthan solutions. This hypothesis of aggregation is supported by dichroism (Meyer *et al.*, 1993) and light scattering (Rodd *et al.*, 2000) experiments. Therefore, the critical concentration c** is also referred to as critical aggregation concentration.

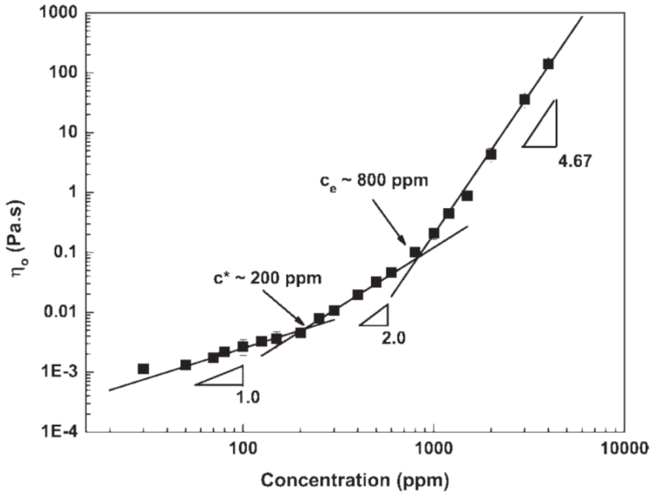

Figure 1-7: Viscosity scaling of xanthan solutions at 0.05M NaCl, the entanglement concentration is indicated by c_e (Wyatt & Liberatore, 2009)

It should be remarked that when heating steps above T_m have been applied, the interpretation of the rheological properties and network structures is further complicated by the formation of intermolecular double-helical junction zones (as described in section 1.1.3.2). It is, however, unclear to which extent both phenomena (parallel aggregation and double-helical association) are related and if both phenomena can coexist. Furthermore, at high xanthan concentrations (± 1%) the formation of anisotropic phases takes place, further complicating the rheological behavior (which is more elaborately described in section 1.1.5).

1.1.4.3. Salt (NaCl) dependence

In most studies, which are also reported in the preceding paragraph, the helical conformation of xanthan is stabilized by the addition of NaCl at different levels. Under these conditions, there is only a limited effect of varying salt concentrations on the rheological properties (Sereno *et al.*, 2007; Takada *et al.*, 1991). At high xanthan concentrations, when anisotropic phases are formed, salt can have more distinct effects as described in paragraph 1.1.5. However, when salt variations give rise to different xanthan conformations, the effects are much more pronounced. In the absence of salts, xanthan occurs as a highly extended disordered polymer. This conformational difference causes distinct changes in rheological behavior. Wyatt & Liberatore (2009) rheologically determined three critical concentrations for salt-free xanthan solutions. Next to the overlap (c*) and entanglement concentration (c**), a third concentration, c_D ,was observed where the viscosity scaling approaches that of an uncharged polymer.

When comparing the xanthan properties in deionized water with their properties in salt solutions, the specific effects are dependent on the xanthan concentration (Pastor *et al.*, 1994; Rochefort & Middleman, 1987; Wyatt & Liberatore, 2009). Salts screen the anionic charges, resulting in a collapse of the side chains and a reduction of the overall hydrodynamic size. In dilute and semi-dilute regimes, the presence of salt causes a reduction in viscosity (Wyatt & Liberatore, 2010). Moreover, more xanthan molecules have to be present in solution to reach a critical concentration at which overlap starts to take place. As a consequence, the overlap and entanglement concentration are much lower in the absence of salt. For higher concentrations, (~ 0.2%) - as claimed by Wyatt and coworkers above c_D, the addition of salt results in a significant increase in viscosity. The enhanced ability of forming hydrogen bonds between chains due to the neutralization of charges dominates the decrease in hydrodynamic volume and the viscosity rises above that of the salt-free solution (Pastor *et al.*, 1994; Wyatt *et al.*, 2011).

1.1.4.4. Influence of thermal transition

The reported effects of the xanthan transition on the rheological properties are rather ambiguous. Depending on the concentration (and molecular weight) the rheological properties are either dominated by conformational changes or changing network properties. Lee & Brant (2002c) observed no marked deflection point during heating of low molecular weight xanthan solutions above T_m. They stated that it was unclear whether the complex viscosity of coils was lower than that of rods. Even with its helical structure lost, the xanthan gum molecules still remain highly extended possibly due to intramolecular steric and electrostatic repulsion, conserving some of the initial solution viscosity (Sereno *et al.*, 2007; Wyatt & Liberatore, 2009). Liu & Norisuye (1988) found that the intrinsic viscosity of xanthan solutions either increases or decreases during denaturation, depending on the molecular weight of the sample.

For high molecular weight samples at concentrations above c**, a drop in viscosity or elastic behavior is often observed upon heating above T_m (Capron *et al.*, 1998b; Choppe *et al.*, 2010; Pelletier *et al.*, 2001; Rochefort & Middleman, 1987; Sereno *et al.*, 2007). The network of associated molecules is stabilized by the helical conformation. By heating these interactions are (partially) disrupted, causing a loss of structural organization.

1.1.5. ANISOTROPY

The stiff extended conformation of xanthan may promote mesomorphic organization. This type of organization is typical for rigid or semi-rigid polymers. Above a certain critical concentration, the molecules tend to spontaneously align side-to-side and form ordered phases to reduce molecular excluded volume. Below a characteristic concentration c_i a completely isotropic phase exists and above c_a a homogeneously anisotropic phase is observed. In the concentration range between c_i and c_a, the system is biphasic and the isotropic and cholesteric liquid crystalline phases coexist at concentrations of c_i and c_a, respectively (Lee & Brant, 2002c). The specific concentrations c_i and c_a depend on the molecular weight, salt concentration, pH, the presence of impurities and temperature (Allain *et al.*, 1988; Lee & Brant, 2002c). Hence, different concentration ranges have been reported in literature. Phase boundaries can be determined by optical birefringence experiments (Allain *et al.*, 1988; Carnali, 1991; Lim *et al.*, 1984; Schorsch *et al.*, 1995). Generally, anisotropy is observed at concentrations around 1% (w/v) and higher. In salt solutions, similar structures are observed but birefringence appears at higher concentration (Lee & Brant, 2002a; Milas & Rinaudo, 1979; Sato *et al.*, 1990). At high salinities, the concentrations c_i and c_a are in the range of 10wt%. Upon heating, birefringence decreases and ultimately disappears. Generally no anisotropy is observed at temperatures above the ordered-disordered transition temperature of the xanthan molecules (Lee & Brant, 2002c; Milas & Rinaudo, 1979; Schorsch *et al.*, 1995).

Few studies describe the rheological behavior of xanthan at concentrations within the biphasic or completely anisotropic region. The steady shear and dynamic viscosities strongly increase with concentration in the isotropic regime, but both decline in the biphasic region as the much less viscous anisotropic phase increases in volume fraction with increasing concentration (Figure 1-8)(Allain *et al.*, 1988; Lee & Brant, 2002a, 2002b; Oertel & Kulicke, 1991). Molecules in the anisotropic phase are parallel oriented so that entanglements are greatly reduced and network formation is suppressed (Lee & Brant, 2002b). For fully anisotropic solutions, the viscosities are generally less dependent on the concentration.

.

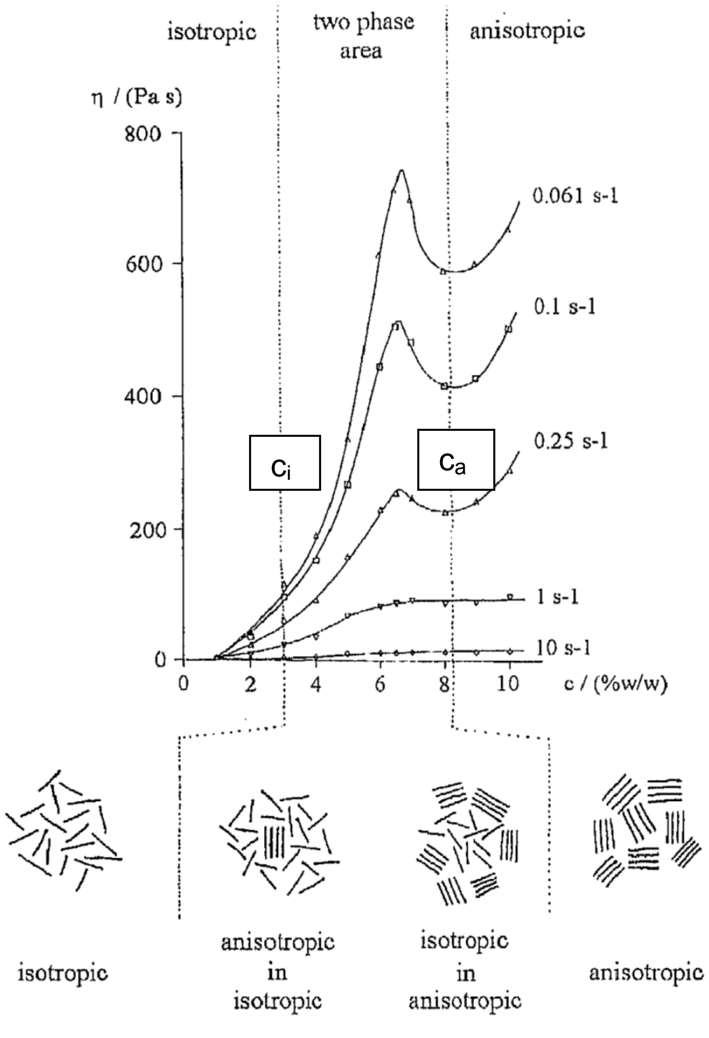

Figure 1-8: Viscosity of 0.1M NaCl xanthan solutions as a function of xanthan concentration and shear rate (25°C)(Jacobs & Kulicke, 1994)

In isotropic solutions the axial ratio and hydrodynamic volume of the stiff xanthan molecules are relatively insensitive to ionic strength and the salt concentration has limited effects on the solution rheology (aside from salt-induced conformation changes or entanglements, see higher). Conversely, in the anisotropic phase the viscosities increase sharply with increasing salt content. The longer range of the lateral electrostatic interactions between the xanthan molecules forces the liquid crystal order parameter to become greater at lower ionic strengths and consequently the viscosity declines as the salt concentration decreases at a given xanthan concentration (Lee & Brant, 2002b)

1.2. STARCH

1.2.1. INTRODUCTION

Starch is present as reserve polysaccharide in cereals (common and durum wheat, maize, rice and rye), in roots and tubers like potato and cassava, and in legumes such as peas. It is one of the most widely used, functional and flexible food stabilizers for both thickening and gelling. As a natural ingredient, it contributes to the characteristic properties of food products made from cereals, rice, potato and maize. Furthermore, it is also added in its native or chemically modified form as a functional ingredient to many foodstuffs ranging from sauces and puddings to confectionery and meat products. Starch is often added to fluid products to increase their viscosity and stability and also to semisolid products to contribute to their texture. In this regard, starches prove to be valuable additives in e.g. low-fat products (Hermansson & Svegmark, 1996; Imeson, 2010).

1.2.2. STRUCTURE

In nature, starch occurs as granules, and their dimensions and morphologies depend on the botanical origin. Starch comprises two different glucose polymers: amylose and amylopectin. Amylose is a linear polymer (MW=10^5 to 10^6 g/mol) of D-glucopyranose units which have α-(1,4) linkages. Amylopectin (MW=10^7 to 10^8 g/mol) has the same backbone but it is highly branched. On the branching points D-glucopyranose has an α-(1,6) linkage. Amylopectin chains are subdivided in so called A-, B- and C-type chains. The A-chains do not carry any other chains, B-chains carry one or more chains and the C-chain is the original chain that carries the reducing end. Normally, starch contains 20-30% amylose and 70-80% amylopectin. Waxy starches are synthetized by mutants that do not have an amylose-producing enzyme and consist exclusively of amylopectin.

When examined under polarized light, native starch granules exhibit birefringence as a result of the internal macromolecular organization perpendicular to the surface (Buleon *et al.*, 1998). As represented in Figure 1-9, the starch granule consists of alternating amorphous and semi-crystalline growth rings. The amorphous shells are less dense and contain amylose and less ordered amylopectin whereas the semi-crystalline shells have alternating amorphous and crystalline lamellae (Tester *et al.*, 2004). There is some convincing evidence that these lamellae are in turn organized into blocklets, ellipsoidal supramolecular structures of 20 to 500 nm in diameter. A blocklet is made up of the semi-crystalline lamellae, which consist of amylopectin double helices, packed in a parallel fashion, and the amorphous lamellae, which incorporate amylopectin branching regions and possibly some amylose (Buleon *et al.*, 1998; Goesaert *et al.*, 2005).

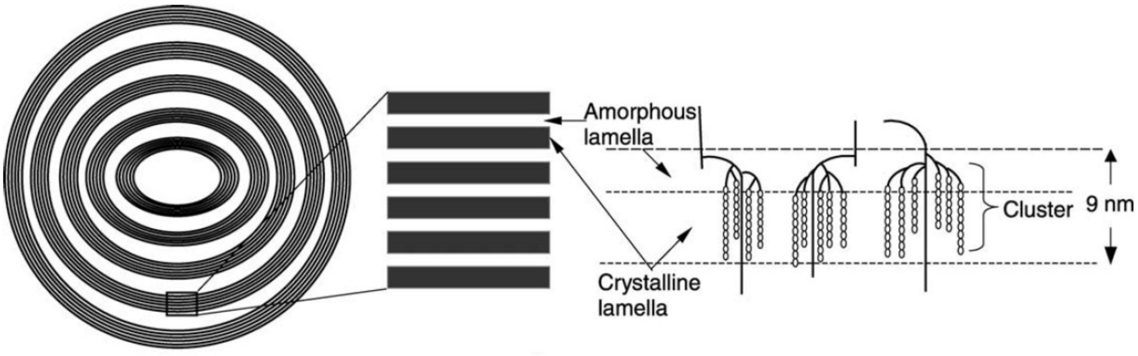

Figure 1-9: Lamellar starch granule structure (Tester *et al.*, 2004)

1.2.3. *GELATINIZATION*

Starch granules are insoluble in cold water. However, they are very hydrophilic due to the high hydroxylation degree which allows a limited water absorption at room temperature. When starch granules are heated in excess water, they undergo a process called gelatinization. At the gelatinization temperature, the granule swells as hydrogen bonds in the amorphous regions are disrupted and water, which acts as a plasticizer, is absorbed. When heating proceeds, further hydration and more swelling occurs in the amorphous regions, pulling apart crystalline zones. Eventually, these regions also undergo hydration and ‘melt’. In this manner, the granules are converted to gel particles (Hermansson & Svegmark, 1996). This disruption of amorphous and crystalline structures results in the loss of birefringence (Parker & Ring, 2001). During the gelatinization process, starch polymer molecules, primarily amylose, diffuse out of the granules and into the surrounding continuous phase. Generally gelatinization of starch granules is determined microscopically, by loss of birefringence, or by differential scanning calorimetry. The latter allows the quantification of an endothermic peak, and the determination of gelatinization onset, peak and conclusion temperatures, describing the gelatinization temperature range.

1.2.4. *PASTING*

The process of pasting follows gelatinization and occurs upon continued heating of starch granules in the presence of excess water. External shear is generally applied. During pasting, considerable granule swelling and leaching of starch polymer molecules take place. Due to the swelling of the granules, the viscosity of the dispersion is markedly increased. The granules can swell up to 50 times their original volume. The swelling degree of the granules is dependent on the available water, the amount of amylose and short chain amylopectines leaching out of the granule. The botanical source, which gives rise to different degrees of polymerization and amylose content, strongly determines the swelling properties. High-amylose corn starch, with a low swelling power, results in small granules compared to waxy varieties which are capable of swelling to greater dimensions. Prolonged heating at temperatures higher than the gelatinization temperature of starch suspensions leads to disruption of the fragile, swollen granules, which is further stimulated by shear. The result is a visco-elastic mass (called a paste) consisting of a continuous phase that is a molecular dispersion of dissolved starch polymer molecules and a discontinuous phase of swollen granules, granule ghosts, and granule fragments (BeMiller, 2011). Already at relatively low concentrations (5-10%) amylose and amylopectin are immiscible. Therefore, a phase separation often occurs within the continuous phase (Kalichevsky & Ring, 1987).

Pasting properties of starch systems are often determined by rapid visco-analyzers (RVA) or Brabender amylographs. Throughout the process, the viscosity is monitored and different parameters are derived from the obtained curves (Figure 1-10). The dispersions are heated (usually to 95°C), held isothermal and finally cooled with continued shearing. The pasting temperature is characterized as the onset of the initial viscosity increase. Although this temperature is related to the gelatinization process, it is affected by other factors as well and might even proceed the actual gelatinization temperature (see section 1.3.2). The peak viscosity is reached when the granules are maximally swollen. During the isothermal step, the fragile swollen granules disintegrate under the shear conditions of the instrument, and the viscosity decreases to a trough viscosity. The difference between the peak and trough viscosity, is defined as ‘breakdown’.

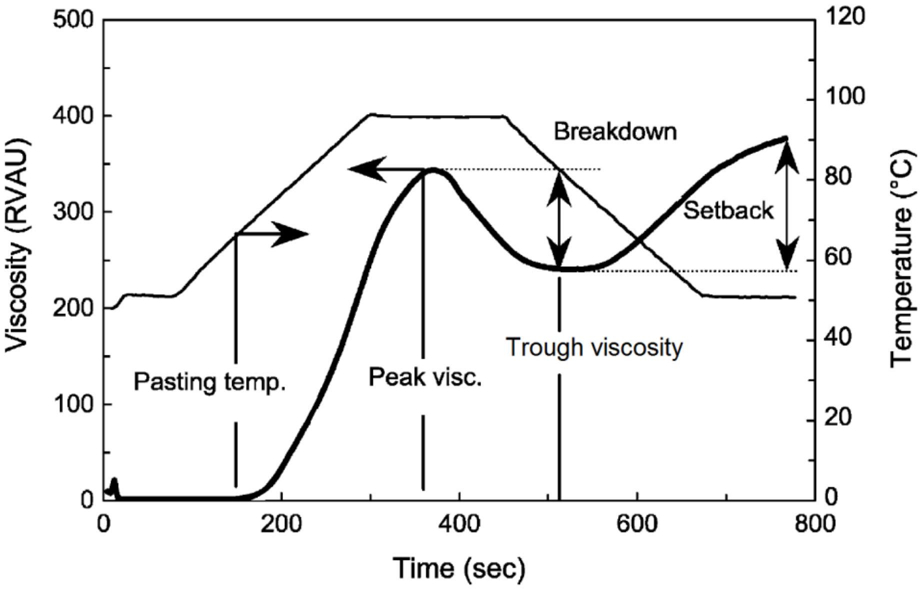

Figure 1-10: Typical starch pasting curve obtained with RVA and corresponding parameters

When the hot pastes begin to cool, they become more elastic and develop distinct solid properties, i.e. gelation occurs. This transition, which is particularly pronounced for amylose containing starches, is called setback. The molecular process causing this setback is called retrogradation and will be treated in the following section.

1.2.5. RETROGRADATION/GELATION

The term retrogradation is used to describe changes that occur during cooling and storage of starch products. It refers to the non-equilibrium polymer association and crystallization processes (Keetels *et al.*, 1996a, 1996b). The rate of retrogradation depends on the type and concentration of the starch as well as the storage temperature (Jouppila *et al.*, 1998; Morikawa & Nishinari, 2000). Retrogradation is usually studied with differential scanning calorimetry (DSC), X-ray diffraction (XRD), turbidimetry and rheological methods (Abd Karim *et al.*, 2000; Farhat *et al.*, 2000; Jouppila *et al.*, 1998; Thygesen *et al.*, 2003).

During the short term phase of retrogradation, leached amylose molecules begin to interact (through entanglements or junction zones) as the paste cools. Subsequently, crystallization in the polymer rich microphase occurs (BeMiller & Whistler, 2009). At low concentrations, amylose precipitates, whereas at higher concentrations (which are more commonly encountered) a network is formed, resulting in a gel. The swollen granules are present as inert fillers within the network. This short term gelation may last up to 48h. In a later stage, lateral association of the helices occurs. This process in particular results in a contraction of the starch gel and water is expelled from the matrix, which is indicated by the term ‘syneresis’. Aged amylose networks consist of double helices, small aggregates of double helices (junction zones), nanocrystals and their aggregates (BeMiller & Whistler, 2009)

Retrogradation of amylopectin is a much slower process that may proceed over several weeks, depending on the concentration and the storage temperature. The external chains of these branched molecules recrystallize (Krystyjan *et al.*, 2013). The rate of amylopectin retrogradation depends on the molecular weight and happens faster with longer chain lengths (Kalichevsky *et al.*, 1990). This crystallization is thermoreversible at temperatures around 40-60°C, as opposed to amylose crystals that melt at much higher temperatures (> 100°C) (Miles *et al.*, 1985). Amylopectin crystallization within the granule results in an increased rigidity of the granules which in turn reinforces the amylose matrix (Miles *et al.*, 1985). The molecular changes occurring during heating and cooling of starch dispersions, are illustrated in Figure 1-11. Retrogradation of waxy starches is strongly influenced by moisture content and initial heating temperature (Liu & Thompson, 1998). At low moisture contents, granules can only swell to a limited extent, resulting in a lot of residual order which facilitates reassociation. A similar mechanism was used to explain the faster retrogradation of waxy starches heated at temperatures just above the gelatinization temperature (Fisher & Thompson, 1997).

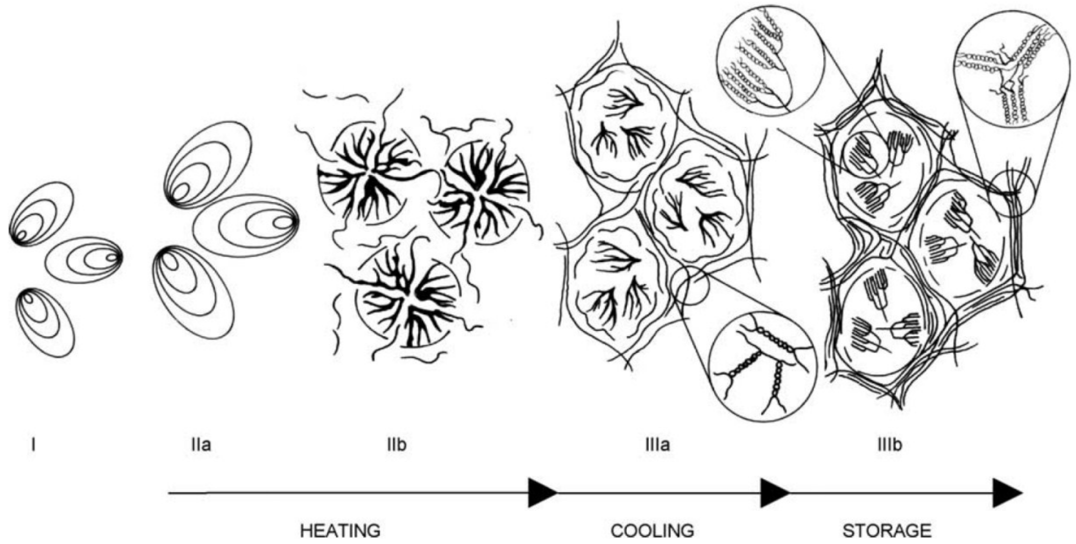

Figure 1-11: Molecular changes occurring during heating, cooling and storage of starch pastes (Goesaert *et al.*, 2005)

1.2.6. RHEOLOGICAL PROPERTIES OF STARCH PASTES

The rheological properties of starch pastes are strongly influenced by the physical state of the present granules, i.e. their swelling/degradation properties (Tattiyakul & Rao, 2000). When the granules disintegrate at high temperatures or under the influence of shear forces, the viscosity of the samples is drastically reduced and the consistency of the paste changes. For these systems which are called ‘overcooked’, the rheological properties are governed by the continuous phase containing the dissolved starch polymers and the texture becomes long or slimy (Hermansson & Svegmark, 1996). This overview focuses on the rheological properties of starch dispersions in which granule breakdown is restricted and swollen granules are the prominent structural feature of the system, which is the case for systems consisting of mildly treated native starches or shear-resistant chemically cross-linked starches.

Gelatinized starch granules can be considered as microgel particles (Evans & Lips, 1992) and the net force between the granules is attractive (Acquarone & Rao, 2003). The rheological behavior of swollen starch dispersions depends on the concentration, the dimensions of the granules, the interactions between the granules, as well as the characteristics of the continuous phase (Rao *et al.*, 1997). The properties of the granules are in turn determined by the temperature and deformation history of the sample (see 1.2.4). For very low concentrations, the viscosity is uniquely determined by the particle volume fraction. In this concentration regime, starches with highest swelling power (i.e. when they can swell freely, the granules adopt the highest volumes) generate the highest viscosities. Generally, they also exhibit a more elastic behavior (higher value of storage modulus G’). When the concentration is increased, a close-packing concentration c_{cp} can be attained where the fully swollen granules just fill up the available space. At higher concentrations, insufficient space is available for the granules to swell to their equilibrium volume (Figure 1-12). The system is completely filled with swollen starch particles and the rheological properties are mainly determined by the particle rigidity of the swollen granules. Under these conditions, starches with the lowest swelling power are more rigid (i.e. they are less deformable) and have the highest storage moduli, which is in contrast with the phenomena observed in the dilute concentration regime. Logically, starches with low swelling power require higher concentrations to attain close-packing (Eerlingen *et al.*, 1997). Furthermore, it has been stated that a network of interacting swollen starch granules is already present at concentrations well below close-packing (Abdulmola *et al.*, 1996b). Hence, for these systems a dominant elastic behavior can be observed at relatively low starch volume fractions (~20%).

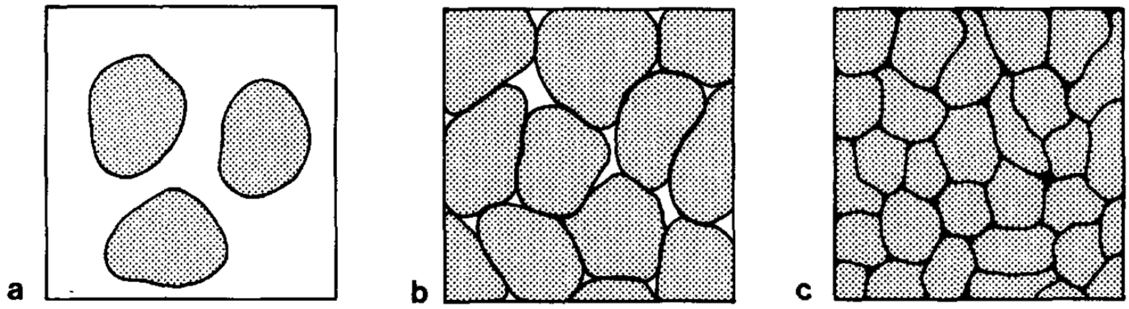

Figure 1-12: Swelling regimes of starch granules at different concentrations: full swelling at c < c_{cp} (a), full swelling at c ≅ c_{cp} (b) and restricted swelling at c > c_{cp} (c) (Eerlingen *et al.*, 1997)

Most gelatinized starch dispersions show a non-newtonian flow behavior. A yield stress is also often observed (Rao *et al.*, 1997). Suspensions of highly swollen granules are generally pseudoplastic or shear-thinning, meaning that the viscosity is reduced, i.e. flow is facilitated, when the shear rate increases. Depending on the type of starch, granules are capable of orienting themselves with the flow (Jacquier *et al.*, 2006). Moreover, Desse *et al.* (2010) demonstrated that swollen starch granules are deformed during flow and that part of the absorbed water can be expelled. Some starch pastes exhibit antitixotropic behavior: the shear stress recorded with increasing shear rate, is lower than the shear rate recorded upon subsequently lowering the shear rate (flow curves represent an anti-clockwise hysteresis loop). This behavior is attributed to the formation of shear-induced granule clusters (Chamberlain *et al.*, 2000; Tattiyakul & Rao, 2000) or a rearrangement of the packed granules (Nayouf *et al.*, 2003).

Concentrated starch dispersions sometimes show dilatant or shear thickening behavior, particularly in the case of poorly swollen granules. For these dispersions, an abrupt rise in viscosity is observed at a characteristic shear rate $\dot{\gamma}_c$ (Rao *et al.*, 1997). This shear thickening is most likely induced by a flow instability of packed granules. When $\dot{\gamma}_c$ is attained, the long range orientational order within the flow field is disturbed resulting in the typical discontinuous viscosity behavior. When more highly swollen granules are present, shear thickening diminishes, due to their more deformable and/or the broader size distribution (Rao *et al.*, 1997).

1.2.7. STARCH MODIFICATIONS

Native starches generally do not comply with the requirements for industrial food applications. Very often, native starches are chemically modified to improve their tolerance to processing conditions (heat, shear and acidic environments) and to provide cold storage and freeze-thaw stability. By introducing chemical modifications to the native starch granules, the resulting pastes or gels exhibit improved textures, which are better preserved over time, and in which syneresis is reduced (Tharanathan, 2005).

The most important chemical modification in the starch industry is cross-linking, in which hydroxyl groups of adjacent polymers are covalently linked with a chemical agent. In this manner, the granule structure is reinforced which results in a restricted swelling power and a higher resistance to elevated shear and temperatures during processing. Distarch phosphates and distarch adipates are the most frequently encountered crosslinked varieties in the food industry. Very often, starch hydroxyl groups are also chemically substituted with monofunctional reagents. Acetylation and hydroxypropylation are the most common examples. Their presence hinders the reassociation of starch polymers during storage. Stabilized starches are therefore less subject to retrogradation effects and contribute to a prolonged shelf-life of the food products (Singh *et al.*, 2007; Tharanathan, 2005).

1.3. STARCH/HYDROCOLLOID COMBINATIONS

Aside from chemical modifications, shortcomings of native starches can partly be overcome or compensated by the incorporation of hydrocolloids (Appelqvist & Debet, 1997). Therefore many experiments have been conducted in order to understand the effects of hydrocolloids on the properties of the starch-based systems. Plenty of diverging effects are reported and one generalizing theory is lacking, because the results greatly depend on the botanical origin of the starch, the nature of the hydrocolloid, the applied concentrations and the preparation conditions (BeMiller, 2011). In this section, the complexity of starch/hydrocolloid systems will be illustrated by summarizing the most commonly reported effects of non-starch hydrocolloids or gums on starch-based systems, along with the proposed mechanisms. This overview is restricted to non-gelling hydrocolloids.

1.3.1. INFLUENCE ON GELATINIZATION

Generally, hydrocolloids do not significantly change the gelatinization temperatures of starches (Chantaro & Pongsawatmanit, 2010; Gonera & Cornillon, 2002; Samutsri & Suphantharika, 2012; Viturawong *et al.*, 2008). Some exceptions are encountered in which a slight increase in gelatinization temperature(s) is observed (Aguirre-Cruz *et al.*, 2005; Ferrero *et al.*, 1996; Kruger *et al.*, 2003; Rojas *et al.*, 1999; Tester & Sommerville, 2003; Yoshimura *et al.*, 1996). Presumably, the results are strongly affected by the concentrations used and apparent increases in gelatinization temperature can be due to reduced heating rates and water diffusivities in a more viscous medium. Nevertheless, the enthalpic transition ΔH is often reduced by the addition of gums (Aguirre-Cruz *et al.*, 2005; Chaisawang & Suphantharika, 2006; Rojas *et al.*, 1999; Satrapai & Suphantharika, 2007; Tester & Sommerville, 2003; Viturawong *et al.*, 2008). It has been proposed that this is caused by a reduction of water availability in the crystalline regions of the granule (Chaisawang & Suphantharika, 2006) or by the occurrence of specific gum starch interactions (Rojas *et al.*, 1999).

1.3.2. INFLUENCE ON PASTING BEHAVIOR

As opposed to the mostly unaffected gelatinization temperatures, the pasting temperature measured by means of RVA or Brabender, is often decreased by the addition of hydrocolloids (Alloncle *et al.*, 1989; Christianson *et al.*, 1981; Liu & Eskin, 1998; Shi & BeMiller, 2002). Christianson *et al.* (1981) proposed that this earlier viscosity onset was due to associations between leached starch molecules and hydrocolloid molecules. Similar conclusions were drawn by Shi & BeMiller (2002), who observed this effect for xanthan and guar gum in combination with several types of starches. In some other cases a delay in pasting onset is observed, particularly in the presence of xanthan gum (Achayuthakan & Suphantharika, 2008; Chaisawang & Suphantharika, 2005; Pongsawatmanit & Srijunthongsiri, 2008; Weber *et al.*, 2009).

A common result of starch-hydrocolloid combinations is an increase in paste viscosity. Generally, a synergistic effect is observed and the mixed systems exhibit higher viscosities than expected from an additive combination of the individual components. Several hypotheses that have been put forward are associated with polymer incompatibility/compatibility. They will be discussed in the following section because the same phenomena can be held responsible for the effects on cold paste viscosity. Aside from the phase behavior of the polymers, some other changes might occur specifically during the pasting process. When heated together, gums can influence the swelling and degradation behavior of the granules, and in this manner indirectly affect the rheological behavior of the mixed pastes.

Depending on the specific starch/gum combination, and the applied preparation conditions, both aspects can be affected. An inhibition of the granule swelling due to the hydrocolloid is often reported (Cai *et al.*, 2011; Kruger *et al.*, 2003; Song *et al.*, 2006; Temsiripong *et al.*, 2005; Tester & Sommerville, 2003). Both kinetic and thermodynamic effects have been put forward to explain this effect. Kruger *et al.* (2003) suggested that in the presence of gums, granule swelling was reduced because of the lower heating rates and the reduced mobility of the water molecules. Kaur *et al.* (2008) observed that the expansion of starches with high swelling capacity was reduced whereas the effect on low swelling starches was limited. By affecting the migration of starch polymers from the granules, hydrocolloids can have an indirect effect on the granule swelling and degradation. Funami *et al.* (2005b), found that guar gum reduced the leaching of amylose from corn starch, with higher molecular weight fractions being more effective. Shi & BeMiller (2002) noticed an inhibited swelling of potato starch in the presence of anionic hydrocolloids, which was attributed to repelling forces between the phosphate groups of the starch and the anionic substituents of the polymer. Furthermore, if their swelling is restricted, the granules also become less sensitive to breakdown. Therefore, by retaining amylose in starch granules, hydrocolloids could possibly also strengthen them (Biliaderis *et al.*, 1997; Hongsprabhas *et al.*, 2007). Conversely, when more starch polymers leach from the granules, they can swell to a higher degree (BeMiller, 2011). In general, increased granule swelling is rarely reported although xanthan gum might be capable of inducing higher granule dimensions (Achayuthakan *et al.*, 2006; Chaisawang & Suphantharika, 2006; Mandala & Bayas, 2004; Samutsri & Suphantharika, 2012).

An increased breakdown as derived from RVA or Brabender pasting curves, has convinced some authors that gums enhance the rupture of the granules. It has been proposed that due to the higher medium viscosity, the shear forces exerted on the granules are increased, which results in more breakdown during pasting (Achayuthakan & Suphantharika, 2008; Chaisawang & Suphantharika, 2006; Christianson *et al.*, 1981; Mandala & Bayas, 2004). In conclusion, it can be stated that the effects of granule swelling (and degradation) are strongly dependent on the specific starch/gum combination and the applied pasting conditions, and are therefore difficult to predict.

1.3.3. INFLUENCE ON RHEOLOGICAL PROPERTIES

The pasting and paste characteristics of starch-hydrocolloid mixtures are affected by at least three factors: the properties of the hydrocolloid solution in the continuous phase, granule swelling in the composite system and interactions between the continuous and dispersed phases (Chaisawang & Suphantharika, 2006). As explained in the preceding paragraph, hydrocolloids could affect granule swelling and/or degradation and hereby the rheological properties of the resulting mixed systems. Some other more direct phenomena have been hypothesized as well, which do not exclude the existence of indirect effects. Most likely a combination of mechanisms contributes to the eventually observed rheological synergies.

Starch-hydrocolloid combinations usually result in increased paste viscosity or gel strength compared with starch alone pastes. Crossland & Favor (1948) proposed that the enhanced viscosity resulted from an increase in the work required to move swollen starch granules past each other in the more viscous medium. Others suggested that the observed synergy was due to associations between starch and hydrocolloid molecules in the continuous phase (Christianson *et al.*, 1981). Comparable conclusions were drawn by Funami *et al.* (2005b) and Shi & BeMiller (2002). The specific interactions depend not only on the gum type and the mixing ratio, but also on molecular characteristics like the molecular weight of the gum and substitution degree (Funami *et al.*, 2008b; Funami *et al.*, 2005b). Hence, for one type of gum, diverging results can be obtained. Possible interactions between gums and (leached) starch polymers can therefore strongly influence the properties of the continuous phase. Others went even further and observed that some hydrocolloid starch polymer interactions could result in collaborative network formation (Freitas *et al.*, 2003).

On the other hand, the enhanced rheological properties are often attributed to mutual exclusion of the starch and the gum fraction. Alloncle *et al.* (1989) first suggested that hydrocolloids remain outside the granules and their concentration in the continuous phase is increased when the granules swell by taking up water. This effect is suggested to cause the often observed synergies, a hypothesis that is embraced by other authors (Achayuthakan & Suphantharika, 2008; Alloncle & Doublier, 1991; Biliaderis *et al.*, 1997; Mandala *et al.*, 2004).

Whereas the viscosities of a mixed paste can be markedly increased, the viscoelastic properties are generally less dramatically affected by gums (Alloncle & Doublier, 1991). In many cases, the elastic modulus G' is slightly elevated by the addition of gums, but the relative increase in viscous behavior (often expressed as loss tangent or tan delta) is higher as well. Kulicke *et al.* (1996) and Biliaderis *et al.* (1997) observed that hydrocolloids can render the starch network more viscous like. They suggested that the formation of permanent cross-links between starch molecules is inhibited. Similar suggestions were made by Eidam *et al.* (1995) and Yoo *et al.* (2005). It has also been proposed that guar gum inhibits starch components from leaching out of the granules, resulting in an increased viscous character of the system (Nagano *et al.*, 2008). Others believed that a phase separation confined the starch components to the discontinuous phase and that the hydrocolloid molecules are concentrated in the continuous phase, therefore dominating the liquid like behavior of composite pastes and gels (Temsiripong *et al.*, 2005). Rodriguez-Hernandez *et al.* (2006) and Savary *et al.* (2008) added that the properties of the composite pastes and gels depend on whether the concentrated molecules could engage in network formation. In the presence of a strongly gelling biopolymer, the increase in composite rheology originates mainly from the continuous gel matrix, whereas in the presence of a non-gelling gum, the major contribution originated from the associated starch granules (Abdulmola *et al.*, 1996a, 1996b).

1.3.4. INFLUENCE ON RETROGRADATION/GELATION

Hydrocolloids can interfere with both short term (amylose gelation and recrystallization) and long term (amylopectin recrystallization) retrogradation. Direct as well as indirect mechanisms have been proposed, which depend on the type of hydrocolloid, preparation methods and storage temperatures (BeMiller, 2011). Similar to the preceding rheological properties, the retrogradation behavior also appears to be strongly affected by the compatibility between the gum and starch molecules.

Most often, short term retrogradation or more specifically amylose gelation is enhanced by hydrocolloids (Alloncle & Doublier, 1991; Eidam *et al.*, 1995; Funami *et al.*, 2008c; Funami *et al.*, 2008d; Yoshimura *et al.*, 1999). It is generally hypothesized that due to their incompatibility, a phase separation exists between gums and the leached amylose molecules. In this manner the concentration of each polymer type in its microphase is increased. Because the molecules are now located more closely to each other, amylose-amylose associations are favored which results in a faster gelation. However, despite the acceleration of gelation, the actual network strength is often weaker in the presence of gums. As described in the preceding section, this might be caused by a phase separation resulting a discontinuity of the present network. Others suggested that gums could also prevent leaching of amylose during pasting and that this results in a weaker gel strength (Funami *et al.*, 2008a; Funami *et al.*, 2005a; Kim & Yoo, 2006; Nagano *et al.*, 2008). Conversely, Funami *et al.* (2005c) found that, depending on the molecular weight, some guar gum molecules can retard short term retrogradation, because guar-amylose associations are formed at the expense of amylose-amylose associations.

The effect of hydrocolloids on longer periods of storage, where crystallization of amylose and amylopectin and cocrystallization between both become predominant, are more vague. Crystallization can be quantified by means of differential scanning calorimetry (DSC) where an endothermic peak is observed upon reheating. The effects on amylose crystallization are mostly not reported, which complicates the interpretation of the changes in overall rheological behavior. As explained above (section 1.2.5), the detected enthalpic transition is only associated with the crystallized amylopectin fraction because the DSC-measurements are generally restricted to temperatures below 100°C. Most studies reveal that the presence of gums initially enhances amylopectin crystallization, which then levels off during longer storage (Biliaderis *et al.*, 1997; Funami *et al.*, 2005a; Temsiripong *et al.*, 2005; Yoshimura *et al.*, 1999). The effects of long term storage on the rheological properties are rarely monitored. It has been hypothesized that also during longer preservation, most gums inhibit the formation of long-ranged continuous network structure but the underlying mechanisms remain vague (Biliaderis *et al.*, 1997; Temsiripong *et al.*, 2005). Others suggested that in case the amylopectin remains inside the granules, and therefore is physically separated from the gums, its retrogradation is not affected by the gum molecules (Ferrero *et al.*, 1994).

2 INFLUENCE OF XANTHAN ON THE RHEOLOGICAL PROPERTIES OF WAXY STARCHES

Relevant publication: Heyman, B., De Hertogh, D., Van der Meeren, P., Depypere, F., Dewettinck, K. (2013). Influence of xanthan transition on the rheological properties of waxy starches. Carbohydrate Polymers, 96 (2), 568-577.

2.1 INTRODUCTION

Non-starch hydrocolloids or food gums prove to be very useful additives when combined with starches. In many cases they act synergistically and the gums are known to improve the rheological properties and stability of starch based systems like sauces and dressings (Arocas *et al.*, 2009; Dolz *et al.*, 2006; Heyman *et al.*, 2010; Sikora *et al.*, 2008a). Moreover, the suggestion is made that gums can compensate the shortcomings of native starches, hence reducing the need for chemically modified starches (BeMiller, 2011).

One particular hydrocolloid of great interest is xanthan gum. In the presence of salt and at low temperatures, xanthan molecules in solution adopt an ordered helical conformation where the side chains are folded-down and associated with the backbone by non-covalent interactions. This high rigidity compared to other polysaccharides is the basis for its distinct rheological behavior and consequently the commercial value of xanthan. This secondary structure exhibits a temperature induced transition at T_m, to a disordered coil structure. T_m is dependent on the ionic strength of the solution, the nature of the electrolyte, as well as the acetyl and pyruvate acetal contents of the polysaccharide (Muller *et al.*, 1986; Rochefort & Middleman, 1987; Smith *et al.*, 1981).

Combinations of starch and gums are discussed extensively in scientific literature. A lot of divergent effects of hydrocolloids on starch based systems are reported. As pointed out by BeMiller (2011), hydrocolloids and starches exhibit strongly varying functionalities, depending on their origin. This natural diversity of the ingredients, combined with the wide variety of procedures used for the preparation of the systems, make it hard to draw general conclusions. Particularly regarding the effects of xanthan gum on the pasting behavior of starches, diverging results are abundant. Some reports describe increases in peak viscosity and/or breakdown (Achayuthakan & Suphantharika, 2008; Aguirre-Cruz *et al.*, 2005; Chaisawang & Suphantharika, 2005; Chantaro & Pongsawatmanit, 2010; Christianson *et al.*, 1981; Korus *et al.*, 2004; Pongsawatmanit & Srijunthongsiri, 2008; Rojas *et al.*, 1999; Samutsri & Suphantharika, 2012; Song *et al.*, 2006; Viturawong *et al.*, 2008). Conversely, in other combinations xanthan induces a decrease in either or both parameters (Cai *et al.*, 2011; Chaisawang & Suphantharika, 2006; Lee *et al.*, 2002; Samutsri & Suphantharika, 2012; Sikora *et al.*, 2008b; Song *et al.*, 2006; Weber *et al.*, 2009)

Most of these discrepancies originate from differences in the concentrations used, the content of amylose (waxy vs. non-waxy) as well as the presence of ionic substituents (e.g.

anionic starch) or salts. In this work, the focus lies on the combination of xanthan gum with waxy starches, which are essentially free of amylose. From a practical point of view waxy starches are very interesting because their chemically modified counterparts are very often used in combination with xanthan gum. Due to the absence of amylose, they do not form strong gels upon cooling, which makes them suited for application in sauces and dressings. Furthermore, the interpretation of the results is not complicated by amylose-xanthan interactions in the continuous phase of the dispersion.

The influence of salts on the transition temperature as well as the final rheological behavior of xanthan gum solutions have been widely documented. Surprisingly, the effects of salt content, and hence the occurrence of the xanthan transition, on mixed starch/xanthan systems is rarely studied. Aside from the contributions of Sudhakar *et al.* (1996), Viturawong *et al.* (2008) and Samutsri & Suphantharika (2012), few or no publications study the functionality of xanthan/starch mixtures at varying salt concentrations. Moreover, the effect of the xanthan gum transition on the functionality of the combined waxy starch/xanthan gum system is to our knowledge never reported. Some authors explicitly mention the use of high salt contents to stabilize the ordered conformation and to avoid the complication of the xanthan denaturation (Abdulmola *et al.*, 1996b; Alloncle & Doublier, 1991), but more often no salts are added to the systems (Achayuthakan & Suphantharika, 2008; Achayuthakan *et al.*, 2006; Biliaderis *et al.*, 1997; Weber *et al.*, 2009).

Furthermore, most studies are also restricted to one type of starch. Different types of waxy starches were included in this setup in order to derive more generalized conclusions. The central aim was to investigate the effects of the xanthan transition on the pasting behavior and the final properties of waxy starches. From a practical point of view, the intention was to help clarifying some of the discrepancies found in literature and to fill the gap between most experimental setups where no salt is added, and practical food applications which generally contain high amounts of salts. In order to buffer differences in ionic content originating from the different starch powders, a NaCl content of 0.01M was used for the low salinity systems. Pastes containing 0.1M NaCl represented the systems with high salinity.

2.2 MATERIALS AND METHODS

2.2.1 *MATERIALS*

Xanthan gum (Satiaxane CX911) was acquired from Cargill Texturizing Solutions (Ghent, Belgium). The supplier indicates that at least 1.5% of the terminal mannose residues are pyruvated and the. molecular weight ranges between 2 and 4 x 10^6 Dalton, an order of magnitude that is also mentioned by other authors (Benna-Zayani *et al.*, 2008; Viturawong *et al.*, 2008). Native waxy maize starch (Merizet 300) and adipate crosslinked acetyl substituted waxy maize starch (Resistamyl 347, further denoted as ‘modified maize’) was supplied by Tate & Lyle Benelux. Native waxy rice starch (Remyline xs) and waxy potato starch (Eliane 100) were provided by Beneo-Remy (Wijgmaal, Belgium) and AVEBE (Veendam, The Netherlands), respectively. Because all starch types used here are of a waxy type, the denomination ‘waxy’ will not be further repeated throughout this chapter.

2.2.2 *PREPARATION OF XANTHAN SOLUTIONS*

Xanthan gum powder was dispersed in deionised water, whilst continuously stirring with a magnetic stirrer. Next, the premix was put in an Ekato Unimix LM3 laboratory mixer (EKATO Rühr- und Mischtechnik GmbH, Schopfheim, Germany), a mixing apparatus equipped with a temperature control system, paravisc agitator with revolving blades and a colloid mill homogenizer (Figure 2-1). To fully dissolve the xanthan gum, the premix was homogenized at room temperature for 15 minutes at 5000 rpm and stirred at an agitation speed of 150 rpm. During homogenization, the unimix system was placed under vacuum to limit air inclusion. The obtained xanthan solutions (0.8% (w/v)) were then diluted with NaCl solutions to the desired xanthan and salt content. An additional heating step could be introduced to solutions containing 0.4% (w/v) xanthan and 0.01M NaCl by means of the Ekato Unimix (heated to 85°C and held at this temperature for 10min). These samples were afterwards diluted to 0.2 % (w/v) xanthan with salt solutions to obtain a final NaCl concentration of 0.1M or 0.01M. Preheated xanthan solutions are indicated by ‘H’ and not-preheated solutions by ‘UH’.

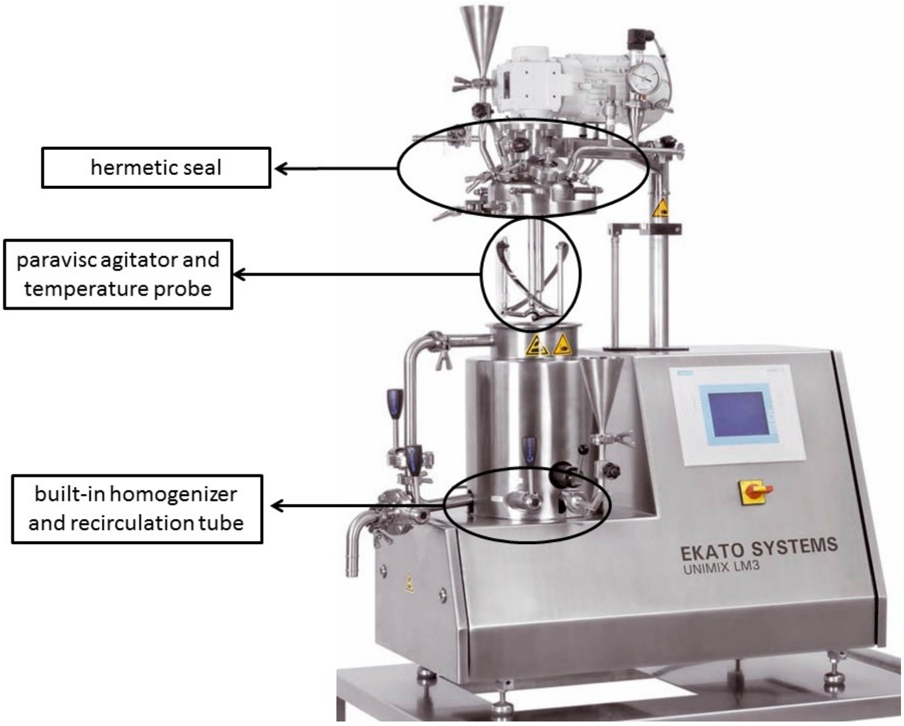

Figure 2-1: Representation of the unimix system

2.2.3 *RHEOLOGY OF XANTHAN SOLUTIONS*

Rheological measurements of xanthan solutions (0.2 and 0.4%) were performed on an AR2000 and AR2000ex rheometer (TA Instruments, New Castle, USA), using 28mm conical concentric cylinders (gap of 500 µm between the inner and outer cylinder) with solvent trap to limit evaporation. A sample size of approximately 20g was used.

To determine the linear visco-elastic region, strain sweeps were performed. First, equilibration was allowed for 2 minutes, at a temperature of 20°C. Next, a strain sweep step was performed: strain was varied from 0.1 to 100% (measuring 10 points per decade), at a constant frequency of 1Hz. A strain of 20% was applied in order to obtain reproducible measurements within the linear visco-elastic region of the different xanthan solutions.

To assess the xanthan transition from ordered to disordered conformation, a temperature ramp was imposed to the unheated xanthan solutions. The temperature was increased from 20°C to 85°C at a rate of 3°C/min, held for 10 minutes and cooled down (3 °C/min) to 20°C. Hereby, the strain was held constant at 20% and the frequency was 1 Hz for samples containing 0.4% (w/w) xanthan gum and 0.5 Hz for samples containing 0.2% (w/w) xanthan gum. The transition temperature T_m was calculated by means of the sudden drop of the complex modulus |*G**|: the temperature at which the change in slope between the 4 preceding and the 4 succeeding data points was maximal, was selected as T_m.

Before and after this heating step, flow curves of the xanthan solutions were recorded. After 2 minutes of equilibration at 20°C, samples were subjected to a stepped flow step: shear rate was varied from 0.01 to 100 s^{-1} (with 10 measuring points per decade).

2.2.4 STARCH/XANTHAN SYSTEMS

Starches were dispersed cold in salt solutions of 0.01M NaCl and 0.1M NaCl or in xanthan solutions (0.2%, 0.01M or 0.1M NaCl) prepared as described above. Either heated xanthan solutions (H) or unheated xanthan solutions were used (UH). The dry starch:continuous phase weight-ratio was always 5:100. Samples from this premix were either transferred to DSC-pans or to the starch pasting cell geometry of the rheometer.

2.2.4.1 Differential scanning calorimetry (DSC) measurements

About 10-15 mg of suspension was accurately weighted in an alodined DSC pan (TA Instruments, New Castle, USA) and hermetically sealed. A DSC Q1000 (TA Instruments, New Castle, USA) was used for all measurements. The instrument was calibrated with Indium (TA Instruments, New Castle, USA) for melting enthalpy and temperature. Additional temperature calibrations were performed with azobenzene (Sigma-Aldrich, Bornem, Belgium) and *n*-undecane (Acros Organics, Geel, Belgium). An empty pan was used as reference. The samples were heated from 20°C to 99°C at a heating rate of 3°C/min. The onset (T_o), peak (T_p) and conclusion (T_c) temperature of gelatinization, as well as the corresponding enthalpy (ΔH) were calculated by means of the Universal Analysis 2000 Software (TA Instruments, New Castle, USA).

2.2.4.2 Pasting experiments

The pasting behavior was studied using a starch pasting cell mounted to a controlled stress rheometer AR2000 (TA Instruments, New Castle, USA). This rheometer geometry (Figure 2-2) consists of a jacket, a removable cup and an impeller. A gap of 5500 µm between rotor and the bottom of the cup is used. Since the impeller produces an ill-defined flow, analytical conversion factors to calculate shear rate or shear stress are not available. Therefore the system was calibrated by the manufacturer with a Newtonian and non-Newtonian oil to determine the conversion factors (4.500 (-) for shear rate and 48,600 m^{-3} for shear stress). For the sake of simplicity, the word ‘shear rate’ is used in this manuscript, although the actual shear rates occurring in the sample will vary throughout the sample volume. The starch pasting cell has a very efficient and accurately controlled heating and cooling system. The temperature is continuously monitored with a Pt-probe in close thermal contact with the bottom of the cup. Heating is accomplished by the electrical elements inside the jacket. Cooling is performed with water circulating in a helical tract inside the jacket and around the sample.

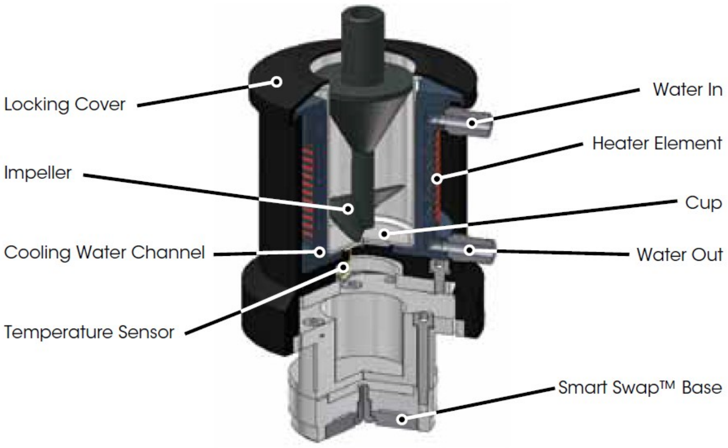

Figure 2-2: Representation of the starch pasting cell (source www.tainstruments.com)

Starch suspensions were pre-sheared at 100 s^{-1} for 2 minutes and then heated to 85°C at a heating rate of 5°C/min, held isothermal for 10 minutes and then cooled down (5 °C/min) to 20°C. Throughout the heating and cooling steps a shear rate of 50 s^{-1} was maintained. The peak viscosity was attained during the heating or the isothermal step, depending on the setpoint temperature. Sometimes, no true peak was observed as the viscosity kept increasing continuously. The peak viscosity then corresponds with the maximum viscosity which is attained at the end of the isothermal step (=’trough viscosity’). The breakdown was calculated as the difference between the peak viscosity and the trough viscosity. Throughout the manuscript, the term ‘breakdown’ refers to parameter derived from the pasting curves. Other terms shall be used to refer to the actual microstructural process of granule disruption (e.g. disintegration, abrasion, break up…). The cooled samples were recollected and stored for 24h in the refrigerator (5°C) for further analysis.

2.2.5 PARTICLE SIZE DETERMINATION

The particle size distribution of the cooled starch pastes was determined by laser light diffraction using a Malvern Mastersizer S (Malvern, UK) equipped with a 300mm reversed Fourier lens and a MSX-17 sample dispersion unit. To measure the starch particle size in the cold paste samples, 4g of paste was diluted to 20g with deionized water and gently shaken manually. Pumping and stirring speeds were put on 30% of the maximum values and the background was determined before each individual measurement. The optical model used was the 3OHD with real refractive index 1.5295 and 1.33 for starch and the continuous phase, respectively (Tecante & Doublier, 1999; Zhu *et al.*, 2009). The imaginary refractive index was set to 0.1.

2.2.6 FLOW CURVES OF COOLED PASTES

The flow curves of the cooled pastes were recorded using 40 mm cross hatched steel plate-plate geometry with solvent trap. To prevent drying of the sample, 1 ml of water was brought in the solvent trap compartment. The gap was set to 1000 µm. After 15 minutes of equilibration at 20°C, a steady state flow step was performed by logarithmically increasing the shear rate from 0.001 s^{-1} to 100 s^{-1}. The absence of wall slip was verified by comparing different gap sizes (1000, 2000 and 3000 µm) for some randomly selected samples as suggested by Barnes (1995).

At very low shear rates (< 0.01 s^{-1}) unreliable data is obtained, resulting from the sample not reaching steady state or signals below the transducer limit of the instrument and the corresponding stresses are believed to be lower than the yield stress (Walls *et al.*, 2003). Flow curves were fitted to the Herschel-Bulkley model with the SigmaPlot 10 software (Systat software inc., San Jose, USA).

$$\sigma_s = \sigma_0 + k.\dot{\gamma}^n \qquad \text{2-1}$$

In this equation, which relates the shear stress σ_s *(Pa)* with the shear rate $\dot{\gamma}$ (s^{-1}), the parameters σ_0 *(Pa)*, *k (Pa.s^n)* and *n (-)* represent the yield stress, the consistency index and the flow behavior index, respectively. All flow curves were fitted from shear rate 0.01 s^{-1} to 100 s^{-1}, except for the potato starch systems (0.1 s^{-1} to 100 s^{-1}) to obtain a better match with the model.

2.2.7 STATISTICAL ANALYSIS

IBM SPSS Statistics software (version 20, SPSS inc., Chicago, USA) was used for statistical comparison of the DSC and pasting data. All the reported values are the average of three replicates. Analysis of variance was carried out to determine significant differences between the results, followed by Tukey's post hoc test for pairwise comparisons. All tests were performed at a 95% significance level.

2.2.8 PRINCIPAL COMPONENTS ANALYSIS

Principal components analysis (PCA) is a mathematical method that transforms a number of possibly correlated variables into a number of uncorrelated variables, called principal components (PC). The central objective of PCA is reducing the dimensionality of the data without losing the original variability. These PCs are linear combinations of the original variables. The coefficients of the original variables in these linear combinations are chosen so that the first principal component accounts for as much of the variability in the data as possible and each succeeding component accounts for as much of the remaining variability as possible. Instead of working with all original variables, PCA can be performed and only the first two or three principal components can be retained in the subsequent analysis (Jolliffe, 2002).

PCA was executed with the SPSS 20 software (SPSS inc., Chicago, USA). A varimax rotation was performed. This additional orthogonal rotation of the principal components optimizes the orientation of the original variables, where each variable has a high loading on a single factor but near-zero loadings on the remaining factors. In this manner the interpretation of the PCs and the scorings is facilitated.

2.3 RESULTS AND DISCUSSION

2.3.1 XANTHAN TRANSITION

Already a low concentrations (> 0.1%), xanthan solutions exhibit marked rheological properties, as described in section 1.1.4. Hence, rheological measurements are sensitive tools to probe temperature induced conformational changes (Capron *et al.*, 1998b; Choppe *et al.*, 2010; Milas & Rinaudo, 1986). Temperature ramps can be imposed to the solutions to monitor the conformational change with oscillatory rheology. The transition temperature is accompanied by a reduction in both moduli, *G'* and *G"*, whereas the phase angle delta increases. The sudden drop in |*G**| was used to derive the transition temperature T_m (Figure 2-3). For high molecular weight samples at concentrations above the entanglement concentration c**, a drop in viscosity and elastic behavior is often observed upon heating above T_m (Capron *et al.*, 1998b; Choppe *et al.*, 2010; Pelletier *et al.*, 2001; Rochefort & Middleman, 1987; Sereno *et al.*, 2007). In ideal xanthan solutions and at low concentrations, double helical molecules convert into random coils. However at intermediate concentrations (0.1-1%), which are studied in this work, aggregates are formed that can mask the behavior of individual macromolecules (Camesano & Wilkinson, 2001). The intermolecular associations – which are stabilized by the helical conformation – are disrupted by additional heating above the denaturation temperature, which may explain the quite pronounced differences observed here. Furthermore, the intrinsic viscosity of the denatured (random coiled) xanthan is much more sensitive to salts than helical molecules (Muller *et al.*, 1986). Consequently, the transition could be accompanied by a reduction in hydrodynamic size of the polymers due to the presence of NaCl, which induces a further reduction in structural features (G', G*) and viscosity.

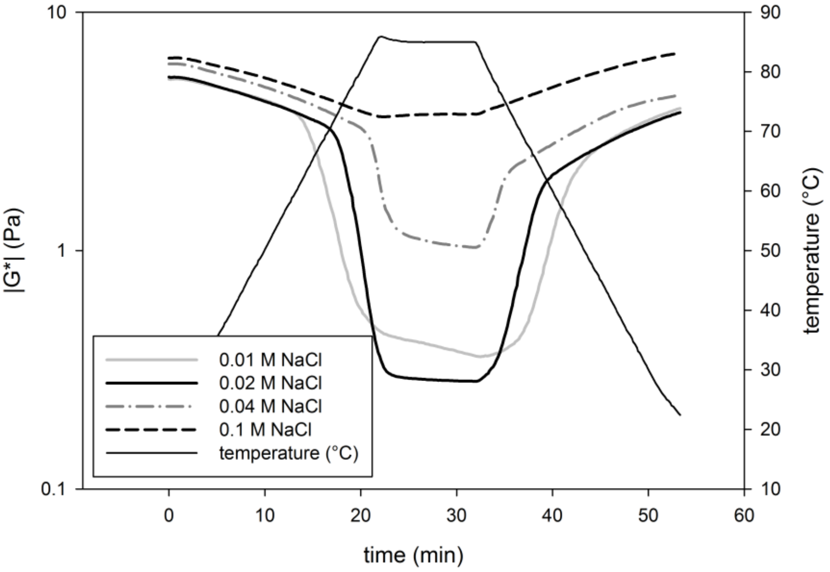

Figure 2-3: Influence of NaCl content on the conformational transition in a 0.4% (w/v) xanthan solution determined by oscillatory rheology. The conversion to random coil is accompanied by a marked reduction of the complex modulus |G*|.

These experiments were performed at two xanthan concentrations (0.2% and 0.4%) and at 5 salt concentrations (0.01, 0.02, 0.03, 0.04, 0.1M NaCl) and the results are summarized in

Table 2-1. As expected, the transition temperature is shifted to higher values when the salt content is increased (Muller *et al.*, 1986; Pelletier *et al.*, 2001). Salts shield the negative charges of the polymer molecules and hence the helical shape of the gum is stabilized, counteracting the thermal energy which forces the molecules to expand. Rheological data show that at a salt content of 0.04M the reduction of $|G^*|$ is limited, most likely because the dissociation is incomplete and/or a fraction of the xanthan molecules remains in the ordered state at 85°C. The transition temperatures do not increase linearly with increasing salt content, as the difference between T_m at 0.01M and 0.02M NaCl is larger than the difference between 0.02M and 0.03M. For the highest salt content, 0.1M, no transition could be observed rheologically within the studied temperature range. Our data reveal slightly higher transition temperatures at a xanthan concentration of 0.4%, although this could not be proven statistically. This effect might be explained by a slightly higher salt content, originating from the xanthan powder and/or by a slower heat transfer within a more viscous solution. Lee & Brant (2002c) state that in more concentrated solutions, the xanthan molecules themselves contribute to the ionic character of the solution, resulting in an increase of T_m.

Table 2-1: Transition temperature T_m (°C) as a function of xanthan concentration and salt content

NaCl (M)	0.2% xanthan	0.4% xanthan
0.01	60.0 ± 2.4 ^{A}	62.6 ± 1.6 ^{A}
0.02	69.6 ± 1.8 ^{B}	73.2 ± 0.4 ^{B}
0.03	77.0 ± 2.3 ^{C}	78.9 ± 0.6 ^{C}
0.04	80.8 ± 1.3 ^{C}	82.7 ± 0.8 ^{D}
0.1	>85	>85

Superscripts A-D indicate significant differences ($p<0.05$) between data within a same column

Flow curves of the xanthan solutions were compared at 20°C before and after the heating step (Figure 2-4). It is generally known that the highly branched, anionic nature of xanthan makes its hydrodynamic volume susceptible to the presence of salt, but the distinct effects depend on the xanthan concentration. At lower xanthan concentrations (approximately up to 0.2%), monovalent and divalent salts are reported to cause a decrease in viscosity. For higher concentrations the addition of salt results in a significant increase in viscosity (Wyatt *et al.*, 2011; Wyatt & Liberatore, 2009, 2010). At low xanthan concentrations, salt causes a screening of the anionic charges, leading to a lower hydrodynamic volume and viscosity. At higher xanthan contents and when charges are shielded, hydrogen bonds can be formed between molecules causing an increase in viscosity. On the contrary, in this setup, no remarkable differences in flow behavior of the unheated xanthan solutions could be observed between the different salt contents, not even at 0.4% (data not represented). It must be stated that in the before mentioned publications high salt contents (>0.1M) are compared with salt free systems in which xanthan gum might adopt a random coil conformation already at room temperature. Furthermore, preference was given here to a commercial xanthan sample, which is used as such in the food industry. No additional purification steps were performed, possibly causing less pronounced differences as compared with highly purified samples.

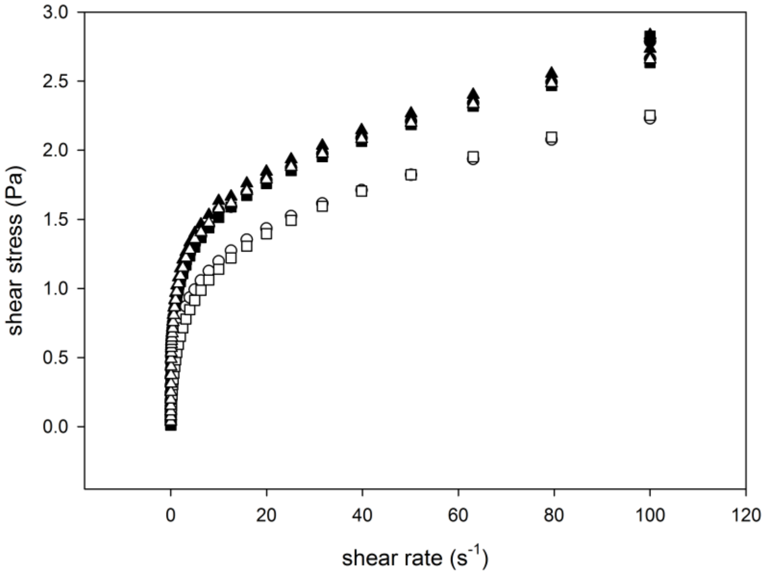

Figure 2-4: Influence of NaCl content (●:0.01M; ■: 0.03M; ▲0.1M) and heat treatment on the flow behavior of xanthan solutions (0.2%). Closed symbols: unheated; Open symbols: heated to 85°C.

However, after imposing a heat treatment, marked effects on the flow behavior of the xanthan solutions were observed, depending on the salt content. Except for the xanthan solutions with 0.1M NaCl, a marked viscosity reduction had taken place after heating and recooling. These results indicate that following a thermal transition, the molecular conformations and/or associations are different compared to those in the unheated solutions. Presumably, some of the molecular aggregates present in the stock solutions were disrupted in the additional heating step above T_m, whereas these associations are better preserved when no conformational transition takes place (Capron *et al.*, 1998b). In order to also incorporate these effects in the pasting experiments, both preheated as well as unheated xanthan solutions were used in combination with the starches.

2.3.2 INFLUENCE OF XANTHAN GUM ON THE GELATINIZATION PROPERTIES OF THE STARCHES

Two NaCl contents were selected for this setup: 0.01M and 0.1M. As indicated in the previous section, no xanthan transition occurs at the highest salt content, whereas a marked transition is observed for the lowest salt content. The temperature onset, peak and conclusion of gelatinization derived from the DSC experiments are summarized in Table 2-2. The gelatinization temperatures are markedly influenced by the salt content. For the samples with 0.1M NaCl, the gelatinization temperatures are shifted to higher values compared to those of the samples with 0.01M NaCl. On the other hand, the gelatinization enthalpy is not significantly influenced.

Salts can have divergent effects on the gelatinization behavior of starches, and the underlying mechanisms are only beginning to be unraveled. Explanations are now generally based on the Hofmeister theory, which states that the structure of water is modified by its solutes, like salts. The Hofmeister series ranks the relative influence of ions on the physical behavior of macromolecules (Chiotelli *et al.*, 2002; Zhang & Cremer, 2006; Zhu *et al.*, 2009). Salts in the upper end of the Hofmeister lyotropic series, called kosmotropes, or water structure makers, have strong electrostatic interactions with water molecules. They reduce the fraction of free water and increase the gelatinization temperature. On the other hand, ions with low charge densities, called chaotropes, or water structure breakers, are less hydrated and increase the fraction of free water by breaking or weakening hydrogen bonds. They decrease the gelatinization temperature. The salts which are located in the middle of the lyotropic series, like NaCl, show an increase of the gelatinization temperatures at low concentrations where higher concentrations induce a decrease.

Xanthan gum did not significantly affect the gelatinization temperatures and enthalpy of the different waxy starches. This conclusion was also drawn by other researchers (Chantaro & Pongsawatmanit, 2010; Samutsri & Suphantharika, 2012; Viturawong *et al.*, 2008). A reduction of the gelatinization enthalpy was reported by some authors (Aguirre-Cruz *et al.*, 2005; Chaisawang & Suphantharika, 2006; Viturawong *et al.*, 2008). However, their setups dealt with amylose-containing starches, which might behave differently than waxy starches. Others mention an increase of gelatinization temperatures, particularly in the case of high starch concentrations, when hydrocolloids are believed to restrict hydration of the granules (Aguirre-Cruz *et al.*, 2005; Tester & Sommerville, 2003). In general, it should be noted that the gelatinization of all starches investigated in this setup, is not influenced by the presence of xanthan gum and consequently not by the occurrence of the xanthan transition.

Table 2-2: Effect of xanthan addition and NaCl concentration on the gelatinization parameters of different starches at a ratio 5:100 (starch:continuous phase). The used xanthan solutions were subjected to heating (85°C) during their preparation

starch type	conc. NaCl (M)	xanthan	T_o (°C)	T_p (°C)	T_c (°C)	ΔH (J/g dry starch)
Maize	0.01	0%	67.03 ± 0.29^{A}	73.02 ± 0.06^{A}	78.68 ± 0.12^{A}	12.76 ± 1.28^{A}
		0.2%	67.28 ± 0.08^{A}	73.16 ± 0.09^{A}	78.93 ± 0.40^{A}	13.50 ± 1.00^{A}
	0.1	0%	70.04 ± 0.20^{B}	75.72 ± 0.19^{B}	81.00 ± 0.11^{B}	12.37 ± 0.33^{A}
		0.2%	70.29 ± 0.08^{B}	76.04 ± 0.18^{B}	81.53 ± 0.28^{B}	12.93 ± 1.04^{A}
Potato	0.01	0%	64.94 ± 0.22^{A}	70.53 ± 0.16^{A}	76.88 ± 0.21^{A}	12.75 ± 0.69^{A}
		0.2%	64.99 ± 0.13^{A}	70.64 ± 0.04^{A}	77.01 ± 0.13^{A}	13.59 ± 0.99^{A}
	0.1	0%	65.93 ± 0.23^{B}	71.34 ± 0.16^{B}	77.55 ± 0.21^{B}	12.15 ± 1.52^{A}
		0.2%	65.93 ± 0.17^{B}	71.43 ± 0.12^{B}	77.98 ± 0.19^{B}	13.35 ± 0.38^{A}
Rice	0.01	0%	61.07 ± 0.21^{A}	68.40 ± 0.13^{A}	74.92 ± 0.06^{A}	10.25 ± 0.09^{A}
		0.2%	60.80 ± 0.44^{A}	68.44 ± 0.25^{A}	74.07 ± 0.41^{A}	10.19 ± 1.11^{A}
	0.1	0%	64.17 ± 0.91^{B}	71.44 ± 0.23^{B}	77.91 ± 0.41^{B}	10.34 ± 1.70^{A}
		0.2%	64.47 ± 0.71^{B}	71.63 ± 0.39^{B}	77.36 ± 0.47^{B}	9.63 ± 0.95^{A}
Modified Maize	0.01	0%	62.01 ± 0.10^{A}	68.54 ± 0.08^{A}	74.31 ± 0.29^{A}	12.06 ± 0.16^{A}
		0.2%	61.73 ± 1.40^{A}	68.89 ± 0.54^{A}	75.31 ± 1.31^{A}	13.18 ± 1.43^{A}
	0.1	0%	64.86 ± 0.54^{B}	71.22 ± 0.16^{B}	77.02 ± 0.36^{B}	11.68 ± 0.98^{A}
		0.2%	65.43 ± 0.28^{B}	71.28 ± 0.18^{B}	77.59 ± 0.60^{B}	11.90 ± 0.27^{A}

For each starch type, superscripts A-B indicate significant differences within columns ($p<0.05$)

2.3.3 INFLUENCE OF XANTHAN TRANSITION ON THE PASTING PROPERTIES

The pasting curves of the different waxy starch systems were recorded at two NaCl contents (0.01M, 0.1M), in the presence and absence of xanthan gum, in order to derive the influence of the xanthan transition for each starch type. The derived peak viscosities and breakdown values are depicted in Figure 2-5. An overview of the different pasting parameters, comprising also the pasting temperatures and statistical analysis can be found in Table 2-3. Due to the absence of amylose, waxy starches exhibit a low pasting temperature, a high peak viscosity, little setback and low final viscosity (Wang *et al.*, 2009). In the current setup, pasting temperatures are mostly very close to the gelatinization onset temperatures. In the case of maize and potato starch, pasting seems to start even at lower temperatures than the gelatinization, but this is uncertain considering standard deviations on both parameters, and the different heating conditions in DSC (small volume, no shear) and starch pasting cell (large volume, with shear). DSC measurements demonstrated that -except for potato starch- the gelatinization temperature of all starches differed about 3-3.5°C between both salt contents, a difference that was also observed in the pasting temperatures of the xanthan free systems. It can also be concluded that the addition of xanthan gum did not significantly affect the pasting temperature. Shi & BeMiller (2002) proposed that hydrocolloids like xanthan gum can induce an advanced viscosity onset by associating with leached molecules. This effect is expected to be more pronounced for non-waxy starches, where some degree of amylose leaching might occur before the actual gelatinization. Although it cannot be proven statistically, a slightly higher pasting temperature is suggested for maize and potato starch in the presence of unheated xanthan at the lowest salt content. A similar delay for pasting of waxy maize starch was also observed by Achayuthakan & Suphantharika (2008) and Weber *et al.* (2009).

Table 2-3: Influence of xanthan gum and salt content on the pasting parameters of different starches at a ratio 5:100 (starch:continuous phase)*. The used xanthan solutions were either heated to 85°C during their preparation (indicated by 'H') or prepared without heating (unheated, indicated by 'UH').

Starch type	conc. NaCl (M)	xanthan	Peak viscosity (Pa.s)	Breakdown (-)**	Pasting temperature (°C)
Maize	0.01	0%	1.27 ± 0.01^{C}	0.52 ± 0.01^{C}	67.1 ± 0.0^{A}
		0.2% H	1.14 ± 0.01^{A}	0.36 ± 0.00^{A,B}	67.3 ± 0.4^{A,B}
		0.2% UH	1.15 ± 0.00^{A}	0.35 ± 0.00^{A,B}	68.4 ± 0.0^{B}
	0.1	0%	1.25 ± 0.02^{B,C}	0.49 ± 0.02^{C}	70 ± 0.7^{C}
		0.2% H	1.23 ± 0.00^{B}	0.34 ± 0.00^{A}	70 ± 0.0^{C}
		0.2% UH	1.28 ± 0.01^{C}	0.37 ± 0.01^{B}	70 ± 0.0^{C}
Potato	0.01	0%	2.18 ± 0.01^{C}	0.89 ± 0.01^{D}	63.6 ± 0.9^{A}
		0.2% H	1.56 ± 0.03^{A}	0.22 ± 0.03^{A}	63.7 ± 0.9^{A}
		0.2% UH	1.56 ± 0.02^{A}	0.22 ± 0.01^{A}	64.6 ± 0.6^{A}
	0.1	0%	1.93 ± 0.09^{B}	0.61 ± 0.06^{C}	64.9 ± 0.2^{A}
		0.2% H	1.97 ± 0.03^{B}	0.49 ± 0.03^{B}	64 ± 0.4^{A}
		0.2% UH	1.99 ± 0.01^{B}	0.49 ± 0.00^{B}	65.1 ± 0.1^{A}
Rice	0.01	0%	0.57 ± 0.01^{A}	N.D.	61.7 ± 0.6^{A,B}
		0.2% H	0.80 ± 0.00^{B}	N.D.	61.1 ± 0.0^{A}
		0.2% UH	0.79 ± 0.01^{B}	N.D.	62.2 ± 0.5^{A,B,C}
	0.1	0%	0.56 ± 0.01^{A}	N.D.	64.6 ± 0.0^{D}
		0.2% H	0.96 ± 0.01^{C}	N.D.	63.5 ± 1.0^{C,D}
		0.2% UH	1.04 ± 0.01^{D}	N.D.	63.0 ± 0.6^{B,C,D}
Modified Maize	0.01	0%	0.68 ± 0.01^{A}	N.D.	63.9 ± 0.3^{A}
		0.2% H	0.77 ± 0.01^{B}	N.D.	62.4 ± 0.6^{A}
		0.2% UH	0.76 ± 0.00^{B}	N.D.	63.6 ± 0.1^{A}
	0.1	0%	0.70 ± 0.01^{A}	N.D.	66.4 ± 0.3^{B}
		0.2% H	1.14 ± 0.00^{C}	N.D.	65.7 ± 0.4^{B}
		0.2% UH	1.24 ± 0.02^{D}	N.D.	66.0 ± 1.1^{B}

*For each starch type, superscripts A-D indicate significant differences within columns

** N.D. indicates parameters that were not detectable

Some representative pasting curves of the rice and native maize starch systems are depicted in Figure 2-6. Except for the potato starch system (not depicted), the pasting curves of the xanthan free systems exhibit a similar behavior at both salt contents. Nevertheless, this is strongly changed when xanthan is present. In all cases the peak viscosities of starch/xanthan systems with 0.01M NaCl are significantly lower than the corresponding systems with 0.1M NaCl. Furthermore, in the case of native maize and potato starch, peak viscosities of the xanthan containing systems are lower (0.01M) or similar (0.1M) to their gum free counterparts. This clearly demonstrates a strong influence of xanthan gum on the rheological properties of the mixed systems, but the exact effects differ between the different starch types. The most obvious explanation for the reduced peak viscosity observed in the potato and maize starch system would be a restricted swelling. However, this effect is unlikely as will be demonstrated by particle size determination (see section 2.3.4).

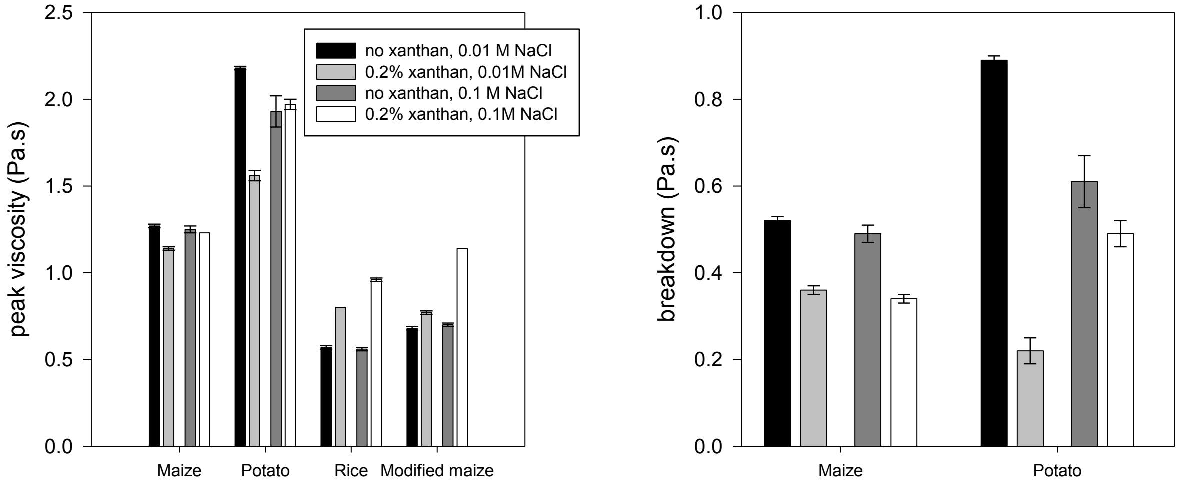

Figure 2-5: Effects of NaCl concentration and the presence of xanthan gum on the pasting parameters of the different starch types.

At least a partial explanation may be found in the xanthan transition. After converting to the random coil shape, the viscosity of the continuous xanthan phase is reduced. Logically more work is required to move granules past each other when the viscosity of the medium is higher. Because xanthan gum exhibits a lower viscosity in the random coil conformation, this might explain the differences between both salt contents of the mixed xanthan/starch systems. Assuming similar granule swelling in both xanthan free and xanthan containing media, this theory does not explain why peak viscosities can be higher in a xanthan free system. Therefore it is probable that xanthan modifies the manner in which particles interact or collide during pasting. It has been suggested that xanthan enwraps the granules as illustrated by Chaisawang & Suphantharika (2006) and Gonera & Cornillon (2002). This layer associated with the granules might act as a stabilizing, lubricating film, which lowers the interaction between the granules and hence the overall viscosity. However, the effects of xanthan gum on the flow properties during pasting will be treated more into detail in chapters 5 and 6.

For the potato starch system with the lowest salt content, the addition of xanthan causes a very marked reduction in peak viscosity (and overall viscosity during the whole pasting process). Probably, this cannot solely be ascribed to the occurrence of the xanthan transition. The distinct pasting behavior of potato starch/xanthan systems was previously attributed to an electrostatic repulsion (Cai *et al.*, 2011; Shi & BeMiller, 2002). It was stated that due to its high degree of phosphorylation, potato starch is slightly anionic, which could repel the anionic xanthan molecules. Similar effects were observed with phosphorylated corn starch (Shi & BeMiller, 2002) and anionic tapioca starch (Chaisawang & Suphantharika, 2006). However, it is unclear whether the altered pasting viscosities due to xanthan gum, originate from differences in swelling properties, an altered interaction during flow or a combination of both. Nevertheless, these effects appear particularly explicit at low salt contents. Presumably salts screen the negative charges and reduce the repulsion, hence diminishing the electrostatic influence on the overall flow behavior.

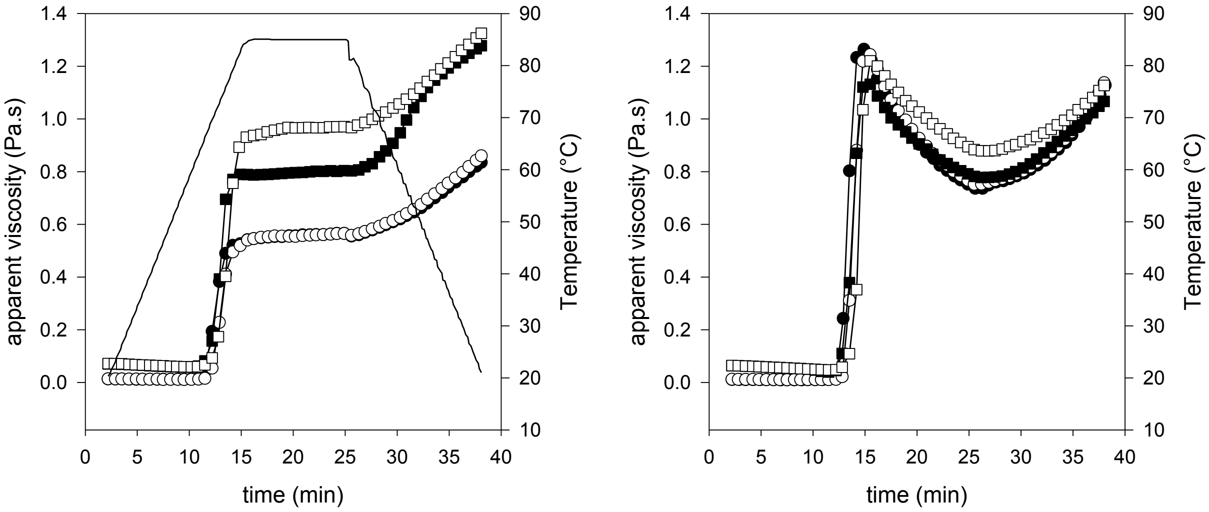

Figure 2-6: Pasting properties of waxy rice starch (L) and native waxy maize starch (R) as influenced by salt content and xanthan gum (● no xanthan, 0.01M NaCl; ○ no xanthan 0.1M NaCl, ■ 0.2% xanthan 0.01 M NaCl; □ 0.2% xanthan 0.1 M NaCl).

For modified maize and rice starch, the presence of xanthan gum caused more pronounced effects as in this case the viscosity during pasting was markedly increased (Figure 2-5). Hence, there is a higher direct contribution of the xanthan gum to the overall viscosity of the system. For the system with 0.01M NaCl the viscosity during pasting was significantly lower, which could again be caused by the xanthan transition. Furthermore, the difference in viscosity of the preheated and the unheated xanthan solutions also became apparent in the pasting viscosities at the highest salt content (see annex II).

Breakdown was not observed in the case of rice or modified maize starch, but this parameter was relatively high for native maize and potato starch. Furthermore, in the xanthan free potato starch systems, this parameter was significantly higher at the lowest salt content, whereas there was no significant salt effect in the native maize starch systems. On the other hand, the presence of xanthan gum markedly reduced the breakdown for both maize and potato starch, which could indicate a reduced degree of granule disruption. However, breakdown values calculated from pasting data should be interpreted cautiously, because the viscosity (hence also viscosity differences) is not solely governed by the starch granules. These phenomena shall be tackled more into detail in the following chapters.

2.3.4 PARTICLE SIZE DISTRIBUTION

The particle size distributions of the pastes were determined 24h after preparation in the starch pasting cell. Table 2-4 summarizes the derived volume weighted equivalent diameters D[4,3]. The average dimensions of pasted starch granules are generally influenced by two phenomena: granule swelling and granule disruption. Pasting data of modified maize starch and rice starch showed no breakdown during pasting, therefore the first effect is assumed to be predominant in these cases. Modified maize starch seems to be only slightly influenced by the presence of xanthan gum and salts whereas rice starch swelling appears to be inhibited by xanthan gum, as well as by salt. Rice starch granules have a low swelling power, and are often present as associated granules in the raw starch powder. These agglomerated granules dissociate when they start to swell. For this starch type the water binding properties of xanthan gum might restrict the water imbibition of the rice starch granules.

Table 2-4: Volume weighted equivalent diameters D[4,3] (µm) of the pastes with different starch types as influenced by salt concentration and xanthan content.

		D[4,3]			
Conc. NaCl (M)	xanthan	maize	potato	rice	modified maize
0.01	0%	29.9 ± 0.5^{A}	143.8 ± 0.0^{C,D}	24.0 ± 0.3^{D}	40.1 ± 1.5^{A}
	0.2% H	37.8 ± 2.0^{C}	145.4 ± 1.8^{C,D}	21.0 ± 0.3^{B}	41.6 ± 1.0^{A}
	0.2% UH	36.1 ± 0.4^{C}	149.1 ± 1.5^{D}	20.8 ± 0.4^{B}	41.8 ± 1.0^{A}
0.1	0%	30.1 ± 1.4^{A}	131.0 ± 0.1^{A,B}	22.2 ± 0.5^{C}	39.9 ± 1.4^{A}
	0.2% H	32.7 ± 0.3^{B}	128.2 ± 4.3^{A}	19.5 ± 0.3^{A}	40.1 ± 0.4^{A}
	0.2% UH	32.6 ± 0.1^{B}	139.6 ± 3.8^{B,C}	19.5 ± 0.3^{A}	40.1 ± 0.1^{A}

For each starch type, superscripts A-B indicate significant differences within columns ($p<0.05$)

The diameters of the maize starch appeared to be clearly higher when xanthan gum was present. When combining these findings with the lower breakdown derived from the pasting curves, it could be hypothesized that xanthan gum restricts the disruption of these granules. The lowest salt content resulted in the highest average diameters for the xanthan containing system, which can suggest an additional beneficial effect of the xanthan transition. Furthermore, because of these higher diameters, the hypothesis of a more restricted swelling caused by xanthan gum seems more unlikely. On the other hand it cannot be fully excluded because the average diameters are always the result of combined swelling and breakdown effects, whereby it is difficult to distinguish between both phenomena. Nevertheless, the observed lower pasting viscosities associated with the xanthan transition, are most probably not due to restricted swelling. This effect was also observed for the modified maize starch pastes, where the particle size distributions demonstrated that there is no effect of salts and xanthan gum on the granule size. For the potato starch systems, there is no significant effect of xanthan gum. The size of these granules is primarily influenced by the salt content as such, where increasing the NaCl concentration to 0.1M leads to a significant reduction in average diameter. Furthermore, it should be remarked that the diverging pasting results caused by xanthan, strongly contrast with the limited differences observed in the particle size distributions of potato starch.

2.3.5 FLOW CURVES OF STARCH PASTES AFTER COOLING

Some characteristic flow curves of the pastes recorded after 1 day of cold storage are represented in Figure 2-7. The derived Herschel-Bulkley parameters of all systems are summarized in Table 2-5. The samples are shear thinning, because the flow behavior index of all pastes was <1. The upward curvature, which is depicted in the graph at higher shear rates, is due to the logarithmic scaling of the shear rate axis. When the data of the different systems are compared, it is clear that the presence of xanthan gum causes a more distinct change in flow behavior of the rice starch and the modified maize starch systems. Comparable observations were made regarding the viscosity differences during pasting. For these starch types, breakdown was not observed during pasting and the pastes are expected to consist largely of intact granules. For the rice and modified maize starch the increase of yield stress and consistency index by the addition of xanthan cannot be attributed to an enhanced swelling of the granules, as demonstrated by particle size distributions. In the case of rice starch even a reduction of the average granule diameter was observed. Therefore, the higher values of these parameters are most likely induced by direct effects of the xanthan gum. The presence of xanthan gum could require a higher shear stress for flow initiation and hence a higher yield stress, due to the presence of molecular entanglements. Furthermore, Abdulmola *et al.* (1996b) suggested that even at relatively low concentrations, swollen starch granules interact and that this interaction can be further enhanced by xanthan gum through the mechanism of depletion flocculation: as two particles approach each other, a point will be reached at which surrounding polymer molecules will be excluded from the intervening gap, creating a region of lower concentration and hence a lower osmotic pressure which forces the two granules together.

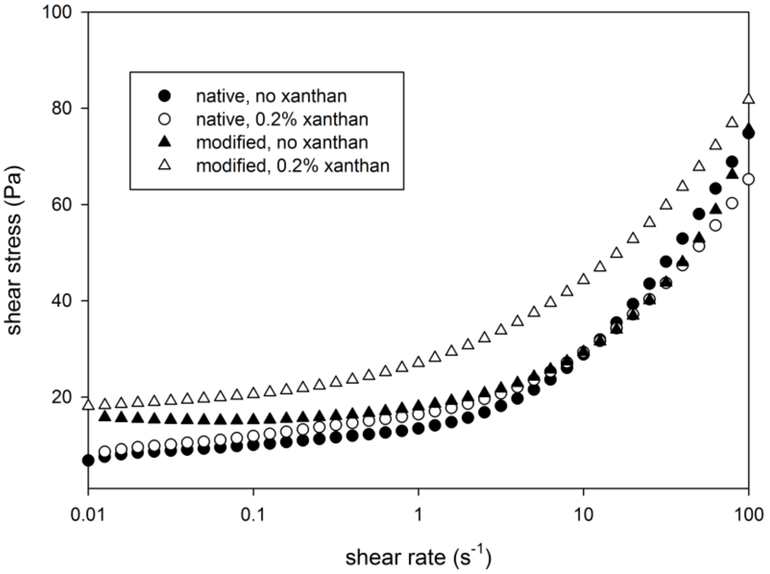

Figure 2-7: The effect of xanthan addition on the flow curves (20°C) of modified maize and native maize starch pastes containing 0.01M NaCl (starch:solvent ratio = 5:100).

Preheating the xanthan solutions generally resulted in limited effects on the rheological properties of the cooled pastes. As mentioned above, the viscosity of the (starch free) unheated xanthan samples is higher than the viscosity of the heated solutions. At the highest salt content, when no transition can occur, the stabilizing action of the ions should preserve this difference during pasting. Nevertheless, this effect fades in the presence of starch, as indicated by the comparable flow curves of starch pastes containing either unheated or preheated xanthan.

The interpretation of the flow behavior of the native maize and potato starch systems is more complex. For these systems some marked differences in granule sizes were induced by the presence of xanthan gum. Nonetheless, it appears that the effects of xanthan gum on the final rheological behavior of these starches were rather limited. It can be assumed that despite the presence of more intact and/or larger granules, the majority of the granules is still disrupted and the remaining ones are highly swollen and consequently have lost their rigidity.

Microstructurally these systems can be described as still intact granules and granule remnants present in a continuous watery phase containing dissolved amylopectin and xanthan molecules. Hermansson & Svegmark (1996) stated that the rheological behavior of overcooked starch pastes is dominated by the continuous phase. The flow properties of such a macromolecular solution are very complex and governed by the phase behavior of both polymers. Unfortunately, there is little or no direct evidence available regarding the phase behavior of amylopectin and xanthan molecules, that could help explaining these phenomena.

Table 2-5: Influence of xanthan gum and salt content on the Herschel-Bulkley parameters fitted to the flow curves of the cooled pastes (20°C) at a ratio of 5:100 (starch:continuous phase). The used xanthan solutions were either heated to 85°C during their preparation (indicated by 'H') or prepared without heating (unheated, indicated by 'UH').

Starch type	NaCl (M)	xanthan	σ_0 (Pa)	k (Pa.s^n)	n (-)	R²
Maize	0.01	0%	7.22 ± 0.23	6.83 ± 0.23	0.505 ± 0.008	0.997
		0.2% H	8.48 ± 0.21	7.81 ± 0.22	0.433 ± 0.006	0.998
		0.2% UH	8.09 ± 0.35	7.34 ± 0.39	0.415 ± 0.011	0.992
	0.1	0%	6.17 ± 0.37	7.94 ± 0.38	0.468 ± 0.010	0.994
		0.2% H	3.86 ± 0.42	13.36 ± 0.47	0.326 ± 0.007	0.996
		0.2% UH	4.18 ± 1.06	15.09 ± 1.19	0.307 ± 0.016	0.981
Potato	0.01	0%	24.82 ± 0.84	6.86 ± 0.69	0.508 ± 0.022	0.987
		0.2% H	25.21 ± 0.36	7.32 ± 0.32	0.460 ± 0.009	0.998
		0.2% UH	24.36 ± 0.49	6.69 ± 0.43	0.453 ± 0.013	0.994
	0.1	0%	27.17 ± 0.91	7.69 ± 0.76	0.491 ± 0.021	0.987
		0.2% H	31.81 ± 0.83	7.78 ± 0.74	0.432 ± 0.020	0.988
		0.2% UH	32.59 ± 0.65	6.33 ± 0.57	0.455 ± 0.019	0.990
Rice	0.01	0%	10.64 ± 0.34	4.88 ± 0.33	0.504 ± 0.015	0.988
		0.2% H	12.01 ± 0.22	12.93 ± 0.25	0.344 ± 0.004	0.999
		0.2% UH	11.92 ± 0.09	11.61 ± 0.11	0.352 ± 0.002	0.999
	0.1	0%	7.89 ± 0.27	4.50 ± 0.27	0.498 ± 0.014	0.990
		0.2% H	11.71 ± 0.78	12.13 ± 0.88	0.370 ± 0.015	0.983
		0.2% UH	12.30 ± 0.42	11.93 ± 0.47	0.357 ± 0.008	0.995
Modified Maize	0.01	0%	14.97 ± 0.08	3.34 ± 0.06	0.627 ± 0.004	0.999
		0.2% H	15.40 ± 0.17	11.80 ± 0.18	0.377 ± 0.003	0.999
		0.2% UH	15.99 ± 0.16	11.50 ± 0.17	0.381 ± 0.003	0.999
	0.1	0%	16.61 ± 0.11	3.70 ± 0.09	0.634 ± 0.005	0.999
		0.2% H	18.28 ± 0.26	12.11 ± 0.28	0.409 ± 0.005	0.998
		0.2% UH	19.67 ± 0.28	13.05 ± 0.31	0.388 ± 0.005	0.997

2.3.6 CLUSTERING OF THE STUDIED PASTES BY PRINCIPAL COMPONENTS ANALYSIS

Throughout this setup, large differences in the derived analytical parameters were observed, depending on the type of starch that was used. In order to get an overview of the variability between the different starches and compositions, PCA was performed on the characteristics derived from pasting (peak viscosity, trough viscosity, breakdown), laser light scattering (D[4,3]) and flow experiments (σ_0, k, n). Because the main focus of this dissertation lies on the (micro-)structural properties, gelatinization and pasting temperatures were not included in this analysis to facilitate the interpretation. Half of the samples (modified maize, rice) exhibited a breakdown equal to 0, this parameter was removed from the PCA, leading to a higher explanation of the total variance by PC1 and PC2 (58.67% and 32.67% respectively). Figure 2-8 represents the score and loading plots for the first two principal components. The loading plot illustrates how the original variables contribute to both principal components. The first PC is governed by the yield stress, the pasting properties and the average granule diameter. These properties can be grouped as swelling and degradation characteristics. PCA confirms the hypothesis that the yield stress is strongly related to the granule diameter. There is also a logical correlation between peak and trough viscosity. The flow parameters k and n determine the second PC and appear inversely correlated, which is expected considering the Herschel-Bulkley equation.

The lower part of the scoring plot contains the samples with xanthan gum (closed symbols), which corresponds with their stronger shear thinning effect (= lower n-value) and higher consistency index k. The graph depicts the aforementioned differences between the starch types more graphically: there is a general similarity between rice starch and modified maize starch. The distinctively larger granule size starch and the corresponding pasting properties, separate the potato starch systems from the other types (PC1). However, their flow properties (PC2) resemble the native maize starch systems (except for 0.1M NaCl with xanthan). Furthermore, the presence of xanthan gum induces very little variation among the potato starch samples. The latter conclusion also holds for the maize starch at a salt content of 0.01M. As stated above, both maize and potato starch granules are prone to degradation, resulting in large amounts of amylopectin in the continuous phase, which could explain the analogies between both types. Conversely, modified maize and rice starch exhibit distinct properties. Their pastes were characterized by a high extent of granule preservation, and can therefore be considered as true swollen starch dispersions. In particular the presence of xanthan gum markedly influenced these pastes, which is reflected in large changes in flow properties (PC2).

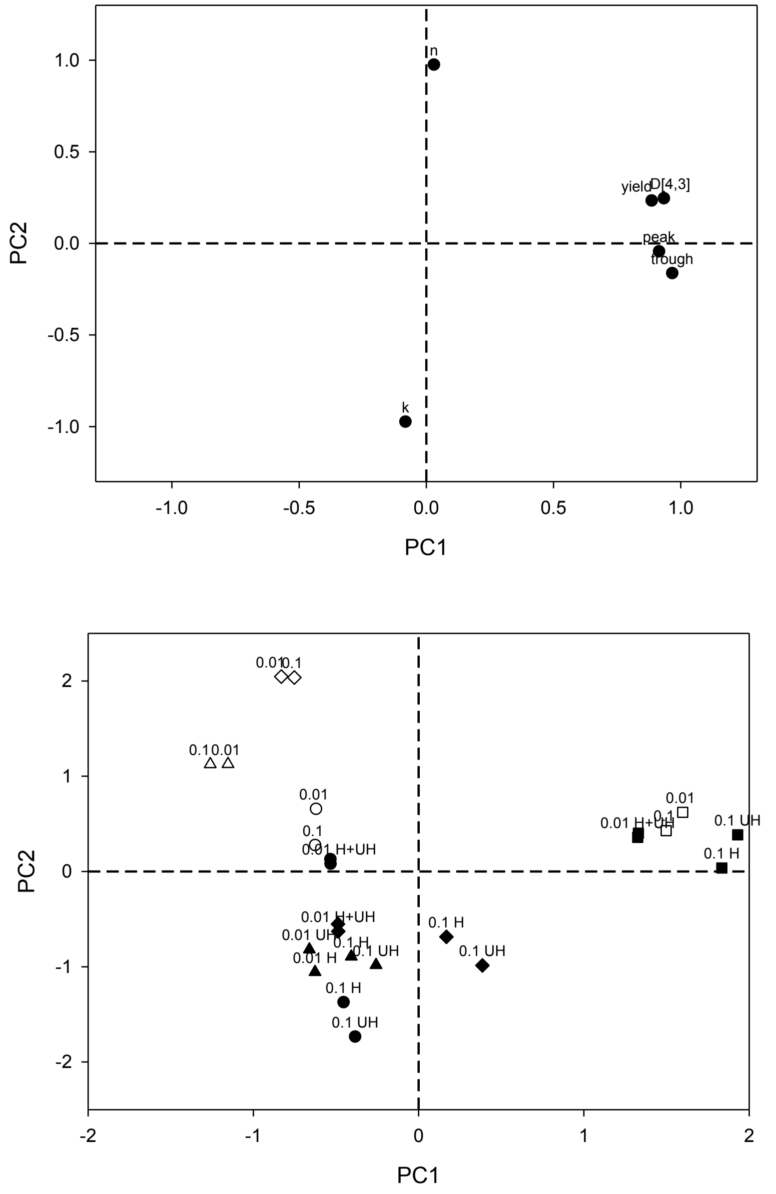

Figure 2-8: Loading (top) and score plots (bottom) of the first two principal components (PC), visualizing the variability among the different starch pastes. The analysis is based on parameters derived from pasting (peak and trough viscosity), flow curves (yield stress, consistency index k and flow behavior index n) and particle size distributions (D[4,3]). Symbols used in score plot: ● native maize; ■ potato; ▲rice; ◆ modified maize. Open symbols: without xanthan, closed symbols: with xanthan.

2.4 CONCLUSIONS

This chapter described the influence of xanthan on the properties of waxy starches, with special focus on the effects of the conformational transition. Different types of waxy starches were assessed within the same setup, in order to develop a more generalized comprehension of these systems. The unique aspects of this work allowed to generate insights that can help understand some of the discrepancies found in literature.

At the investigated concentrations, the xanthan transition did not influence the gelatinization of waxy starches but it clearly affected the pasting behavior. When starch/xanthan systems were heated above the xanthan transition temperature, the conformational change of xanthan in the continuous phase gave rise to reduced pasting viscosities. However, the effect of this transition is not directly noticeable in the flow behavior of the pastes after cooling.

Furthermore, xanthan gum appears capable of reducing breakdown of shear sensitive waxy starches (native maize, potato). This stabilizing action might be enhanced by the xanthan transition but further research is required to confirm this. Nevertheless, the possible granule protecting effect of xanthan gum only had a limited effect on the flow behavior after cooling. Most likely, the majority of the granules is broken down under these pasting conditions, even in the presence of xanthan gum. Therefore these pastes behave as macromolecular solutions, whose flow behavior is dominated by the dissolved starch fraction.

The specific effects of xanthan gum on the flow properties of the systems, during pasting but also after cooling, strongly depended on the type of starch. Whereas its addition at the concentrations used here only caused slight (relative) changes in the native maize and potato starch systems, xanthan gum had a large influence on the flow behavior of the starches with a large extent of granule preservation (modified maize, rice). Therefore granule integrity appears to be a prerequisite for optimal xanthan functionality.

The fragile nature of native waxy maize and potato starches is clearly their main technological disadvantage. A better preservation of their granular structure would not only result in better sensory properties, it might also lead to improved synergies with xanthan gum. In the following chapter, it will be attempted to better protect the granules during processing, by lowering the heating temperatures.

3 PROCESSING OF WAXY STARCH/XANTHAN GUM MIXTURES WITHIN THE GELATINIZATION TEMPERATURE RANGE

Relevant publication: Heyman, B., Depypere, F., Van der Meeren, P., Dewettinck, K. (2013). Processing of waxy starch/xanthan gum mixtures within the gelatinization temperature range. Carbohydrate Polymers, 96 (2), 560-567.

3.1 INTRODUCTION

When starch granules are heated in excess water, they undergo gelatinization. During this process, the hydrogen bonds in amorphous regions are disrupted and the internal order in the granules is lost. Water, which acts as a plasticizer, is absorbed and causes swelling of the starch granules. The process of pasting follows gelatinization and occurs with continued heating and shearing of starch granules in the presence of excess water. During this step, granule swelling proceeds, amylose leaches from the granules and some of the fragile, swollen granules are disrupted. The resulting paste consists of a dispersed phase of swollen granules, granule ghosts, and granule fragments within a continuous aqueous phase of dissolved starch polymer molecules (BeMiller, 2011; Hermansson & Svegmark, 1996). When granule degradation becomes predominant, undesired textures are formed and the rheological properties are governed by the continuous phase (Hermansson & Svegmark, 1996). In food products such as sauces and puddings containing many broken starch granules, the texture becomes long or slimy. Conversely, it is generally known that sufficiently swollen starch granules, with limited breakdown, yield products with a good sensory perception.

The swelling of starch granules becomes significant when heated above the gelatinization temperature (Choi & Kerr, 2004; Jacquier *et al.*, 2006; Li & Yeh, 2001; Zhu *et al.*, 2009). In food production processes, heating is usually performed at more elevated temperatures (>85°C) which can be advisable to impart microbial stability. However, these temperatures are not necessarily optimal for starch functionality, particularly because starch degradation might occur. Therefore, in most commercial applications cross-linked starches are used, which can withstand or even require more elevated temperatures and higher levels of shearing. Few studies suggest that when heated at temperatures slightly higher than the gelatinization temperature, granule swelling is incomplete, but their rigidity is preserved (Bagley & Christianson, 1982; Jacquier *et al.*, 2006; Mandala & Bayas, 2004; Rao *et al.*, 1997). However, these setups are mostly restricted to static heating procedures (no shear) at low starch concentrations to determine the swelling power and polymer leaching as a function of different heating temperatures. On the contrary, little information is available regarding the actual pasting behavior of (native) starches under these conditions and how it affects the final properties of the resulting systems. Particularly for native waxy starches, which are extremely sensitive to thermal breakdown, it is a great challenge to preserve their granular integrity during production processes. It should therefore be interesting to know whether the use of mild temperatures can result in improved performance of the waxy starch granules.

When heated together, food gums in general (see section 1.3.2) and xanthan gum in particular are known to affect the granule swelling and degradation during pasting. At high starch contents swelling of the starch is reduced in the presence of xanthan, probably as a consequence of restricted water availability (Kruger *et al.*, 2003; Song *et al.*, 2008; Song *et al.*, 2006; Tester & Sommerville, 2003; Weber *et al.*, 2009). At lower starch concentrations (<6%) the granule swelling is sometimes enhanced by xanthan gum (Chaisawang & Suphantharika, 2006; Mandala & Bayas, 2004; Samutsri & Suphantharika, 2012). Shi & BeMiller (2002) attributed this to an interaction between xanthan and amylose in the continuous phase, causing increased amylose leaching, which in turn leads to a higher water absorption. It should also be remarked that, when swollen to higher dimensions, the granules become more vulnerable to disruption (BeMiller, 2011). In anionic starches an opposite effect was observed due to the repelling forces between the xanthan molecules and the starch polymers, leading to reduced swelling and lower viscosities (Cai *et al.*, 2011; Shi & BeMiller, 2002). Xanthan gum is also reported to reduce the breakdown during pasting (Chaisawang & Suphantharika, 2006; Samutsri & Suphantharika, 2012; Sikora *et al.*, 2008b; Song *et al.*, 2006; Weber *et al.*, 2009). Possibly, this can be related to its ability to enwrap the surface, hence stabilizing the granule (Abdulmola *et al.*, 1996b; Achayuthakan & Suphantharika, 2008; Achayuthakan *et al.*, 2006; Gonera & Cornillon, 2002).

In the preceding chapter, it was demonstrated that waxy maize and potato starches are easily disrupted during heating, even when a mild shear rate (50 s^{-1}) is imposed. Furthermore, it was found that for these starches, the addition of xanthan gum can result in larger granule sizes. However, this effect was not noticeable in the final rheological properties because granule breakdown was abundant in all systems and the rheological properties were dominated by the amylopectin moiety present in the continuous phase. The purpose of this experimental setup was to investigate whether the use of temperatures within the gelatinization range, along with the addition of xanthan gum, could lead to a more controlled swelling and a more limited breakdown of the native starch granules. In a first step the optimal preparation temperatures were derived by DSC. Secondly, pasting experiments were performed at the selected temperatures and at two different shear rates (50 s^{-1} and 150 s^{-1}). The use of the starch pasting cell, mounted to a controlled stress rheometer offers the opportunity to work at accurately controlled heating and shearing conditions. Due to the sensitivity of this system small differences during the pasting process can be monitored. The same samples were stored overnight and further characterized by means of laser light scattering and rheology (flow curves).

3.2 MATERIALS AND METHODS

3.2.1 MATERIALS

The same type of xanthan gum, native waxy maize starch and waxy potato starch was used as described in the preceding chapter. Because both starch types are from a waxy variety the denomination 'waxy' will further not be repeated throughout the chapter. The preparation of the xanthan gum solutions (0.2% w/v) occurred in a similar manner as described in paragraph 2.2.2.

3.2.2 STARCH/XANTHAN SYSTEMS

Starches were dispersed at room temperature in salt solutions of 0.01M NaCl and 0.1M NaCl or in xanthan solutions (0.2% w/v) containing either 0.01M NaCl or 0.1M NaCl. Samples from this premix were either transferred to DSC-pans or to the starch pasting cell. The starch:solvent ratio (w:w) was always 5:100, except for the last part of the experimental setup where ratios of 3:100 and 7:100 were used as well.

3.2.2.1 DSC measurements

The gelatinization properties of the different systems have been derived in section 2.3.2. The total enthalpy of the gelatinization is denoted as ΔH_{tot}. Within the same starch type, the ΔH_{tot} of the different compositions were not significantly different (α=0.05), as verified by ANOVA (see section 2.3.2). Therefore, one single averaged value of ΔH_{tot} was calculated for each starch type.

Isothermal gelatinization was performed by heating (3°C/min) to the desired setpoint temperature and holding this isothermally for 10 minutes (Figure 3-1). Next a rapid cooling step (20°C/min) to 45°C was introduced and after holding for 5 minutes, the remaining gelatinization was determined by heating to 99°C at a ramp of 3°C/min. The enthalpic transition during this second ramp is denoted by ΔH_{ungel}. The fraction of the starch that did not gelatinize during the isothermal step was quantified as $\Delta H_{ungel}/\Delta H_{tot}$ (assuming no recrystallization).

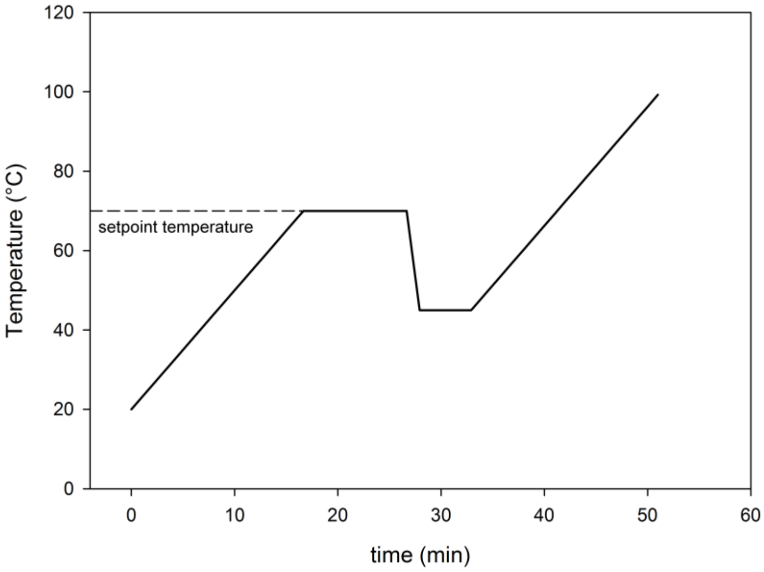

Figure 3-1: Temperature profile imposed during DSC-measurements for quantification of the starch fraction that remains ungelatinized after an isothermal step at the setpoint temperature

3.2.2.2 Pasting experiments

The pasting behavior was studied using the starch pasting cell conformation of the AR2000 rheometer (TA Instruments, New Castle, USA). Starch suspensions were presheared at 100 s^{-1} for 2 minutes and then heated to the desired holding temperature (67.5, 70 or 72.5°C) at a heating rate of 3°C/min, held isothermal for 10 minutes and then cooled down to 20°C (5°C/min). Throughout the heating and cooling steps a shear rate of either 50 or 150 s^{-1} was imposed. The peak viscosity was attained during the heating or the isothermal step, depending on the setpoint temperature. In many cases, no true peak was observed as the viscosity kept continuously increasing. The reported peak viscosity then corresponds with the maximum viscosity which is attained at the end of the isothermal step. The relative breakdown was calculated as the difference between the peak viscosity and the viscosity at the end of the isothermal step, divided by the peak viscosity (expressed as percent). Throughout the manuscript, the term ‘breakdown’ refers to parameter derived from the pasting curves. Other terms shall be used to refer to the actual microstructural process of granule disruption (e.g. disintegration, abrasion, break up…).

The cooled samples were recollected and stored for 24h in the refrigerator (5°C) for further analysis. The pasting data were statistically compared by ANOVA and Tukey's post hoc test as described in §2.2.7

3.2.3 *ANALYSIS OF THE COLD PASTES*

Flow curves and particle size distributions of the cold pastes were performed as described in section 2.2.6 and section 2.2.5, respectively.

3.2.4 *CONFOCAL SCANNING LASER MICROSCOPY (CSLM)*

Stock solutions of rhodamine B (Sigma-Aldrich, Diegem, Belgium) reagent were prepared by dissolving the right amount (0.2 w/v%) in distilled water (Nagano *et al.*, 2008). To prepare the stained samples, 20 µl of rhodamine stock solution was dropped onto to glass bottom dishes (MatTek corp., MA, USA). Subsequently approximately 200 mg of paste was added. Paste samples were covered and stored for at least 2h at 20°C to allow diffusion of the dye into the system.

The samples were examined under a confocal microscope (Nikon A1R; Nikon Instruments Inc., Paris, France), using a 40x/1.4 oil Plan Apo objective. A multi-line Ar laser was used for excitation (562 nm) and fluorescence was detected with a 595/50 nm bandpass filter. The pinhole was set to 1 A.U. Digital image files were acquired at a resolution of 0.41µm/pixel and annotated using FIJI, a packaged version of ImageJ freeware (Rasband, W.S., ImageJ; US National Institutes of Health, Bethesda, MD, http://www.fiji.sc).

3.3 RESULTS AND DISCUSSION

3.3.1 *DETERMINATION OF PROCESSING TEMPERATURES AND ISOTHERMAL GELATINIZATION*

The setpoint temperatures (i.e. temperatures of the isothermal heating step) for the pasting experiments were based on the previously determined gelatinization characteristics (section 2.3.2). The intention is to use temperatures as low as possible, but which still allow swelling of the granules, i.e. gelatinization should still take place. For the maize starch system, gelatinization was not influenced by the xanthan content, as there were no statistical differences between the gelatinization temperatures and gelatinization enthalpy of the samples when heated in a continuous ramp to 99°C. Between the two NaCl contents there is a difference in gelatinization temperatures of about 3°C. The average temperature between the gelatinization onset and the gelatinization peak of the systems at 0.01M NaCl and 0.1M NaCl, i.e. 70°C and 72.5°C respectively, were chosen as processing temperature for the isothermal step. In order to control the size of the setup, only discrete temperature steps of 2.5°C were considered.

The fraction of the starch that remained ungelatinized was quantified by DSC. For the maize starch, these experiments revealed that after heating at 70°C for 10 minutes, about 11% of the starch is ungelatinized for the xanthan free system and 17% for the xanthan containing system at the lowest salt content (Figure 3-2). This illustrates that particularly under these low temperature conditions xanthan gum might affect the gelatinization process, for example by slowing down water diffusion into the starch granules. At the highest salt content (0.1M), the larger part of the granules remained ungelatinized (±63%) at this temperature. The gelatinization occurs over a quite broad temperature range, and the preceding isothermal step has thus caused a fractionation between the granules gelatinizing at the lowest temperatures and the ones gelatinizing at the higher temperatures. After an isothermal step at 72.5°C, the systems with a salt content of 0.01M were fully gelatinized, whereas approximately 20% remained ungelatinized in the presence of 0.1M NaCl.

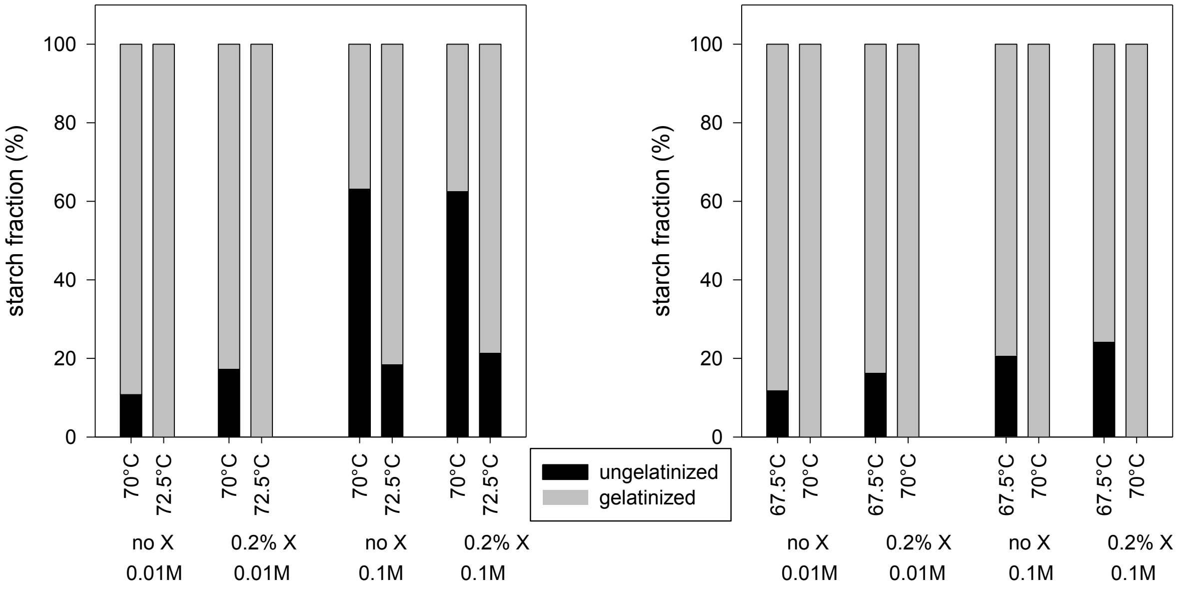

Figure 3-2: Influence of xanthan (X) concentration and NaCl (0.01M, 0.1M) content on the degree of gelatinization after heating for 10 min to temperatures within the gelatinization range, as determined by DSC-measurements. Left: maize starch, right: potato starch

For the waxy potato starch, it has been demonstrated that the differences in salt content have a less strong effect on the gelatinization temperatures, only a slight shift of less than 1°C was detected when increasing the salt content from 0.01 to 0.1M (section 2.3.2). A temperature of 67.5°C was chosen as isothermal processing temperature, along with 70°C. All samples appeared to be fully gelatinized after an isothermal step at 70°C of 10 minutes, but this was not the case when heated at 67.5°C. For the xanthan free system 12% of the starch was ungelatinized at the lowest salt content and 22% for the systems with 0.1M NaCl. In the case of the xanthan containing dispersions, this was 16% and 24%, respectively.

3.3.2 INFLUENCE OF PROCESSING CONDITIONS ON PASTING BEHAVIOR

Native waxy starches swell quickly when heated above the gelatinization temperature (Jacquier *et al.*, 2006; Schirmer *et al.*, 2013). This rapid swelling which leads to large granule sizes, is at least partially responsible for their high shear sensitivity. The selected processing temperatures in this setup were kept as closely as possible to the gelatinization temperature range to avoid excessive swelling and consequently rupture of the granules. Furthermore, the heating rate was kept relatively low (3°C/min) to allow an equal temperature distribution all over the sample and to avoid local temperature overshoot. In this manner, it was possible to work at different degrees of gelatinization as demonstrated in the preceding section. Pasting experiments were performed at two different shear rates (50 s^{-1} and 150 s^{-1}). At too low shear rates, sedimentation of starch granules could occur, particularly in the xanthan-free systems. High shear rates (>200 s^{-1}) appeared to be too destructive for some of the samples.

Figure 3-3 depicts the pasting behavior of the maize starch systems at a temperature of 72.5°C and a shear rate of 150 s^{-1}. Peak viscosities and breakdown derived from the different pasting experiments are represented in Table 3-1. For maize starch it is clear that the limited amount of gelatinization of the samples with 0.1M NaCl at 70°C led to a largely incomplete swelling of the starch granules, as illustrated by the low viscosities. For the lowest salt contents a significant viscosity increase indicated a fair extent of granule swelling at this temperature. When processed at a shear rate of 50 s^{-1} no breakdown was exhibited (i.e. no peak was observed in the curve), and the xanthan containing sample did not even show breakdown at the highest shear rate. Conversely, when pasting was performed at 72.5°C, all samples at the lowest salt content exhibited breakdown. However, this parameter was clearly lower when xanthan was present. At this temperature, the swelling within the samples containing 0.1M resulted in a siginificant viscosity increase. When sheared at 50 s^{-1} no equilibrium viscosity was attained during the isothermal step. However, plateau values were recorded at a shear rate of 150 s^{-1}. Similar to the processes at 70°C, there was significantly less breakdown of the systems when xanthan gum was present.

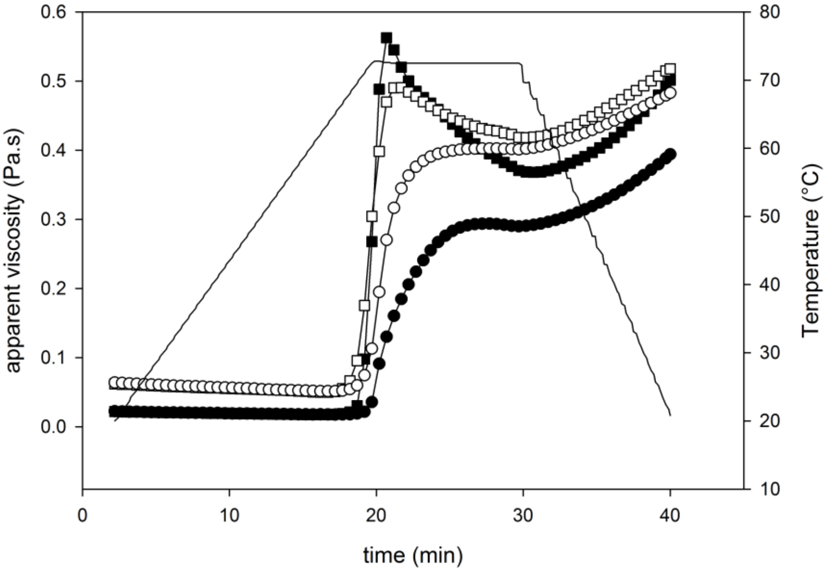

Figure 3-3: The salt content, which controls the gelatinization temperature, and the presence of xanthan gum, strongly affects the pasting behavior of waxy maize starch (starch:solvent = 5:100) at 72.5°C and a shear rate of 150 s^{-1} (■ no xanthan 0.01M NaCl; □ 0.2% xanthan 0.01M NaCl; ● no xanthan, 0.1M NaCl; ○ 0.2% xanthan 0.1M NaCl).

The differences in gelatinization temperature between the highest and the lowest salt content were much lower for the potato starch systems. Nonetheless at 67.5°C the systems at 0.1M NaCl showed an incomplete swelling when processed at 50 s^{-1} as indicated by the continuously increasing viscosity (not depicted), but at 150 s^{-1}, plateau values (xanthan containing paste) and even breakdown (xanthan free paste) was observed (see Figure 3-4). Elevating the temperature to 70°C allowed more granules to gelatinize and swell at 0.1M NaCl, whereas the samples with the lowest salt content became more fragile as illustrated by the observed breakdown for the sample without xanthan at 50 s^{-1} and for both samples at 150 s^{-1} (Table 3-1).

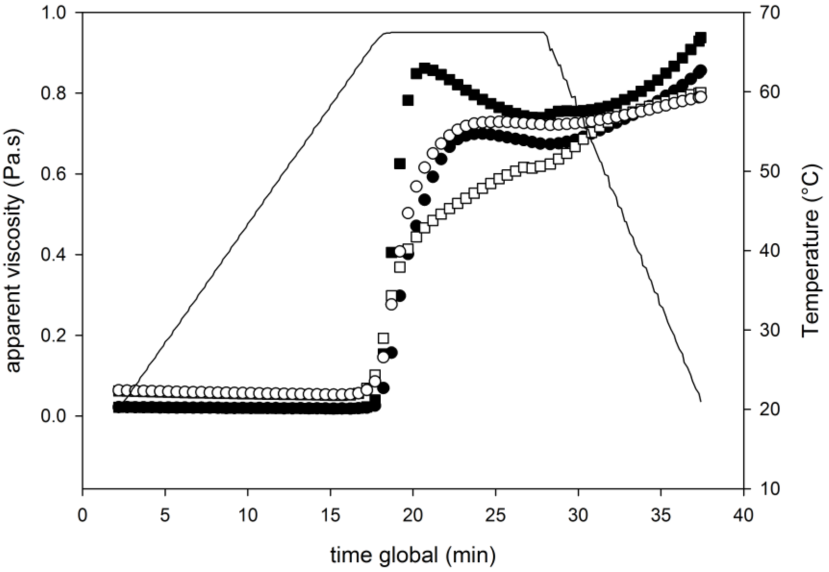

Figure 3-4: Pasting behavior of waxy potato starch (starch:solvent=5:100) systems at 67.5°C and a shear rate of 150 s^{-1} as affected by xanthan and salt content (■ no xanthan 0.01M NaCl; □ 0.2% xanthan 0.01M NaCl; ● no xanthan, 0.1M NaCl; ○ 0.2% xanthan 0.1M NaCl).

These results clearly demonstrate that the pasting behavior of shear sensitive starches can be better controlled at low temperatures. By selecting a processing temperature slightly higher than the gelatinization onset, breakdown can be reduced. Furthermore an increased shear rate facilitates the viscosity build-up at slowly swelling conditions, similar phenomena have been observed with cross-linked starches (Nayouf *et al.*, 2003). Presumably, the imposed shear weakens the internal bonds in the granules and facilitates water uptake of the granules. Conversely, increasing the shear can lead to breakdown at higher temperatures. In practice, operation temperatures can be chosen slightly lower when higher shear rates are applied and vice versa. Nonetheless, a correct choice of the operating temperature appears to be most decisive.

Xanthan gum can play a mediating role in starch pasting at these moderate temperatures. Breakdown was significantly reduced for all investigated samples. In addition, DSC experiments suggested that at these temperature conditions, gelatinization is partially inhibited by xanthan. This could imply a more restricted swelling of the granules and consequently an additional reduction in breakdown. Particularly at the lowest salt content, pasting viscosities of the xanthan containing samples are lower than for the xanthan free systems. However, it was demonstrated in chapter 2 that this marked viscosity reduction is also observed at conditions where granule swelling is not restricted. These observations suggest that a restriction in swelling, if it occurs, is probably not the only reason for the stabilizing effect of xanthan gum. When xanthan gum is heated at low salt contents, its rigid helical structure transforms to a random coil with much lower viscosity (Capron *et al.*, 1998b; Choppe *et al.*, 2010; Milas & Rinaudo, 1986). At higher salt contents this transition does not take place, which explains the differences between the two salt contents. Furthermore, xanthan gum most likely can change the impact between the granules during the pasting process. It was suggested before that xanthan gum is capable of enwrapping the starch granules (Cai *et al.*, 2011; Chaisawang & Suphantharika, 2006; Gonera & Cornillon, 2002). This envelope might physically stabilize the particle by acting as a lubricating layer. Another explanation might be that an increased viscosity in the presence of xanthan in the continuous phase reduces the turbulence in the starch pasting cell and hence the Reynolds number, which leads to a lower collision rate of the granules (Walstra, 2003). These phenomena might explain why systems, even with the same extent of granule swelling, can exhibit lower viscosities when xanthan gum is present and will be studied more into detail in chapter 5.

Table 3-1: Pasting properties of different starch/xanthan mixtures at two NaCl levels (0.01M, 0.1M) as influenced by temperature and shear rate imposed during pasting

Starch type	Setpoint temp. (°C)	NaCl (M)	xanthan	Shear rate 50 s^{-1}		Shear rate 150 s^{-1}	
				Peak viscosity (Pa.s)	Relative break-down (%)	Peak viscosity (Pa.s)	Relative break-down (%)
Maize	70	0.01	0%	0.79 ± 0.01^{E}	0.0	0.37 ± 0.01^{D}	7.5
			0.2%	0.66 ± 0.00^{D}	0.0	0.38 ± 0.01^{D}	0.0
		0.1	0%	0.02 ± 0.00^{A}	0.0	0.04 ± 0.00^{A}	0.0
			0.2%	0.14 ± 0.00^{B}	0.0	0.12 ± 0.00^{B}	0.8
	72.5	0.01	0%	1.21 ± 0.01^{G}	15.9	0.56 ± 0.01^{F}	34.1
			0.2%	1.06 ± 0.01^{F}	3.3	0.49 ± 0.00^{E}	14.6
		0.1	0%	0.50 ± 0.03^{C}	0.0	0.29 ± 0.02^{C}	1.7
			0.2%	0.69 ± 0.01^{D}	0.0	0.40 ± 0.01^{D}	0.5
Potato	67.5	0.01	0%	1.89 ± 0.03^{C}	0.0	0.86 ± 0.01^{C}	14.2
			0.2%	1.13 ± 0.03^{A}	0.0	0.62 ± 0.00^{A}	1.1
		0.1	0%	1.23 ± 0.18^{A}	0.0	0.70 ± 0.01^{B}	3.7
			0.2%	1.41 ± 0.03^{B}	0.0	0.73 ± 0.02^{B}	1.1
	70	0.01	0%	2.20 ± 0.05^{D}	9.2	1.03 ± 0.01^{E}	29.5
			0.2%	1.33 ± 0.07^{B}	0.0	0.73 ± 0.02^{B}	4.1
		0.1	0%	1.88 ± 0.01^{C}	0.8	0.95 ± 0.02^{D}	18.6
			0.2%	1.90 ± 0.00^{C}	0.5	0.88 ± 0.00^{C}	13.4

For each starch type, superscripts A-G indicate significant differences within columns ($p<0.05$)

3.3.3 PARTICLE SIZE DISTRIBUTION

Particle size distributions of the cooled pastes were determined in order to derive the effects of the different pasting conditions and the addition of xanthan gum on the granules. Two different derived diameters were taken into consideration. Besides the volume-weighted mean diameter D[4,3], the 10th percentile of the volume-weighted particle size distribution D(0.1) was considered. The latter accounts for the smaller fragments, as 10% (V) of the particles have a diameter smaller than this one. Consequently, this parameter can be regarded as a measure for the fragments originating from disrupted granules. The granule size distribution is determined by two phenomena: granule swelling and granule disruption. Hence, a combined interpretation of both parameters provides additional information on the microstructural changes that took place during the heating and cooling steps. The derived diameters are summarized in Table 3-2.

For the maize starch systems processed at 70°C, differences in particle diameters could only be observed at the lowest salt content (Table 3-2). In these cases the granule size was lower when pasted at a shear rate of 150 s^{-1}. However this reduction was much less pronounced when xanthan gum was present. Similar trends are observed for the pastes prepared at 72.5°C. Likewise, at a salt content of 0.1M (and heating temperature of 72.5°C), varying the shear rates was more noticeable in the xanthan free pastes than in the xanthan containing pastes. In general, these results are in line with the conclusions of the pasting experiments: the effect of increasing the shear rate during preparation resulted in smaller granule sizes for samples where breakdown was exhibited during pasting. Granules of samples where swelling was limited or incomplete, and breakdown seemed not to occur, appeared not to be influenced by xanthan gum (e.g. the pastes with 0.1M NaCl and prepared at 70°C with shear rate 50 s^{-1}). This could prove that xanthan gum does not restrict swelling of the granules at the concentrations considered here. Although it should be noted that – based on the DSC measurements – xanthan gum might reduce the number of granules that can gelatinize in the given conditions. This does not necessarily mean that the ones that are capable of swelling, adopt smaller diameters. As the volume-weighted mean diameter D[4,3] is dominated by the size of the fully swollen granules, the contribution of the unswollen granules might be overlooked. Conversely, it cannot be fully excluded that xanthan actually enhances the swelling of the granules. In chapter 5 it will be attempted to elucidate the precise effects of xanthan gum on these waxy maize starch systems.

Table 3-2: The volume-weighted mean diameter D[4,3] and the 10th percentile of the volume-weighted particle size distribution D(0.1) as influenced by xanthan gum, NaCl content and pasting conditions (shear rate, temperature)

			maize		potato	
NaCl (M)	Xanthan	shear rate (s^{-1})	D(0.1)	D[4,3]	D(0.1)	D[4,3]
			70°C		67.5°C	
0.01	0%	50	15.2 ± 0.2^{C}	34.0 ± 0.7^{B}	46.0 ± 2.0^{C}	144.1 ± 3.5^{C}
		150	12.5 ± 0.1^{A}	29.3 ± 0.5^{A}	$37.1 \pm 0.3^{A,B}$	123.1 ± 2.2^{B}
	0.2%	50	15.9 ± 0.4^{C}	35.7 ± 2.2^{B}	60.0 ± 0.7^{E}	175.0 ± 1.8^{E}
		150	14.3 ± 0.2^{B}	34.6 ± 1.1^{B}	$48.2 \pm 0.8^{C,D}$	$149.6 \pm 1.5^{C,D}$
0.1	0%	50	13.1 ± 0.4^{A}	28.0 ± 0.5^{A}	$47.7 \pm 1.3^{C,D}$	$148.9 \pm 2.4^{C,D}$
		150	12.8 ± 0.2^{A}	27.9 ± 0.3^{A}	35.3 ± 0.6^{A}	110.3 ± 1.1^{A}
	0.2%	50	12.6 ± 0.3^{A}	27.4 ± 0.3^{A}	49.3 ± 1.0^{D}	156.3 ± 4.0^{D}
		150	12.3 ± 0.9^{A}	27.0 ± 1.2^{A}	38.4 ± 2.3^{B}	122.6 ± 5.7^{B}
			72.5°C		70°C	
0.01	0%	50	$13.8 \pm 0.1^{B,C}$	34.0 ± 0.6^{C}	$45.3 \pm 0.8^{C,D}$	$140.5 \pm 1.1^{C,D}$
		150	11.3 ± 1.0^{A}	29.0 ± 0.6^{A}	37.3 ± 1.1^{B}	$124.1 \pm 2.4^{B,C}$
	0.2%	50	$14.7 \pm 0.6^{B,C}$	36.8 ± 1.6^{D}	52.4 ± 1.4^{E}	175.1 ± 12.0^{E}
		150	11.0 ± 0.2^{A}	$33.0 \pm 0.7^{B,C}$	43.1 ± 0.4^{C}	$136.9 \pm 2.5^{C,D}$
0.1	0%	50	15.2 ± 0.1^{C}	$32.6 \pm 0.8^{B,C}$	42.9 ± 0.8^{C}	$134.6 \pm 2.1^{B,C,D}$
		150	13.4 ± 0.1^{B}	29.9 ± 0.2^{A}	32.1 ± 0.7^{A}	108.3 ± 4.8^{A}
	0.2%	50	$14.6 \pm 0.1^{B,C}$	32.1 ± 0.6^{B}	48.6 ± 3.2^{D}	$148.5 \pm 8.3^{C,D}$
		150	$14.5 \pm 1.0^{B,C}$	32.3 ± 0.1^{B}	36.6 ± 1.7^{B}	$121.0 \pm 7.3^{A,B}$
			85°C		85°C	
0.01	0%	50	9.6 ± 0.2^{A}	29.9 ± 0.5^{A}	44.3 ± 0.1^{A}	143.8 ± 0.0^{A}
	0.2%	50	9.4 ± 0.7^{A}	37.8 ± 2.0^{B}	46.4 ± 0.6^{A}	145.3 ± 1.8^{A}

For each starch type/temperature combination, superscripts A-E indicate significant differences within columns ($p<0.05$)

The results obtained for the potato starch pastes were comparable with those derived for the maize starch systems. Nevertheless, the differences induced by both shear rates were more distinct, even in the presence of xanthan gum (Table 3-2). Considering the large dimensions of potato starch granules, a lower shear-tolerance is not unlikely. In all of these systems the average diameters were much lower when processed at 150s^{-1}, indicating a stronger shear sensitivity than for the maize starch. Nonetheless, the granules of the xanthan containing pastes proved to be larger compared to the gum free systems. In this case the effect of xanthan gum appears to be much more pronounced at the lowest salt content. This might be related to either the occurrence of the xanthan transition or to a higher electrostatic repulsion at low salt concentrations. Some researchers have suggested an electrostatic incompatibility between xanthan gum and the potato starch which has an anionic nature due to its high degree of phosphorylation (Cai *et al.*, 2011; Shi & BeMiller, 2002). This repulsion might in turn be (partially) shielded by the present ions, explaining the differences between both salt contents. The xanthan transition as such did not seem to have a distinct effect in the case of the maize system because comparable effects could be noted at the lowest as well as the highest salt content. Of course, one should be cautious when comparing systems with high and low salt content, given their difference in gelatinization temperature.

In Table 3-2 the diameters of starches pasted at 85°C are represented as well (i.e. samples from chapter 2). These results demonstrate the positive effects of processing near the gelatinization temperature: the number of small granule fragments is reduced (higher D(0.1) values), as a result of the reduced starch disruption. In general, the value of D[4,3] is also lower when heated to 85°C, although the relative differences between the different temperatures are smaller. This is rather expected because its value is largely determined by the size of the largest (i.e. fully swollen) granules. Furthermore, it should be remarked that the averaged granule diameters are based on the granules which are actually present in the system. Particularly when heated to 85°C, it can be expected that a significant fraction of the starch granules is completely degraded (hence they do not contribute to the averaged diameters), resulting in a significantly lower granule concentration.

3.3.4 MICROSTRUCTURE OF PASTES AS AFFECTED BY HEATING TEMPERATURE

Lowering the heating temperature, clearly affected the pasting behavior, and as a result also the particle size distributions. These effects are also clearly noticeable on a macroscopic level. Figure 3-5 visually demonstrates the textures of the waxy maize starch pastes induced by different heating temperatures. When heated to 85°C, the granules have been broken down to a large extent, which results in slimy textures. Granules remain largely intact when heated to 70°C and give rise to a more yoghurt-like appearance.

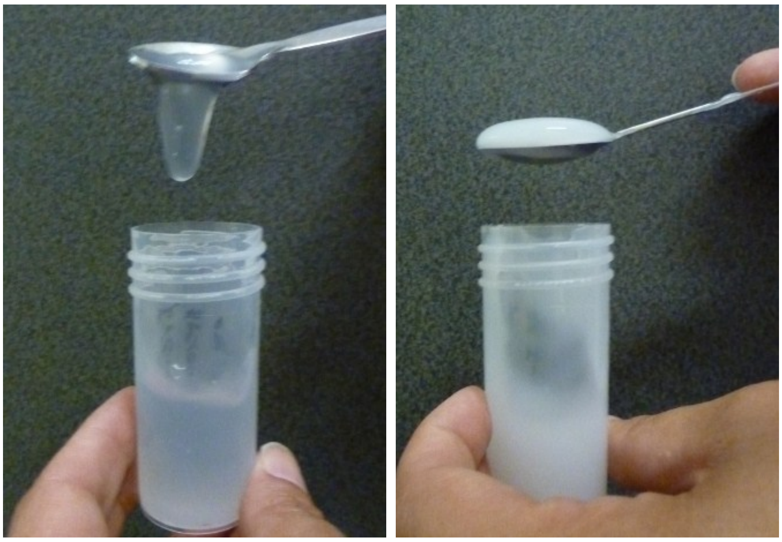

Figure 3-5: Translucent long texture of waxy maize starch paste (5:100, no xanthan) heated to 85°C (L) and short opaque paste (R) heated to 70°C (5:100, no xanthan)

Micrographs of maize starch pastes heated to different temperatures (70, 72.5 and 85°C) were recorded in order to illustrate the effects on their microstructure. Figure 3-6 depicts representative micrographs for each system. All pastes were sheared at 50 s^{-1} during the heating step. Visually it was not possible to detect differences between the xanthan-containing and the xanthan-free systems, hence only the latter are shown.

These micrographs confirm the beneficial effects of using mild temperature heating to prepare the waxy starch pastes: compared with more customary heating temperatures (c), significantly more granules remain intact (figure a and b). Furthermore, as suggested by the particle size determinations, a slight temperature increase from 70°C to 72.5°C already results in marked effects. Although the size of the granules present is not markedly different, the number of intact granules is lower when heated to 72.5°C. The temperatures imposed in the preceding chapter (85°C) are clearly too elevated to obtain true starch dispersions. As hypothesized in section 2.3.5, those systems are better described as macromolecular solutions containing only a limited number of remaining starch granules.

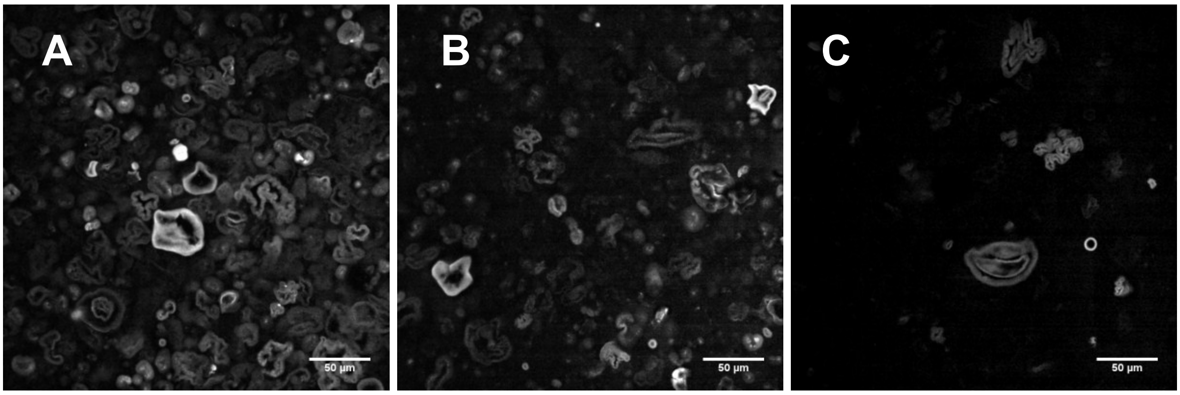

Figure 3-6: Confocal micrographs of maize starch pastes at a starch to solvent ratio of 3:100 (0% xanthan, 0.01M NaCl). The samples are sheared at 50 s^{-1} and heated to 70°C (A), 72.5°C (B) or 85°C (C)

3.3.5 FLOW CURVES OF PASTES AFTER COOLING

Following pasting, the samples were stored (5°C) for 24h and subsequently analyzed rheologically. As an example, flow curves of the cooled maize starch pastes prepared at 70°C are represented in Figure 3-7. For this temperature, only the samples with a NaCl concentration of 0.01M were considered. Granule swelling was too limited at 0.1M NaCl, resulting in a watery suspension of largely ungelatinized starch granules.

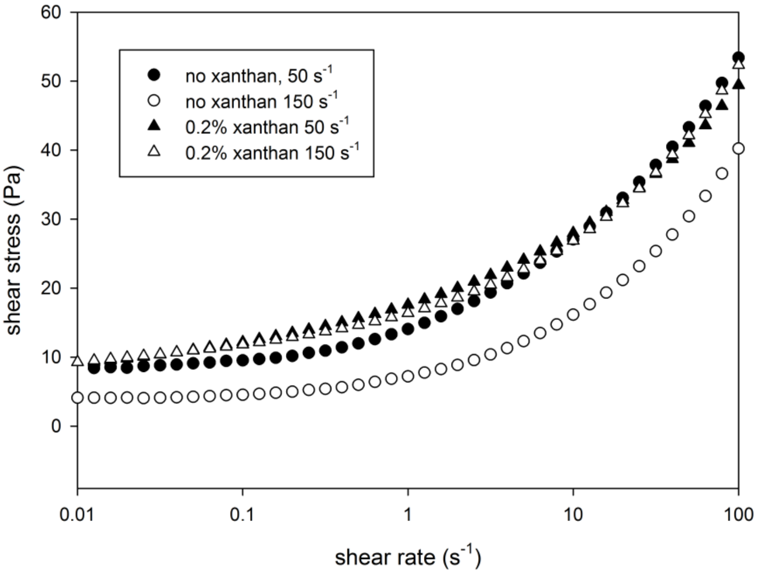

Figure 3-7: Flow curves of cooled waxy maize starch pastes (0.01M NaCl) as influenced by imposed shear rate and the presence of xanthan gum (all pasted at 70°C). The curves illustrate the protective effects of xanthan gum

Table 3-3 and Table 3-4 summarize the derived Herschel-Bulkley parameters for all the investigated systems. The higher shear during pasting, and consequently the higher extent of granule degradation, shifts the flow curves to lower values, which is translated in lower values of the yield stress and consistency index. The difference between both imposed shear rates was more pronounced in the case of the gum free pastes. This effect is also illustrated by the flow curves depicted in Figure 3-7. However, the increased values of the yield stress and the consistency index, cannot solely be attributed to differences in granular preservation, but the properties of the continuous phase might play a role as well. In dilute systems, the rheological behavior is governed by the properties of the continuous phase, e.g. the dissolved hydrocolloids, as well as the volume occupied by the swollen starch granules. In this manner, strongly swelling starches induce higher viscosities (Steeneken, 1989). At the given concentrations, the maize starch occupies a volume of ± 20% which is far below close packing (calculation based on the volume equivalent average diameter D[3,0] of the swollen and unswollen granules). Consequently, it can be assumed that the continuous phase, which contains xanthan gum, still strongly influences the rheological behavior. However, Abdulmola *et al.* (1996b) stated that even below close packing swollen starch granules interact and influence the small deformation rheology. Most likely the adjoining starch granules dominate the rheological behavior at low shear rates, whereas the influence of the continuous phase is more noticeable at higher shear rates.

Table 3-3: Influence of xanthan content, NaCl concentration and preparation conditions (shear rate, temperature) on the Herschel-Bulkley parameters fitted to the flow curves (20°C) of waxy maize starch pastes (starch:solvent=5:100)

NaCl (M)	xanthan	Shear rate (s^{-1})	σ_0	k ($Pa.s^n$)	n (-)	R²
			70°C			
0.01	0%	50	5.9 ± 0.3	8.8 ± 0.3	0.37 ± 0.01	0.997
		150	3.1 ± 0.4	4.4 ± 0.4	0.47 ± 0.02	0.977
	0.2%	50	6.5 ± 0.2	11.0 ± 0.2	0.29 ± 0.00	0.999
		150	8.3 ± 0.3	8.0 ± 0.3	0.37 ± 0.01	0.994
0.1	0%	50		Not determined		
		150		Not determined		
	0.2%	50		Not determined		
		150		Not determined		
			72.5°C			
0.01	0%	50	7.9 ± 0.2	9.8 ± 0.3	0.40 ± 0.01	0.998
		150	6.3 ± 0.1	4.3 ± 0.1	0.56 ± 0.01	0.999
	0.2%	50	12.6 ± 0.4	9.0 ± 0.4	0.39 ± 0.01	0.989
		150	9.8 ± 0.5	6.3 ± 0.5	0.44 ± 0.02	0.981
0.1	0%	50	3.9 ± 0.3	6.0 ± 0.4	0.39 ± 0.01	0.989
		150	2.4 ± 0.1	4.1 ± 0.1	0.48 ± 0.00	0.999
	0.2%	50	5.3 ± 0.2	9.2 ± 0.2	0.33 ± 0.00	0.998
		150	5.1 ± 0.3	12.1 ± 0.3	0.29 ± 0.00	0.998

The Herschel-Bulkley model appeared to be less suitable to fit the flow curves of the potato starch systems. Hence, the low shear data (< 0.1 s^{-1}) were omitted in the fit. As a consequence, the absolute values of σ_0 and k varied more strongly among the different samples than the actual flow curves would suggest. There is a strong correlation between both fitted parameters, because higher values of k give rise to lower values of σ_0 and vice versa, as illustrated in the loading plots depicted in section 2.2.8. Purely as an interpretation aid, the sums of the yield stress and consistency index are included in Table 3-4. This value corresponded well with the differences seen in the location of the flow curves. However, this is a purely empirical finding and the value of the sum holds no physical meaning (addition of different units). For the xanthan free systems, flow curves of systems pasted at 150 s^{-1} were systematically located below the curves of pastes prepared at 50 s^{-1}, as expected.

However, as opposed to the maize starch systems, the location of the flow curves appeared more difficult to predict based on the interpretation of the pasting curves (presence of breakdown) and the particle size distributions. At 0.01M NaCl, pasting experiments and particle size distributions showed less granule disruption when xanthan was present, but when processed at 50 s^{-1} the flow curves of these systems were located lower than their gum free counterparts (when pasted at 150 s^{-1} the differences were less pronounced). At 0.1M NaCl, the addition of xanthan gum shifted the flow curves upwards, which was expressed as higher values of the yield stress and the consistency index. For all samples processed at 50 s^{-1}, the addition of xanthan gum led to a significant reduction of the yield stress, an increased consistency index, and a lower flow behavior index. This distinct behavior may suggest a specific interaction between starch and xanthan, that modifies the way particles interact, as it was also observed during the pasting experiments. As suggested above, electrostatic repulsion probably plays a role. Furthermore the interpretation of the flow behavior of these potato starch systems is complicated by the fact that they cannot be considered as simple particles imbedded in a continuous phase of dissolved xanthan gum. Potato starch granules swell to relatively large dimensions, even when processed at moderate temperatures, they take in large effective volume fractions. Therefore they are likely to deform and even break up within a flow field.

Table 3-4: Influence of xanthan content, NaCl concentration and preparation conditions (shear rate, temperature) on the Herschel-Bulkley parameters fitted to the flow curves (20°C) of waxy potato starch pastes (starch:solvent=5:100)

NaCl (M)	xanthan	shear rate (s^{-1})	σ_0	k ($Pa.s^n$)	sum (σ_0 +k)	n (-)	R²
			67.5°C				
0.01	0%	50	16.6 ± 0.5	9.0 ± 0.5	25.7	0.39 ± 0.01	0.996
		150	14.6 ± 0.3	6.3 ± 0.2	20.9	0.48 ± 0.01	0.998
	0.2%	50	3.6 ± 0.5	16.5 ± 0.5	20.1	0.25 ± 0.01	0.999
		150	16.6 ± 0.4	6.1 ± 0.4	22.7	0.42 ± 0.01	0.994
0.1	0%	50	4.8 ± 1.0	5.7 ± 0.9	10.5	0.40 ± 0.03	0.966
		150	8.3 ± 0.4	5.0 ± 0.4	13.2	0.45 ± 0.02	0.992
	0.2%	50	0.2 ± 0.5	14.1 ± 0.5	14.3	0.27 ± 0.01	0.999
		150	13.2 ± 0.8	10.3±0.8	23.5	0.31 ± 0.01	0.992
			70°C				
0.01	0%	50	30.6 ± 0.6	6.1 ± 0.5	36.7	0.51 ± 0.02	0.990
		150	22.6 ± 0.3	4.0 ± 0.2	26.6	0.58 ± 0.01	0.996
	0.2%	50	13.2 ± 0.4	11.8 ± 0.4	25.0	0.32 ± 0.01	0.998
		150	22.1 ± 0.5	5.3 ± 0.4	27.3	0.47 ± 0.02	0.991
0.1	0%	50	18.8 ± 1.1	7.8 ± 1.0	26.6	0.43 ± 0.03	0.979
		150	16.8 ± 0.1	4.7 ± 0.1	21.5	0.54 ± 0.00	1.000
	0.2%	50	10.9 ± 1.3	15.9 ± 1.3	26.8	0.30 ± 0.01	0.991
		150	20.4 ± 1.2	12.9 ± 1.2	33.3	0.33 ± 0.02	0.988

3.3.6 EFFECT OF VARYING STARCH CONCENTRATIONS

The previous results showed the beneficial effects of both moderate temperature processing and xanthan gum on the stabilization of waxy starch granules during pasting at a fixed starch:water ratio of 5:100. The differences observed between maize starch and potato starch might be attributed to their strongly differing swelling power and hence their effective volume fraction in the dispersion. At higher starch volumes, the mutual friction between the granules is most likely further increased. Therefore it might be possible that the aforementioned effects of xanthan gum, namely the higher degree of starch granule preservation, are cancelled out at higher starch concentrations. To examine this, pasting experiments were compared at different starch contents (starch:solvent ratio 3:100; 5:100; 7:100). For maize starch an isothermal temperature of 70°C was selected and for potato starch this was 67.5°C (all systems contained 0.01M NaCl). Figure 3-8 represents the pasting behavior of the different potato starch systems.

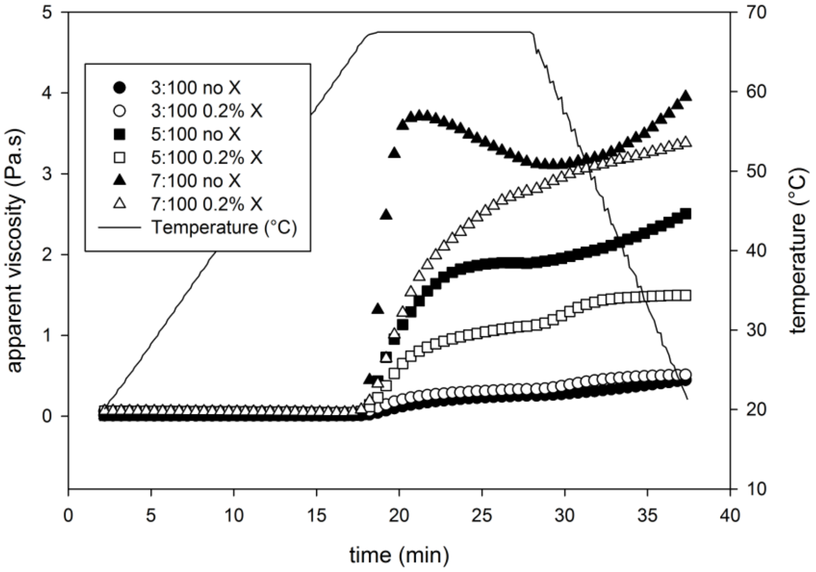

Figure 3-8: Effect of xanthan gum (X) on pasting behavior of waxy potato starch at different concentrations (67.5°C; 0.01 M NaCl; shear rate 50 s^{-1})

The peak exhibited for the highest starch concentration, demonstrates a more predominant granule disruption. This confirms the hypothesis that the denser packing leads to more abrasion of the granules. Similar results were observed for the maize starch system at a ratio of 7:100 (data not represented). Furthermore the positive effects of xanthan gum are clearly demonstrated as no breakdown could be observed for all systems. Specifically at higher starch contents, xanthan could restrict the swelling of the granules, due to competition for the available water or by slowing down the diffusion. This is suggested by a clearly less steep viscosity increase during pasting. When the granules remain less swollen, they are also less easily disrupted.

For the potato starch systems, the varying starch concentrations resulted in marked effects in particle size distributions (Figure 3-9). These effects were more limited for the maize starch systems (not depicted). Potato starch has a high swelling power and at a 7:100 ratio, the higher concentration clearly limits granule swelling (Steeneken, 1989). When xanthan gum was present, higher diameters were measured, most likely due to less granule degradation. Surprisingly, an exception could be observed at the lowest starch content where the average diameter of the xanthan containing system was lower than its gum-free counterpart. In these dilute systems it is very likely that starch granules swell freely to high dimensions without breaking up. In a more viscous medium this expansion of the granule might be more limited. These phenomena could be caused by effects of conformational entropy: swelling reduces the conformational freedom (and entropy) of the dissolved polymers between the granules, hence counteracting the driving forces for swelling.

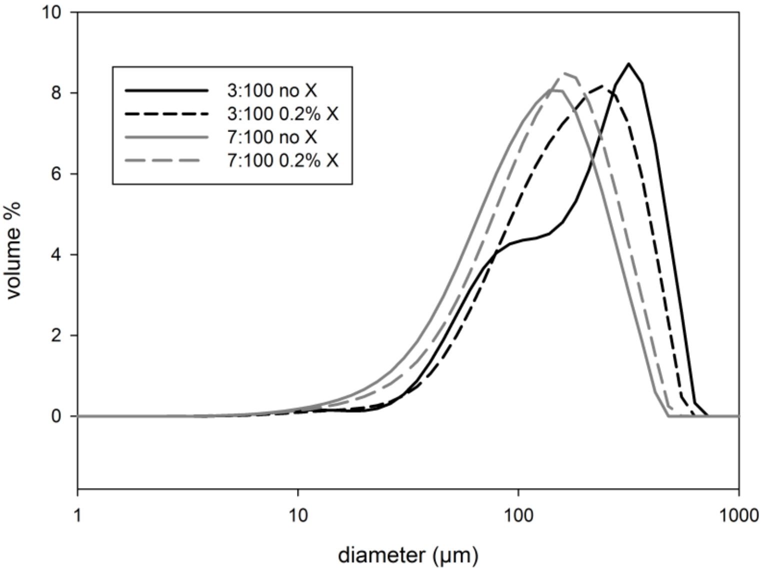

Figure 3-9: Influence of xanthan gum (X) on particle size distributions of two different concentrations of potato starch (pasted at 67.5°C, shear rate 150 s^{-1}, 0.01 M NaCl)

3.4 CONCLUSIONS

When native waxy starches (maize or potato) are pasted at temperatures slightly higher than the gelatinization onset temperature, their swelling can be more controlled, but a limited fraction of the starch will remain ungelatinized. Under these conditions granule disruption can be limited and a higher shear rate can even be beneficial towards complete viscosity development. The correct choice of processing conditions allows to tune the (primarily rheological) properties of these waxy starch systems. The heating temperature is therefore a critical process-parameter. When the temperature is too low, swelling will be incomplete and at more elevated temperatures granule disintegration will become more predominant. In the latter case the presence of xanthan may help to stabilize the granules, probably by altering the impact between the granules although further research is required to elucidate the exact role of xanthan gum (see chapter 5).. In conclusion it can be stated that processing at temperatures within the gelatinization range, combined with the addition of xanthan gum may improve the performance of native starches in food systems.

4 LONG-TERM STABILITY OF WAXY MAIZE STARCH/XANTHAN GUM MIXTURES PREPARED AT A TEMPERATURE WITHIN THE GELATINIZATION RANGE

Relevant publication: Heyman, B., Van Bockstaele, F., Van de Walle, D., Dewettinck, K. (2013). Long-term stability of waxy maize starch/xanthan gum mixtures prepared at a temperature within the gelatinization range. Food Research International (submitted).

4.1 INTRODUCTION

Aside from their weak processing tolerance, native starches are preferentially not incorporated in industrially produced foodstuffs because of their tendency to retrograde during storage. Particularly for amylose containing starches, strongly gelled pastes are obtained after a few hours, making them unsuitable for applications requiring a more liquid behavior (BeMiller & Whistler, 2009). Moreover, during longer storage, the amylose gel further contracts, resulting in syneresis, which in turn may lead to consumer rejection. Due to the absence of amylose, waxy starches retrograde relatively slowly, where depending on the concentration and temperature, amylopectin chains recrystallize over several days to weeks (Kalichevsky *et al.*, 1990; Ring *et al.*, 1987). Unfortunately, native waxy starches are very sensitive to shear and/or elevated temperatures, which results in slimy products when processed under conventional circumstances. It was demonstrated in the preceding chapter that when processed within the gelatinization temperature range, waxy starches can better preserve their integrity and withstand shear forces. In this chapter, the retrogradation behavior of waxy maize starch pastes prepared at mild temperatures is studied.

Keetels *et al.* (1996c) observed that the rate of retrogradation of maize starch systems was slower when subjected to mild heating. They proposed that the phase separation between amylose and amylopectin in the continuous phase was incomplete, resulting in a slower rearrangement of amylopectin moiety. For waxy starches, no amylose is present and the effects of mild heating differ. When heated to temperatures within the gelatinization temperature range, some residual gelatinization is observed during reheating in DSC. This is caused by some granules not being fully gelatinized during the first heating step, or not being gelatinized at all and/or the occurrence of annealing (Fisher & Thompson, 1997). As a direct consequence, a lower fraction of gelatinized amylopectin is available for recrystallization, resulting in a lower degree of retrogradation. However, when the starch granules are heated at temperatures just above the gelatinization range, all granules are fully gelatinized and all crystalline regions are melted, but some residual order among the molecules is still present. This in turn serves as a template for recrystallization and leads to a more rapid retrogradation (Fisher & Thompson, 1997; Liu & Thompson, 1998). Although these effects have been demonstrated experimentally, it is unclear how these mild heating conditions affect the microstructure and rheological properties of the formed pastes throughout longer periods of preservation.

The addition of hydrocolloids is generally known to affect the retrogradation behavior of starch pastes. However, the effects strongly vary and depend on the specific combination of gum and starch. Most studies focus on amylose gelation, which is mostly enhanced by gum addition. This effect is generally attributed to a phase separation between the gum molecules and amylose (see section 1.3.4). The phase behavior of gum molecules and amylopectin is remarkably rarely studied. Consequently, a mechanistic interpretation of their effects on waxy starch retrogradation is inconclusive. Biliaderis *et al.* (1997) observed a much slower gelation of waxy maize starch in the presence of gums, whereas DSC revealed a higher degree of crystallinity during preservation. They suggested a phase separation between the gums and the (largely degraded) waxy maize starch, favoring the short range amylopectin association, but inhibiting the long range associations required for gel formation. Although it has never been studied with direct methods, a phase separation between xanthan and amylopectin was also proposed by Ptaszek *et al.* (2009). Ferrero *et al.* (1994) claimed at least the absence of specific interactions between both polymers.

Low-field ^{1}H-NMR can provide valuable information on the molecular mobility of the various components in starch systems, and consequently their retrogradation behavior. In relation with other direct methods like DSC and XRD, NMR offers some advantages. Because it is a non-destructive test, the same sample can be analyzed repeatedly as a function of preservation time. Furthermore, relatively large amounts of sample are analyzed, making the technique suitable for less concentrated and more heterogeneous pastes (Farhat *et al.*, 2000). However, the interpretation of the NMR data is less straightforward. When studying ^{1}H spin-spin relaxation (= transverse or T_2 relaxation) of polysaccharide systems, the obtained relaxation signal originates from hydrogen nuclei belonging to different classes of molecules. Each class is characterized by its physical state, its diffusion rate and its bonding or interaction with other molecules (Thygesen *et al.*, 2003). For dilute polysaccharide systems, the T_2 relaxation time is dominated by the signal originating from the water molecules, which is in turn modulated by the chemical exchange between the water protons and the protons of the macromolecules (Hills *et al.*, 1990). As a result, the NMR transverse relaxation time of water in polysaccharide systems is significantly reduced in comparison with bulk water. The extent of this reduction, depends on the state of aggregation and gelation of the polysaccharide (Hills *et al.*, 1991; Rayment *et al.*, 2009). It should be remarked that as a consequence, proton relaxation measurements do not provide much useful information regarding the state of water (water binding and immobilization) in dilute polysaccharide systems (Hills *et al.*, 1990). The observed relaxation rate and the corresponding T_2-value is a complex function of the number of exchangeable protons, the rate of exchange (k_{gel}) with those sites and the relaxation time of the protons at those exchangeable sites (T_{2gel}) as expressed by following equation (Potter *et al.*, 1993):

$$\frac{1}{T_{2measured}}=\frac{1}{T_{2bulk\ water}}+\frac{K.\ [polysaccharide]}{T_{2gel}+k_{gel}^{-1}} \qquad 4\text{-}1$$

In this equation, the parameter K relates the polysaccharide concentration to the relative number of exchangeable protons. When aggregation occurs, the relaxation behavior of the hydroxyl groups changes (T_{2gel}). Furthermore, conformational changes can alter the accessibility of the polysaccharide hydroxyl groups and therefore the exchange rate. Hence, transverse relaxation measurements were proven to be a sensitive probe for changes in the polymer conditions, although the exact physical explanation is complicated.

The evaluation of starch retrogradation in pastes containing relatively low amounts of starch is associated with a lot of practical difficulties, particularly when the microstructure changes continuously during storage. For the study of those systems, pulsed field NMR can be a valuable option. In starch pastes, the molecular interpretation is further complicated by the presence of different phases: some polymers are dissolved, others are present in dispersed granules or crystallized aggregates. Nonetheless, the technique proved to be very useful in sensitively detecting molecular ‘reordening’ of starch systems during retrogradation, where changes within the same sample can be monitored (Hansen *et al.*, 2009; Thygesen *et al.*, 2003). This relative approach partly excludes the complex interpretation of the absolute signals as such. A marked reduction of the transverse relaxation time of the starch pastes was successfully related with the extent of retrogradation as measured by X-ray diffraction (Farhat *et al.*, 2000).

4.2 EXPERIMENTAL SETUP

The samples were not prepared by means of the starch pasting cell, because larger amounts of sample were required. Hence, this setup markedly differs from the other chapters. Stock solutions of xanthan gum (0.8%, 0.01M NaCl) were prepared by means of the unimix system as described elsewhere (section 2.2.2). For the preparation of the xanthan free pastes, the starch powder was first dispersed in a NaCl (0.01M) solution and this slurry was transferred to the unimix system. For the xanthan-containing pastes, the xanthan stock solution was added as well. Two different starch contents were used in order to obtain a starch to solvent ratio of 5:100 or 7:100 (w:w) in the final products. A schematic overview of the production steps is depicted in Figure 4-1. The NaCl concentration in the water phase of the slurry was 0.01M, to allow the same gelatinization behavior as described in the preceding chapter.. The dispersions were heated to either 70°C or 72°C (a temperature of 72.5°C, which was used in the preceding chapter, could not be programmed in the system) under continuous stirring with the agitator (150 rpm). The setpoint temperature was maintained for 15 minutes and the system was subsequently cooled down to 30°C (cooling time ± 10 minutes).

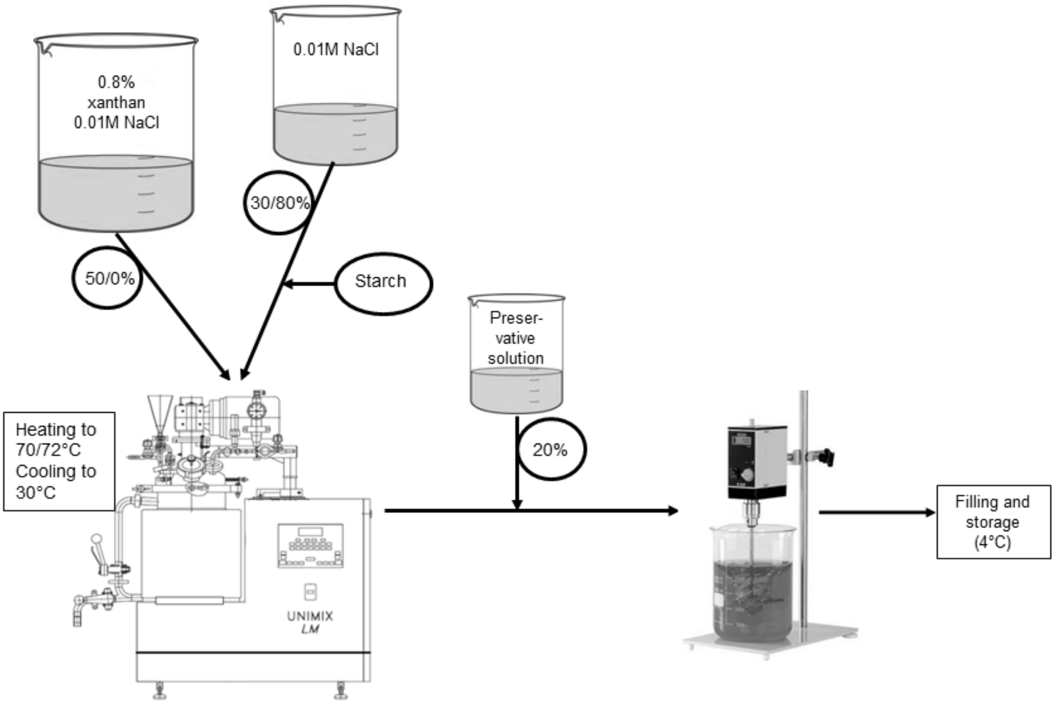

Figure 4-1: Schematic overview of the starch paste production

The resulting concentrated paste was split up in two parts and further mixed with either an acid or a neutral preservative solution. In this manner, the possible effects of the additives (primarily the acid) on the pasting behavior were excluded and the differences in stability observed between the different compositions can be related solely to changes which take place during storage. Mixing the paste with the preservative solution was performed with a laboratory overhead mechanical stirrer. The neutral preservative solution contained sodium azide (0.1% w/v) and 0.01M NaCl. The acid solution consisted in practice of two separate solutions, one containing 1% potassium-sorbate and 0.01M NaCl and the other one containing 2.5% citric acid and 0.01M NaCl. This separation was required to avoid precipitation of sorbic acid in the concentrated blend. NaN_3 is preferentially not used in acid environment where the highly toxic hydrazoic vapor can be formed. The resulting 'neutral' pastes contained 0 or 0.4% (w/v) xanthan, 0.01M NaCl and 0.02% (w/v) NaN_3. The acid pastes consisted of 0 or 0.4% (w/v) xanthan, 0.01M NaCl, 0.1% K-sorbate and 0.25% (w/v) citric acid. It is important to remark that these final concentrations are expressed on water phase volume and not on total volume, hence with exclusion of the volume occupied by the raw starch powder. This approach is similar to the setups of the preceding chapters and allows to use the same stock solutions for both starch contents. The pH of the resulting pastes was measured and equaled 3.3±0.1 and 6.5±0.1, respectively for the acid and the neutral pastes. The finished pastes were filled into jars (± 100ml), NMR- (10ml) and centrifuge tubes (25g) and stored at 7°C for further analysis. In total, this setup comprised 16 different systems. An overview is given in Table 4-1. Each composition was prepared in duplicate (i.e. two completely independent production sets.

Table 4-1: Composition and processing conditions of the pastes studied in this chapter

Starch:solvent ratio	heating temperature (°C)	xanthan concentration	acidity
5:100	70	0%	neutral
			acid
		0.4%	neutral
			acid
	72	0%	neutral
			acid
		0.4%	neutral
			acid
7:100	70	0%	neutral
			acid
		0.4%	neutral
			acid
	72	0%	neutral
			acid
		0.4%	neutral
			acid

The aim of this setup was to study the retrogradation effects of these pastes which were prepared at temperatures within the gelatinization range. The samples were stored for 8 weeks (7°C) and analyzed on day 1, 7, 14, 28 and 56. Texture analysis and rheology (flow curves, frequency sweeps) were used to evaluate macro- and microstructural changes, pulsed-field NMR was chosen to study the molecular aggregation. The amount of syneresis was quantified gravimetrically.

4.3 MATERIALS AND METHODS

4.3.1 TEXTURE ANALYSIS

Back extrusion tests were performed with an Instron 5942 materials testing system (Instron, Norwood, US) equipped with a 500N load cell (measurement accuracy: +/- 0.5% of reading down to 1/1000 of load cell capacity). A flat cylindrical probe (polypropylene, diameter 50.6mm, height 20.0mm) was pressed into the sample cups (polystyrene, diameter 56.3mm, height 51.4mm) at a rate of 10mm/min. As soon as the disc is submersed and the sample starts to overflow, a maximum load plateau is attained (Figure 4-2). This value was selected for further analysis. The raw date were analyzed with the Bluehill 3 software (Instron, Norwood, US).

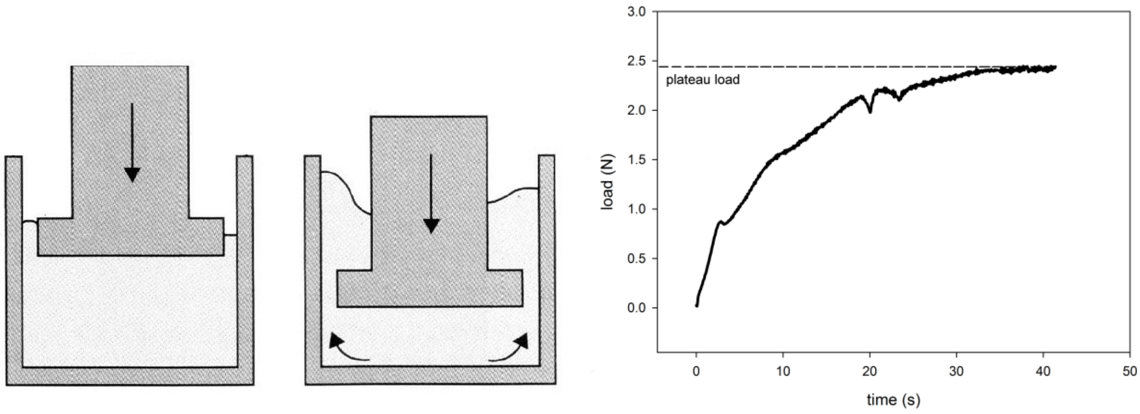

Figure 4-2: Back extrusion test with corresponding time-load plot

4.3.2 RHEOLOGICAL PROPERTIES OF THE PASTES

The flow curves of the cooled pastes were recorded using a 40 mm cross hatched steel plate-plate geometry with solvent trap. To prevent drying of the sample, 1 ml of water was brought in the solvent trap compartment. The gap was set to 1000 µm. Before each measurement (flow curves and frequency sweeps) the sample was allowed to equilibrate for 15 minutes at 20°C.

A steady state flow step was performed by logarithmically increasing the shear rate from 0.01 s^{-1} to 100 s^{-1}. The measurements were performed in duplicate (i.e. based on two independently produced batches). Because the texture of some samples evolved slowly from fluid to strongly gelled during storage, the samples could not be molded into readily measurable gel discs immediately after preparation. Hence, for analysis a small amount of paste was taken out of the jar and placed between the rheometer plates. Due to the sampling, part of the long range interactions in the gelled samples could be broken. A similar methodology was applied by Temsiripong *et al.* (2005).

The frequency sweeps were recorded from 0.01 to 5 Hz (the frequency was increased logarithmically) at a stress amplitude of 1 Pa. This value was within the linear visco-elastic region of the samples, as determined by recording stress amplitude sweeps at 1 Hz. The measurements were also performed in duplicate (based on two independently produced batches).

4.3.3 T_2-MEASUREMENTS

4.3.3.1 Principle of T_2- relaxation

Pulsed field gradient NMR is a fast, sensitive and non-invasive technique based on the spin of nuclei. The spinning motion causes a magnetic moment in the direction of the spin axis. This phenomenon is illustrated in Figure 4-3. When an external magnetic field B_0 is imposed, the magnetic moments or spins are constrained to adopt parallel or anti-parallel orientations with respect to B_0.

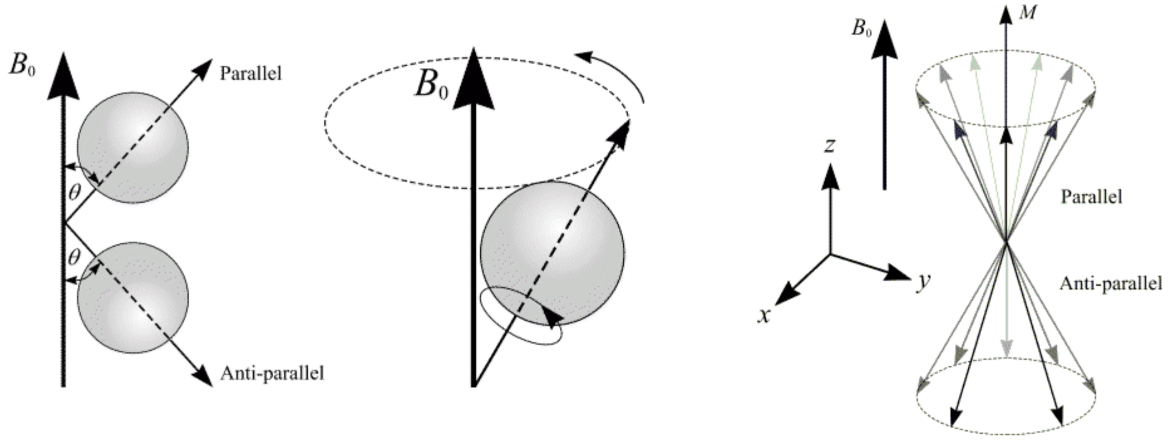

Figure 4-3: Orientation of spins in the presence of external magnetic field (Puddephat, 2010)

The application of a radio frequent pulse causes nuclear spins to shift between parallel and anti-parallel states. When the magnetic field component of an RF pulse is parallel with the xy-plane, the pulse will cause the magnetization M to rotate from the z direction into the xy plane. The return of M to its equilibrium state (the direction of the z-axis) is known as relaxation. T_2-relaxation (also known as transverse relaxation or spin-spin relaxation) is the decrease in the xy component of magnetization (Figure 4-4). Immediately following a 90 degree pulse, the net magnetization M is rotated into the xy-plane. Due to the absence of a perfectly uniform magnetic field strength, nuclei throughout the sample will experience slightly differing B_0's. These local variations of B_0 are constant in time. As a result, the nuclei experience different precessional frequencies depending on their location, and the spins dephase and expand over the xy-plane. Consequently, the net signal detected in the xy-plane will decay, because the opposed vectors cancel each other out (Ridgway, 2010).

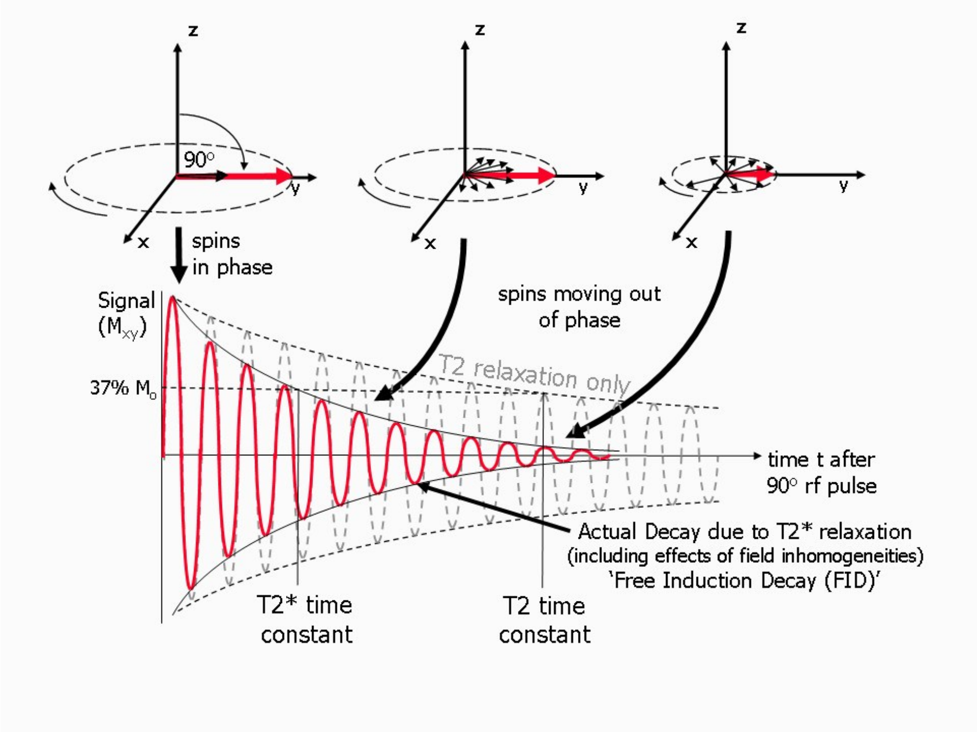

Figure 4-4: Signal decay following a 90° RF pulse (Ridgway, 2010)

A second type of transverse decay is caused by the nature of the sample. Within a sample, the magnetic moments of different protons interact with each other and modify the electric field that is experienced by each individual proton. Due to the random nature of the spin-spin interactions, this effect is not constant over time. The decrease in transverse magnetisation is described by a time constant, T_2*, that is the time it takes for the transverse magnetisation to decay to 37% of its original magnitude. This effect is generally described as free induction decay (FID). T_2^* characterizes dephasing due to both B_0 inhomogeneity and transverse relaxation (Ridgway, 2010). In order to obtain signal with a T_2 dependence rather than a T_2^* dependence, a pulse sequence known as the Carr-Purcell-Meiboom-Gill (CPMG) spin-echo has been developed (Meiboom & Gill, 1958). This sequence consists of a 90° radio frequency pulse followed by an echo train induced by successive 180° pulses, characterized by a pulse spacing time τ and an echo time TE (= 2* τ). The process is represented in Figure 4-5.

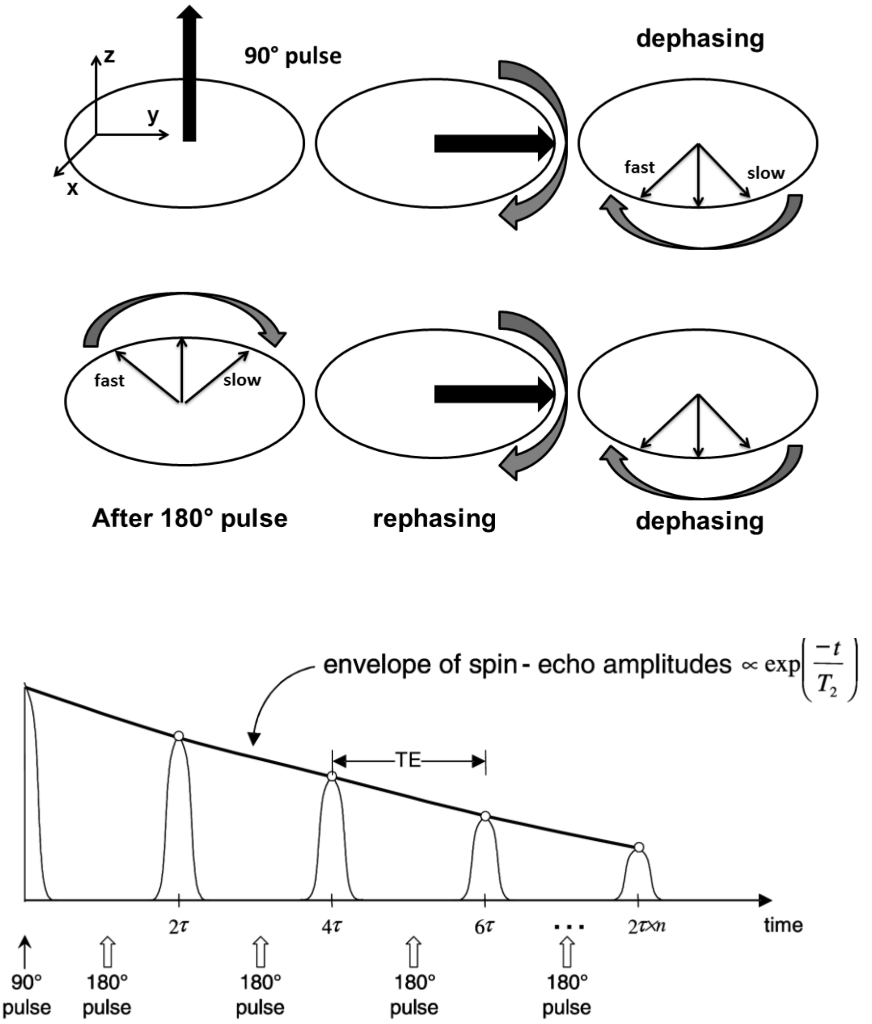

Figure 4-5: Spin echo's induced by rephasing following 180° pulses (adapted from Puddephat (2010) and Zhang & Hirasaki (2003))

First a 90° pulse is applied, followed by an 180° degree pulse at time τ which causes the three spins to invert. In this manner, the faster spins catch up with the slower ones. At time TE, the spins become coherent again so that an echo is produced and a signal is detected. If an additional 180° pulse is applied at time TE/2 after the peak signal of the first spin echo, then a second spin echo signal will form at time TE after the first spin echo. The peak signal amplitude of each spin echo is reduced from its previous peak amplitude due to T_2 dephasing, which is a random and irreversible process and therefore cannot be rephased by the 180° pulses (as opposed to magnet inhomogeneity dephasing). Figure 4-5 shows how the signal from a spin echo sequence decays over time. A line drawn through the peak amplitude of a large number of spin echoes describes the T_2 decay, while individual spin echoes exhibit T_2^* decay (Ridgway, 2010) .

4.3.3.2 Setup T_2-measurements

A 23 MHz ^{1}H NMR Maran instrument from Oxford Instruments (Tubney Woods, Abingdon, Oxfordshire, UK) was used to obtain Carr–Purcell–Meiboom–Gill (CPMG) relaxation curves of the pastes at 7°C. The temperature in the measuring cell was lowered by means of externally circulating cooled water. For each sample, three test tubes (diameter 8 mm) were filled with 10 mL of paste, immediately after preparation. The tubes were then covered with Parafilm flexible film and stored at 7°C. Before each measurement, the samples were allowed to equilibrate in a waterbath for at least 1h. Four scans (acquisitions) were accumulated during each measurement. The recycle delay between the scans was 10 s to allow full spin relaxation. For each composition and measuring day, 6 replicates were measured originating from two different production sets. The pulse spacing (τ) was set to 400 µs and the number of recorded echoes was set to 8192. A short pulse spacing was chosen in order to record spin-echo relaxation of all liquid-like proton populations, particularly those representing the mobility of the hydrocolloids through proton exchange (Hansen *et al.*, 2009). Relaxation curves were fitted to a mono-exponential decay curve by the WinDXP software (Resonance instruments, Skokie, Il, USA), providing the T_2- relaxation times.

The evolution of the T_2-values as a function of preservation time t (days), could be well described ($R^2 > 0.98$) by a three parameter exponential decay function:

$$T_2 = A + B.\ e^{-C.t} \qquad 4\text{-}2$$

Curves were fitted by means of the SigmaPlot 10 software to obtain the parameters A, B and C (Systat software inc., San Jose, USA). As the measurements started after 1 day of preservation, a hypothetical value T_{20} was calculated to describe the relaxation time of the fresh pastes, i.e. at t = 0:

$$T_{20}=A+B \qquad 4\text{-}3$$

4.3.4 SYNERESIS

The freshly prepared pastes (25g) were transferred to screw cap tubes and stored at 7°C. These samples were centrifuged at 8000g for 15 minutes after 1 day and after 8 weeks of storage. The watery top layer was removed and weighted. Syneresis was expressed as percentage of total water in the system.

4.4 RESULTS AND DISCUSSION

4.4.1 TEXTURE ANALYSIS

Due to the microstructurally largely differing nature of the samples, particularly after longer storage times, a back extrusion test was preferred for texture evaluation of the starch pastes at different moments (day 1, 7, 14, 28 and 56) throughout the preservation period. This type of test is suitable for fluid as well as gelled samples. For the fresh pastes (day 1), the composition of the systems strongly influenced their strength (Figure 4-6). Especially at the lowest starch content, there was a relatively large effect due to the presence of xanthan gum which induces a higher resistance to flow. During further preservation, the specific evolution of the textures strongly varied among the samples. Particularly the differences caused by both preparation temperatures were marked. In all cases, the pastes prepared at 72°C proved to be more susceptible to structural changes during storage, in which a slow but strong gelling occurred. Conversely, the texture of the pastes heated at 70°C remained much more constant.

The pasting behavior as described in the preceding chapter, demonstrated that the breakdown of starch granules was restricted at these mild temperatures. However, disruption of the granules cannot be fully excluded, particularly at temperatures higher than 70°C. Therefore, the presence of significant amounts of amylopectin in the continuous phase should be taken into account, particularly for the pastes heated to 72°C. Associations between these amylopectin molecules can cause the observed gelling, but enhanced interactions between peripheral amylopectin molecules in the granules may occur as well. Considering the mild preparation conditions, a large fraction of the granules is undisrupted and closely packed, which allows the formation of granule bridges. Furthermore, the higher extent of gelatinization and swelling may increase the mutual interaction or even interpenetration of neighboring granules.

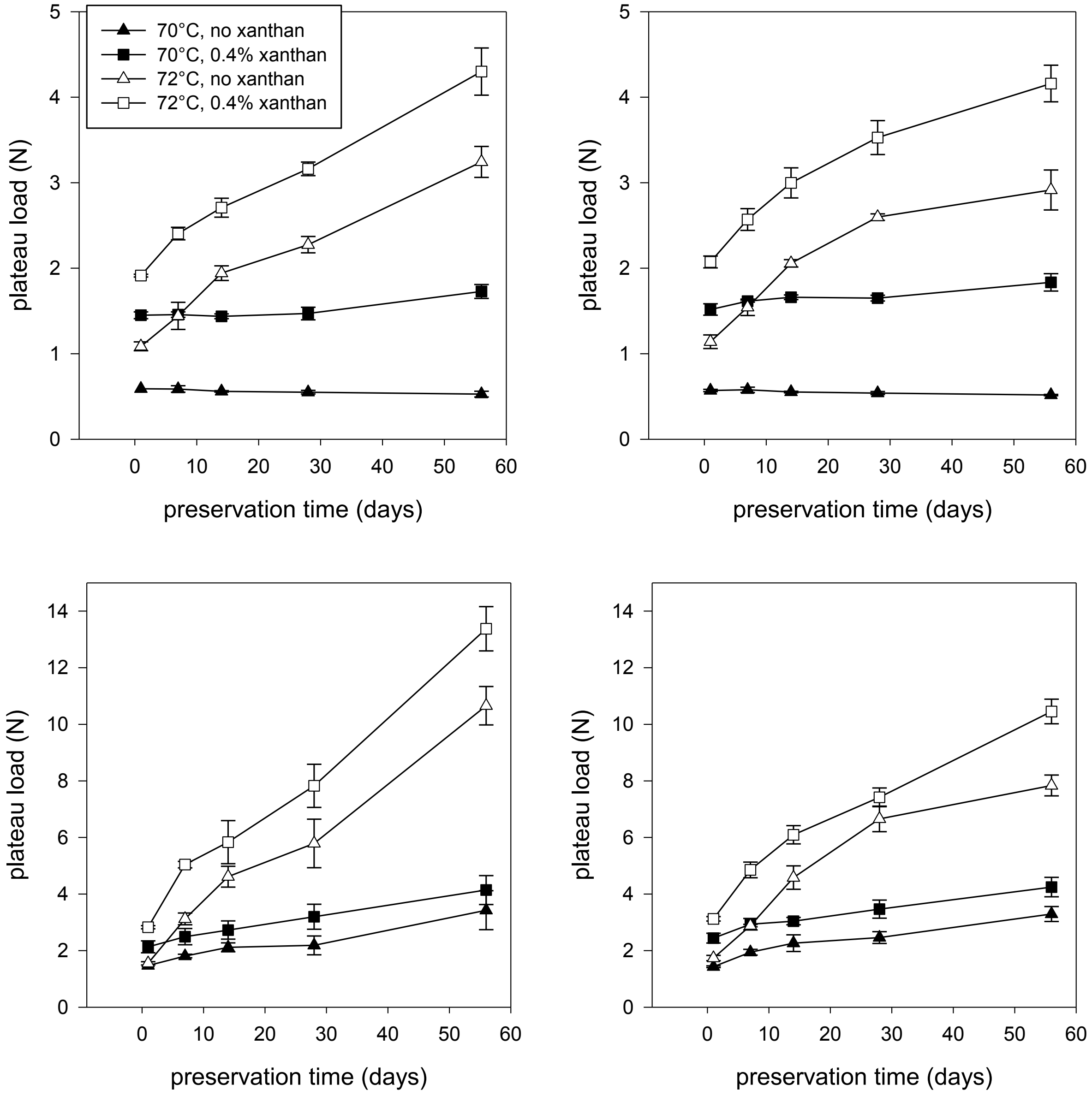

Figure 4-6: Effect of composition and preparation temperature on the textural properties of starch/xanthan pastes. Top row: starch content 5:100, bottom row: starch content 7:100. Left column: neutral pastes, right column: acid pastes.

As demonstrated in the preceding chapter, the granules of the pastes prepared at 70°C are less degraded. It can therefore be assumed that due to the large extent of granule integrity, the amylopectin largely remained inside the granules. Hence, polymer associations in the continuous phase are inhibited, resulting in a higher stability. At the highest starch content (7:100), a limited structure build up was observed for all pastes prepared at 70°C. Presumably, a higher extent of granule disruption had occurred during pasting of more concentrated dispersions. In this way more amylopectin would be present between the granules. A second hypothesis is that amylopectin molecules at the surface of the intact granules associate, inducing a network of granules, which is logically favored by the presence of a higher number of granules.

For both preparation temperatures, the texture evolution was not affected by xanthan: the texture of the xanthan free and the xanthan containing systems evolved comparably. It was suggested in chapter 3 that xanthan gum could restrict granule breakdown during pasting. This effect, however, did not result in a higher stability of the systems. At the lowest starch content, there was a limited progression in strength for the pastes heated to 70°C. This change could either be attributed to a xanthan-induced aggregation of the granules and/or the formation of xanthan aggregates. It has been suggested before that xanthan gum can affect the interparticle bonding of waxy starches through mechanisms of bridging or depletion flocculation (Abdulmola *et al.*, 1996b; Achayuthakan *et al.*, 2006), which could proceed during storage. In addition, xanthan molecules are capable of aggregating during storage, further increasing the structural features of the mixed system. However, this effect is expected to occur during the first days of storage (Rochefort & Middleman, 1987).

The differences between the acid and the neutral pastes are limited. Initially, the course of both curves is comparable, whereas the gel strength at the end of preservation is lower for the acid systems. The latter could possibly be caused by a higher extent of amylopectin hydrolysis, yielding softer gels (Sae-Kang & Suphantharika, 2006). This illustrates that the influence of acid addition is limited when dosed after the heating step. When heating is performed in acidic environment, the extent of hydrolysis is generally more profound, which leads to higher textural losses.

4.4.2 RHEOLOGY

4.4.2.1 Flow behavior

Flow curves of the pastes were recorded at fixed days during the preservation period. The strongly varying flow behavior of the different samples did not allow the use of a rheological model to fit all the obtained curves. Therefore the shear stresses corresponding with shear rates of 1 s^{-1} and 100 s^{-1} were used for sample comparison (Figure 4-7).

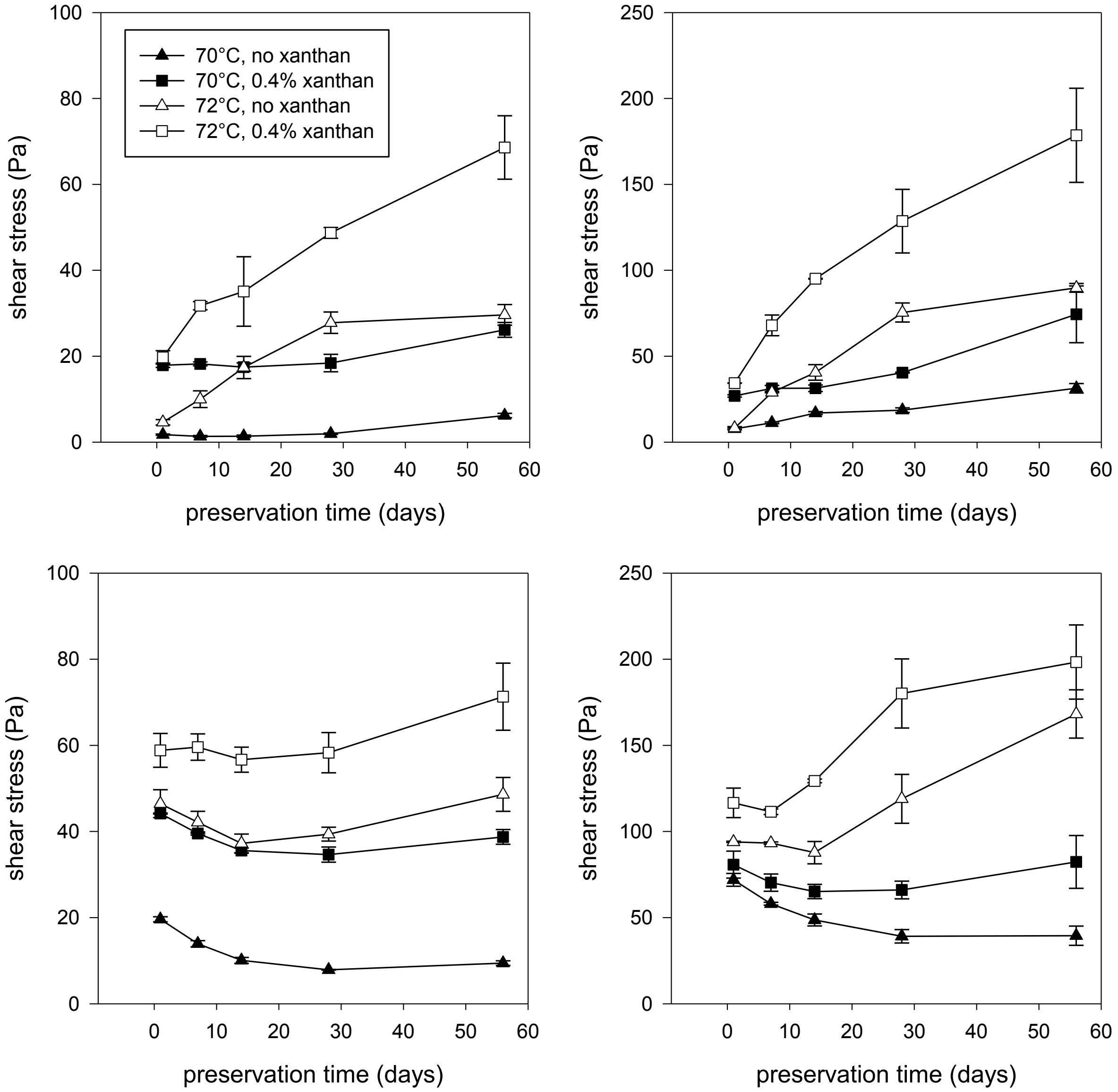

Figure 4-7: Influence of preparation temperature (70 or 72°C) and xanthan content on the evolution flow behavior of the neutral pastes during storage. Top row: shear stress recorded at shear rate 1 s^{-1}, bottom row: shear stress recorded at shear rate 100 s^{-1}. Left column: starch content 5:100, right column: starch content 7:100

At a shear rate of 1 s^{-1} the flow behavior of the fresh samples (day 1) was more affected by the composition than by the heating temperature. The samples with xanthan exhibited a higher shear stress (and hence a higher apparent viscosity) than the gum free samples. However, during storage a diverging behavior was observed between both preparation temperatures. A strong increase took place for the pastes heated to 72°C, and this behavior was slightly enhanced by the presence of xanthan. Again, the acid samples (see Figure 4-8) behaved very similar to the neutral pastes. It can therefore be stated that the findings from these flow measurements at low shear rates are entirely in line with the texture analysis.

At higher shear rates (100 s^{-1}), a different behavior was observed. Large differences between both production temperatures were present already at day 1. Furthermore, at the lowest starch content, the effect of xanthan gum was much more pronounced for pastes heated to 70°C. These results are in line with the findings from chapter 2, where a large extent of granule integrity was found to be a prerequisite for synergistic rheological effects between xanthan and starch. At this shear rate, the corresponding shear stress of the pastes heated to 70°C decreased during storage, eventually leading to a plateau value. In the presence of xanthan gum, a slight increase towards the end is suggested. For pastes heated to 72°C, a reduction was observed during the first days, but for longer storage times, the shear stress was enhanced. In combination with the results obtained at 1 s^{-1}, this indicates that the interactions developed within the mildly heated samples (70°C) – if they occur - are rather weak and can easily be disrupted by shear. This behavior is presumably caused by a network of flocculated starch granules. The occurring viscosity reduction can most likely be attributed to a shrinking of the starch granules. Morikawa & Nishinari (2000) demonstrated that the size of native potato starch granules decreased during long-term preservation. They concluded that (amylopectin) retrogradation in the granules caused the release of water. For pastes heated to 72°C, this effect also possibly occurs, accounting for the decrease at the beginning of the storage period, however, it is overruled by another phenomenon as the shear stress increases again at longer storage times. During preservation, amylopectin chains present in the continuous phase between the granules will associate and crystallize. These interactions are quite strong and are not so easily disrupted by shear. The presence of these strongly aggregated structures are most likely responsible for the observed viscosity increase. Logically, this effect is more pronounced at higher starch concentrations, due to a higher number of possible junction points.

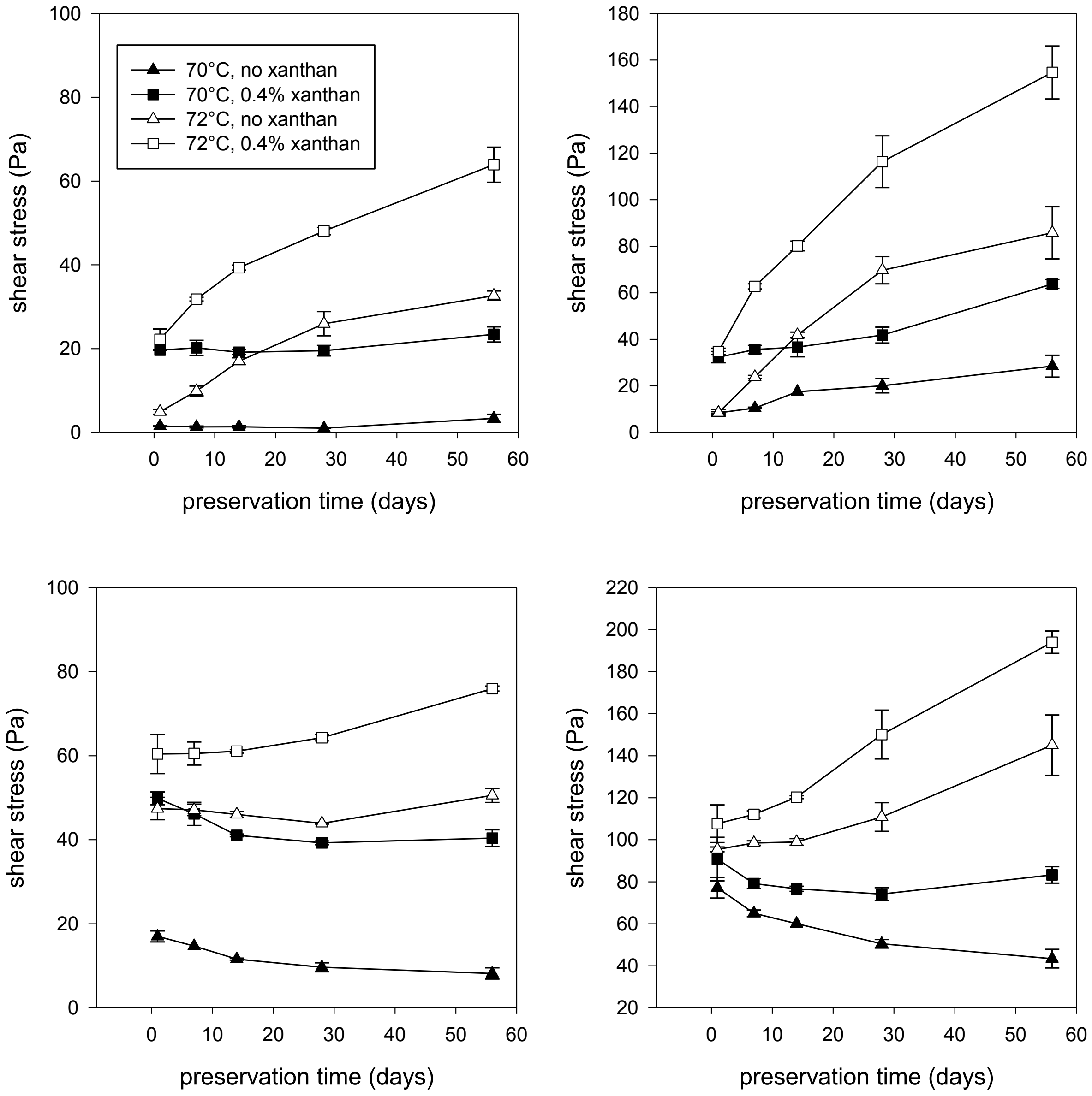

Figure 4-8: Influence of preparation temperature (70 or 72°C) and xanthan content on the evolution flow behavior of the neutral pastes during storage. Top row: shear stress recorded at shear rate 1 s-1, bottom row: shear stress recorded at shear rate 100 s^{-1}. Left column: starch content 5:100, right column: starch content 7:100

4.4.2.2 Visco-elastic behavior

So far, the samples have been analyzed rheologically by destructing their microstructure (texture analysis and flow behavior). Oscillatory rheology was performed on the samples to study their stability in a non-destructive manner. This technique provides very useful information regarding the development of the present networks and the microstructural changes occurring over time. Xanthan free samples at the lowest starch content (5:100) were not included because they exhibited a dominant viscous behavior throughout the whole storage period. In their initial state (day 1), the gum free systems with the highest starch content exhibited a dominant elastic behavior (G' > G") but with a strong frequency dependence. This behavior is typical for flocculated (micro-) gel particles at concentrations below close packing (Genovese & Rao, 2003; Kaneda & Sogabe, 2005). In the case of more severely disrupted granules (heated to temperatures > 90°C), the system would be governed by entangled amylopectin molecules, resulting in a less strong effect of the frequency on the moduli (Achayuthakan & Suphantharika, 2008; Kulicke *et al.*, 1996). As stated above, the pastes prepared at 70°C consist of more intact and rigid granules compared with the pastes heated to 72°C. This can be derived from a higher value of G' and relatively less viscous behavior (lower tan delta).

Upon the addition of xanthan gum, the viscoelastic properties are radically modified (Figure 4-9). The elastic behavior (G') is significantly increased and the moduli are much less dependent on the applied frequency. This profile, typical for weak gels, demonstrated a dominant effect of xanthan gum, where its ability to engage in strong molecular entanglements is therefore clearly reflected in the profiles of the mixed pastes. The absolute increase of G' is higher for the samples heated to 70°C than for the samples prepared at 72°C. Particularly when using non-gelling hydrocolloids, both the continuous and the dispersed phase contribute to the rheological properties (Alloncle & Doublier, 1991; Alloncle *et al.*, 1989; Samutsri & Suphantharika, 2012). In the case more disruption of the granules took place, as it is the case for pastes heated to 72°C, the volume occupied by the swollen granules is decreased and therefore the effective xanthan concentration is lower as well. Consequently, both components contribute less to the overall rheology of the system. Moreover, the continuous phase does not solely contain dissolved xanthan molecules, but consists of a complex mixture of xanthan and amylopectin, which in turn can affect the continuity of the xanthan network.

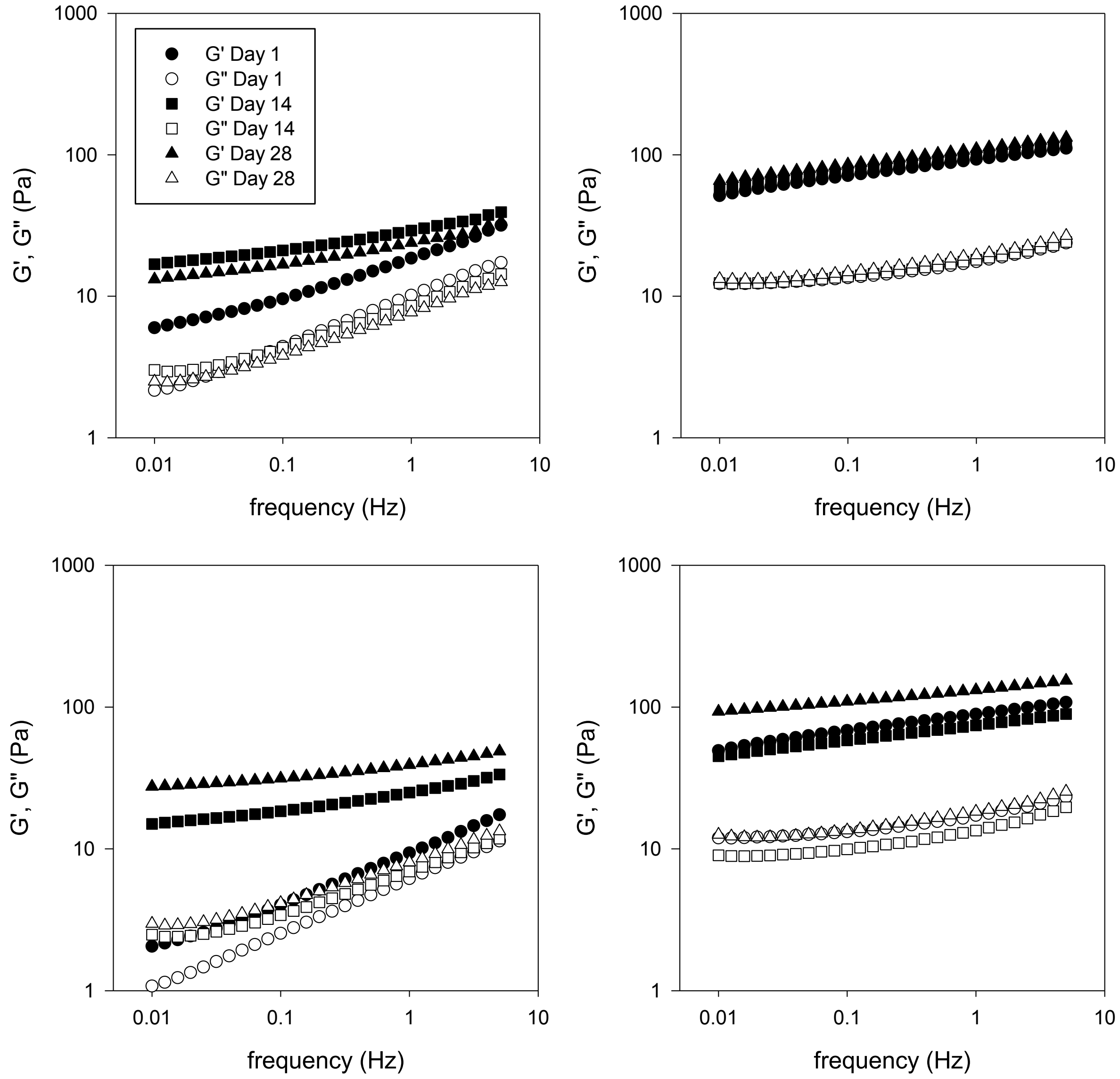

Figure 4-9: Influence of preparation temperature and xanthan content on the evolution of the viscoelastic behavior of the acid pastes (starch content 7:100) during storage. Top row: pastes heated to 70°C, bottom row: pastes heated to 72°C. Left column: no xanthan, right column: 0.4% xanthan

During prolonged storage, changes induced by different heating temperatures, result in diverging effects. For the pastes without xanthan, the increased elasticity, lower phase angle and reduced dependence of frequency suggest the creation of a gel network (Figure 4-10). In line with the preceding results, the changes are the most predominant for the systems heated to 72°C, although some marked changes also occur for the pastes subjected to the lowest temperature. The latter observation confirms that, aside from amylopectin associations within the continuous phase, interactions between flocculated intact granules are also enhanced during storage. This higher stability can be caused either by a reduced degree of retrogradation or the absence of a space-filling network (implying that the amylopectin associations occur intragranular). The exact molecular changes occurring in the pastes heated to 72°C are more difficult to assign. Rheologically, it is not obvious to distinguish a pure amylopectin polymer network from a mixed network of associated starch gel particles and dissolved molecules. Considering the pasting properties as described in the preceding chapter, a significant amount of intact granules is still present, and the latter hypothesis is more likely.

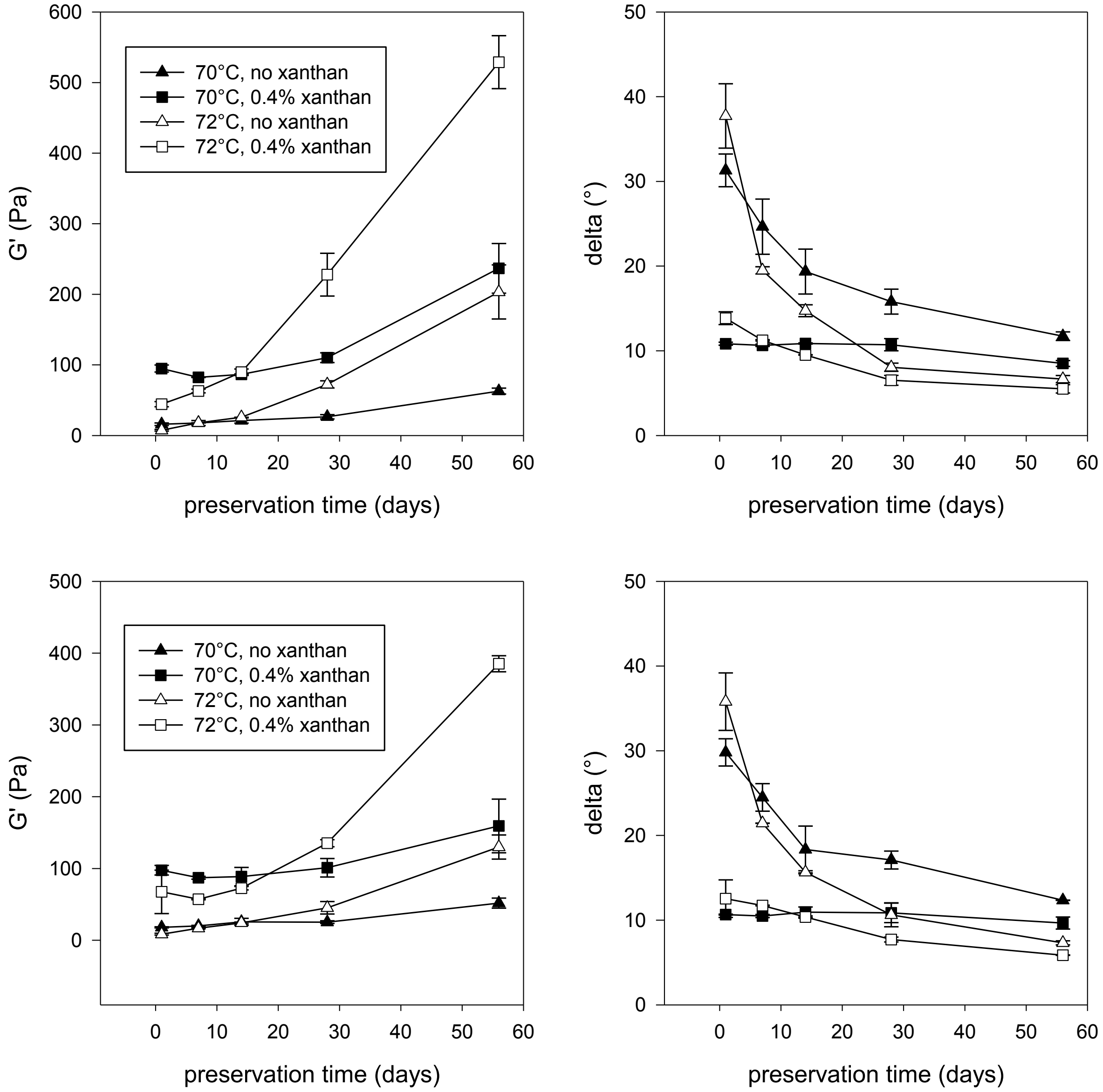

Figure 4-10: Influence of xanthan content and preparation temperature (70 or 72°C) on the evolution of storage modulus G' and phase angle delta during preservation (starch content 7:100). Top row: neutral pastes, bottom row: acidic pastes

In the presence of xanthan, the evolution of the microstructure becomes even more complicated. When prepared at the lowest temperature, the changes in elasticity are much more subtle, indicating a more limited tendency of associating. During the first 4 weeks of storage, xanthan gum even appears to exhibit a stabilizing effect, where the recorded curves vary less over time (Figure 4-9). However, the absolute changes of G’ are comparable for the xanthan free and the xanthan containing systems, and the curves of pastes with and without xanthan even diverge towards the end of the storage period. As stated higher, both xanthan and starch contribute to the viscoelastic properties of the mixed system. Due to the direct effects of xanthan gum in the bulk, the retrogradation effects occurring in the starch moiety result in relatively less changes in the overall visco-elastic behavior as illustrated in Figure 4-9. This is also visible in the nearly constant value of the phase angle delta of the xanthan systems (Figure 4-10).

For the pastes prepared at 72°C, an additive effect of xanthan on the network development is suggested as the curves of the gum free and xanthan containing pastes are explicitly diverging. These results in turn confirm that xanthan gum has no beneficial effect on the retrogradation effects. The observed effects could result from a phase separation between xanthan and the amylopectin, raising the effective concentration of the starch polymers and favoring their intermolecular associations. Another hypothesis could be that xanthan and amylopectin engage in the formation of a mixed network. The latter, however, seems unlikely considering the molecular differences between both types of polymers. Furthermore in the case of such a direct interaction, the association (which is no crystallization) is expected to occur much faster, resulting in firmer gels shortly after preparation, as it is also observed for synergistic xanthan-galactomannan gels (Lu *et al.*, 2008; Tsai *et al.*, 1997).

In general, the evolution of the visco-elastic properties is comparable for both acidity levels. For longer preservation times (> 14 days), the neutral pastes exhibit higher values of G’ and lower values of delta, which suggests the presence of a stronger network. This is particularly the case for pastes heated to 72°C. Hence, these results are in line with the texture analysis reported above. Most likely, some hydrolysis of the amylopectin chains had taken place, which results in a reduced gelling capacity.

4.4.3 STARCH POLYMER ASSOCIATION MEASURED BY T_2-RELAXATION

NMR was selected as a complementary technique to the rheological methods, which were used to characterize the macroscopic (texture analysis, flow curves) and microstructural (oscillatory rheology) properties. By evaluating the proton relaxation, information is gathered on a molecular level. As explained in the introduction, this technique is suitable for monitoring relative changes in polymer mobility, rather than for quantifying an absolute degree of crystallization. Figure 4-11 shows the initial T_2-values of all pastes. Pastes prepared at 70°C systematically exhibited lower values of this parameter than the pastes prepared at 72°C. The lower degree of gelatinization is expected to result in a higher extent of residual order and lower mobility of the starch polymers within the granules. The addition of xanthan gum always induced a faster relaxation. This could incorrectly be interpreted as a result of reduced water mobility. As stated before, proton relaxation provides little information on the state of water in these dilute systems (> 93% water). The reduction is due to the presence of an additional number of hydroxyl protons with their own characteristic relaxation time and which are available for exchange as observed for pure polysaccharide systems. Similarly, higher starch concentrations also result in lower values of T_2. Finally, there is also a marked effect of pH. The presence of citric acid induces a remarkable reduction of T_2 values. It has been stated before that pH variations significantly affect the proton exchange rate (Rabenstein & Fan, 1986). For this reason, the behavior of the neutral and acidic pastes will not be compared directly with this technique. Moreover, the relative reduction induced by xanthan gum is significantly larger at lower pH (±35% vs. ±20%). Rabenstein & Fan (1986) demonstrated that the optimal pH for the exchange of labile protons may vary among different molecules. It could therefore be assumed that in acidic conditions the exchange rate of protons originating from xanthan is more enhanced than for those originating from the starch molecules. Consequently, the starch fraction contributes less to the overall signal of the acid pastes.

In order to allow a better comparison between the different samples, the initial variation is eliminated by dividing the obtained T_2-values by the T_{20}-value. In this manner, changes relative to their initial state are represented (Figure 4-12). As expected, the transitions occurring in the acid pastes result in more explicit signal changes compared with the neutral pastes. Considering the striking similarities in rheological behavior, it can be expected that these differences are not primarily caused by an altered retrogradation behavior. Hirashima *et al.* (2012) demonstrated that the effects of different pH values on the retrogradation behavior are rather limited. The chemical exchange rate is clearly enhanced at lower pH, hence molecular changes are more explicitly manifested for the citric acid containing systems. In general, it could be stated that the signal of pastes prepared at 70°C changes slightly less over longer storage periods. This corresponds with the hypotheses proposed by Fisher & Thompson (1997): a fraction of the starch molecules remains ungelatinized, hence crystallized, and is therefore not available for retrogradation.

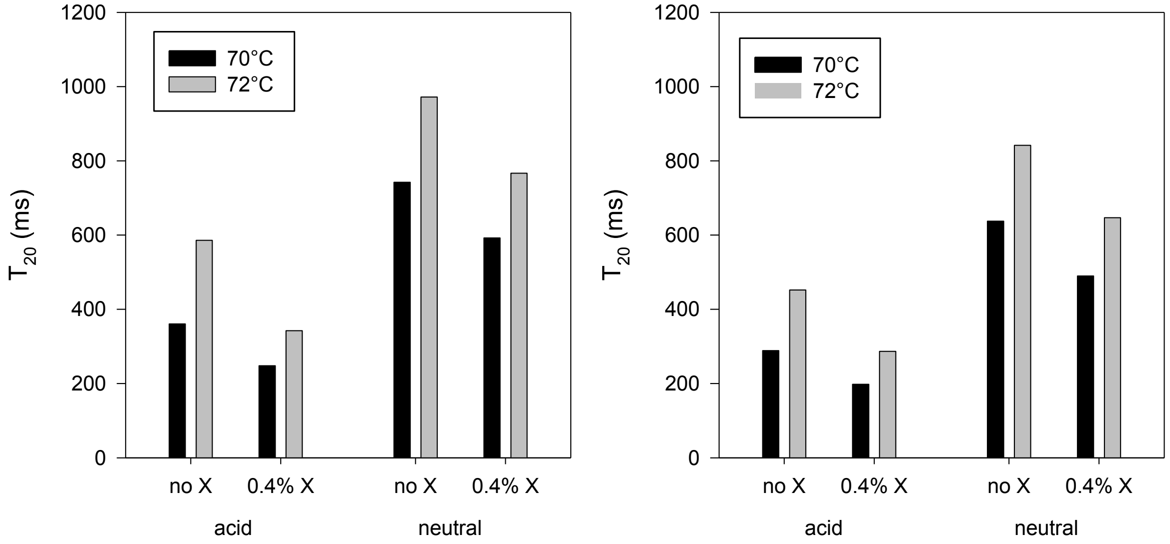

Figure 4-11: The effects of preparation temperature (70 or 72°C), acidity and xanthan content on the extrapolated T_2-relaxation times at the start of the stability experiment (T_{20}). Left: starch content 5:100, right: starch content 7:100

Xanthan can also aggregate in solutions, although this is known to proceed more rapidly. Therefore the contribution of xanthan gum associations was assumed to be negligible throughout the preservation period. However, the indirect effect of xanthan gum on the mixed pastes is more ambiguous. The data from the acidic pastes suggest a slower amylopectin reassociation and therefore a lower extent of retrogradation whereas the neutral pastes indicate the opposite effect. As stated before, the relative contribution of the xanthan fraction to the signal is higher at acidic pH. This could explain why the relative change during storage is lower in the case of the acidic starch/xanthan pastes. When interested in the state of the starch molecules, the neutral pastes might therefore be a more appropriate choice for comparison.

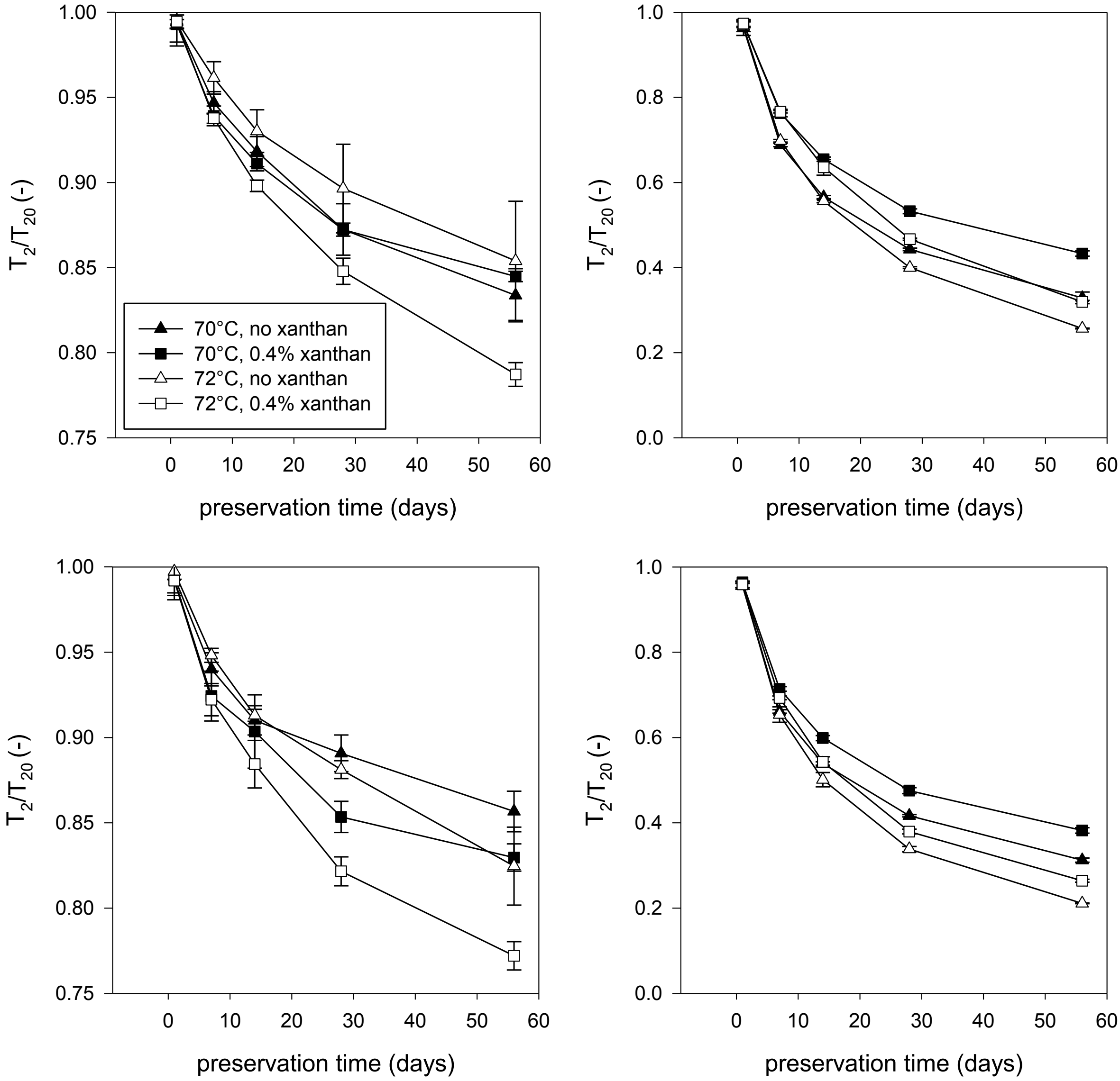

Figure 4-12: T_2-reduction during preservation as affected by xanthan content, acidity and preparation temperature (70 or 72°C). Top row: starch content 5:100, bottom row: starch content 7:100. Left column: neutral pastes, right column: acid pastes.

For the pastes prepared at 70°C, the differences between xanthan-containing and xanthan-free pastes are more limited. However, when heated to the highest temperature, there is a marked effect of xanthan as a significantly larger reduction of T_2 value is observed. This result could further evidence that xanthan gum enhances the association of amylopectin molecules provided that they are not present within the granules. As stated higher, this phenomenon could arise from phase separation between both polymers, concentrating the starch molecules in their microdomain and stimulating reassociation.

These results demonstrated that on a molecular level, strong changes take place during storage for pastes prepared at both heating temperatures. However, the rheological data demonstrated that for the pastes heated to 70°C, these changes are much less reflected in the macroscopic properties as compared with the pastes prepared at 72°C. It could be hypothesized that in the former case, molecular reassociations take place inside the granules. This should result in a reinforcement of the granules. Considering the restricted swelling at 70°C, the granules were supposed to be quite rigid from the start, and therefore this additional reinforcement only induces limited rheological changes.

4.4.4 SYNERESIS

Centrifuge tubes were filled with the different pastes after preparation and stored at 7°C. By using centrifugation, unbound water is forced out of the pastes. However, the external centrifugal forces could also induce a compression of the structure e.g. in case of a particulate network, resulting in a watery top layer after centrifugation. Data should therefore always be interpreted cautiously because both effects cannot be separated. Syneresis at the end of the storage period, expressed as relative percentage of expelled water, is listed for the different pastes in Table 4-2. The pastes with the lowest starch content that were prepared at 70°C (and without xanthan) exhibited water separation at day 1. Due to the restricted swelling of the granules, the swollen granules did not occupy a close packing volume nor created a space filling network like the other pastes. The amount of separated liquid on day 1 was subtracted from the values on day 56, to obtain an absolute change. For all the other pastes this was not required because they did not show syneresis after centrifugation on day 1.

It is clear from the data that xanthan gum inhibits the separation of liquid from the systems as its addition induces a significant reduction in syneresis at the end of the storage period. However, for the pastes prepared at 72°C - even without xanthan - syneresis was not observed at the end of the considered period. Presumably, as opposed to amylose gels, the tendency to strongly contract is much less present in amylopectin gels. As retrogradation proceeds, the network might develop without expelling water. Furthermore, it can be expected that the complex mixture of dissolved amylopectin and swollen granules is incompressible at day 1, hence sedimentation cannot be achieved through centrifugation.

The marked increase in expellable water for the pastes heated to 70°C suggests a different microstructural evolution. As mentioned above, retrogradation may result in a release of water from the swollen granules. Consequently, more water can be removed by centrifugation and indirectly, the total volume occupied by the granules decreases. The latter leads to a more dense precipitate and in turn a higher observed syneresis. As demonstrated by the centrifugation results on day 1, xanthan inhibits sedimentation of the swollen granules. This effect is believed to cause the absolute difference in separated water layer on day 1. The water expelled from the xanthan containing pastes is therefore supposedly caused by changes in water holding capacity of the granules. For the xanthan pastes, the pH value did not significantly affect the results. However, for the systems pasted at 70°C, syneresis is significantly lower in the presence of citric acid, which suggests a lower extent of contraction of the granules. However, further research is required to clarify this pH effect.

Table 4-2: Syneresis for the different compositions at the end of storage period (Day 56), expressed as % of total water

		Starch content 5:100		Starch content 7:100	
		no xanthan	0.4% xanthan	no xanthan	0.4% xanthan
70°C	acid	36.9 ± 1.7	7.6 ± 4.0	7.6 ± 2.9	0.0 ± 0.0
	neutral	44.3 ± 0.8	8.7 ± 9.9	32.0 ± 1.1	0.0 ± 0.0
72°C	acid	0.0 ± 0.0	0.0 ± 0.0	0.0 ± 0.0	0.0 ± 0.0
	neutral	3.7 ± 5.4	0.0 ± 0.0	5.6 ± 7.3	0.0 ± 0.0

4.5 CONCLUSIONS

The effects of xanthan gum addition and the use of mild preparation conditions on the long-term retrogradation behavior of waxy maize starch systems were studied in this setup. Texture analysis, rheology and pulsed field NMR were used to evaluate structural changes at different length scales.

Pastes heated to 70°C are composed of swollen and largely intact granules. These systems behaved as flocculated dispersions and the rheological evaluations demonstrated that their structural properties remained largely constant during the preservation period. Slight changes were attributed to shrinking of the granules and intensified granule associations. The addition of xanthan gum did not induce a higher stability of the starch fraction. However, due to its direct contribution to the structural features of the systems, changes occurring in the starch fraction are partly masked.

When the granules are heated to a higher temperature (72°C), the pastes contain a significant amount of dissolved amylopectin in addition to the fully swollen granules. This higher degree of gelatinization and degradation, rendered the systems structurally unstable. A slow but significant gelation was observed for the pastes heated to this temperature. This behavior was attributed to the association and crystallization of amylopectin molecules in both the continuous phase and the granules. Under these circumstances, xanthan gum was found to enhance the gelation process. A phase separation between both polymers in the continuous phase was proposed as an underlying mechanism. In this manner the effective concentration of amylopectin is raised in its microdomain, favoring molecular interactions.

The use of T_2-relaxation to monitor the molecular reassociation during preservation clearly offers some practical advantages over other techniques. The results confirm that this is a sensitive probe to detect changes in these complex matrices. Hence, this technique holds a lot of potential for future setups. On the other hand, samples with different compositions should be compared with care, because even at low concentrations acids and hydrocolloids strongly affect the overall relaxation behavior. Nevertheless, in this setup it was strongly suggested that pastes heated to 72°C exhibit a higher tendency for molecular reassociation as compared to the pastes heated to 70°C, which is in line with the rheological results.

It was previously demonstrated (see chapter 3) that the use of preparation temperatures within the gelatinization range, results in a higher extent of starch granule preservation. In this chapter it was found that as a direct consequence, the stability of the pastes is improved. However, the choice of heating temperature appears of utmost importance: a slight temperature increase could suffice to render the systems highly unstable. It was also suggested that xanthan gum may restrict the granule disruption during preparation. However, this beneficial effect on the freshly prepared pastes, did not result in an improved stability during storage.

5 INFLUENCE OF GUAR AND XANTHAN GUM ON THE SHEAR INDUCED BREAKDOWN OF WAXY MAIZE STARCH

Relevant publication: Heyman, B., De Vos, W., Depypere, F., Van der Meeren, P., Dewettinck, K. (2013). Guar and xanthan gum differentially affect shear induced breakdown of native waxy maize starch. Food Hydrocolloids (in press).

5.1 INTRODUCTION

Along with xanthan, guar is one of the most commonly used gums in combination with starches. This non-ionic polysaccharide is derived from the ground endosperm of guar seeds (*Cyamopsis tetragonoloba*). Its molecular weight is generally in the order of 5-10 x 10^5 g/mol. Guar galactomannan is composed of galactose and mannose units in 1:2 ratios. The linear backbone consists of (1→4)-linked β-D-mannose units with single α-D-galactose units attached to the O-6 position. The galactose substitutions are not randomly distributed on the main chain, but exist as so-called hairy regions (Casas *et al.*, 2000; Mudgil *et al.*, 2012).

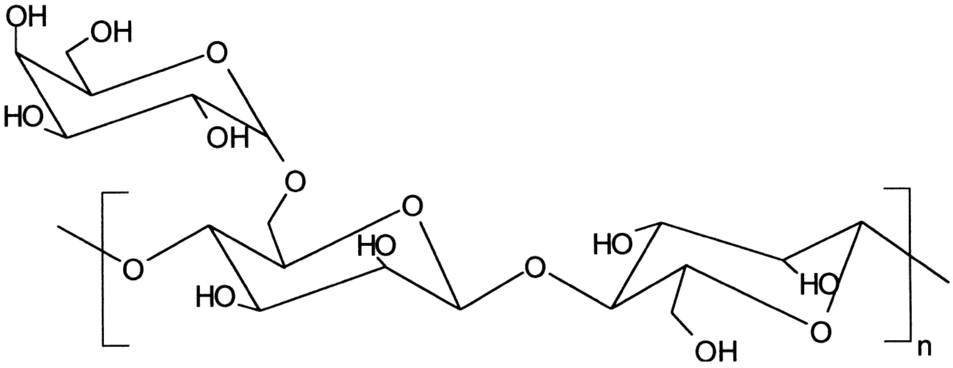

Figure 5-1: Molecular structure of guar gum (Sostar & Schneider, 1998)

Aside from their direct rheological effects, which will be treated in the next chapter, gums can also indirectly influence the rheological behavior of starch pastes by modifying the properties of the granules. When heated together, gums can affect the swelling and degradation behavior of the starch as described in section 1.3.2 and 3.1. In most experimental setups dealing with waxy starch systems, the intense heating of the starches causes extensive disruption of the granules. These treatments result in microstructurally complex systems of granule remnants and granule ghosts within a macromolecular solution of amylopectin and gums (Hermansson & Svegmark, 1996; Tsai *et al.*, 1997). Therefore, it is difficult to draw conclusions regarding the effect of gums on their swelling and degradation behavior. Furthermore, when waxy starches are heated to elevated temperatures (> 85°C, see chapter 2), differences in granule sizes hold little rheological relevance because the vast majority of the granules is disrupted and the continuous phase dominates the rheological behavior of the pastes.

As demonstrated in chapter 3, the processing of waxy starches at temperatures close to the gelatinization range, helps to limit their breakdown. Furthermore it was found that at these mild temperatures, the presence of xanthan gum induced larger granule diameters in the final paste. Although a reduced granule disruption was suggested, the exact underlying mechanism was not certain. Based on those results and the available literature, several hypotheses could be raised to explain this effect of xanthan gum:

- Xanthan gum enhances the swelling of the starch granules through a yet unknown mechanism;
- Swelling of the granules is slowed down due to competition for the available water and/or inhibited diffusion, as a result of the restricted swelling, breakdown is reduced as well;
- The presence of a viscosity increasing agent like xanthan gum reduces the turbulence inside the starch pasting cell, which diminishes the collisions of the granules during pasting and inhibits breakdown;
- The increased viscosity causes a less effective heat transfer inside the starch pasting cell, leading to a reduced thermal breakdown;
- Xanthan gum associates with the starch granule surface, hereby slowing down the diffusion of water inside the granules. This reduces the swelling and results in less disruption of the granules;
- Xanthan gum associates with the granule surface which creates a lubricating film around them and reduces the impact between the granules during pasting.

All of these proposed mechanisms appear plausible. However, due to the complexity of gum/starch systems, it is difficult to directly demonstrate the effects. The aim of this setup was to gather circumstantial evidence for one or more hypotheses, by varying the preparation conditions. Two different heating temperatures were imposed (70°C and 72.5°C) and pasting was performed under oscillatory (i.e. no shear flow) as well as under shearing conditions (50 s^{-1} and 150 s^{-1}). Furthermore, it was investigated whether the addition of guar gum can induce similar effects as xanthan gum. The comparison of both gums should clarify if the observed phenomena can be attributed to effects of the increased viscosity of the continuous phase – in this case guar should induce similar effects as xanthan gum - or to a more specific feature of xanthan gum.

Due to its anionic nature, xanthan gum is sensitive to variations in salt content, which in turn affects its functionality when combined with starches (Samutsri & Suphantharika, 2012; Viturawong *et al.*, 2008). Throughout the chapter, a salt concentration of 0.01M will be maintained for the major part of this setup, however, the effect of varying salt concentrations will be briefly touched as well.

5.2 MATERIALS AND METHODS

5.2.1 GUM STOCK SOLUTIONS

The preparation of the xanthan gum stock solutions is described elsewhere (see section 2.2.2). Guar gum (Viscogum MP41230) was acquired from Cargill Texturizing Solutions (Ghent, Belgium). Guar gum stock solutions (1L) were prepared by dissolving the gum powder (0.8% w/v) in deionized water by means of a magnetic stirrer, followed by heating to 70°C and continued stirring at room temperature for 4 hours. NaCl was added at a concentration of 0.01M. Both hydrocolloid stock solutions were allowed to rest overnight (at 5°C) before use.

5.2.2 PASTING EXPERIMENTS

The same type of native waxy maize starch was used as described in the preceding chapters (Merizet 300, provided by Tate & Lyle Benelux). The starch powder was suspended either in a 0.01M NaCl solution (for preparation of the gum-free pastes), or in a mixture of the NaCl solution and gum stock solutions. In this manner, starch slurries were obtained with three different gum concentrations in the continuous phase: 0%, 0.2% and 0.4% (w/v), all of which had a salt concentration of 0.01M NaCl. The resulting starch:solvent ratio in all cases was kept constant at 5:100 (w:w).

The dispersions were transferred to the starch pasting cell of the rheometer (see 2.2.4.2). Starch suspensions were pre-sheared at 100 s^{-1} for 2 minutes and then heated to either 70°C or 72.5°C at a heating rate of 3°C/min, held isothermal for 10 minutes and then cooled down to 20°C (5°C/min). Throughout the heating and cooling steps a shear rate of either 150 or 50 s^{-1} was maintained.

A similar time-temperature combination was employed for the preparation of the 'unsheared' samples. A heating ramp of 3°/min was imposed and the granules were sheared at 100 s^{-1} to avoid sedimentation until a temperature of 70°C was attained and granules started to swell. Preliminary tests at varying shear rates and temperatures ($\leq$70°C) demonstrated that these preparatory steps had a negligible effect on the paste properties. From this temperature onwards an oscillatory step was imposed with constant stress (1 Pa) and frequency (1 Hz). The set point temperature (70°C or 72.5°C) was maintained for 10 minutes and subsequently the sample was cooled to 20°C at 5°/min.

Following these temperature/shear treatments, the cooled samples were recollected and stored for 24h in the refrigerator (5°C) for further analysis.

5.2.3 FLOW CURVES OF GUM SOLUTIONS

To characterize the continuous phases of the unheated starch dispersions, starch was suspended in the gum solutions as described for the pasting experiments. Without prior heating, the suspensions were centrifuged (Sigma 4K15, Sigma GmbH, Germany) at room temperature (8000g, 15 minutes). In this manner, viscosity differences induced by the gum powder (small amounts solutes and salts) are taken into account. The supernatant was transferred to an AR2000ex rheometer (TA Instruments, New Castle, USA), using 28mm conical concentric cylinders (gap of 500 µm between the inner and outer cylinder) with solvent trap to limit evaporation. A sample size of approximately 20g was used. Subsequent to an equilibration step at the desired temperatures, flow curves were recorded at 20°C and 72.5°C by logarithmically increasing the shear rate from 0.001 s^{-1} to 1000 s^{-1}.

5.2.4 PARTICLE SIZE DISTRIBUTION

The particle size distributions of the cooled starch pastes were determined by laser light scattering as described in section 2.2.5.

5.2.5 FLOW CURVES OF THE PASTES AFTER COOLING

The flow curves of the pastes were recorded and subsequently fitted to the Herschel-Bulkley model (see equation 2-1). When fitting the flow curves of the guar containing pastes, a yield stress close to zero was observed. This is a consequence of the steeper slope of the flow curve at low shear rates, leading to an underestimation of σ_0 by extrapolation of the model. Therefore, the yield stress was predetermined and its value was fixed in the Herschel-Bulkley equation before fitting. The yield stress was estimated by plotting the apparent viscosity as a function of the shear stress. The stress at which a sudden drop in apparent viscosity was observed, was assigned as the yield stress. For the sake of uniformity, this approach was also used for the xanthan containing pastes and the gum free pastes.

5.2.6 OSCILLATORY RHEOLOGY OF COOLED PASTES

Frequency sweeps of the cooled pastes were recorded using the 40 mm cross hatched steel plate-plate geometry with solvent trap. To prevent drying of the sample, 1 ml of water was brought in the solvent trap compartment. The gap was set to 1000 µm. The samples were allowed to equilibrate for 15 minutes. Subsequently the frequency sweeps were recorded from 0.01 to 5 Hz (the frequency was increased logarithmically) at a stress amplitude of 1 Pa. This value was within the linear visco-elastic region of the samples, as determined by recording stress amplitude sweeps.

5.2.7 COVALENT LABELING OF THE GUMS

Gums were labeled with fluorescein isothiocyanate (FITC, Sigma-Aldrich, Germany) by a procedure adapted from Tromp *et al.* (2001). For this reaction polysaccharide (250 mg), FITC (40 mg), pyridine (100ml), and dibutyltin dilaurate (20 ml) were dissolved in dimethyl sulfoxide (DMSO) (25 ml). The reaction mixture was heated for 4 h at 100 °C, precipitated with isopropyl alcohol (100 ml) and centrifuged for 30 min at 9000g. The labeled gums were dissolved in water (50ml, deionized for guar gum, 0.1M NaCl for xanthan gum) and precipitated with isopropyl alcohol (2 times). The polysaccharide was redissolved in hot water (50 ml) and dialysed against NaCl-solution (0.1 M; 4x4l) and deionized water (4x2l). Finally, the samples were freeze-dried. Guar gum was also labeled with 5-([4,6-Dichlorotriazin-2-yl]amino)fluorescein hydrochloride (DTAF, Sigma-Aldrich, Germany), based on the procedure described by Wei *et al.* (2011). Guar gum (300 mg) and DTAF (10mg) were separately dissolved in 50ml of sodium carbonate buffer (0.1 M, pH= 9.5). After mixing both solutions, the mixture was stirred gently at room temperature overnight. The labeled polysaccharide was precipitated with isopropyl alcohol and redissolved in water twice. For further purification, dialysis was performed using 4x4l of NaCl solution (0.1M, pH adjusted to 9.5) and 4x4l of deionized water. The labeled guar was freeze-dried and stored. All dialysis purifications were performed using a cellulose membrane with a molar mass cut off of 12,000–14,000 g/mol (Spectra/Por 2, Spectrum Europe, Breda, The Netherlands). Dialysis duration was determined by deriving the dialysis time required for full visual decoloration of a non-reacted solution of gum and coloring agent within the membrane.

5.2.8 CONFOCAL LASER SCANNING MICRSOSCOPY

Starch pastes containing labeled gums were prepared similarly to the procedure described in section 5.2.2, but in this case the starch to solvent ratio (w:w) was 3:100, to allow a better distinction of the swollen granules in the micrographs. The pastes were heated to 72.5°C at a shear rate of 50 s^{-1} and subsequently analyzed by transferring a small amount (200µl) to glass bottom dishes (MatTek corp., MA, USA). The samples were examined under a confocal microscope (Nikon A1R; Nikon Instruments Inc., Paris, France), using a 60x/1.4 oil Plan Apo objective. A multi-line Ar laser was used for excitation (488 nm) and fluorescence was detected through a 525/50 nm band-pass filter. The pinhole was set to 1 A.U. Digital image files were acquired in at a resolution of 0.41µm/pixel and annotated using FIJI, a packaged version of ImageJ freeware (Rasband, W.S., ImageJ; US National Institutes of Health, Bethesda, MD, http://www.fiji.sc).

5.2.9 STATISTICAL ANALYSIS

IBM SPSS Statistics software (version 20, SPSS inc., Chicago, USA) was used for statistical comparison of the rheological data. Analysis of variance was carried out to determine significant differences between the results, followed by Tukey's post hoc test for pairwise comparisons. All tests were performed at a 95% significance level.

5.3 RESULTS AND DISCUSSION

5.3.1 FLOW BEHAVIOR OF THE GUM SOLUTIONS

The hydrocolloid solutions that were later on used to perform the pasting experiments, were first rheologically characterized. Two concentrations were selected for both hydrocolloids: 0.2% and 0.4% (w/v). The flow curves of the obtained gum solutions were recorded at two temperatures: 20°C and 72.5°C (example curves are depicted in Figure 5-2). The curves confirm a strong shear thinning behavior of xanthan gum as the viscosity drops over several logarithmic scales with increasing shear rate. This effect was less pronounced for guar gum solutions. Xanthan molecules are subject to strong disentanglement and alignment under shear. At 20°C, viscosity differences between the solutions are therefore strongly shear rate dependent. Initially the xanthan solutions exhibit the highest viscosity, but at more elevated shear, the solution containing 0.4% guar exceeds the xanthan solutions. At 72.5°C the viscosity of all solutions is markedly reduced. The temperature increase strongly affected the xanthan solutions, due to the occurrence of a xanthan transition. At this NaCl content (0.01M), the T_m is situated below 70°C (see chapter 2). For high molecular weight samples, this transition is accompanied by a viscosity reduction (Capron *et al.*, 1998b; Choppe *et al.*, 2010; Milas & Rinaudo, 1986). Guar gum is not subject to conformational transitions, hence the thermal effect on guar gum is more limited. For this temperature, the order of the flow curves is preserved over the whole shear rate range: 0.4% xanthan > 0.4% guar > 0.2% xanthan > 0.2% guar.

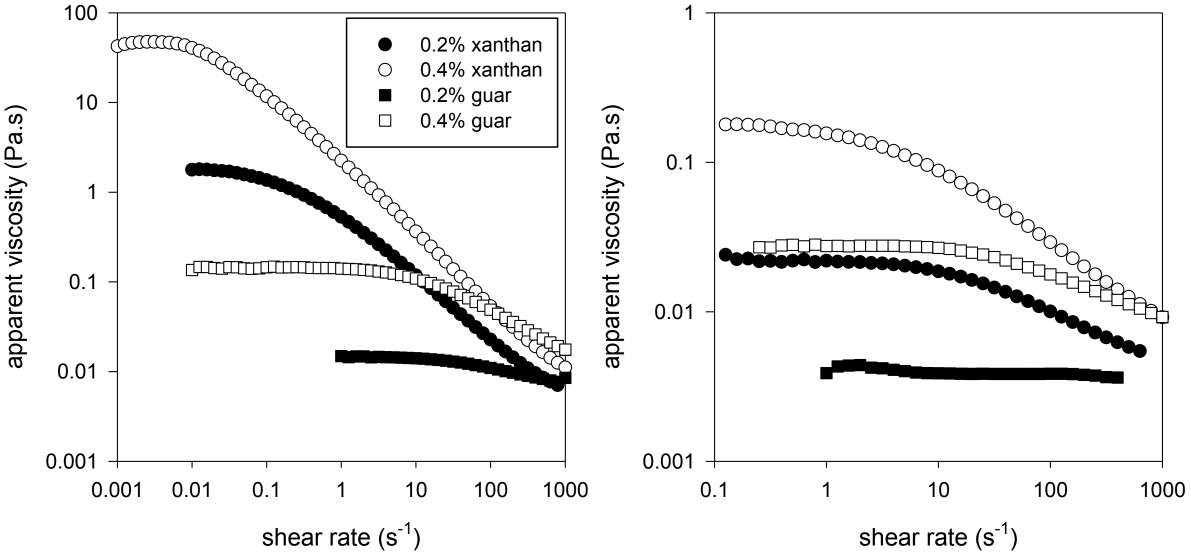

Figure 5-2: Flow curves of gum solutions: 0.4% xanthan (○), 0.2% xanthan (●), 0.4% guar (□) and 0.2% guar (■) at 20°C (L) and 72.5°C (R) and a NaCl concentration of 0.01M

Gums can affect the pasting properties of starches in various ways, as described in section 1.3.2. Some of these phenomena could directly result from the increased viscosity of the continuous phase for example by slowing down the convective heat transfer (and hence the effective heating rate of the granules) or by changing the turbulence in the cell during pasting. In this regard it is particularly interesting to compare the samples containing 0.4% guar gum with the samples containing 0.2% xanthan gum. If the previously reported effects of xanthan gum are caused solely by a viscosity effect during pasting, this should be more pronounced in the case of the 0.4% guar gum solution, which exhibits an even higher viscosity at the shear rates and temperatures studied here. However, it should be remarked that the effective gum concentration in the pastes increases due to water absorption of the starch granules. Hence, the presence of simultaneous swelling and degradation phenomena complicate the calculation of effective gum concentrations. Part of these difficulties can be overcome by using chemically cross-linked starches, which will be demonstrated in chapter 6.

5.3.2 EFFECT OF GUM SOLUTIONS ON THE PASTING BEHAVIOR

Similar to the setup of chapter 3, the maximum temperature of the pasting experiments was set to either 70°C or 72.5°C. The gelatinization temperatures were not significantly affected by the presence of both gums at the concentrations studied here (data not shown). Figure 5-3 depicts the pasting curves of the different samples when pasted at 50 s^{-1}, the curves are the average of three replicates. Comparable curves were obtained at a shear rate of 150 s^{-1} (not depicted). This mild temperature pasting behavior is elaborately described in chapter 3. The exhibited breakdown (i.e. viscosity reduction following the peak) is lower in the presence of both gums, and the lowest breakdown was observed for the xanthan-containing paste. From these graphs it is also clear that the additive effect of guar gum to the viscosity of the hot paste is larger than the contribution of xanthan gum.

Remarkably, the order of the pasting curves at the isothermal step differs from the order observed in the flow curves of the gum alone systems. Although there is a strong correlation between with the viscosity of the dispersion before the pasting onset, the situation changes as the granules start to swell. These differences could result from an indirect effect, where both gums differently influence the interaction, swelling or degradation of the granules, or it could result from a direct effect in which both gums deliver a differential contribution to the overall viscosity. Furthermore, aside from the location, the shape of the pasting curves is affected as well. Whereas the effect of guar gum is primarily additive – the curves have shifted to higher values – xanthan gum changes its shape. The peak is less prominent in the presence of xanthan gum and the viscosity build up proceeds more slowly. These results suggest that both gums affect the pasting process of waxy maize starch differently.

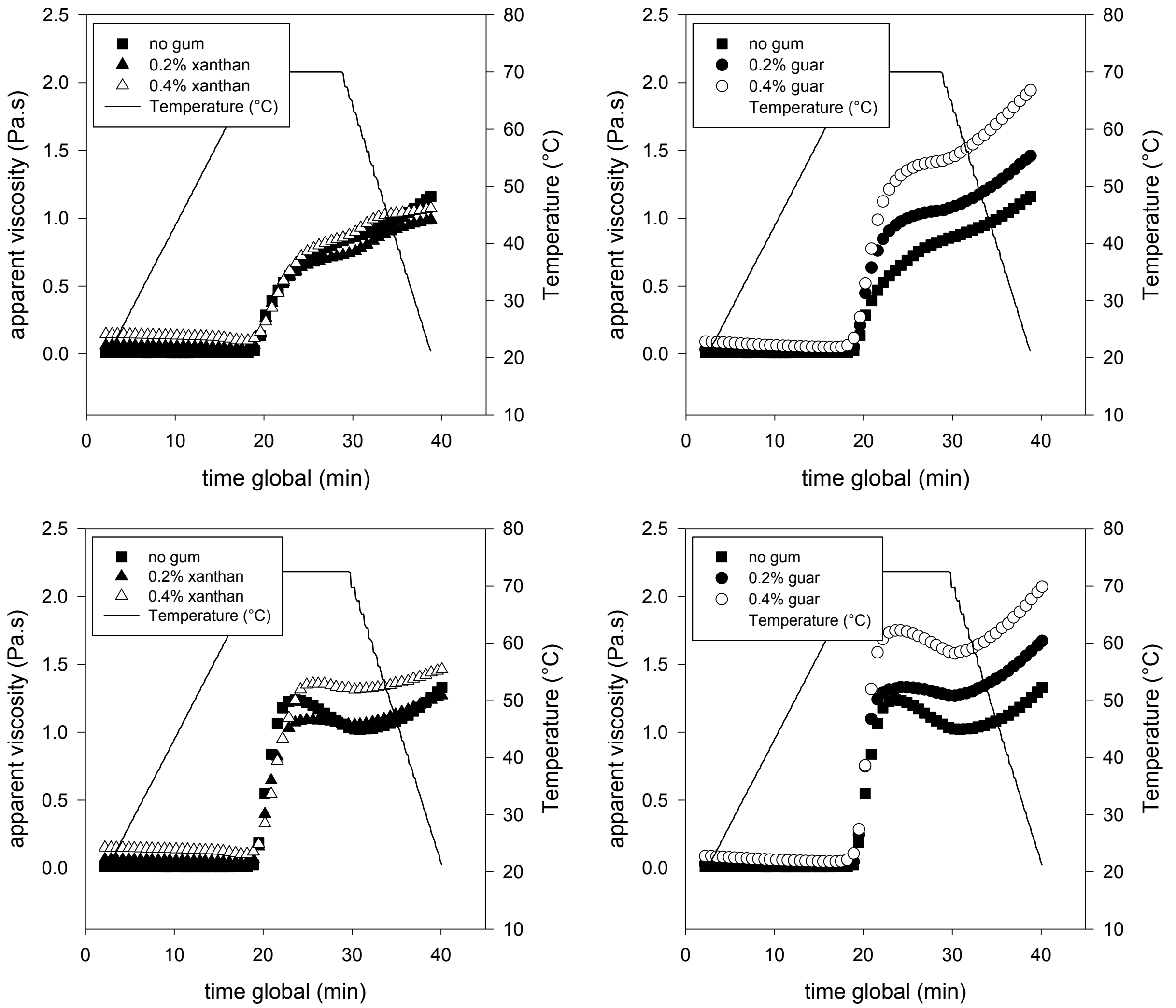

Figure 5-3: Effects of xanthan (left column) and guar (right column) on the pasting behavior of waxy maize starch (starch:solvent ratio = 5:100) at 70°C (top row) and 72.5°C (bottom row) and at a shear rate of 50 s^{-1}

In most setups dealing with starches and xanthan gum, salts are either not added or high salt contents (> 0.1M) are used to stabilize the helical xanthan gum conformation. For these waxy maize starch/xanthan systems, the comparison between 0.01M NaCl and 0.1M NaCl is described elaborately in chapter 3. Both salt contents not only affected the xanthan conformation but also induced differences in gelatinization temperature, which complicated the comparison of the samples when pasted at these moderate temperatures. Furthermore, it should also be interesting to study the effects for a system where no salt is added.

Figure 5-4 illustrates the differences between a system containing 0.01M NaCl and a system without added salt. The changes caused by these low salt differences are surprisingly high. The salt free (of course salts are never absent, but present in both the gum and the starch powder) system better resembles the additive behavior of xanthan as it is more often documented (Achayuthakan & Suphantharika, 2008; Viturawong *et al.*, 2008) and exhibits a pasting behavior similar to the guar gum systems as described above. In this case the curves are shifted to higher viscosities and breakdown is more explicitly manifested. A closer look into the rheological behavior of the pure gum solutions partly clarifies the observed differences in pasting behavior. The flow behavior of 0.2% xanthan solutions with 0.01M NaCl versus without added NaCl is shown in Figure 5-4. At 72.5°C the solution without salt exhibits a significantly higher viscosity. This could explain the viscosity differences recorded during pasting of the starch samples. It can be assumed that for both salt contents, the xanthan molecules were present in the random coil conformation at 72.5°C, but the presence of 0.01M NaCl causes a stronger shielding of the anionic charges, hence reducing the hydrodynamic volume of the polymer. Apparently, at 0.01 M NaCl an interesting condition is created, in which the viscosity of the xanthan solution is very low, but on the other hand is capable of strongly dominating the flow within the starch suspension. It should be noted that the pasting curve of the gum free systems also differed between both salt contents (0 M and 0.01M NaCl), due to a slight shift in gelatinization temperature. In order not to further increase the number of variables, a salt content of 0.01M was maintained throughout the rest of this setup.

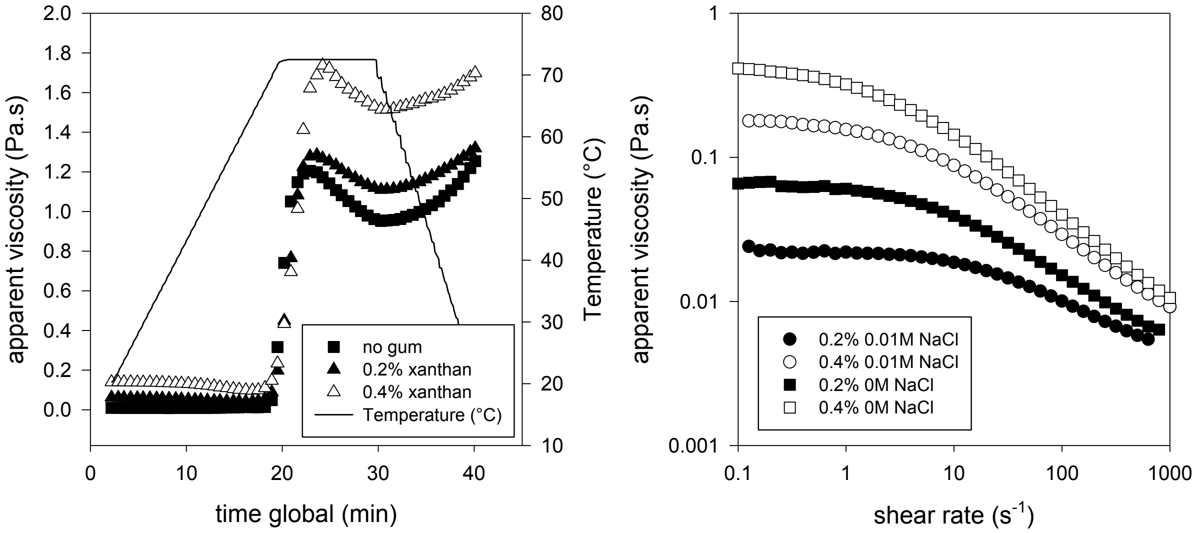

Figure 5-4: Effects of xanthan concentration on the pasting behavior of waxy maize starch (starch:solvent ratio = 5:100) without added salt (L) and effects of NaCl on the flow behavior of xanthan solutions at 72.5°C (R)

5.3.3 PARTICLE SIZE DISTRIBUTION

Pastes prepared at three different shearing conditions (no shear, 50s^{-1}, 150s^{-1}) and two temperatures (70 and 72.5°C) were analyzed by laser diffraction. To limit the size of the experimental setup, three compositions were studied: no gum, 0.2% xanthan gum and 0.4% guar gum. The choice for these gum concentrations was based on their rheological properties, as mentioned above. The different imposed shear rates during pasting clearly affected the particle size distributions (PSD). When the shear rate is increased, the PSD gradually shifts to lower values and the peak is broadened (Figure 5-5). It is difficult to capture both effects in one averaged diameter, therefore preference was given to plotting the whole curve. The depicted curves are the average of three (independent) repetitions. The clear differences between the varying shear rates demonstrate that granule degradation effects take place even for the systems where no peak was observed in the pasting curves. When a starch paste is heated above the gelatinization onset temperature, a fraction of the granules will gelatinize very quickly and break up, even at these low temperatures. This however does not necessarily result in a reduction in paste viscosity because this effect is overruled by the other granules which are still swelling. Therefore, the absence of a viscosity drop does not indicate the absence of granule disintegration. When an actual drop is observed (i.e. breakdown is exhibited in the pasting curve), this means that degradation effects have become predominant. As expected, the effect of shear is more pronounced at the highest temperature (72.5°C). This slight increase in temperature not only enhances temperature induced breakdown – which is visible by comparing the unsheared samples at both temperatures – but also results in stronger shear effects.

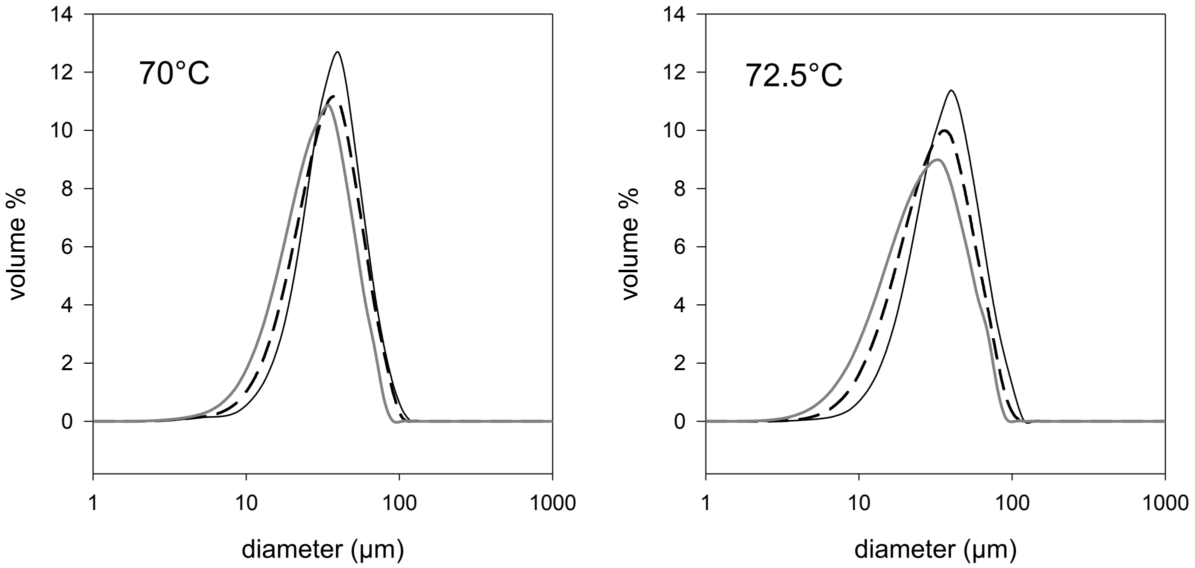

Figure 5-5: Effect of shear (__: no shear; ---: 50 s^{-1}; __: 150 s^{-1}) and temperatures imposed during pasting on the particle size distribution of waxy maize starch dispersions (starch:solvent ratio = 5:100, without gum)

Figure 5-6 illustrates the effects of the gums at different pasting conditions. For the unsheared samples, the granule size of the xanthan system strongly resembles the gum free paste. In the presence of guar gum, the curve is slightly shifted to lower diameters. However, when the highest shear rate (150 s^{-1}) was imposed during preparation, the differences between the compositions become more apparent. The granule sizes are clearly larger in the presence of xanthan. Remarkably this effect is not noticeable when guar gum is present. In fact, at 72.5°C the granules in the guar paste exhibit a very broad distribution and appear even more damaged than the granules in the pure starch system. From the viscosity drop in the pasting curves, a lower extent of granule disintegration in the presence of xanthan gum was expected, but this was also suggested for the guar gum systems. Although the paste viscosity is strongly related to the volume occupied by the granules, pasting data should be interpreted with caution, particularly when comparing gum free with gum containing systems. The contribution of the gum to the rheological properties of starch pastes is strongly determined by the integrity of the granules (Closs *et al.*, 1999). In case the granules are largely intact, waxy starch pastes can be considered as swollen granules within a concentrated gum solution. When the granules are more disrupted, the rheological properties are governed by the continuous phase, which is in turn dependent on the phase behavior of the gum and the dissolved amylopectin molecules. Consequently, the synergistic effect of gums is not simply additive over the entire range of the pasting curve. As breakdown increases in the course of the process, the system changes from a gum-continuous starch dispersion to a macromolecular solution consisting of amylopectin and gum polymers. These factors can give rise to a different viscosity drop at a similar extent of actual granule disruption (Chantaro *et al.*, 2013) and complicates the comparison of systems with different compositions.

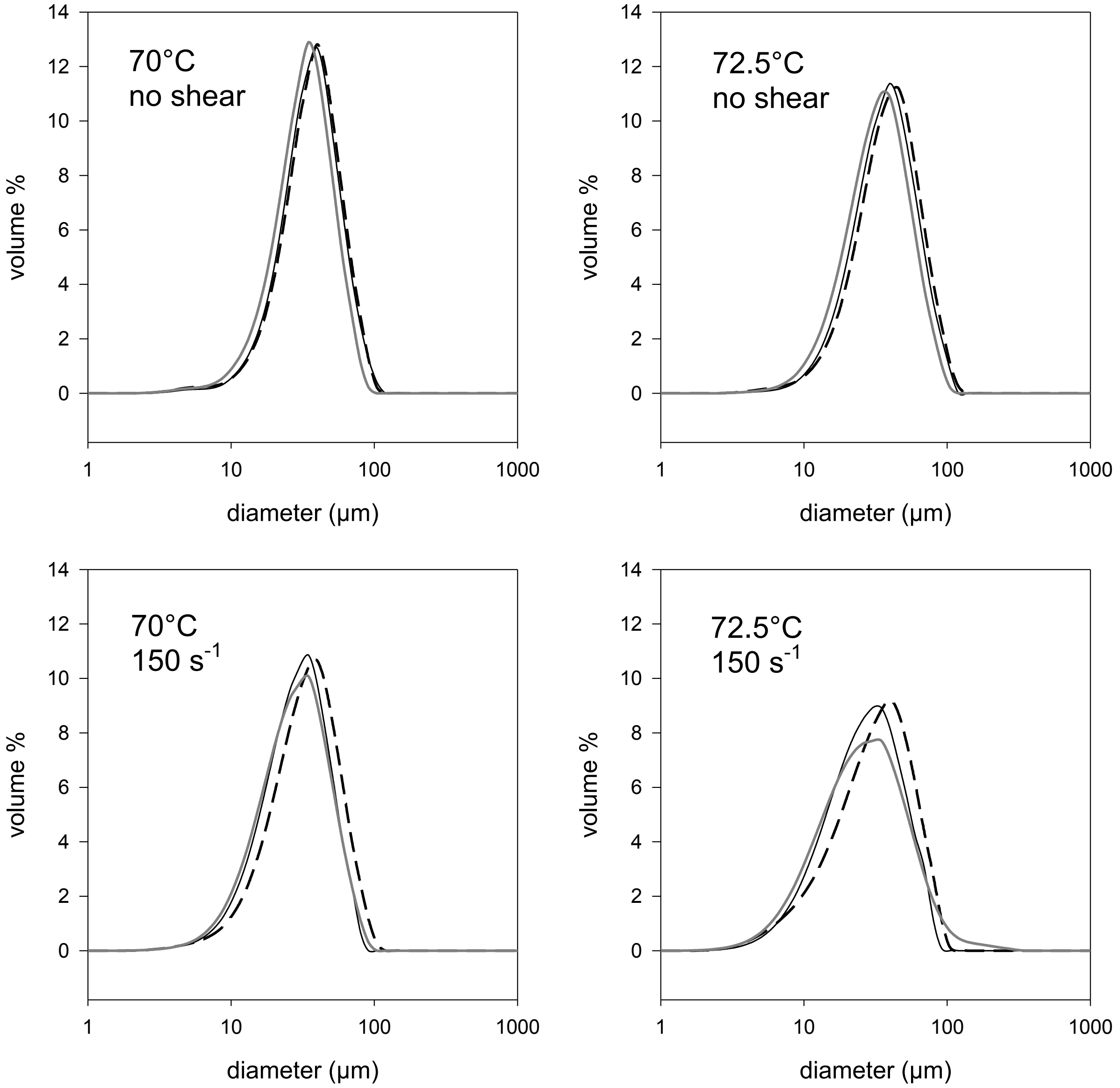

Figure 5-6: Effect of gum presence (black: no gum; dotted: 0.2% xanthan; grey: 0.4% guar) on the particle size distributions after varying temperature and shear conditions during pasting

Several hypotheses could be postulated in order to explain the higher granule size in the presence of xanthan gum. By including samples that have not been subjected to shear, some of these mechanisms can be refuted. If xanthan gum should slow down the swelling of the granules, leading to less disruption, the particle size distribution of the unsheared samples containing xanthan is expected to be lower than the gum free system. This is definitely not the case. On the contrary, this effect is more likely displayed for the samples containing 0.4% guar gum, which show slightly lower diameter sizes. Conversely, because the particle size distributions of the unsheared samples with and without xanthan are very similar, an enhanced swelling induced by xanthan gum can also be excluded.

It has also been suggested that due to their high viscosity, gums induce a slower heat transfer. This could result in a reduced (thermal) degradation of the granules. Because both gums increase the viscosity (the guar solution is even more viscous than the xanthan solution), similar effects should be observed for both gums, but this was clearly not the case. However, it should be noted that when performing pasting experiments with rapid visco-analyzers or Brabender amylographs using high heating rates, the medium viscosity could change the actual heating rate. With the accurate temperature control in the starch pasting cell and the rather low heating rate, this effect is kept to a minimum in the current setup.

Consequently, it can be concluded that the larger granule size in the presence of xanthan is induced by effects of shearing. Gums increase the viscosity of the continuous phase which can affect the impact between starch granules by reducing the turbulence within the starch pasting cell (Walstra, 2003). A higher viscosity of the continuous medium gives rise to lower Reynolds number (i.e. less turbulence). Building further on the viscosity profiles of the gum solutions, this would mean that there should be less turbulence in the systems containing 0.4% guar than the systems containing 0.2% xanthan. Therefore, the guar pastes should have resulted in a higher extent of granule preservation. This was not the case, these observations rather indicate a specific feature of xanthan gum, which is not exhibited by guar gum. Hence, it can be stated that under these conditions, xanthan can reduce the shear induced breakdown of waxy maize starch, and this property is not induced by a viscosity effects, nor is it the result of competition for the available water.

A first possibility could be the presence of shear induced anisotropy of xanthan gum. Within a flow field, the elongated xanthan molecules strongly align to reduce their molecular excluded volume, hence leading to mesomorphic organization (see also section 1.1.5). This property is observed for both the ordered and disordered state (Laneuville *et al.*, 2013). The strong alignment of the xanthan molecules between the starch granules could guide them in a specific flow pattern, in which mutual friction and turbulent collisions are restricted. Unfortunately, little information is available on how mesophase formation in the continuous phase affects the flow of dispersions.

A second possible explanation is the specific association of xanthan gum with the surface of the starch granules. Several authors claim the unique ability of xanthan gum to enwrap starch granules (Chaisawang & Suphantharika, 2005, 2006; Gonera & Cornillon, 2002). If xanthan is associated with the outside of the granules, it might act as a physical barrier, slowing down the diffusion of water molecules into the starch granules. As a result, the granule swelling would occur more slowly. It was proposed before (see chapter 2 and 3) that this association could also modify the manner in which starch granules interact during pasting. A concentrated xanthan film surrounding the granules might also act as a lubricating layer, reducing the friction exerted during granule collisions. This property of granule association is studied more in detail in the following paragraph.

5.3.4 CONFOCAL LASER SCANNING MICROSCOPY

Gonera & Cornillon (2002) demonstrated that DTAF-labeled xanthan associated with the surface of unheated and heated normal maize starch. Xanthan gum also appeared to cover the surface of heated cationic and normal tapioca starch (Chaisawang & Suphantharika, 2005, 2006). The same authors concluded that guar gum did not have this ability. The authors remain vague regarding exact mechanism, but non-covalent interactions like hydrogen bonding, van der Waals forces, which are also proposed for xanthan-galactomannan interactions, appear very likely (Tako *et al.*, 2010). In all of those setups, the possible interaction of xanthan gum with amylose could have caused these results because they dealt with non-waxy starches, for cationic starches an electrostatic interaction was suggested as well. This specific feature of xanthan has not been demonstrated in waxy starch systems, which are essentially free of amylose.

Both guar gum and xanthan gum were covalently labeled with a fluorescent dye. After intensive purification, they were dissolved and subsequently cold mixed with the waxy maize starch and pasted at 72.5°C in the starch pasting cell (at 50 s^{-1}). For the xanthan systems, the effects of the NaCl concentration were studied as well (0 M, 0.01M). Figure 5-7 depicts some representative micrographs of each system. It should be marked that the CLSM-micrographs are taken from samples with a starch to solvent ratio of 3:100 (w:w) which allowed the granules to swell more freely, causing slightly larger dimensions.

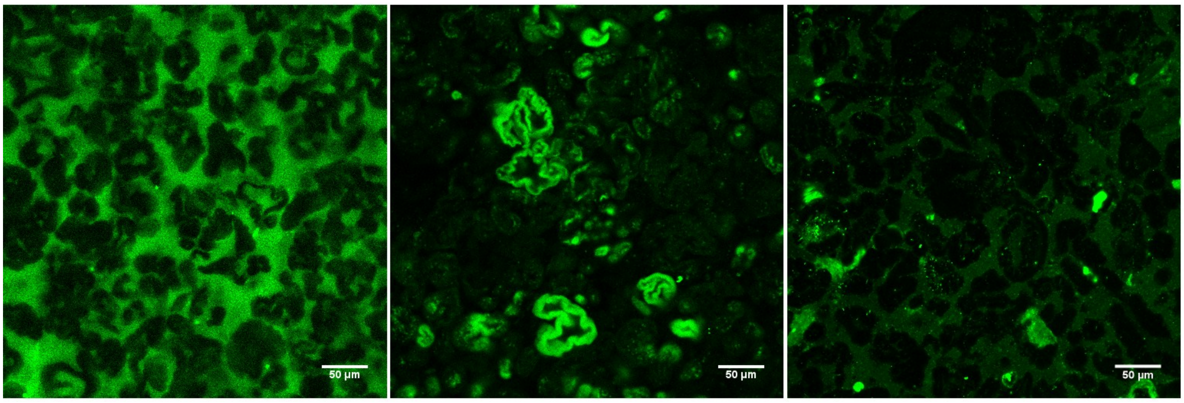

Figure 5-7: Confocal micrographs (recorded at room temperature) of waxy maize starch dispersions (starch:solvent ratio = 3:100) indicate presence of labeled gums (left: 0.2% DTAF-guar; middle: 0.2% xanthan-FITC no salt; right: 0.2% xanthan-FITC 0.01M NaCl). The dispersions are pasted at 72.5°C at a shear rate of 50 s^{-1}.

In case of the guar paste, the majority of the gum is present in the continuous phase. The starch granules can be observed as dark structures in a fluorescent medium. For the xanthan containing systems, the presence of NaCl and consequently the xanthan conformation appeared to greatly affect the results. In the salt free system, xanthan is mainly associated with the granule surface. At 0.01M NaCl the behavior is intermediate: an occasional association with the granules was observed, but the xanthan is predominantly present in the continuous phase. Moreover, these pastes (0.01M NaCl) were more heterogeneous, showing local accumulations of xanthan.

These results suggest that, when present in the random coil conformation (no salt), xanthan can associate with the swollen starch granules. Possibly a similar effect can take place at higher salt contents when the xanthan is heated above the transition temperature, e.g. during pasting. If associations between xanthan and gelatinized waxy starch granules occur, these micrographs suggest that the xanthan, at least partly, desorbs upon reconverting to its helical form during cooling. The question however should be raised whether these associations are also present during the isothermal heating step, where the highest degree of granule disruption takes place. It has been stated before that molecular associations between polysaccharides are less likely to occur at elevated temperatures (BeMiller, 2011). More advanced equipment, capable of recording micrographs at elevated temperatures could further clarify this hypothesis. Nevertheless, these results invalidate the hypothesis that association of xanthan with the granule surface causes the stabilizing effect during shear. As described in chapter 3, xanthan also exhibited granule stabilizing properties at 0.1M NaCl, when no transition and likely no association with the granules is taking place. Furthermore, the association of xanthan gum is not responsible for the specific flow behavior observed during pasting of the samples at 0.01M NaCl. If this were true, the salt free system should exhibit comparable changes in pasting behavior, which was not observed. Consequently, it can be stated that xanthan gum, present in the continuous phase protects the starch granules from breaking, irrespective of its molecular conformation. This observation favors the hypothesis of shear anisotropy as stated above.

5.3.5 RHEOLOGICAL PROPERTIES OF THE COOLED PASTES

Unlike guar gum, xanthan gum limited the shear induced breakdown of the starch granules, as shown in the particle size distributions. However, laser light diffraction allows only to characterize the present granules and fragments. This technique provides no information about the fraction of the starch that has been completely broken down to its molecular constituents. Therefore, additional measurements were performed to evaluate the rheological relevance of the observed differences between the varying shear regimes and the differences induced by the gums. For practical reasons, the rheological analyses of the pastes were always performed after 24h of storage at 5°C. Because these waxy starches contain no amylose, retrogradation effects are limited, but can still induce minor changes in paste structure. Lu *et al.* (2008) demonstrated that the heating temperature can affect the structure buildup of waxy starch pastes during storage. In order to exclude differences induced by retrogradation effects, samples that only differed in shear rate during pasting were directly compared (i.e. same composition and the same heating temperature).

5.3.5.1 Visco-elastic properties

The viscoelastic properties of starch pastes are governed by the volume and the rigidity of the swollen granules, the continuous phase and the interaction between both (Chaisawang & Suphantharika, 2006). Therefore small deformation rheology is a sensitive probe for detecting microstructural differences within the samples. Figure 5-8 summarizes the effect of temperature and shear conditions on the elastic modulus *G’* (recorded at 0.5 Hz). The effect of increased shear during pasting is clearly noticeable as *G’* is significantly reduced when more shear was applied. Furthermore, this effect is more apparent when pasting was performed at 72.5°C. This illustrates that preparation conditions can induce modest changes in average granule size but with large rheological implications.

The effect of the shearing conditions is most pronounced for the gum free system, which exhibits the strongest fallback of *G'*. This is rather expected because the starch component is in this case the only ingredient that can contribute to the rheological properties. When gums are present, they inevitably have a direct influence as well, which is not affected by the shear conditions used in these experiments. At 70°C the xanthan containing system is the least affected by the different shear conditions. When comparing the samples sheared at 150 s^{-1} with the unsheared samples, a reduction of about 30% can be observed for G' in the presence of xanthan gum, whereas there is a reduction of 50% in the presence of guar gum. For those samples, the granule preserving effect of xanthan is clearly noticeable. At 72.5°C the effects of increasing the shear rate during production are comparable for guar gum and xanthan gum. Based on the PSD of the samples, this result is unexpected because the granule sizes differed the most when the pastes were prepared at this temperature. When heated at 72.5°C, an important fraction of the starch is broken down for all the sheared samples (see confocal micrographs section 3.3.4) and the dynamic rheology is more affected by the gums and the starch amylopectin present in the continuous phase, than by the intact granules.

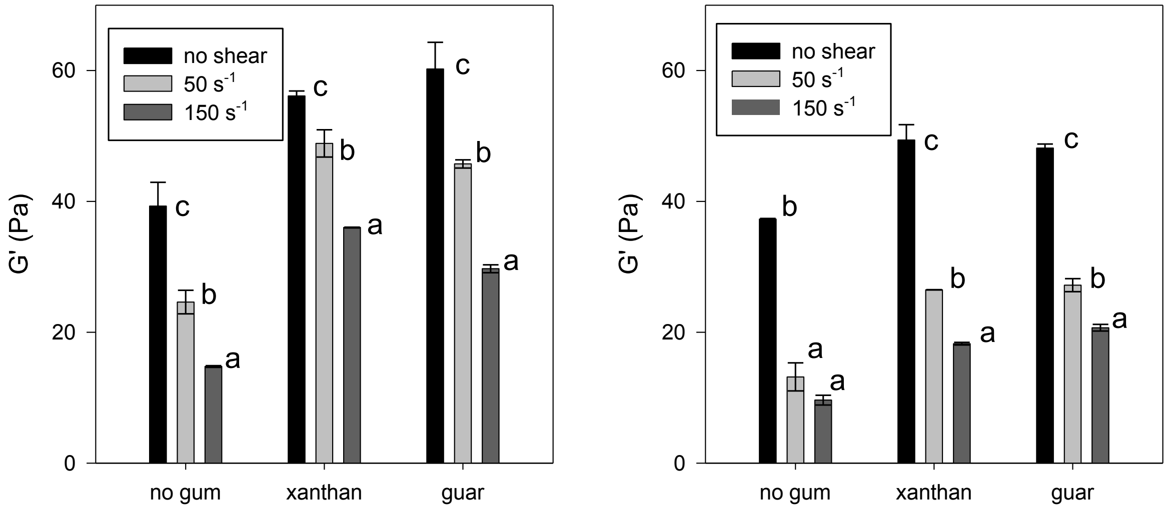

Figure 5-8: Effects of processing temperature (left: 70°C; right 72.5°C) and shear on the value of G' (0.5 Hz) of the resulting pastes. For a given composition and preparation temperature, letters a, b and c indicate significant differences ($p<0.05$) induced by the applied shear conditions.

5.3.5.2 Flow parameters

The flow curves of the samples and the derived Herschel-Bulkley parameters are strongly affected by the presence of both gums (Figure 5-9). The flow behavior index of all samples was smaller than 0.5 (not depicted), hence they all exhibited shear thinning behavior. Compared with the pure starch systems, the addition of guar gum gave rise to a reduced yield stress, whereas this parameter is significantly increased by xanthan. Xanthan gum solutions exhibit weak gel properties due to their rigid conformation and the presence of molecular entanglements. Therefore an increased yield stress is not unexpected. Moreover, it has been suggested that xanthan gum can enhance the granule association of waxy maize starch systems (Abdulmola *et al.*, 1996b; Achayuthakan *et al.*, 2006). The proposed mechanisms were bridging or depletion flocculation. De latter appears rather unlikely considering the size of the swollen granules and the rather high (effective) xanthan concentrations in the continuous phase. Several hypotheses could be formulated to explain the lower yield stress observed for the guar pastes. Because this effect is the clearest for the unsheared samples, the lower yield stress could be the result of a lower granule swelling, as suggested by the PSD. Guar gum might also affect the granule packing. Upon swelling, the guar gum concentration in the continuous phase is raised, thus encumbering granule-granule interactions and possibly lowering the yield stress.

Conversely, the consistency index is strongly increased by guar gum while there is only a moderate influence of xanthan on this parameter. The consistency index (k) characterizes the behavior of the systems under flow, i.e. when the yield stress is exceeded. Their high values for the consistency indices demonstrate that the guar gum systems are more resistant to flow. Similar to the increased viscosities during pasting, a higher stress is required to move starch granules past each other in a more viscous medium.

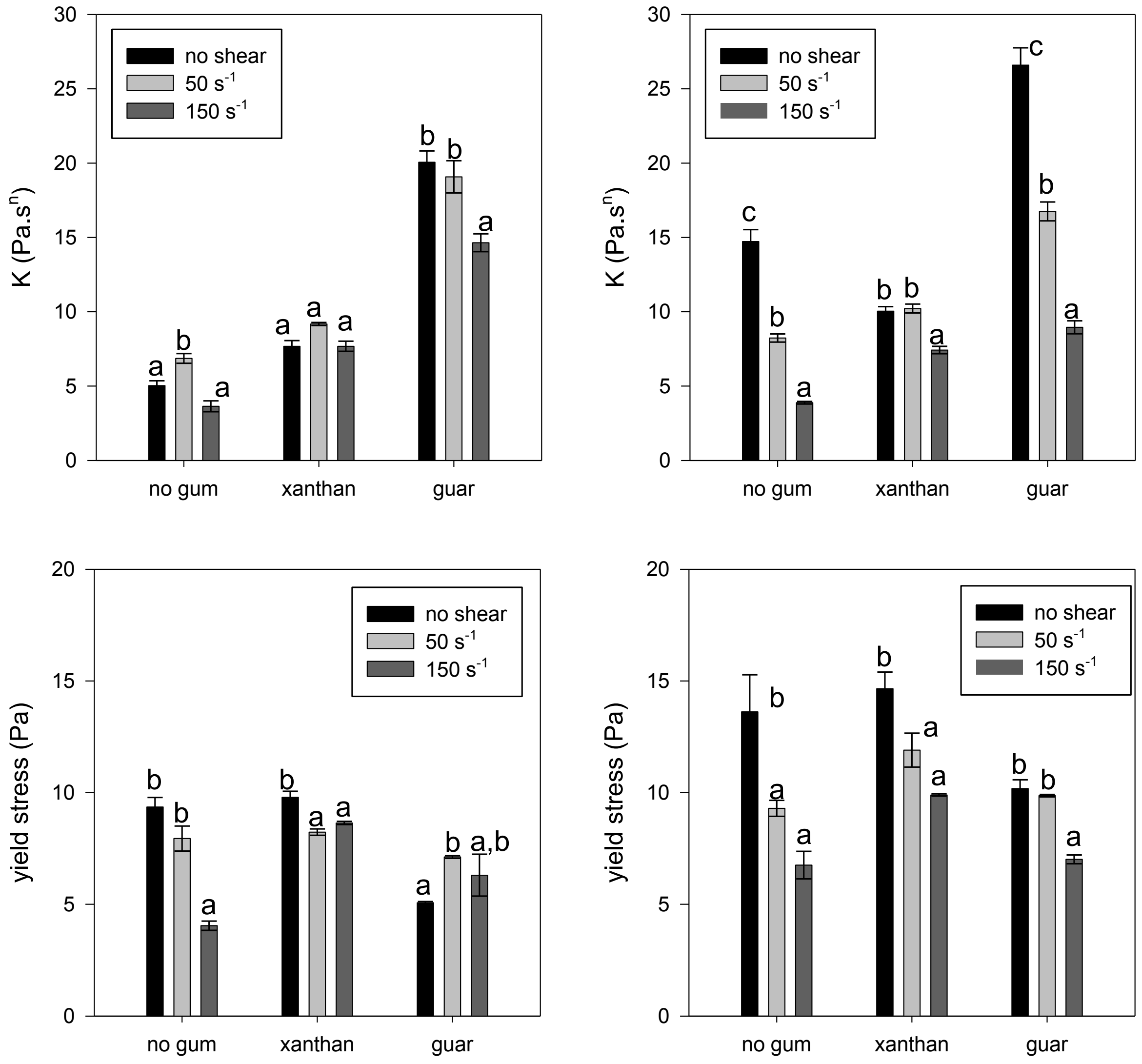

Figure 5-9: Effects of processing temperatures (left: 70°C; right 72.5°C) and shear rate on the value of the Herschel-Bulkley parameters of the resulting waxy maize starch pastes. For a given composition and preparation temperature, letters a, b and c indicate significant differences ($p<0.05$) induced by the applied shear conditions.

Based on the yield stress and the consistency index, the effect of the different preparation conditions was evaluated. In general, it could be stated that there is a marked effect from the imposed shear rates on both parameters (Figure 5-9). For pastes heated to 70°C, changing the shear rate from no shear to 50 s^{-1}, results in limited effects. However, upon further increasing the shear rate to 150 s^{-1}, the consistency index is significantly reduced except in the presence of xanthan gum. Pastes heated to 72.5°C exhibit more marked differences in both yield stress and consistency index. Particularly for the latter parameter, the limited differences for the xanthan pastes strongly contrast with the large shear induced effects which are observed for the gum free and the guar system. Their large influence on the consistency index demonstrates the strong effects of the processing conditions on the macroscopic properties of these systems.

These results further evidence the granule preserving properties of xanthan gum and illustrate that both gums enhance the rheological properties differently. The effect of guar gum is mainly additive because this component increases the consistency without affecting the granule properties. Xanthan gum also exhibits this feature, but more importantly it can protect the granules at varying shear conditions, hence improving the intrinsic contribution of the starch.

5.4 CONCLUSIONS

The effects of guar and xanthan gum on the mild temperature pasting behavior of waxy maize starch were studied in this setup. The use of the starch pasting cell geometry of the rheometer allowed to accurately control the preparation conditions of the pastes. In particular the effects of different shearing conditions (no shear, 50 s^{-1} and 150 s^{-1}) were compared to elucidate the influence of the gums on granule swelling and breakdown (Figure 5-10).

At the concentrations studied here, the gums did not induce marked differences in granule swelling. However, breakdown was clearly affected by their presence. The ability of xanthan to inhibit granule disruption was confirmed, whereas guar gum appeared not to have this property. As a consequence, large differences in pasting profiles as well as particle size distributions were observed between guar and xanthan systems. This specific feature of xanthan gum was attributed to its ability to modify the impact between the granules. The latter is possibly caused by a shear induced anisotropic organization of the xanthan molecules, rather than by an association with the granule surface.

Furthermore, differences induced by the pasting conditions were also reflected in the rheological behavior of the pastes after cooling. For the gum free and the guar pastes, the consistency index as well as the elastic modulus were significantly reduced by an increased shear rate. In the presence of xanthan, these effects could be more restricted. In conclusion, it could be stated that both gums can enhance the rheological properties of these waxy starch pastes, but guar gum rather masks the shortcomings of the starch, whereas xanthan gum can actively improve the performance of the granules by preserving their structure.

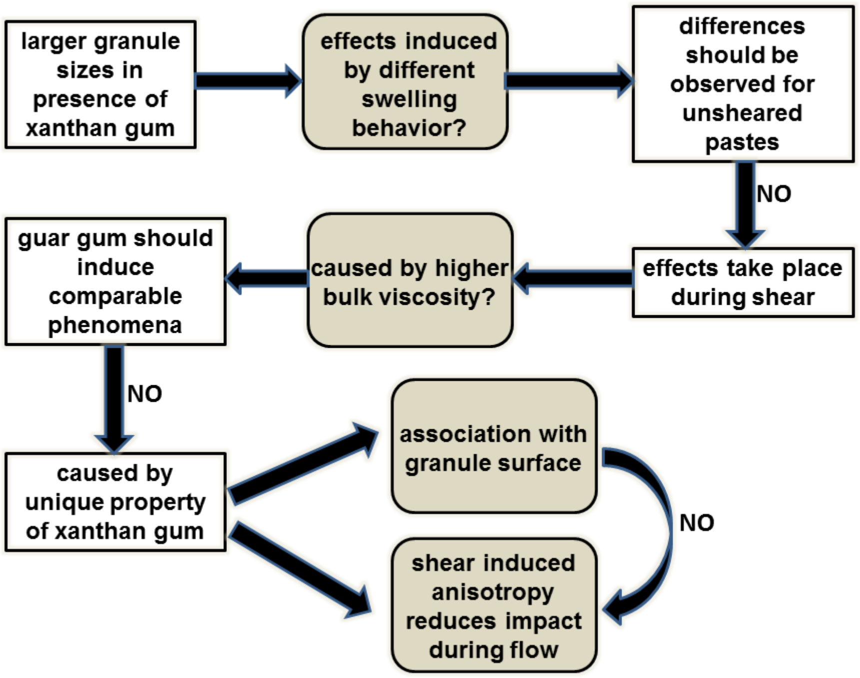

Figure 5-10: Deductive decision scheme to explain the effect of xanthan gum

These results demonstrated that gums indirectly influence the rheological properties of native waxy maize starch, by changing the granule properties. However, a deeper look into the existing literature shows that their direct rheological contributions are also not fully understood, which is also illustrated repeatedly in this chapter. If effects of gums on granule swelling and degradation could be excluded, a more fundamental insight in their rheological effects could be developed, which in turn could help interpreting the behavior of these more complex systems. Therefore, the following chapter will focus on cross-linked starch systems in which granule degradation effects are limited.

6 RHEOLOGY OF MODIFIED STARCH/GUM SYSTEMS: COMPARISON BETWEEN GUAR AND XANTHAN

Relevant publication: Heyman, B., De Vos, W., Van der Meeren, P., Dewettinck, K. (2013). Gums tuning the rheological properties of modified maize starch pastes: differences between guar and xanthan. Food Hydrocolloids (submitted).

6.1 INTRODUCTION

For numerous industrial food applications chemically modified starches and gums are combined in order to improve their sensory and rheological properties as well as their physicochemical stability. Chemically cross-linked starches are very popular, because the strengthened granules can much better withstand the elevated temperatures and high shear forces often encountered in production processes (Singh *et al.*, 2007; Tharanathan, 2005). However, the swelling of cross-linked starch is restricted by the presence of cross-link junctions. Therefore, in many liquid and semisolid foods, polysaccharide gums are added as the second thickening component to adjust the viscosity and texture in the final products (Fuongfuchat *et al.*, 2012). Surprisingly, modified starch/ gum mixtures are far less studied than their native counterparts, despite their industrial abundance.

The specific effects of gums on the rheological properties of starch systems appear to strongly depend on the type of gum, the type of starch as well as the applied concentrations and preparation conditions (BeMiller, 2011). Associations between starch and hydrocolloid molecules (Christianson *et al.*, 1981; Freitas *et al.*, 2003; Funami *et al.*, 2005b; Shi & BeMiller, 2002) as well as their mutual exclusion (Achayuthakan & Suphantharika, 2008; Alloncle & Doublier, 1991; Alloncle *et al.*, 1989; Biliaderis *et al.*, 1997; Conde-Petit *et al.*, 1997; Mandala *et al.*, 2004) have been proposed to explain the observed rheological phenomena. The hypothesis of mutual exclusion – which is embraced by many authors – states that gum molecules are confined to the continuous phase of the starch dispersion. This model is particularly important for cross-linked waxy starches where granules remain intact and no amylose is present. Consequently, the pastes are regarded as discontinuous systems: the swollen starch granules are surrounded by the continuous watery phase containing the gum molecules (Abdulmola *et al.*, 1996b; Alloncle & Doublier, 1991). Due to the water absorption of the starch, the effective concentration of the polysaccharides present in the external phase is raised. The latter is believed to cause the often observed synergistic effects in the rheological behavior of starch/gum systems.

Under the impulse of granule swelling in mixed starch/gum systems, the concentration regime of the gum could differ before and after heating. Particularly for xanthan gum solutions, the rheological behavior strongly depends on the applied concentration and the corresponding molecular organization. Two characteristic concentrations are generally defined. The critical overlap concentration c* marks the start of the semi-dilute regime. Above the entanglement concentration c**, molecules start to engage in intermolecular interactions

(Meyer *et al.*, 1993; Wyatt & Liberatore, 2009). At more elevated concentrations (~2% w/v), anisotropic phases are observed due to the spatial alignment of the stiff molecules and the rheological properties depend less strongly on the xanthan concentration (Allain *et al.*, 1988; Lee & Brant, 2002a; Oertel & Kulicke, 1991; Sato *et al.*, 1990). In this regard, it is interesting to compare the effects of guar gum and xanthan because both are high molecular weight polymers that induce high viscosities in solution. However, guar gum does not engage in strong molecular entanglements and does not exhibit mesophase formation.

In this chapter, a comprehensive study on the rheological effects of xanthan and guar gum on waxy starch systems is presented. In contrast with the preceding chapters dealing with native starch systems, preference was given to chemically cross-linked and acetyl substituted waxy maize starch. This type of modified starch is not subject to degradation effects under the conditions used in this study, which facilitates the interpretation of the results, and allows to calculate the effective starch volume in the system (see further). More specifically, it was evaluated to which extent the unique rheological effects of xanthan gum, as observed in the preceding chapters, are also reflected in modified starch systems. For that reason, results of the xanthan systems are compared with guar containing and gum free pastes. A better insight in the effects of gums on the rheological properties of modified starches can not only result in a more sensible use of both components, but it might also assist in the search for native starch alternatives that can mimic the rheological behavior of their modified counterparts.

6.2 MATERIALS AND METHODS

6.2.1 MATERIALS

Xanthan gum (Satiaxane CX911, pyruvic acid content >1.5%) and guar gum (Viscogum MP41230) were acquired from Cargill Texturizing Solutions (Ghent, Belgium). For the covalent labeling, a clarified version of the xanthan gum was used (Satiaxane CX931) to avoid complications during purification and noise within the micrographs due to residual cell debris and other fermentation impurities. Adipate cross-linked and acetyl substituted waxy maize starch (Resistamyl 347) was provided by Tate & Lyle Benelux.

6.2.2 PREPARATION OF GUM SOLUTIONS

Gum solutions were prepared as described in the preceding chapter (see section 5.2.1).

6.2.3 PASTING EXPERIMENTS

By means of a magnetic stirrer, the starch powder was suspended in 0.1M (or 0.01M, for the last part of the setup) NaCl solutions or first suspended in 0.19 M NaCl (or 0.01M, for the last part of the setup) solutions and further diluted (50/50) with the gum stock solutions to obtain a final NaCl concentration of 0.1M in the continuous phase. The resulting gum concentration in the continuous phase was 0, 0.2 or 0.4% (w/w). As it will be remarked repeatedly throughout the text, the effective xanthan concentration in the systems is raised due to starch granule swelling in the heating step. When reference is made to ‘gum concentrations’, these initial concentrations (0.2%, 0.4%) in the continuous phase are intended, otherwise the term ‘effective gum concentration’ is used. Different starch:continuous phase ratios (w:w) were applied: 3:100, 4:100, 5:100, 6:100 and 7:100.

Pasting experiments were performed by means of the starch pasting cell. Starch suspensions were presheared at 100 s^{-1} for 2 minutes and then heated to 85°C at a heating rate of 5°C/min, held isothermal for 10 minutes and finally cooled down to 20°C (5°C/min). Throughout the heating and cooling steps a shear rate of 100 s^{-1} was maintained. The cooled samples were recollected and stored for 24h in the refrigerator (5°C) before further analysis.

6.2.4 PARTICLE SIZE DISTRIBUTIONS

The particle size distribution of the cooled starch pastes was determined by laser light scattering using a Malvern Mastersizer S (Malvern, UK) equipped with a 300mm reversed Fourier lens and a MSX-17 sample dispersion unit. To measure the starch particle size in the cold paste samples, approximately 4 g paste was diluted to 20g with deionized water and gently shaken manually. Pumping and stirring speeds were put on 30% of the maximum values and the background was measured. For the optical model, the refractive indices were 1.6 and 1.33 for starch and the continuous phase, respectively. The average diameter of the unheated starch granules was determined with the dry powder feeder MSX-64. The refractive indices were 1.6 for the particles and 1.00 for air.

The volume fraction occupied by the swollen granules is calculated from the starch concentration c (g/ml), the raw starch volume-equivalent mean granule diameter $D_0[3,0]$, the swollen starch volume-equivalent mean diameter D[3,0] and the starch density δ (g/ml). The calculations are similar to the procedure of Jacquier *et al.* (2006). As a starting point, it is assumed that the number of granules present remains constant, i.e. each raw granule results in a swollen granule, hence no disruption into smaller fragments takes place. The number of granules present in the system (n) can be calculated as follows:

$$n = \frac{\text{total volume of raw starch}}{\text{volume of 1 raw starch granule}} = \frac{m_s/\delta}{\pi/6 \, . \, D_0[3,0]^3} \tag{6-1}$$

The swollen starch volume fraction can now be calculated:

$$\Phi = \frac{\text{Volume occupied by swollen starch}}{\text{Total volume of the system}} = \frac{n \, . \, \pi/6 \, . \, D[3,0]^3}{\text{Total volume of the system}} = \frac{c \, . D[3,0]^3}{\delta \, . \, D_0[3,0]^3} \tag{6-2}$$

The density of the raw starch was determined experimentally and equaled 1.47 g/ml. The value of $D_0[3,0]$ was experimentally determined to be 11.2 ± 0.2 µm, the average of 3 replicates. This average size is comparable with other reports (BeMiller & Whistler, 2009; Tester *et al.*, 2004). In this setup, starch/continuous phase ratios are used rather than starch concentrations. The concentration c can easily be calculated from the starch mass m_s (g) and the corresponding solvent mass m_w (g) and solvent density δ_w (g/ml).

$$c = \frac{m_s}{\frac{m_s}{\delta} + \frac{m_w}{\delta_w}} \tag{6-3}$$

The solvent (water or gum solutions) largely constituted of water. Therefore, the value of δ_w was for all systems fixed to 1 g/ml.

6.2.5 *FLOW CURVES OF THE PASTES AFTER COOLING*

The flow curves of the cooled pastes were recorded using a 40 mm cross hatched steel plate-plate geometry with solvent trap. To prevent drying of the sample, 1 ml of water was brought in the solvent trap compartment. The gap was set to 1000 µm. After 15 minutes of equilibration at 20°C, a steady state flow step was performed by logarithmically increasing the shear rate from 0.01 s^{-1} to 100 s^{-1}.

A comparable procedure was used for recording the flow curves at 85°C. The sample was applied at room temperature and heated to 85°C. After an equilibration time of 5 minutes, the flow curve was recorded (0.1 s^{-1} to 1000 s^{-1}). In addition to the solvent trap, a liquid paraffin oil was wrapped around the edge of the sample to restrict evaporation.

6.2.6 EMPIRICAL MODELING OF RHEOLOGICAL DATA

The apparent viscosities (η) of both the hot and cooled pastes were plotted as a function of the starch volume fraction Φ. For the hot paste viscosity (η_{85}), the final viscosity of the isothermal step during pasting was selected. The cold paste viscosity (η_{20}) at a shear rate of 100 s^{-1} was derived from the flow curves recorded at 20°C. Within the studied volume fraction range, the course of the plots could be described by a three parameter power function:

$$\eta = a + b \,.\, \phi^{c} \qquad 6\text{-}4$$

Curves were fitted to data obtained from pastes with a fixed initial gum concentration (no gum, 0.2% or 0.4%) by means of the SigmaPlot 10 software (Systat software inc., San Jose, USA). In order to depict the contribution of the gums relative to the gum free systems as a continuous function of Φ, the ratio of both equations was plotted:

$$\text{viscosity ratio}= \frac{a_g + b_g.\phi^{c_g}}{a_0 + b_0.\phi^{c_0}} \qquad 6\text{-}5$$

The fitted parameters (a,b,c) with subscript ‘g’ refer to the fits of the gum containing systems and subscript ‘0’ indicates the gum free systems.

6.2.7 OSCILLATORY RHEOLOGY OF COOLED PASTES

Frequency sweeps of the cooled pastes were recorded using a 40 mm cross hatched steel plate-plate geometry with solvent trap as described in section 5.2.6.

6.2.8 COVALENT LABELING OF THE GUMS AND CONFOCAL SCANNING LASER MICROSCOPY

Gums were labeled with fluorescein isothiocyanate (FITC) as described in section 5.2.7. Labeled gums were dissolved (0.2%) in distilled water and if necessary NaCl was added (0.1M, 0.01M). Starch pastes containing labeled gums were prepared and analyzed as described in section 5.2.8. However, for this setup the pastes (starch to solvent ratio 3:100) were heated to 85°C, by the same procedure as described in section 6.2.3.

6.3 RESULTS AND DISCUSSION

6.3.1 CONFOCAL SCANNING LASER MICROSCOPY

Starch/gum pastes and gels are mostly considered as swollen starch granules within a watery gum solution. Particularly in the case of xanthan gum, it was suggested as well that this polysaccharide is capable of associating with the granule surface (Chaisawang & Suphantharika, 2006; Gonera & Cornillon, 2002). In the previous chapter, it was demonstrated that this effect is also occurring for native waxy maize starch/xanthan systems. Furthermore, the extent of association appeared dependent on the salt content. To verify whether similar phenomena take place in these modified starch systems, the location of labeled gums in the pastes was visualized. Depending on the location of the xanthan within the systems, rheological data should be interpreted differently.

Figure 6-1 represents the confocal micrographs of the different systems studied. Due to its strong salt sensitivity, three NaCl contents were applied for the xanthan pastes (no salt, 0.01M and 0.1M). The starch dispersions containing xanthan but without the addition of salt, clearly differed from the others. Whereas xanthan and guar gum are clearly present in the continuous phase of the other dispersions, it is in this case (at least partly) associated with the surface of the granules. It should be remarked that also in the work of Gonera & Cornillon (2002), as well as Chaisawang & Suphantharika (2006) associations between xanthan and starch granules were observed in systems where no salts were added. At 0.01M NaCl, a somewhat intermediate behavior is observed, where a slight degree of granule association can be perceived, but the majority is present in the continuous phase. The degree of association appears therefore dependent on the salt content of the dispersions, which confirms the findings from the preceding chapter. It is generally known that when cooling from above T_m to lower temperatures, xanthan converts to its helical form. At low salt contents xanthan molecules occur in random coil (Muller *et al.*, 1986; Stokke *et al.*, 1989) and the driving force for renaturation is less strong (Camesano & Wilkinson, 2001). Xanthan gum is known to be able to engage in non-electrostatic interactions with polysaccharides, like guar gum or locust bean gum during cooling and it was proven that these interactions are suppressed by the helical conformation (Mao *et al.*, 2012; Renou *et al.*, 2013). Possibly the same mechanism is responsible for xanthan interactions with the starch polymers present at the periphery of the swollen granules. This topic deserves a separate study, and will not be the focus in the current setup. On the other hand, it is clear that the systems studied here, containing 0.1M NaCl (and presumably also at 0.01M) can be considered as discontinuous systems of swollen starch granules dispersed in a gum containing medium.

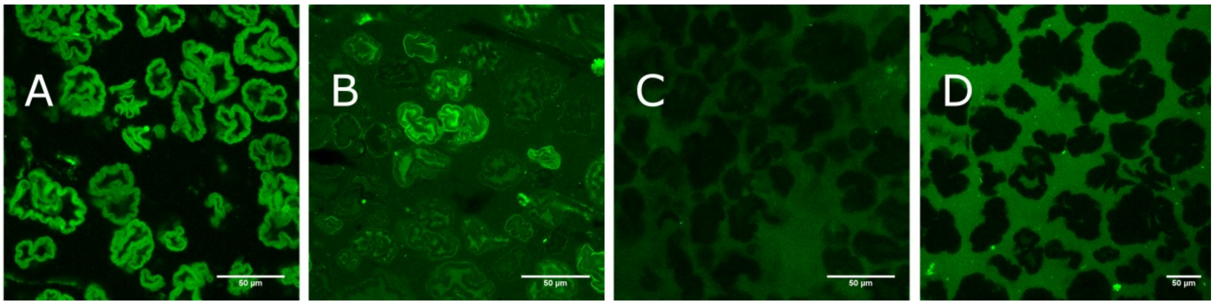

Figure 6-1: Confocal micrographs (recorded at room temperature) of adipate crosslinked and acetylated starch (starch:solvent ratio 3:100) with FITC-labeled gums (A: 0.2% xanthan 0 M NaCl; B: 0.2% xanthan 0.01 M NaCl, C: 0.2% xanthan, 0.1 M NaCl; D: 0.2% guar 0 M NaCl). Dispersions are prepared at 85°C and a shear rate of 100 s^{-1}.

6.3.2 VERIFICATION OF THE ADSORPTION HYPOTHESIS

Although CSLM proves to be a powerful technique to visualize these complex systems, one should interpret the micrographs cautiously. First of all, the addition of fluorescent groups could modify the affinity of the polymer for the starch. Secondly, the labelling reaction as such might partially depolymerize the molecules which can also lead to a functionality change. Demonstrating whether or not xanthan gum adheres to the swollen granules is not easy. Generally, adsorption or association phenomena could be confirmed by concentration differences before and after centrifugation of the dispersed phase. In the case of starch dispersions, the particles as such absorb a large fraction of the water, hence increasing the concentrations of the gum, as described higher. Moreover, due to the irregular shape and the deformable nature of the swollen granules, the exact volume fraction of the starch is not known and can only be approximated. Furthermore, the quantification of polysaccharide gums poses a lot of practical difficulties. Chemical quantification methods like total organic carbon (TOC) determination, which has been used for xanthan quantification (Van Nevel *et al.*, 2012), are affected by the impurities (e.g. leached polymers) originating from the starch. In order to avoid these complications, the continuous phase of the starch/gum dispersions was analyzed rheologically and compared with a reference solution. The starch pastes were prepared in the same manner as described in 6.2.3. And these pastes were transferred to screw cap tubes and centrifuged at 8000g for 15 minutes. A low starch to solvent ratio (3:100) was chosen in order to allow separation of the granules. Flow curves of the solvent phase were recorded by means of the concentrical cylinder geometry.

The volume equivalent average diameter D[3.0] allowed to calculate the starch volume fraction in the systems and hence the corresponding theoretical gum concentration (assuming no association with the granules). For these tests, a starch-to-solvent ratio of 3:100 was used (in this case, based on starch powder instead of dry starch). When the starting concentration of both gums was 0.2%, this should result in an effective gum concentration of 0.31%. Therefore, for all systems, the flow behavior of the supernatant was compared with solutions containing 0.3% of gum. The reference solutions were subjected to the same temperature-shear treatment as the starch pastes in the starch pasting cell. The resulting flow curves are represented in Figure 6-2. It is clear that in all cases, the viscosity of the reference solutions (0.3%) was below the supernatant curves. This indicates that the actual starch and gum concentrations were underestimated. However, there was one exception. The curves of the xanthan systems without salt were almost identical (reference solution and supernatant). This could demonstrate that the effective gum concentration in the supernatant of the salt free system was lower than for all the other systems, which in turn supports the findings of the confocal microscopy measurements. However, viscosity differences demonstrate a limited extent of association whereas the micrographs suggest much stronger effects. This could be caused by a higher affinity of the fluorescent xanthan gum for the granules. Another hypothesis is the occurrence of a contrast induced bias. The intensity of the perceived color is not linearly related with the actual concentration of the chromophores. Increased local concentrations might result in a much stronger visual signal, hence diminishing the signal originating from the more dilute regions. Therefore, it does not necessarily mean that all of the fluorescently labeled xanthan is associated with the granules. Finally, it cannot be excluded that part of the xanthan molecules are stripped from the granules during the centrifugation step e.g. due to molecular entanglements between the xanthan molecules.

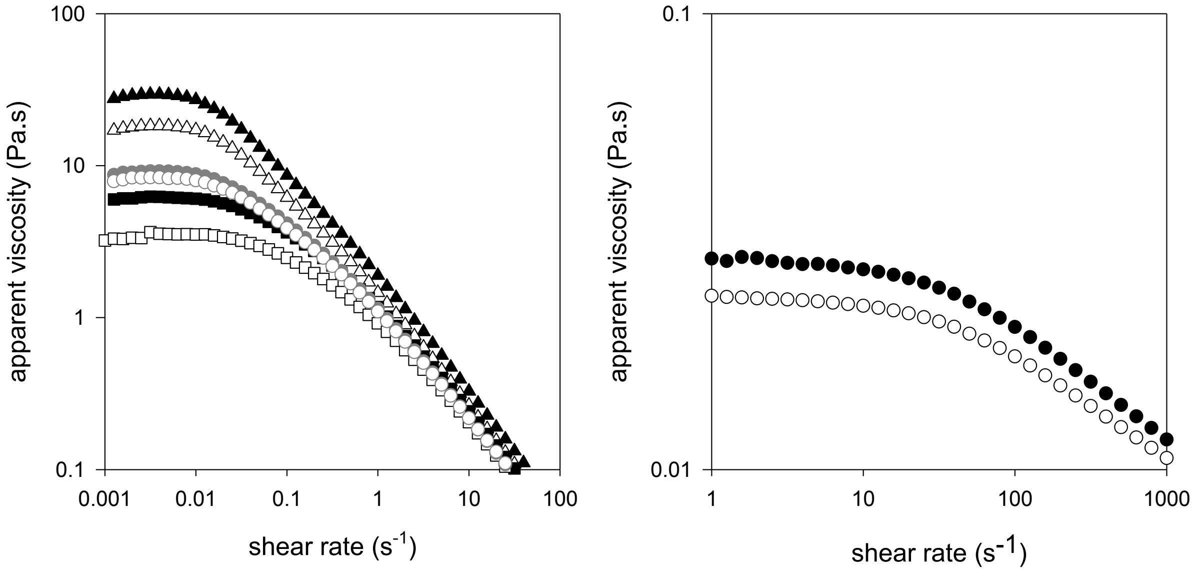

Figure 6-2: Left figure: flow curves of the xanthan solutions after centrifugation and separation of the starch granules (full symbols) and the reference solutions containing 0.3% of gum (open symbols) at different salt concentrations (▲ 0.1M, ■ 0.01M and ● 0M NaCl). Right figure: flow curves of the supernatant guar solution (●) and the reference (0.3%) guar solution (○)

These preliminary tests demonstrate the complexity of xanthan-starch associations. Particularly the search for applicable techniques appears a challenge. The specific effects that are taking place e.g. at varying salt concentrations could therefore be one of the major topics of future research. The use of high salt contents, like e.g. 0.1M in this setup, avoids these complications and allows to consider these systems as discontinuous: swollen granules dispersed in a gum solution.

6.3.3 COMPARISON BETWEEN GUAR GUM AND XANTHAN GUM

6.3.3.1 Flow behavior during pasting

The pasting profiles for the different compositions are depicted in Figure 6-3 for a starch: solvent ratio of 5:100. As expected, both hydrocolloids increase the viscosity during the pasting process. At a level of 0.2% the effect of guar gum and xanthan is comparable. For the samples containing 0.4% of gum, the effect of guar gum is significantly stronger. This already illustrates that the mixed paste viscosities are quite complex, not simply additive and that the obtained result for a given gum/starch ratio is strongly dependent on the type of gum. The shape of the curves is more or less the same for all systems. Because the cross-linked starches studied here are considered not to break up under the given processing conditions

(85°C, shear rate 100 s^{-1}), the pasting curves attain a plateau viscosity rather quickly within the isothermal heating step. During the cooling step, the slope of the guar curves is much steeper than the other ones. This could be due to a stronger temperature dependency of guar gum and/or an altered interaction between the granules, and will be discussed more into detail later on.

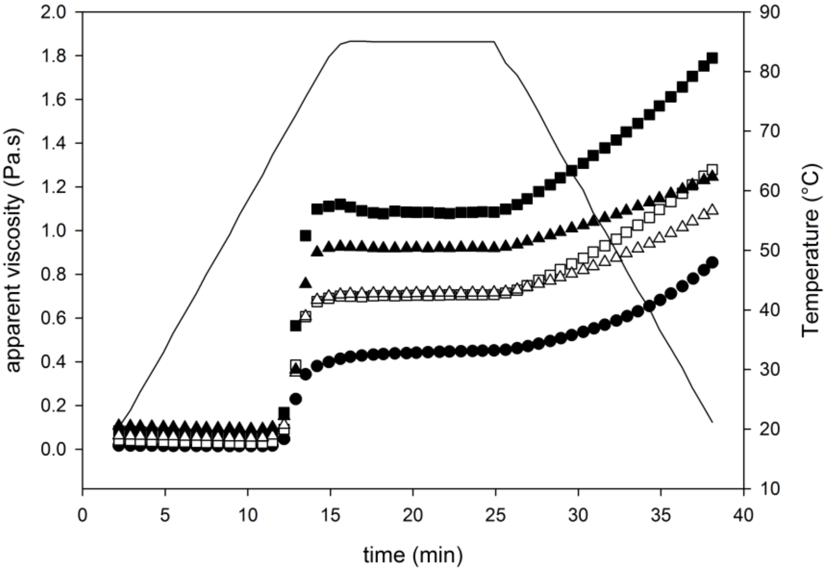

Figure 6-3: Pasting behavior as affected by gums at starch:continuous phase ratio 5:100 (● no gum; ☐ 0.2% guar; ■ 0.4 % guar; △ 0.2% xanthan; ▲ 0.4% xanthan)

The final viscosities of the isothermal step (85°C) are plotted as a function of starch volume fraction (Figure 6-4). Guar and xanthan increase the viscosity of the starch paste in the studied concentration range. Nonetheless, there are some marked differences between both gum systems. Firstly, the concentration increase from 0.2 to 0.4% is more pronounced in the case of guar gum. Secondly, the viscosity increases less strongly by elevating the starch volume in the presence of xanthan gum. At a given starch volume, the viscosity is determined by the properties of the granules (size, distribution, deformability), their interactions, the viscosity of the continuous medium and the interactions between both phases (Genovese *et al.*, 2007; Genovese & Rao, 2003). Along with the increasing starch content, the concentration of the gum in the continuous phase, and hence its viscosity, is increased as well. Therefore, the guar gum systems behave synergistically, as expected: compared to the gum-free system, the viscosity increases more quickly with increasing starch content. In the case of xanthan gum, the curves are more parallel or even slightly converging with the gum free systems. This suggests that there is an antagonistic effect cancelling out the viscosity increase of the continuous phase.

The addition of the gums induces limited (largest variation 5.4%) differences in average granule sizes. However, due to the large number of granules present in the system, this can result in relatively strong variations in total starch volumes. Consequently, the calculated starch volume fraction for a given starch/solvent ratio depends on the type of gum. In order to compare the effect of the gums for a fixed volume fraction, a three-parameter power function was fitted through the data. It should be remarked that the fitted parameters contain no physical meaning and are only valid for the systems and concentration range studied here, but allow an accurate continuous description of the data ($R^2>0.99$). Modeling the viscosity of starch dispersions by two frequently used models, Krieger-Dougherty (Krieger & Dougherty, 1959) and Quemada (Quemada, 1977) is complicated by the presence of gums. Both equations assume a constant fluidum viscosity. When gums are present, their concentration increases by swelling of the starches. Consequently, the fluidum viscosity varies as well with increasing volume fractions.

Figure 6-4 shows the evolution of the paste viscosities of the gum systems relative to the gum free paste. Although it is clear that particularly upon the addition of guar gum, the absolute differences increase with starch content, the relative contributions become smaller (Figure C). At low volume fractions, the viscosity can be raised 3 to 5 times by addition of the gums. At high volume fractions the flow behavior is largely determined by the starch component and for each gum, both curves converge. Initially, the viscosity of the xanthan samples is higher than the viscosities of the guar samples and the gum free system. When the starch concentration becomes higher, the viscosity of the 0.2% guar systems surpasses those of the xanthan pastes. Furthermore, it is remarkable that the relative viscosity of the guar paste decreases much more slowly than the xanthan systems, suggesting that the direct contribution of guar to the overall viscosity is stronger.

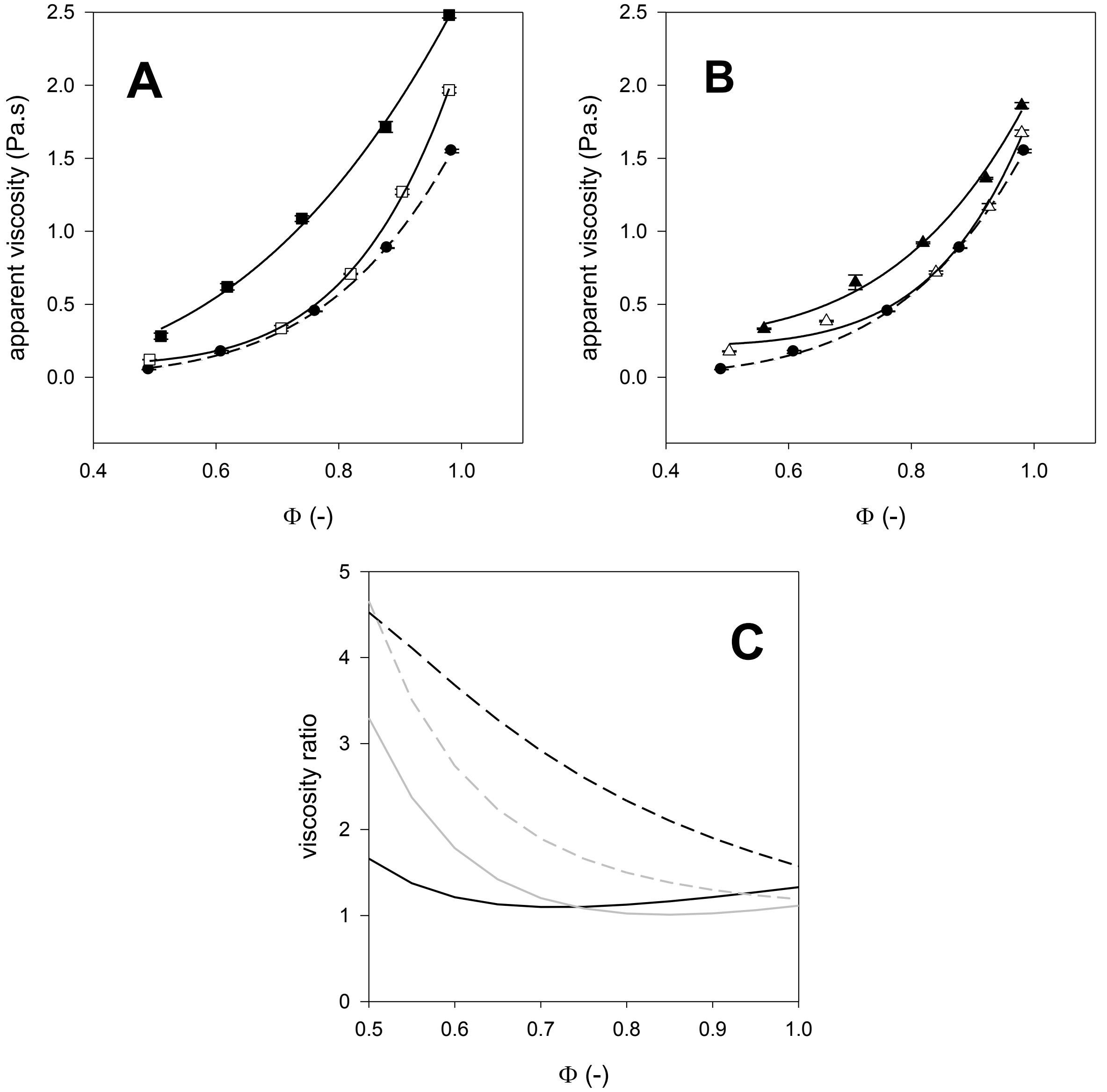

Figure 6-4: Apparent viscosity (shear rate 100 s^{-1}, 85°C) at varying starch volume fractions as affected by guar (A) and xanthan (B) (● no gum; ☐ 0.2% guar; ■ 0.4 % guar; △ 0.2% xanthan; ▲ 0.4% xanthan). Figure C represents the continuous viscosity ratio gum/no gum (__0.2 % guar ; --- 0.4% guar ; __ 0.2% xanthan; --- 0.4 % xanthan)

The different behavior between xanthan and guar gum is marked. This could be a direct effect of the increased viscosity of the continuous phase. At more elevated effective gum concentrations, due to a higher starch volume, the viscosity of the guar containing continuous phase might therefore exceed the viscosity of the xanthan phase. The viscosities of pure guar and xanthan of 1% are approximately the same when measured at 85°C and a shear rate of 100 s^{-1} (0.21 Pa.s for guar, 0.22 Pa.s for xanthan, determined with conical concentric cylinders with solvent trap, data not depicted). This gum concentration corresponds to the effective gum concentrations at starch volume fractions of 60% and 80%, provided that the initial concentration was 0.4% and 0.2% respectively. In both cases, the viscosity of the guar/starch paste was significantly higher than the viscosity of the xanthan/starch paste (0.55 vs. 0.41 Pa.s at Φ=0.60 and 0.4% gum; 0.64 Pa.s vs. 0.58 Pa.s at Φ=0.80 and 0.2% gum). This illustrates that the observed differences in viscosity cannot be based on differences in gum viscosity alone. It was assumed that at an equal volume fraction, the rigidity/deformability was not affected by the gums. Therefore, it can be stated that within flow either the interactions between the granules or the interactions between the granules and the continuous phase were different in the presence of guar and xanthan. In an attempt to further explain the observed phenomena, comparable experiments were executed on the resulting pastes at room temperature, as it will be described in the following paragraph.

6.3.3.2 Flow behavior of cold pastes

The viscosity of the pastes at 100 s^{-1} was determined with a steady state flow step (at 20°C), 24h after preparation in the pasting cell. The data are summarized in Figure 6-5, as a function of starch volume fraction. The guar and gum free systems exhibit a comparable behavior as observed at 85°C. In the case of guar gum there is again a strong effect of gum concentration. In the presence of xanthan gum, the difference between both concentrations is very limited. Remarkably, at high volume fractions the observed viscosities are lower than the ones of the gum free system. Based on the hypothesis raised in 6.3.3.1, this suggests that at high volume fractions – and high effective xanthan concentrations – the flow behavior of swollen starch suspensions can even be facilitated by xanthan, a property that is not observed for guar gum. Furthermore, this property is more explicitly manifested at 20°C than at 85°C.

Figure 6-5 also depicts the evolution of the paste viscosity relative to the gum free systems. Similarly to the viscosities at 85°C the relative contribution of the gum is reduced with increasing starch volume fraction. The shape of the curves is very comparable with the ones obtained at 85°C, although their location has shifted. Whereas for all systems the absolute viscosities are higher at lower temperatures, the relative contributions of the gums as such are lower at 20°C. Aside from the thermal effects on the gums, there is also a clear effect on the starch component. Presumably the rigidity and/or volume of the modified starches does not significantly change during cooling. Abdulmola *et al.* (1996b) demonstrated that upon cooling of cross-linked waxy starch dispersions, the elastic modulus was not significantly increased. A more likely suggestion is that the interaction between the granules is higher at low temperatures. Starch granules can be considered as microgel particles that cannot really interpenetrate but ‘overlap’ with polymers present on the surface (Kaneda & Sogabe, 2005; Ketz *et al.*, 1988). Within flow, these particle interactions contribute to the viscosity and could – as many polymer interactions – be more predominant a lower temperatures. This behavior could also account for the viscosity increase during the cooling step of the pasting experiments. For some starch dispersions, it has even been demonstrated that these interparticle interactions can result in the formation of shear-induced aggregates (Nayouf *et al.*, 2003; Tattiyakul & Rao, 2000).

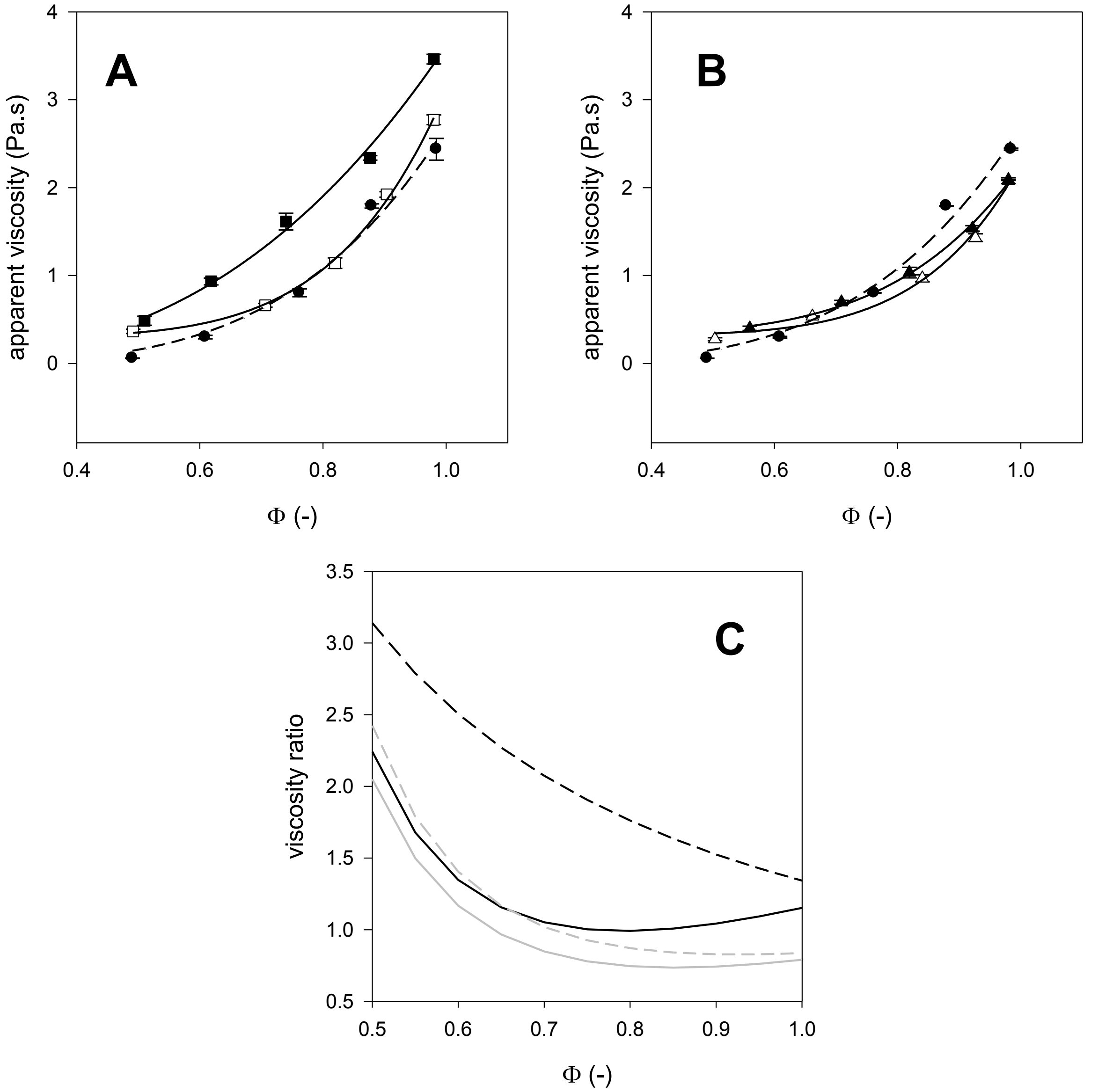

Figure 6-5: Apparent viscosity (shear rate 100 s^{-1}, 20°C) at varying starch volume fractions as affected by guar (A) and xanthan (B) (● no gum; □ 0.2% guar; ■ 0.4 % guar; △ 0.2% xanthan; ▲ 0.4% xanthan). Figure C represents the continuous viscosity ratio gum/no gum (__0.2 % guar ; --- 0.4% guar ; __ 0.2% xanthan; --- 0.4 % xanthan)

As mentioned before, the viscosity of the paste is governed by the starch interactions, the viscosity of the continuous phase and the interaction between the granules and the gums solution. The relative contribution of each phase strongly depends on the used concentration. It is assumed that for an equal granule size and volume fraction, the rigidity of the swollen granules is not affected by the gum. Based on these premises and the fact that in the presence of xanthan lower viscosities can be obtained than in the gum free systems, it can be suggested that xanthan can reduce the interactions of starch granules within flow. Although this cannot be directly demonstrated, other hypotheses can be ruled out. The viscosity of the continuous phase of the xanthan systems cannot be lower than that of the gum-free system (i.e. water). Similarly, it is unlikely that the hydrodynamic forces of the solvent, acting on the granules are higher in the gum free system. Furthermore, these observed effects are most predominant at high starch concentrations, where logically granule-granule interactions are more important than granule-continuous phase interactions.

Because this facilitated flow is most predominant at higher starch and consequently at higher effective xanthan concentrations, a possible explanation could lie in mesophase formation of xanthan. When a critical concentration c_i is exceeded, rigid molecules like xanthan are known to align, leading to the formation of anisotropic phases that can be observed as birefringence under polarized light (Allain *et al.*, 1988; Oertel & Kulicke, 1991; Sato *et al.*, 1990). In this setup, effective gum concentrations are generated around and above this critical concentration range (>2%), due to the swelling of the starch. Moreover, there is a strong alignment of the molecules in the presence of shear, causing a flow induced birefringence at even lower concentrations (Laneuville *et al.*, 2013; Lim *et al.*, 1984). This behavior is not observed for randomly coiled polymers like guar. Under these conditions, the viscosity of xanthan gum solutions is less dependent on the concentration, partly explaining the large viscosity differences with guar gum. Furthermore, the presence of a dense array of aligned xanthan molecules between the granules might restrict their interaction and further facilitate their flow.

Although their specific effects are strongly differing, it can be stated that the flow behavior of the starch pastes, both at elevated and low temperatures, is strongly affected by the gums even at high volume fractions of starch. It is therefore interesting to find out if this is also the case at small deformations, which is described in the following paragraph.

6.3.3.3 Visco-elastic properties of the pastes after cooling

The frequency dependent behavior of the different pastes is represented in Figure 6-6 for starch:solvent ratios of 5:100. A dominant elastic response with limited frequency dependency is observed for all systems. Similar curves are usually obtained for particulate gel networks of starch granules (Abdulmola *et al.*, 1996b; Genovese & Rao, 2003; Steeneken, 1989). Although the results are dominated by the starch component, the effects of the gums are clearly noticeable. Compared to the gum-free paste, the slope of the elastic modulus G’ is steeper. Moreover, the values of the loss modulus G” are significantly increased. Particularly in the case of guar, there is a strong concentration dependency for this parameter. Such behavior suggests that, compared with the gum-free paste, different dissipation mechanisms are present in the mixed pastes and consequently that the microstructural nature of the network is modified by the gums.

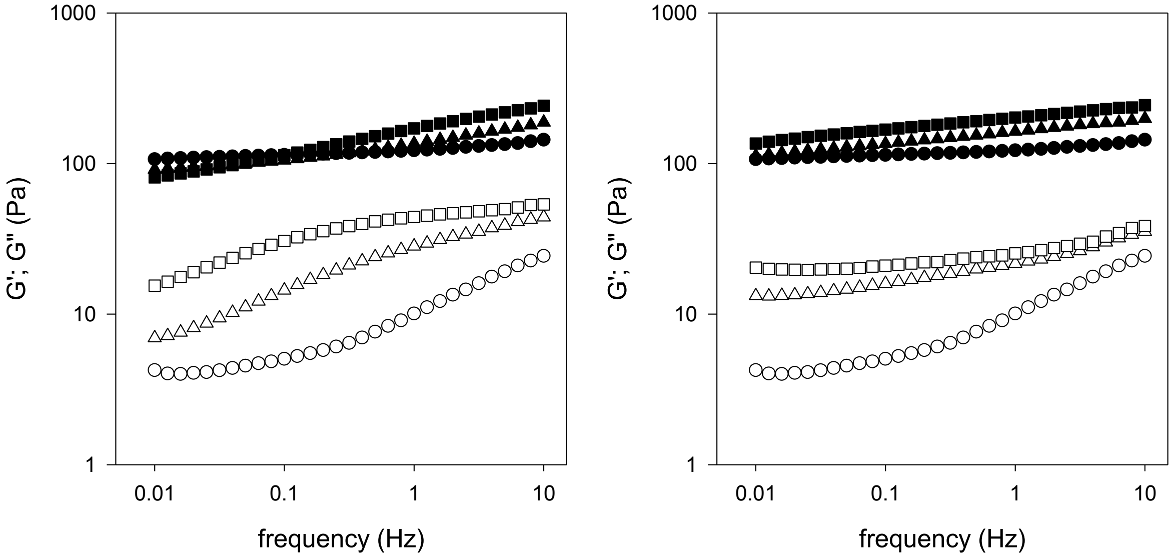

Figure 6-6: Frequency sweeps of starch pastes (5:100; 20°C) as affected by guar (L) and xanthan (R). (● no gum; ▲ 0.2% gum; ■ 0.4 % gum; closed symbols G’, open symbols G”)

Figure 6-7 depicts the behavior of both G’ and G” as function of starch volume fraction. Similar to the viscosity data, power curves are fitted to the G’ data as a guide for the eye. A linear relation was used for G”. When examining the values of G’, the effect of xanthan appears to be purely additive over the whole concentration range. In the case of the lowest guar gum concentration, the pastes are less elastic than the reference system at low volume fractions, but become more elastic at increasing starch volume fractions. The values of the loss modulus (G”) on the other hand, suggest a more viscous behavior due to the gums over the whole starch concentration range. With increasing starch content, G” is further increased relative to the reference system. These results demonstrate that the network synergy between gums and starches is not purely additive and depends strongly on the concentration of both. For the lowest starch volume fractions, a starch granule network is non-existing and the rheology is governed by the continuous phase. At volume fractions of 60% and higher, dominant elastic behavior is observed for all systems. The sharp reduction of the phase angle (Figure 6-7) suggests a network by interacting starch granules. This reduction happens much more gradually in the presence of gums. These curves demonstrate that due to the incorporation of gums, the network is not purely composed of interacting granules. Most likely, a starch network and a network of interacting gum molecules coexist, both contributing to the visco-elastic properties (Achayuthakan & Suphantharika, 2008; Alloncle & Doublier, 1991). When the starch concentration is increased, the interactions between the gum polymers are enhanced by further concentrating the continuous phase. As a consequence, granule-granule interactions might be partly inhibited. The presence of these antagonistic effects is most explicitly manifested by the pastes with 0.2% guar, where the elastic moduli G’ are largely below the ones of the gum-free pastes.

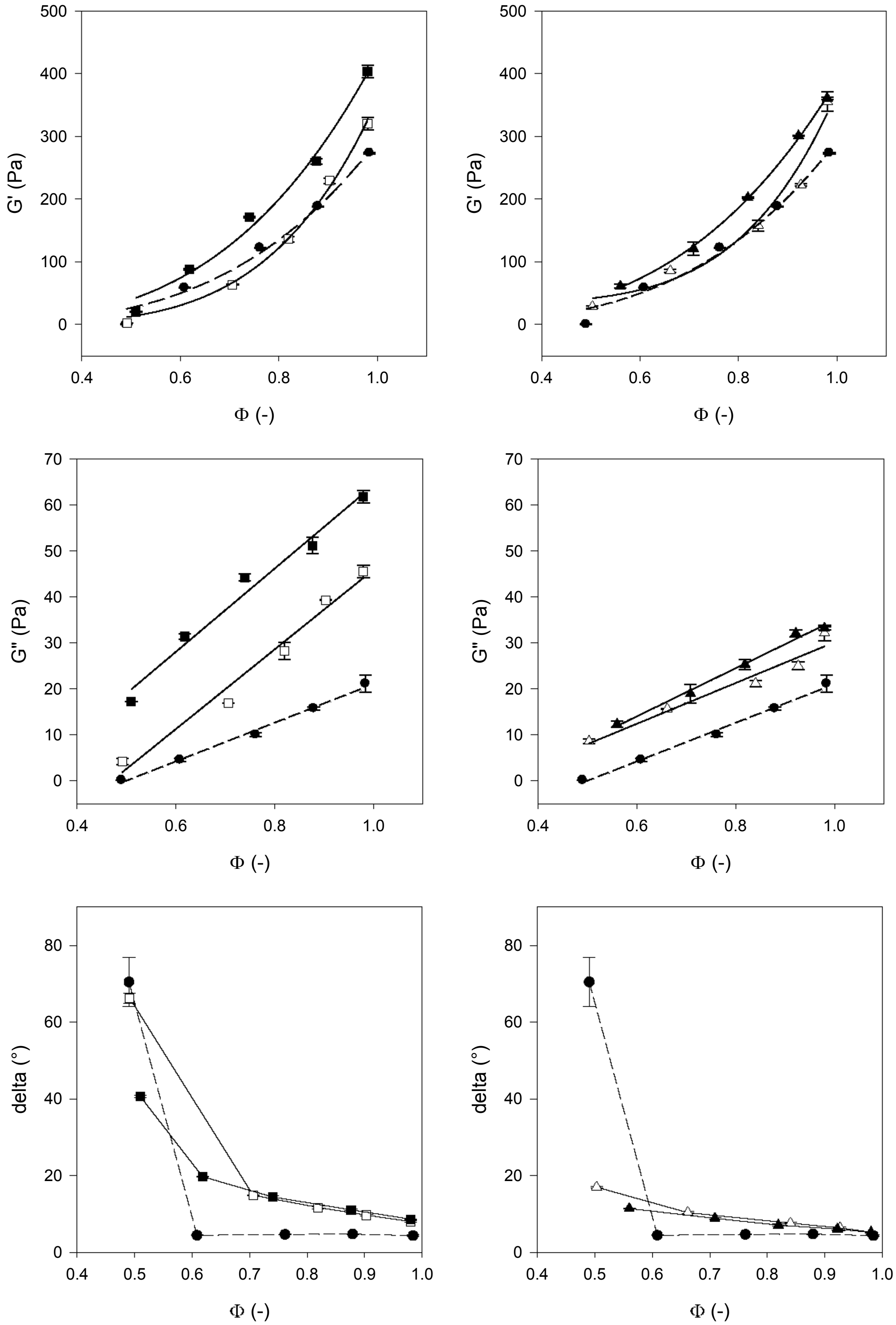

Figure 6-7: Influence of guar (left column) and xanthan (right column) on the dynamic rheological parameters (20°C) at different starch volume fractions (● no gum; □ 0.2% guar; ■ 0.4 % guar; △ 0.2% xanthan; ▲ 0.4% xanthan)

Most likely, both guar and xanthan induce these effects, and the specific dissimilarities between both are due to the differing nature of their intermolecular interactions. Xanthan induces an overall increase in elastic behavior whereas the effect of guar gum depends on the concentrations and the applied frequency. Xanthan generally engages in strong intermolecular associations, resulting in a weak gel while guar molecules associate less strongly. Based on the increased elasticity of the mixed xanthan/starch systems, Abdulmola *et al.* (1996b) suggested that xanthan can strengthen the interactions between the starch granules by e.g. depletion flocculation. They observed that the elastic modulus of the mixed system was higher than the purely additive contribution of both the starch and xanthan component. Unfortunately, they did not take into account the increased xanthan concentration due to granule swelling, and the corresponding enhanced rheological properties of the continuous phase. Their conclusion was based largely on the effects on G' and cannot account for the increased viscous behavior. Furthermore, considering the high effective xanthan contents and the large size of the granules, depletion flocculation seems unlikely. As demonstrated by the CSLM data, xanthan might associate with starch granules in salt free media. Under these circumstances, bridging between the granules might be possible. However, in the current setup relatively high salt contents are used. Under these conditions, association of xanthan with the granules does not occur and the occurrence of bridging flocculation can be ruled out as well.

6.3.4 EFFECT OF XANTHAN TRANSITION

So far, a constant NaCl content of 0.1 M was maintained throughout the setup. In this way, complications induced by the xanthan transition were excluded. It was demonstrated in chapter 2 that the occurrence of a xanthan transition strongly affects the pasting behavior of waxy starch systems. Furthermore, it was proposed repeatedly that during heating steps above the xanthan transition temperature, the flow behavior of the swollen granules is also strongly modified by xanthan gum. However, the interpretation was often complicated by possible effects on granule breakdown and/or differences in gelatinization behavior due to varying salt contents (particularly important when heated to temperatures around the gelatinization range). The use of cross-linked starches and elevated temperatures during pasting excludes these complications and allows to more directly compare the flow behavior of the systems with and without xanthan transition. In the perspecitve of this chapter, experiments were performed at different starch contents. There was only a limited effect of the salt content – and corresponding transition – on the flow and oscillatory rheology of the cooled pastes (data not shown). At 20°C, xanthan exists in its renatured form for both salt contents (0.01M and 0.1M). A slight downward shift in flow curve as well as moduli occurred, presumably due to disruption of xanthan aggregates during the heating step and/or a different degree of renaturation during cooling. Therefore, the focus of this part lies on the effects during pasting.

For the xanthan free systems there were no differences in rheological behavior between 0.01M NaCl and 0.1M NaCl, aside from a minor shift in gelatinization temperature and consequently a shift in pasting onset. Therefore, only one salt content (0.1M) was considered for the xanthan free systems. The conformational transition of xanthan solutions is accompanied by a reduction in the solution viscosity. As mentioned above, this is largely caused by the dissociation of helically linked molecules. This is depicted in Figure 6-8 for a xanthan concentration of 0.8% (corresponding with the effective xanthan concentration at $\Phi = 0.75$). This viscosity drop is comparable with the marked inflection point as observed in the oscillatory temperature sweeps performed in chapter 2 (section 2.3.1).

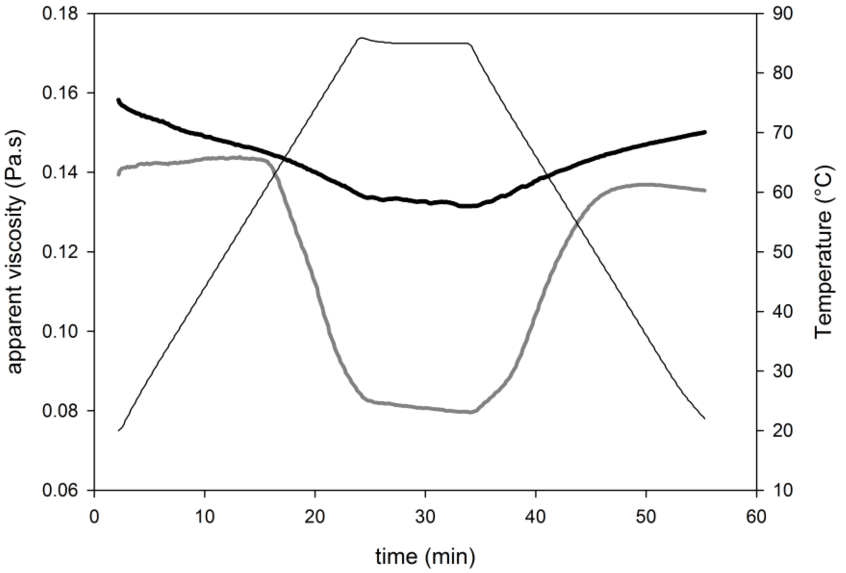

Figure 6-8: Influence of xanthan transition on the apparent viscosity (at shear rate 100s^{-1}) of xanthan gum (0.8%) (black: 0.1M NaCl; grey: 0.01M NaCl)

As depicted in Figure 6-8, the transition-induced viscosity reduction is also reflected in the pasting behavior, where the curve with the lowest salt content is below the one with 0.1M for both starch concentrations. In the cooling ramp a distinct kink can also be observed due to renaturation of the xanthan, comparable with the behavior of the pure xanthan solutions. For the pastes with the highest starch content, the viscosity of the xanthan containing system (with 0.01 M NaCl) was lower than the viscosity of the xanthan free system during the isothermal step. These results confirm that particularly at high starch volume fractions, xanthan gum markedly changes the flow behavior of the pastes.

In order to better understand the flow behavior at elevated temperatures, flow curves were recorded at 85°C using serrated plates and solvent trap. For clarity reasons shear stress instead of the viscosity is plotted as function of the shear rate (Figure 6-9). Except for the gum free paste with the lowest starch content, the derived viscosities at 100 s^{-1} showed a good correlation with the plateau viscosities obtained from the pasting data. At high starch volume fractions flow within the starch-pasting cell is presumed not to be very turbulent, therefore a good agreement between both geometries was expected. Interestingly, both at 4:100 and 6:100 ratio the viscosity of the xanthan sample with 0.01M NaCl is lower than the one of the gum free paste. It should be remarked that at more elevated shear rates there is also a crossover point at the highest salt content. This in turn confirms that in the close-packing region, xanthan can facilitate the flow of starch suspensions, provided that the applied shear is high enough. Furthermore, the effect is more explicit when xanthan can convert into its random coil conformation. It can be remarked that these effects could also be the result of shear-induced anisotropy, which is observed in the random coil conformation as well (Laneuville *et al.*, 2013)

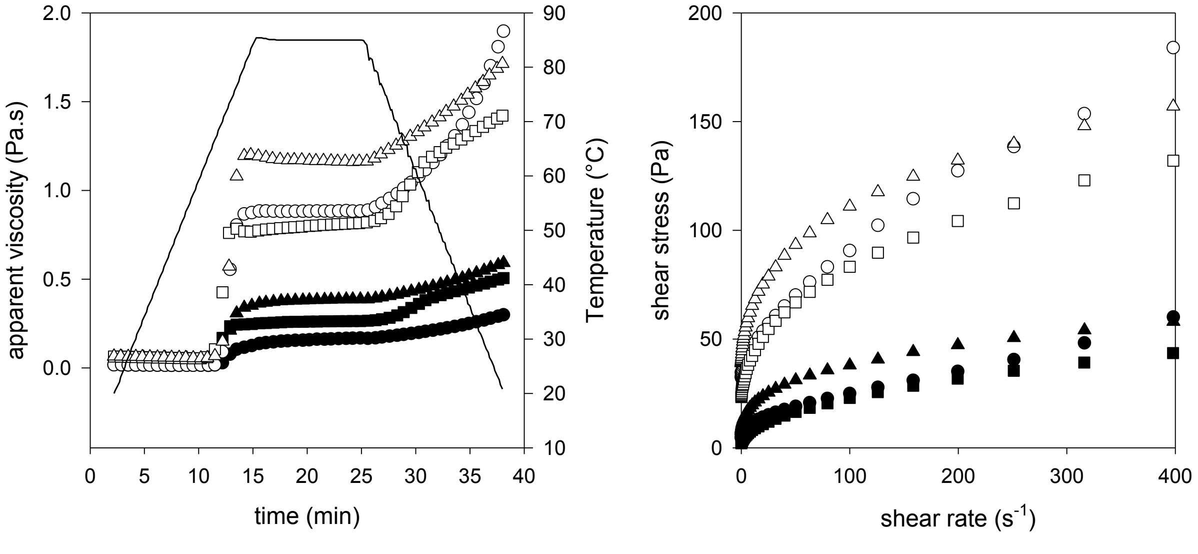

Figure 6-9: Influence of salt concentration on the pasting behavior (L) and flow behavior at 85°C (R) of starch/xanthan pastes (● no gum 0.1M NaCl; ■ 0.2 % xanthan 0.01M NaCl; ▲ 0.2% xanthan 0.1M NaCl) at two different starch:continuous phase ratios (open symbols 6:100; closed symbols 4:100)

6.4 CONCLUSIONS

Despite their commercial relevance, the rheological properties of mixed starch/gum systems are not fully understood. The results of the current setup contribute to this field by providing new insights, and by combining existing knowledge on starch systems and pure gum solutions . The use of shear-resistant starch allowed to consider the pastes as swollen, intact granules, surrounded by a continuous phase containing the gum molecules, which was confirmed by confocal micrographs. More specifically, the effects of two frequently used gums, guar and xanthan, were evaluated at different (swollen) starch volume fractions.

First of all it was demonstrated that the effects of gums on the flow behavior strongly depended on the starch content. At low starch volume fractions, the viscosity is primarily determined by the continuous phase. Due to the absorption of water by the starch granules, the effective gum concentration is raised, leading to an apparent synergy. At starch volume fractions around and above close packing, the flow properties were governed by granule-granule interactions, hereby reducing the relative contribution of the gums. The effect of guar gum was purely additive over the studied concentration range. Conversely, xanthan gum possesses the unique property of facilitating the flow in concentrated starch dispersions, presumably by restricting the interactions between the granules during flow. This specific effect of xanthan gum was observed at low temperatures as well as at elevated temperatures and occurs in both the ordered and the disordered conformation. It was hypothesized that this is caused by the anisotropic arrangement of the xanthan molecules in the continuous phase.

Small deformation rheology demonstrated that already at relatively low starch volume fractions, a network of associated granules is formed. Under these circumstances the network is further strengthened by a coexisting network of interacting gum molecules. With this regard, xanthan gum proved to be more effective due to its capacity of forming weak gel entangled networks. As the starch fraction increases, the concentrated continuous gum phase partly hinders granule interactions, thus enhancing the viscous character of the resulting pastes.

Figure 6-10 summarizes the proposed effects of both guar and xanthan gum on dilute and concentrated starch dispersions both under quiescent state and under externally applied shear.

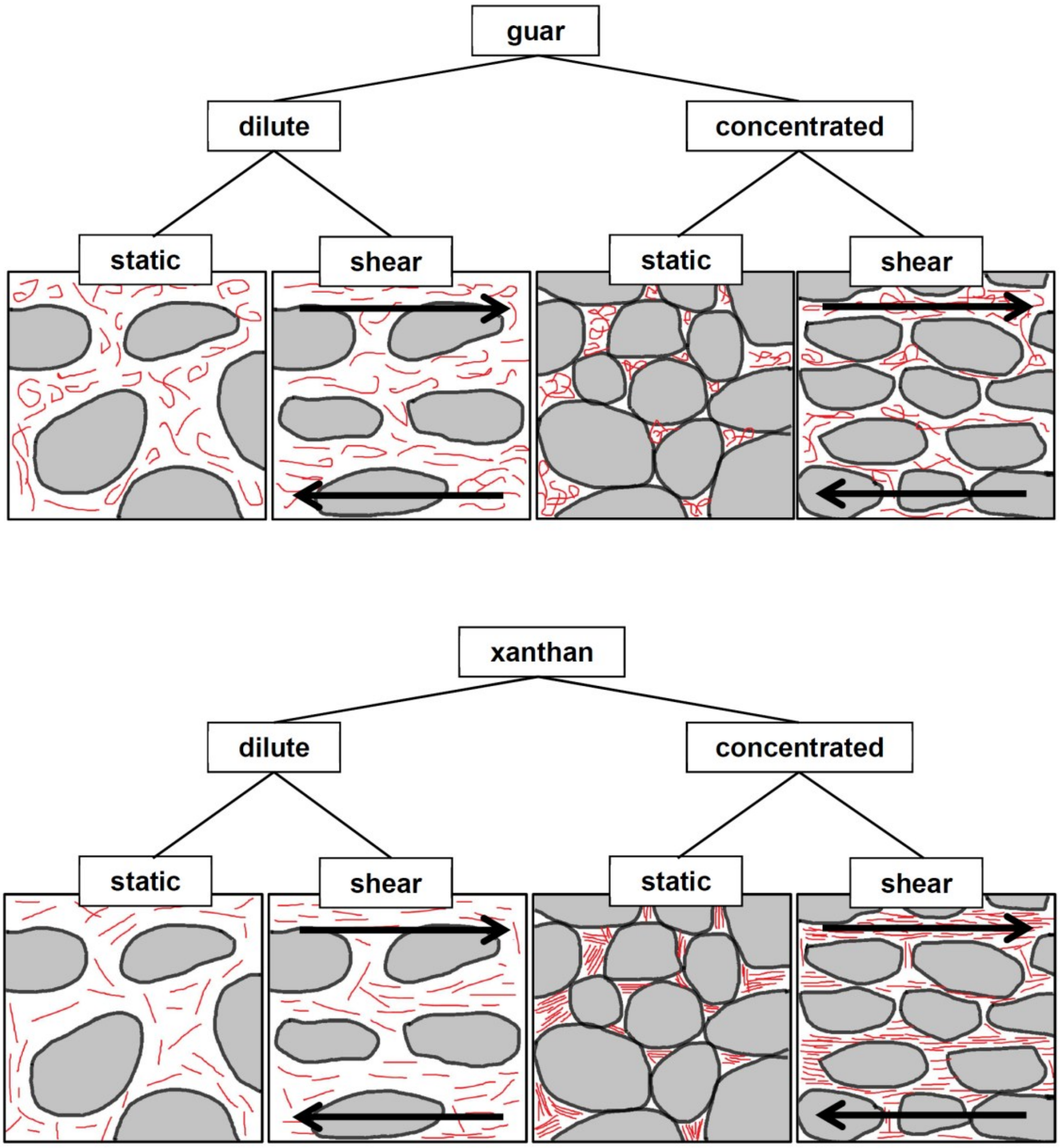

Figure 6-10: Summary of the proposed microstructural models for modified starch/gum systems, depending on the starch concentration regime and the applied shear

GENERAL CONCLUSIONS

Combinations of starches and non-starch hydrocolloids or gums are used abundantly in the food industry. As a consequence of their commercial popularity, starch/gum systems are extensively studied. However, scientific literature is riddled with assertions and contradictory observations, due to the differing concentrations and preparation conditions and the wide variety of starch and gum types. Because of its unique properties, xanthan gum is very often combined with starches. However, due to its different molecular conformations and its tendency to aggregate, this biopolymer offers a lot of challenges as a research subject. A thorough overview on xanthan gum and starch functionality is presented in chapter 1.

In the second chapter, the effects of xanthan gum on various types of waxy starches (potato, rice, native and modified maize) were studied. This setup aimed at deriving more generalized conclusions that could help explaining some of the discrepancies found in literature. More specifically, the possible effects of the conformational transition of xanthan gum were studied. The obtained results strongly depended on the specific type of starch that was combined with the xanthan gum. The flow behavior of modified maize and rice starch systems during pasting at 85°C, but also after cooling, was markedly affected by xanthan gum. Conversely, its relative influence was much smaller for potato and native maize starch systems. These differences were attributed to variations in swelling power and more importantly, variations in degradation behavior. As opposed to the types of modified maize and rice starch used here, potato and native maize starch exhibited a significant degree of breakdown during the pasting step. It was stated that the rheological properties for the latter systems were primarily governed by the continuous phase, which surrounds the remaining granules. Therefore, granule integrity appears to be a prerequisite for optimal xanthan functionality.

The pasting properties of the starch/xanthan systems were studied at two NaCl concentrations: 0.01M and 0.1M. For the lowest salt content, xanthan converts to a random coil during the heating step (85°C), at 0.1M the helical conformation of xanthan is maintained over the whole temperature range. At the concentrations studied here, the transition exhibited no significant effect on the gelatinization behavior of the starches. The conformational change of xanthan in the continuous phase was accompanied by a viscosity reduction, which was also clearly reflected in the pasting curves of all systems. However, the effect of this transition was not directly noticeable in the flow behavior of the pastes after cooling.

The fragile nature of native waxy maize and potato starches towards elevated temperatures and shear is clearly their main technological disadvantage. In chapter 3, it was attempted to better preserve the granule structure by varying the processing conditions. It became clear that the properties of the dispersions can be tuned by choosing a specific temperature/shear combination during pasting. When native waxy starches (maize or potato) are heated to temperatures slightly higher than the gelatinization onset temperature, it appears that their swelling can be more controlled. Nevertheless, a limited fraction of the starch will remain ungelatinized. Under these conditions, granule breakdown could be limited and a higher shear rate was even beneficial towards complete viscosity development. The heating temperature therefore proved to be a critical process parameter. When the temperature is too low, swelling will be incomplete and at more elevated temperatures granule breakdown will become more predominant. It was demonstrated that in the latter case, the presence of xanthan gum can help to restrict the breakdown. Several hypotheses for this effect were formulated, however the underlying mechanisms were further unraveled in chapter 5 and 6.

The mild temperature processing of fragile waxy maize starch proved to be beneficial towards preserving its granular integrity. However, it was not known to which extent the microstructure of these pastes would change during preservation and how this was affected by xanthan gum. Therefore, chapter 4 was devoted to the physicochemical stability of these systems. Texture analysis, rheology and pulsed field NMR were used to evaluate structural changes at different scales during a storage period of 8 weeks. The pastes were prepared by means of the unimix system, which allows the production of larger batches (3L). Two different heating temperatures (70 and 72°C) were chosen within the gelatinization range. T_2-relaxation revealed that molecular reassociations took place in all samples, although the rheological consequences varied strongly among the different systems. The pastes heated to 70°C consisted of partially swollen and largely intact granules and behaved as flocculated dispersions, which were structurally stable throughout the storage period. Slight rheological changes were attributed to shrinking of the granules and intensified granule associations. The addition of xanthan gum did not induce a higher stability, however, due to its direct contribution to the structural features of the systems, changes occurring in the starch fraction were partly masked. When the pastes were heated to a slightly more elevated temperature (72°C), a higher fraction of the granules was broken down. This rendered the systems more unstable: a slow but marked gelation was observed for all systems, presumably due to the association and crystallization of amylopectin molecules, which are present in both the continuous phase and the granules. Under these circumstances, xanthan gum was found to enhance the gelation process. A phase separation between both polymers (amylopectin and xanthan) in the continuous phase was proposed as an underlying mechanism. By exclusion from the xanthan containing phase, the effective concentration in the amylopectin phase is increased and intermolecular associations are favored.

In order to unravel the earlier suggested granule protecting features of xanthan gum, experiments of chapter 5 were designed in such a manner that several proposed underlying mechanisms could be challenged. The effects of xanthan gum were evaluated at different processing conditions (shear, temperature) and thoroughly compared with systems containing guar gum or no gum. At the concentrations studied here, both gums did not induce marked differences in granule swelling. However, breakdown was clearly affected by their presence. The ability of xanthan to inhibit granule disruption was confirmed, and guar gum appeared not to have this property. As a consequence, large differences in pasting profiles as well as particle size distributions were observed between guar and xanthan systems. This effect was attributed to a specific property of xanthan gum which modifies the impact between the granules under shear. In this light, the ability of xanthan gum to associate with the starch granule surface, which is claimed by some authors, was investigated. This unique property of xanthan gum was demonstrated by confocal microscopy. However, its role in the granule stabilizing effects is unlikely. Even at higher salt contents, where it was proven that associations with the starch do not occur, xanthan gum protects the granules against shear. Furthermore, xanthan-starch associations are unlikely at elevated (pasting) temperatures, at which the largest extent of granule disruption takes place. Therefore it was suggested that during pasting, xanthan gum reduces the impact between the granules by the formation of a shear-induced anisotropic organization in the continuous phase. This strong molecular alignment, which is typical for extended molecules like xanthan gum, may guide the granules and induce a smooth flow and protects them from breaking down. The different effects of guar and xanthan gum that took place during pasting were also reflected in the rheological behavior of the cooled pastes. It was concluded that gums can enhance the rheological properties of these systems. However, guar gum rather masks the shortcomings of the starch by its direct rheological contribution to the bulk phase. Next to a similar direct contribution, xanthan gum can actively improve the performance of the granules by better preserving their structure.

Repeatedly throughout this research, it became clear that the interpretation of rheological data of starch/gum systems is very complicated, primarily because many different concomitant effects can take place during pasting. This complicates a targeted tuning of their rheological properties. The final chapter aimed at gaining a more fundamental rheological understanding of waxy starch/gum systems. By using chemically cross-linked waxy maize starch, degradation effects could be excluded. The pastes were composed of swollen, intact granules, surrounded by a continuous phase containing the gum molecules, as confirmed by confocal micrographs. It was demonstrated that the effects of gums on the flow behavior strongly depended on the starch content. At low starch volume fractions, the viscosity is primarily determined by the continuous phase. Due to the absorption of water by the starch granules, the effective gum concentration is raised, leading to an apparent synergy. At starch volume fractions around and above close packing, the flow properties were governed by granule-granule interactions, hereby reducing the relative contribution of the gums. The effect of guar gum was purely additive over the studied concentration range. Conversely, xanthan gum exhibited the unique property of facilitating the flow in concentrated starch dispersions. Because of the explicit effects at high starch volume fractions, and therefore high effective gum concentrations, these results favored the aforementioned hypothesis of anisotropic arrangement of the xanthan molecules in the continuous phase. Moreover, this specific effect of xanthan gum was observed at low temperatures as well as at elevated temperatures and occurs in both the ordered and the disordered conformation.

It was demonstrated by small deformation rheology that already at relatively low starch volume fractions, a network of interacting granules is formed. Under these circumstances the network is further strengthened by a coexisting network of interacting gum molecules. With this regard, xanthan gum proved to be more effective due to its capacity of forming weak gel entangled networks. As the starch fraction increases, the concentrated continuous gum phase partly hinders granule interactions, thus enhancing the viscous character of the resulting pastes.

FUTURE PERSPECTIVES

The central aim of this PhD research was to better understand waxy starch/xanthan functionality and to investigate whether the performance of native waxy starches can be improved by varying processing conditions and by the incorporation of xanthan gum. The setup was intended as an exploratory study and was designed to derive generally applicable principles that can assist in tuning the final properties of these systems. Although this work could assist in the search for chemically modified starch alternatives, the goal was not to develop clean-label products. Nevertheless, some more directly applicable conclusions could be drawn.

For native waxy starch systems, it was demonstrated that when the maximum heating temperature is kept as closely as possible to the gelatinization onset, the disruption of the granules can be restricted. Furthermore, the resulting pastes exhibit an acceptable physicochemical stability. Throughout this work, short heating times were imposed, but it could be worthwhile to maintain longer isothermal steps to allow the granules to swell more gradually and to develop optimal functionality. The latter strategy was not included in this work, but is most likely more effective than further elevating the temperature, at which thermal breakdown starts to dominate. The addition of xanthan gum not only imparts a unique flow behavior to the pastes, but when prepared under these mild heating temperatures, this polysaccharide further protects the fragile granules against shear.

Chemically modified starches have been used for many years and impart very unique properties to food products. It is becoming clear that there is no miraculous clean-label substitute. The major part of this work focused on waxy maize starch, which is a rather cheap but extremely fragile type of starch. For some commercial products, its application might therefore remain restricted, even with the adjustment of the processing conditions. However, by applying the findings of this dissertation – adaptation of processing conditions and the incorporation of xanthan gum – to other, better performing starches, it might be possible to produce satisfactory commercial products. For instance the use of waxy rice starches or even enzymatically or physically modified starches could provide a valid alternative. From a practical point of view, it could also be interesting to evaluate the performance of these native starch granules at more elevated shear rates (200-1000 s^{-1}).

Aside from studying the performance of native starches, some important insights were also developed regarding the rheological behavior of starch/xanthan systems. Swollen granules cannot be considered as solid and regularly shaped particles, nor as true polymer systems, which strongly restricts the number of available analytical techniques. Hence, many researchers prefer rheological methods for starch functionality evaluation. However, this technique provides indirect information and requires a correct interpretation. The findings presented in this work can assist in the understanding of the rheological behavior, both during pasting and after cooling. Furthermore, the conclusions presented in the final chapter could contribute to a more sensible formulation of modified starch/xanthan systems, which are currently used abundantly in commercial products.

Some scientific aspects were not covered or only briefly touched in this dissertation. These topics deserve a more specific, separate study. Throughout the manuscript, a standard commercial xanthan type was used. However, it could be interesting to study the functionality of xanthan at varying molecular weights or with varying substitutions (acetyl and pyruvate). Such an approach could be particularly useful to study the phase behavior of xanthan and amylopectin as well as its association behavior with swollen starch granules. In this perspective, the effect of salts and the corresponding xanthan conformations should also be further elucidated.

The presence of flow anisotropy has been proposed as one of the major mechanisms causing the unique flow properties of mixed starch/xanthan systems. Due to the microstructural complexity, direct evidence for this behavior is lacking. Therefore, the flow behavior of more simplified and standardized dispersions should be studied. The use of purified xanthan samples is advised, but the replacement of starch granules by another type of particles will offer a challenge. Ideally, monomodal spherical microgels are used, but with the same dimensions, density and deformability as starch granules.

The effect of varying processing conditions on the sensory properties of finished products has not yet been evaluated. More specifically, it could be interesting to see whether the taste of real products, which also contain flavors and seasonings is affected by the presence of ungelatinized granules. Furthermore, for many light-applications, chemically modified starches are used to impart viscosity. However, the properties of the original products are often difficult to copy (e.g. in the case of light-mayonnaise). The textures induced by mildly heated native starches differ from those of cross-linked starches and could possibly better approach the desired mouthfeel.

REFERENCES

Abd Karim, A., Norziah, M. H., & Seow, C. C. (2000). Methods for the study of starch retrogradation. *Food Chemistry, 71*(1), 9-36.

Abdulmola, N. A., Hember, M. W. N., Richardson, R. K., & Morris, E. R. (1996a). Application of polymer blending laws to starch-gelatin composites. *Carbohydrate Polymers, 31*(1-2), 53-63.

Abdulmola, N. A., Hember, M. W. N., Richardson, R. K., & Morris, E. R. (1996b). Effect of xanthan on the small-deformation rheology of crosslinked and uncrosslinked waxy maize starch. *Carbohydrate Polymers, 31*(1-2), 65-78.

Achayuthakan, P., & Suphantharika, M. (2008). Pasting and rheological properties of waxy corn starch as affected by guar gum and xanthan gum. *Carbohydrate Polymers, 71*(1), 9-17.

Achayuthakan, P., Suphantharika, M., & Rao, M. A. (2006). Yield stress components of waxy corn starch-xanthan mixtures: Effect of xanthan concentration and different starches. *Carbohydrate Polymers, 65*(4), 469-478.

Acquarone, V. M., & Rao, M. A. (2003). Influence of sucrose on the rheology and granule size of cross-linked waxy maize starch dispersions heated at two temperatures. *Carbohydrate Polymers, 51*(4), 451-458.

Aguirre-Cruz, A., Mendez-Montealvo, G., Solorza-Feria, J., & Bello-Perez, L. A. (2005). Effect of carboxymethylcellulose and xanthan gum on the thermal, functional and rheological properties of dried nixtamalised maize masa. *Carbohydrate Polymers, 62*(3), 222-231.

Allain, C., Lecourtier, J., & Chauveteau, G. (1988). Mesophase Formation in High Molecular-Weight Xanthan Solutions. *Rheologica Acta, 27*(3), 255-262.

Alloncle, M., & Doublier, J. L. (1991). Viscoelastic Properties of Maize Starch Hydrocolloid Pastes and Gels. *Food Hydrocolloids, 5*(5), 455-467.

Alloncle, M., Lefebvre, J., Llamas, G., & Doublier, J. L. (1989). A Rheological Characterization of Cereal Starch-Galactomannan Mixtures. *Cereal Chemistry, 66*(2), 90-93.

Appelqvist, I. A. M., & Debet, M. R. M. (1997). Starch-biopolymer interactions - A review. *Food Reviews International, 13*(2), 163-224.

Arocas, A., Sanz, T., & Fisman, S. M. (2009). Improving effect of xanthan and locust bean gums on the freeze-thaw stability of white sauces made with different native starches. *Food Hydrocolloids, 23*(8), 2478-2484.

Bagley, E. B., & Christianson, D. D. (1982). Swelling Capacity of Starch and Its Relationship to Suspension Viscosity - Effect of Cooking Time, Temperature and Concentration. *Journal of Texture Studies, 13*(1), 115-126.

Barnes, H. A. (1995). A Review of the Slip (Wall Depletion) of Polymer-Solutions, Emulsions and Particle Suspensions in Viscometers - Its Cause, Character, and Cure. *Journal of Non-Newtonian Fluid Mechanics, 56*(3), 221-251.

Bejenariu, A., Popa, M., Picton, L., & Le Cerf, D. (2010). Effect of concentration, pH and temperature on xanthan conformation: a preliminary study before crosslinking. *Revue Roumaine De Chimie, 55*(2), 147-152.

BeMiller, J. N. (2011). Pasting, paste, and gel properties of starch-hydrocolloid combinations. *Carbohydrate Polymers, 86*(2), 386-423.

BeMiller, J. N., & Whistler, R. (2009). *Starch - Chemistry and Technology* (3rd ed.).

Benna-Zayani, M., Kbir-Ariguib, N., Trabelsi-Ayadi, M., & Grossiord, J. L. (2008). Stabilisation of W/O/W double emulsion by polysaccharides as weak gels. *Colloids and Surfaces a-Physicochemical and Engineering Aspects, 316*(1-3), 46-54.

Biliaderis, C. G., Arvanitoyannis, I., Izydorczyk, M. S., & Prokopowich, D. J. (1997). Effect of hydrocolloids on gelatinization and structure formation in concentrated waxy maize and wheat starch gels. *Starch-Starke, 49*(7-8), 278-283.

Born, K., Langendorff, V., & Boulenguer, P. (2005). Xanthan. In *Biopolymers Online*: Wiley-VCH Verlag GmbH & Co. KGaA.

Born, K., Langendorff, V., & Boulenguer, P. (2010). Xanthan. In *Wiley-VCH Verlag GmbH & Co.*

Bresolin, T. M. B., Milas, M., Rinaudo, M., & Ganter, J. L. M. S. (1998). Xanthan-galactomannan interactions as related to xanthan conformations. *International Journal of Biological Macromolecules, 23*(4), 263-275.

Buleon, A., Colonna, P., Planchot, V., & Ball, S. (1998). Starch granules: structure and biosynthesis. *International Journal of Biological Macromolecules, 23*(2), 85-112.

Cai, X. R., Hong, Y., Gu, Z. B. A., & Zhang, Y. Y. (2011). The effect of electrostatic interactions on pasting properties of potato starch/xanthan gum combinations. *Food Research International, 44*(9), 3079-3086.

Camesano, T. A., & Wilkinson, K. J. (2001). Single molecule study of xanthan conformation using atomic force microscopy. *Biomacromolecules, 2*(4), 1184-1191.

Capron, I., Alexandre, S., & Muller, G. (1998a). An atomic force microscopy study of the molecular organisation of xanthan. *Polymer, 39*(23), 5725-5730.

Capron, I., Brigand, G., & Muller, G. (1997). About the native and renatured conformation of xanthan exopolysaccharide. *Polymer, 38*(21), 5289-5295.

Capron, I., Brigand, G., & Muller, G. (1998b). Thermal denaturation and renaturation of a fermentation broth of xanthan: rheological consequences. *International Journal of Biological Macromolecules, 23*(3), 215-225.

Capron, I., Brigand, G., & Muller, G. (1998c). Thermal denaturation and renaturation of a fermentation broth of xanthan: rheological properties. *International Journalm of Biological Macromolecules, 23*, 215-225.

Carnali, J. O. (1991). A Dispersed Anisotropic Phase as the Origin of the Weak-Gel Properties of Aqueous Xanthan Gum. *Journal of Applied Polymer Science, 43*, 929-941.

Casas, J. A., Mohedano, A. F., & Garcia-Ochoa, F. (2000). Viscosity of guar gum and xanthan/guar gum mixture solutions. *Journal of the Science of Food and Agriculture, 80*(12), 1722-1727.

Chaisawang, M., & Suphantharika, M. (2005). Effects of guar gum and xanthan gum additions on physical and rheological properties of cationic tapioca starch. *Carbohydrate Polymers, 61*(3), 288-295.

Chaisawang, M., & Suphantharika, M. (2006). Pasting and rheological properties of native and anionic tapioca starches as modified by guar gum and xanthan gum. *Food Hydrocolloids, 20*(5), 641-649.

Chamberlain, E. K., Rao, M. A., & Cohen, C. (2000). Shear thinning and antithixotropic behavior of a heated cross-linked waxy maize starch dispersion (vol 2, pg 63, 1999). *International Journal of Food Properties, 3*(1), 171-171.

Chantaro, P., & Pongsawatmanit, R. (2010). Influence of sucrose on thermal and pasting properties of tapioca starch and xanthan gum mixtures. *Journal of Food Engineering, 98*(1), 44-50.

Chantaro, P., Pongsawatmanit, R., & Nishinari, K. (2013). Effect of heating–cooling on rheological properties of tapioca starch paste with and without xanthan gum. *Food Hydrocolloids, 31*(2), 183-194.

Chaplin, M. (2009). Xanthan Gum. In *London South Bank University*.

Chiotelli, E., Pilosio, G., & Le Meste, M. (2002). Effect of sodium chloride on the gelatinization of starch: A multi measurement study. *Biopolymers, 63*(1), 41-58.

Choi, S. G., & Kerr, W. L. (2004). Swelling characteristics of native and chemically modified wheat starches as a function of heating temperature and time. *Starch-Starke, 56*(5), 181-189.

Choppe, E., Puaud, F., Nicolai, T., & Benyahia, L. (2010). Rheology of xanthan solutions as a function of temperature, concentration and ionic strength. *Carbohydrate Polymers, 82*(4), 1228-1235.

Christianson, D. D., Hodge, J. E., Osborne, D., & Detroy, R. W. (1981). Gelatinization of Wheat-Starch as Modified by Xanthan Gum, Guar Gum, and Cellulose Gum. *Cereal Chemistry, 58*(6), 513-517.

Closs, C. B., Conde-Petit, B., Roberts, I. D., Tolstoguzov, V. B., & Escher, F. (1999). Phase separation and rheology of aqueous starch/galactomannan systems. *Carbohydrate Polymers, 39*(1), 67-77.

Conde-Petit, B., Pfirter, A., & Escher, F. (1997). Influence of xanthan on the rheological properties of aqueous starch-emulsifier systems. *Food Hydrocolloids, 11*(4), 393-399.

Crossland, L. B., & Favor, H. H. (1948). Starch gelatinization studies II. A method for showing the stages in swelling of starch during heating in the amylograph. *Cereal Chemistry, 25*, 213-220.

Cuvelier, G., & Launay, B. (1986). Concentration Regimes in Xanthan Gum Solutions Deduced from Flow and Viscoelastic Properties. *Carbohydrate Polymers, 6*(5), 321-333.

Desse, M., Fraiseau, D., Mitchell, J., & Budtova, T. (2010). Individual swollen starch granules under mechanical stress: evidence for deformation and volume loss. *Soft Matter, 6*(2), 363-369.

Dolz, M., Hernandez, M. J., & Delegido, J. (2006). Oscillatory measurements for salad dressings stabilized with modified starch, xanthan gum, and locust bean gum. *Journal of Applied Polymer Science, 102*(1), 897-903.

Eerlingen, R. C., Jacobs, H., Block, K., & Delcour, J. A. (1997). Effects of hydrothermal treatments on the rheological properties of potato starch. *Carbohydrate Research, 297*(4), 347-356.

Eidam, D., Kulicke, W. M., Kuhn, K., & Stute, R. (1995). Formation of Maize Starch Gels Selectively Regulated by the Addition of Hydrocolloids. *Starch-Starke, 47*(10), 378-384.

Evans, I. D., & Lips, A. (1992). Viscoelasticity of Gelatinized Starch Dispersions. *Journal of Texture Studies, 23*(1), 69-86.

Farhat, I. A., Blanshard, J. M. V., & Mitchell, J. R. (2000). The retrogradation of waxy maize starch extrudates: Effects of storage temperature and water content. *Biopolymers, 53*(5), 411-422.

Ferrero, C., Martino, M. N., & Zaritzky, N. E. (1994). Corn Starch Xanthan Gum Interaction and Its Effect on the Stability during Storage of Frozen Gelatinized Suspensions. *Starch-Starke, 46*(8), 300-308.

Ferrero, C., Martino, M. N., & Zaritzky, N. E. (1996). Effect of hydrocolloids on starch thermal transitions, as measured by DSC. *Journal of Thermal Analysis and Calorimetry, 47*(5), 1247-1266.

Fisher, D. K., & Thompson, D. B. (1997). Retrogradation of maize starch after thermal treatment within and above the gelatinization temperature range. *Cereal Chemistry, 74*(3), 344-351.

Freitas, R. A., Gorin, P. A. J., Neves, J., & Sierakowski, M. R. (2003). A rheological description of mixtures of a galactoxyloglucan with high amylose and waxy corn starches. *Carbohydrate Polymers, 51*(1), 25-32.

Funami, T., Kataoka, Y., Noda, S., Hiroe, M., Ishihara, S., Asai, I., Takahashi, R., Inouchi, N., & Nishinari, K. (2008a). Functions of fenugreek gum with various molecular weights on the gelatinization and retrogradation behaviors of corn starch-2: Characterizations of starch and investigations of corn starch/fenugreek gum composite system at a relatively low starch concentration; 5 w/v%. *Food Hydrocolloids, 22*(5), 777-787.

Funami, T., Kataoka, Y., Noda, S., Hiroe, M., Ishihara, S., Asai, I., Takahashi, R., & Nishinari, K. (2008b). Functions of fenugreek gum with various molecular weights on the gelatinization and retrogradation behaviors of corn starch - 1: Characterizations of fenugreek gum and investigations of corn starch/fenugreek gum composite system at a relatively high starch concentration; 15 w/v%. *Food Hydrocolloids, 22*(5), 763-776.

Funami, T., Kataoka, Y., Omoto, T., Goto, Y., Asai, I., & Nishinari, K. (2005a). Effects of non-ionic polysaccharides on the gelatinization and retrogradation behavior of wheat starch. *Food Hydrocolloids, 19*(1), 1-13.

Funami, T., Kataoka, Y., Omoto, T., Goto, Y., Asai, I., & Nishinari, K. (2005b). Food hydrocolloids control the gelatinization and retrogradation behavior of starch. 2a. Functions of guar gums with different molecular weights on the gelatinization behavior of corn starch. *Food Hydrocolloids, 19*(1), 15-24.

Funami, T., Kataoka, Y., Omoto, T., Goto, Y., Asai, I., & Nishinari, K. (2005c). Food hydrocolloids control the gelatinization and retrogradation behavior of starch. 2b. Functions of guar gums with different molecular weights on the retrogradation behavior of corn starch. *Food Hydrocolloids, 19*(1), 25-36.

Funami, T., Nakauma, M., Noda, S., Ishihara, S., Asai, I., Inouchi, N., & Nishinari, K. (2008c). Effects of some anionic polysaccharides on the gelatinization and retrogradation behaviors of wheat starch: Soybean-soluble polysaccharide and gum arabic. *Food Hydrocolloids, 22*(8), 1528-1540.

Funami, T., Noda, S., Hiroe, M., Asai, I., Ikeda, S., & Nishinari, K. (2008d). Functions of iota-carrageenan on the gelatinization and retrogradation behaviors of corn starch in the presence or absence of various salts. *Food Hydrocolloids, 22*(7), 1273-1282.

Fuongfuchat, A., Seetapan, N., Makmoon, T., Pongjaruwat, W., Methacanon, P., & Gamonpilas, C. (2012). Linear and non-linear viscoelastic behaviors of crosslinked tapioca starch/polysaccharide systems. *Journal of Food Engineering, 109*(3), 571-578.

Garcia-Ochoa, F., Santos, V. E., Casas, J. A., & Gomez, E. (2000). Xanthan gum: production, recovery, and properties. *Biotechnology Advances, 18*(7), 549-579.

Genovese, D. B., Lozano, J. E., & Rao, M. A. (2007). The rheology of colloidal and noncolloidal food dispersions. *Journal of Food Science, 72*(2), R11-R20.

Genovese, D. B., & Rao, M. A. (2003). Role of starch granule characteristics (volume fraction, rigidity, and fractal dimension) on rheology of starch dispersions with and without amylose. *Cereal Chemistry, 80*(3), 350-355.

Goesaert, H., Brijs, K., Veraverbeke, W. S., Courtin, C. M., Gebruers, K., & Delcour, J. A. (2005). Wheat flour constituents: how they impact bread quality, and how to impact their functionality. *Trends in Food Science & Technology, 16*(1-3), 12-30.

Gonera, A., & Cornillon, P. (2002). Gelatinization of starch/gum/sugar systems studied by using DSC, NMR, and CSLM. *Starch-Starke, 54*(11), 508-516.

Hamman, J. H. (2010). Chitosan Based Polyelectrolyte Complexes as Potential Carrier Materials in Drug Delivery Systems. *Marine Drugs, 8*(4), 1305-1322.

Hansen, M. R., Blennow, A., Farhat, I., Norgaard, L., Pedersen, S., & Engelsen, S. B. (2009). Comparative NMR relaxometry of gels of amylomaltase-modified starch and gelatin. *Food Hydrocolloids, 23*(8), 2038-2048.

Hermansson, A. M., & Svegmark, K. (1996). Developments in the understanding of starch functionality. *Trends in Food Science & Technology, 7*(11), 345-353.

Heyman, B., Depypere, F., Delbaere, C., & Dewettinck, K. (2010). Effects of non-starch hydrocolloids on the physicochemical properties and stability of a commercial bechamel sauce. *Journal of Food Engineering, 99*(2), 115-120.

Hills, B. P., Cano, C., & Belton, P. S. (1991). Proton Nmr Relaxation Studies of Aqueous Polysaccharide Systems. *Macromolecules, 24*(10), 2944-2950.

Hills, B. P., Takacs, S. F., & Belton, P. S. (1990). A New Interpretation of Proton Nmr Relaxation-Time Measurements of Water in Food. *Food Chemistry, 37*(2), 95-111.

Hirashima, M., Takahashi, R., & Nishinari, K. (2012). The gelatinization and retrogradation of cornstarch gels in the presence of citric acid. *Food Hydrocolloids, 27*(2), 390-393.

Holzwarth, G. (1976). Conformation of Extracellular Polysaccharide of Xanthomonas-Campestris. *Biochemistry, 15*(19), 4333-4339.

Hongsprabhas, P., Israkarn, K., & Rattanawattanaprakit, C. (2007). Architectural changes of heated mungbean, rice and cassava starch granules: Effects of hydrocolloids protein-containing envelope. *Carbohydrate Polymers, 67*(4), 614-622.

Imeson, A. (2010). *Food Stabilisers, Thickeners and Gelling Agents*: Blackwell Publishing Ltd.

Jacobs, A., & Kulicke, W.-M. (1994). Characterization and flow properties of lyotropic ultrahigh-molar-mass polysaccharide mesophases. *Macromolecular Symposia, 84*(1), 197-207.

Jacquier, J. C., Kar, A., Lyng, J. G., Morgan, D. J., & McKenna, B. M. (2006). Influence of granule size on the flow behaviour of heated rice starch dispersions in excess water. *Carbohydrate Polymers, 66*(4), 425-434.

Jolliffe, I., T. (2002). *Principal Component Analysis* (2nd ed.). Springer, New York.

Jouppila, K., Kansikas, J., & Roos, Y. H. (1998). Factors affecting crystallization and crystallization kinetics in amorphous corn starch. *Carbohydrate Polymers, 36*(2-3), 143-149.

Kalichevsky, M. T., Orford, P. D., & Ring, S. G. (1990). The Retrogradation and Gelation of Amylopectins from Various Botanical Sources. *Carbohydrate Research, 198*(1), 49-55.

Kalichevsky, M. T., & Ring, S. G. (1987). Incompatibility of Amylose and Amylopectin in Aqueous-Solution. *Carbohydrate Research, 162*(2), 323-328.

Kaneda, I., & Sogabe, A. (2005). Rheological properties of water swellable microgel polymerized in a confined space. *Colloids and Surfaces a-Physicochemical and Engineering Aspects, 270*, 163-170.

Katzbauer, B. (1998). Properties and applications of xanthan gum. *Polymer Degradation and Stability*(59), 81-84.

Kaur, L., Singh, J., Singh, H., & McCarthy, O. J. (2008). Starch-cassia gum interactions: A microstructure - Rheology study. *Food Chemistry, 111*(1), 1-10.

Kawakami, K., Okabe, Y., & Norisuye, T. (1990). Dissociation of Dimerized Xanthan in Aqueous-Solution. *Carbohydrate Polymers, 14*(2), 189-203.

Keetels, C. J. A. M., vanVliet, T., & Walstra, P. (1996a). Gelation and retrogradation of concentrated starch systems .1. Gelation. *Food Hydrocolloids, 10*(3), 343-353.

Keetels, C. J. A. M., vanVliet, T., & Walstra, P. (1996b). Gelation and retrogradation of concentrated starch systems .2. Retrogradation. *Food Hydrocolloids, 10*(3), 355-362.

Keetels, C. J. A. M., vanVliet, T., & Walstra, P. (1996c). Gelation and retrogradation of concentrated starch systems .3. Effect of concentration and heating temperature. *Food Hydrocolloids, 10*(3), 363-368.

Ketz, R. J., Prudhomme, R. K., & Graessley, W. W. (1988). Rheology of Concentrated Microgel Solutions. *Rheologica Acta, 27*(5), 531-539.

Kim, C., & Yoo, B. (2006). Rheological properties of rice starch-xanthan gum mixtures. *Journal of Food Engineering, 75*(1), 120-128.

Korus, J., Juszczak, L., Witczak, M., & Achremowicz, B. (2004). Influence of selected hydrocolloids on triticale starch rheological properties. *International Journal of Food Science and Technology, 39*(6), 641-652.

Krieger, I. M., & Dougherty, T. J. (1959). A Mechanism for Non-Newtonian Flow in Suspensions of Rigid Spheres. *Transactions of the Society of Rheology, 3*, 137-152.

Kruger, A., Ferrero, C., & Zaritzky, N. E. (2003). Modelling corn starch swelling in batch systems: effect of sucrose and hydrocolloids. *Journal of Food Engineering, 58*(2), 125-133.

Krystyjan, M., Adamczyk, G., Sikora, M., & Tomasik, P. (2013). Long-term storage stability of selected potato starch – Non-starchy hydrocolloid binary gels. *Food Hydrocolloids, 31*(2), 270-276.

Kulicke, W. M., Eidam, D., Kath, F., Kix, M., & Kull, A. H. (1996). Hydrocolloids and rheology: Regulation of visco-elastic characteristics of waxy rice starch in mixtures with galactomannans. *Starch-Starke, 48*(3), 105-114.

Laneuville, S. I., Turgeon, S. L., & Paquin, P. (2013). Changes in the physical properties of xanthan gum induced by a dynamic high-pressure treatment. *Carbohydrate Polymers, 92*(2), 2327-2336.

Lee, H. C., & Brant, D. A. (2002a). Rheology of concentrated isotropic and anisotropic xanthan solutions. 1. A rodlike low molecular weight sample. *Macromolecules, 35*(6), 2212-2222.

Lee, H. C., & Brant, D. A. (2002b). Rheology of concentrated isotropic and anisotropic xanthan solutions. 2. A semiflexible wormlike intermediate molecular weight sample. *Macromolecules, 35*(6), 2223-2234.

Lee, H. C., & Brant, D. A. (2002c). Rheology of concentrated isotropic and anisotropic xanthan solutions: 3. Temperature dependence. *Biomacromolecules, 3*(4), 742-753.

Lee, M. H., Baek, M. H., Cha, D. S., Park, H. J., & Lim, S. T. (2002). Freeze-thaw stabilization of sweet potato starch gel by polysaccharide gums. *Food Hydrocolloids, 16*(4), 345-352.

Li, J. Y., & Yeh, A. I. (2001). Relationships between thermal, rheological characteristics and swelling power for various starches. *Journal of Food Engineering, 50*(3), 141-148.

Lim, T., Uhl, J. T., & Prudhomme, R. K. (1984). Rheology of Self-Associating Concentrated Xanthan Solutions. *Journal of Rheology, 28*(4), 367-379.

Liu, H., & Eskin, N. A. M. (1998). Interactions of native and acetylated pea starch with yellow mustard mucilage, locust bean gum and gelatin. *Food Hydrocolloids, 12*(1), 37-41.

Liu, Q., & Thompson, D. B. (1998). Effects of moisture content and different gelatinization heating temperatures on retrogradation of waxy-type maize starches. *Carbohydrate Research, 314*(3-4), 221-235.

Liu, W., & Norisuye, T. (1988). Thermally Induced Conformation Change of Xanthan - Interpretation of Viscosity Behavior in 0.01-M Aqueous Sodium-Chloride. *International Journal of Biological Macromolecules, 10*(1), 44-50.

Liu, W., Sato, T., Norisuye, T., & Fujita, H. (1987). Thermally Induced Conformational Change of Xanthan in 0.01m Aqueous Sodium-Chloride. *Carbohydrate Research, 160*, 267-281.

Lu, T. J., Duh, C. S., Lin, J. H., & Chang, Y. H. (2008). Effect of granular characteristics on the viscoelastic properties of composites of amylose and waxy starches. *Food Hydrocolloids, 22*(1), 164-173.

Mandala, I., & Bayas, E. (2004). Xanthan effect on swelling, solubility and viscosity of wheat starch dispersions. *Food Hydrocolloids, 18*(2), 191-201.

Mandala, I., Michon, C., & Launay, B. (2004). Phase and rheological behaviors of xanthan/amylose and xanthan/starch mixed systems. *Carbohydrate Polymers, 58*(3), 285-292.

Mao, C. F., Klinthong, W., Zeng, Y. C., & Chen, C. H. (2012). On the interaction between konjac glucomannan and xanthan in mixed gels: An analysis based on the cascade model. *Carbohydrate Polymers, 89*(1), 98-103.

Matsuda, Y., Biyajima, Y., & Sato, T. (2009). Thermal Denaturation, Renaturation, and Aggregation of a Double-Helical Polysaccharide Xanthan in Aqueous Solution. *Polymer Journal, 41*(7), 526-532.

Meiboom, S., & Gill, D. (1958). Modified Spin-Echo Method for Measuring Nuclear Relaxation Times. *Review of Scientific Instruments, 29*(8), 688-691.

Meyer, E. L., Fuller, G. G., Clark, R. C., & Kulicke, W. M. (1993). Investigation of Xanthan Gum Solution Behavior under Shear-Flow Using Rheooptical Techniques. *Macromolecules, 26*(3), 504-511.

Milas, M., & Rinaudo, M. (1979). Conformational investigation on the bacterial polysaccharide xanthan. *Carbohydrate Research, 76*, 189-196.

Milas, M., & Rinaudo, M. (1986). Properties of Xanthan Gum in Aqueous-Solutions - Role of the Conformational Transition. *Carbohydrate Research, 158*, 191-204.

Milas, M., Rinaudo, M., Duplessix, R., Borsali, R., & Lindner, P. (1995). Small-Angle Neutron-Scattering from Polyelectrolyte Solutions - from Disordered to Ordered Xanthan Chain Conformation. *Macromolecules, 28*(9), 3119-3124.

Milas, M., Rinaudo, M., Knipper, M., & Schuppiser, J. L. (1990). Flow and Viscoelastic Properties of Xanthan Gum Solutions. *Macromolecules, 23*(9), 2506-2511.

Miles, M. J., Morris, V. J., Orford, P. D., & Ring, S. G. (1985). The Roles of Amylose and Amylopectin in the Gelation and Retrogradation of Starch. *Carbohydrate Research, 135*(2), 271-281.

Morikawa, K., & Nishinari, K. (2000). Effects of concentration dependence of retrogradation behaviour of dispersions for native and chemically modified potato starch. *Food Hydrocolloids, 14*(4), 395-401.

Mudgil, D., Barak, S., & Khatkar, B. S. (2012). X-ray diffraction, IR spectroscopy and thermal characterization of partially hydrolyzed guar gum. *International Journal of Biological Macromolecules, 50*(4), 1035-1039.

Muller, G., Anrhourrache, M., Lecourtier, J., & Chauveteau, G. (1986). Salt Dependence of the Conformation of a Single-Stranded Xanthan. *International Journal of Biological Macromolecules, 8*(3), 167-172.

Muller, G., & Lecourtier, J. (1988). Temperature-Induced Extension and Dissociation of Native Xanthan. *Carbohydrate Polymers, 9*(3), 213-225.

Nagano, T., Tamaki, E., & Funami, T. (2008). Influence of guar gum on granule morphologies and rheological properties of maize starch. *Carbohydrate Polymers, 72*(1), 95-101.

Nayouf, M., Loisel, C., & Doublier, J. L. (2003). Effect of thermomechanical treatment on the rheological properties of crosslinked waxy corn starch. *Journal of Food Engineering, 59*(2-3), 209-219.

Oertel, R., & Kulicke, W. M. (1991). Viscoelastic Properties of Liquid-Crystals of Aqueous Biopolymer Solutions. *Rheologica Acta, 30*(2), 140-150.

Oviatt, H. W., & Brant, D. A. (1993). Thermal-Treatment of Semidilute Aqueous Xanthan Solutions Yields Weak Gels with Properties Resembling Hyaluronic-Acid. *International Journal of Biological Macromolecules, 15*(1), 3-10.

Parker, R., & Ring, S. G. (2001). Aspects of the physical chemistry of starch. *Journal of Cereal Science, 34*(1), 1-17.

Pastor, M. V., Costell, E., Izquierdo, L., & Duran, L. (1994). Effects of Concentration, Ph and Salt Content on Flow Characteristics of Xanthan Gum Solutions. *Food Hydrocolloids, 8*(3-4), 265-275.

Pelletier, E., Viebke, C., Meadows, J., & Williams, P. A. (2001). A rheological study of the order-disorder conformational transition of xanthan gum. *Biopolymers, 59*(5), 339-346.

Pongsawatmanit, R., & Srijunthongsiri, S. (2008). Influence of xanthan gum on rheological properties and freeze-thaw stability of tapioca starch. *Journal of Food Engineering, 88*(1), 137-143.

Potter, K., Carpenter, T. A., & Hall, L. D. (1993). Mapping of the Spatial Variation in Alginate Concentration in Calcium Alginate Gels by Magnetic-Resonance-Imaging (Mri). *Carbohydrate Research, 246*, 43-49.

Ptaszek, A., Berski, W., Ptaszek, P., Witczak, T., Repelewicz, U., & Grzesik, A. (2009). Viscoelastic properties of waxy maize starch and selected non-starch hydrocolloids gels. *Carbohydrate Polymers, 76*(4), 567-577.

Puddephat, M. (2010). Principles of Magnetic Resonance Imaging. Web-link: http://www.mikepuddephat.com/page/1603/principles-of-magnetic-resonance-imaging.

Quemada, D. (1977). Rheology of Concentrated Disperse Systems and Minimum Energy-Dissipation Principle .1. Viscosity-Concentration Relationship. *Rheologica Acta, 16*(1), 82-94.

Rabenstein, D. L., & Fan, S. (1986). Proton Nuclear-Magnetic-Resonance Spectroscopy of Aqueous-Solutions - Complete Elimination of the Water Resonance by Spin Spin Relaxation. *Analytical Chemistry, 58*(14), 3178-3184.

Rao, M. A., Okechukwu, P. E., Da Silva, P. M. S., & Oliveira, J. C. (1997). Rheological behavior of heated starch dispersions in excess water: role of starch granule. *Carbohydrate Polymers, 33*(4), 273-283.

Rayment, P., Wright, P., Hoad, C., Ciampi, E., Haydock, D., Gowland, P., & Butler, M. F. (2009). Investigation of alginate beads for gastro-intestinal functionality, Part 1: In vitro characterisation. *Food Hydrocolloids, 23*(3), 816-822.

Renou, F., Petibon, O., Malhiac, C., & Grisel, M. (2013). Effect of xanthan structure on its interaction with locust bean gum: Toward prediction of rheological properties. *Food Hydrocolloids, 32*(2), 331-340.

Richardson, R. K., & Rossmurphy, S. B. (1987). Nonlinear Viscoelasticity of Polysaccharide Solutions .2. Xanthan Polysaccharide Solutions. *International Journal of Biological Macromolecules, 9*(5), 257-264.

Ridgway, J. P. (2010). Cardiovascular magnetic resonance physics for clinicians: part I. *Journal of Cardiovascular Magnetic Resonance, 12*(7), 1-28.

Ring, S. G., Colonna, P., Ianson, K. J., Kalichevsky, M. T., Miles, M. J., Morris, V. J., & Orford, P. D. (1987). The Gelation and Crystallization of Amylopectin. *Carbohydrate Research, 162*(2), 277-293.

Rochefort, W. E., & Middleman, S. (1987). Rheology of Xanthan Gum - Salt, Temperature, and Strain Effects in Oscillatory and Steady Shear Experiments. *Journal of Rheology, 31*(4), 337-369.

Rodd, A. B., Dunstan, D. E., & Boger, D. V. (2000). Characterisation of xanthan gum solutions using dynamic light scattering and rheology. *Carbohydrate Polymers, 42*(2), 159-174.

Rodriguez-Hernandez, A. I., Durand, S., Garnier, C., Tecante, A., & Doublier, J. L. (2006). Rheology-structure properties of waxy maize starch-gellan mixtures. *Food Hydrocolloids, 20*(8), 1223-1230.

Rojas, J. A., Rosell, C. M., & de Barber, C. B. (1999). Pasting properties of different wheat flour-hydrocolloid systems. *Food Hydrocolloids, 13*(1), 27-33.

Sae-Kang, V., & Suphantharika, M. (2006). Influence of pH and xanthan gum addition on freeze-thaw stability of tapioca starch pastes. *Carbohydrate Polymers, 65*(3), 371-380.

Samutsri, W., & Suphantharika, M. (2012). Effect of salts on pasting, thermal, and rheological properties of rice starch in the presence of non-ionic and ionic hydrocolloids. *Carbohydrate Polymers, 87*(2), 1559-1568.

Sato, T., Kakihara, T., & Teramoto, A. (1990). Isotropic Liquid-Crystal Phase-Equilibrium in Semiflexible Polymer-Solutions - Xanthan, a Rigid Polyelectrolyte. *Polymer, 31*(5), 824-828.

Sato, T., Norisuye, T., & Fujita, H. (1984). Double-Stranded Helix of Xanthan - Dimensional and Hydrodynamic Properties in 0.1-M Aqueous Sodium-Chloride. *Macromolecules, 17*(12), 2696-2700.

Satrapai, S., & Suphantharika, M. (2007). Influence of spent brewer's yeast beta-glucan on gelatinization and retrogradation of rice starch. *Carbohydrate Polymers, 67*(4), 500-510.

Savary, G., Handschin, S., Conde-Petit, B., Cayot, N., & Doublier, J. L. (2008). Structure of polysaccharide-starch composite gels by rheology and confocal laser scanning microscopy: Effect of the composition and of the preparation procedure. *Food Hydrocolloids, 22*(4), 520-530.

Schirmer, M., Höchstötter, A., Jekle, M., Arendt, E., & Becker, T. (2013). Physicochemical and morphological characterization of different starches with variable amylose/amylopectin ratio. *Food Hydrocolloids, 32*(1), 52-63.

Schorsch, C., Garnier, C., & Doublier, J. L. (1995). Microscopy of xanthan/galactomannan mixtures. *Carbohydrate Polymers, 28*(4), 319-323.

Sereno, N. M., Hill, S. E., & Mitchell, J. R. (2007). Impact of the extrusion process on xanthan gum behaviour. *Carbohydrate Research, 342*(10), 1333-1342.

Shi, X. H., & BeMiller, J. N. (2002). Effects of food gums on viscosities of starch suspensions during pasting. *Carbohydrate Polymers, 50*(1), 7-18.

Sikora, M., Badrie, N., Deisingh, A. K., & Kowalski, S. (2008a). Sauces and dressings: A review of properties and applications. *Critical Reviews in Food Science and Nutrition, 48*(1), 50-77.

Sikora, M., Kowalski, S., & Tomasik, P. (2008b). Binary hydrocolloids from starches and xanthan gum. *Food Hydrocolloids, 22*(5), 943-952.

Singh, J., Kaur, L., & McCarthy, O. J. (2007). Factors influencing the physico-chemical, morphological, thermal and rheological properties of some chemically modified starches for food applications - A review. *Food Hydrocolloids, 21*(1), 1-22.

Smith, I. H., Symes, K. C., Lawson, C. J., & Morris, E. R. (1981). Influence of the Pyruvate Content of Xanthan on Macromolecular Association in Solution. *International Journal of Biological Macromolecules, 3*(2), 129-134.

Song, J. Y., Kim, Y. C., & Shin, M. (2008). Textural properties and structures of wheat and maize starch-gum mixed gels during storage. *Food Science and Biotechnology, 17*(1), 20-25.

Song, J. Y., Kwon, J. Y., Choi, J., Kim, Y. C., & Shin, M. (2006). Pasting properties of non-waxy rice starch-hydrocolloid mixtures. *Starch-Starke, 58*(5), 223-230.

Sostar, S., & Schneider, R. (1998). Guar gum as an environment-friendly alternative thickener in printing with reactive dyes. *Dyes and Pigments, 39*(4), 211-221.

Southwick, J. G., Jamieson, A. M., & Blackwell, J. (1981). Quasi-Elastic Light-Scattering-Studies of Semi-Dilute Xanthan Solutions. *Macromolecules, 14*(6), 1728-1732.

Steeneken, P. A. M. (1989). Rheological Properties of Aqueous Suspensions of Swollen Starch Granules. *Carbohydrate Polymers, 11*(1), 23-42.

Stokke, B. T., Smidsrod, O., & Elgsaeter, A. (1989). Electron-Microscopy of Native Xanthan and Xanthan Exposed to Low Ionic-Strength. *Biopolymers, 28*(2), 617-637.

Sudhakar, V., Singhal, R. S., & Kulkarni, P. R. (1996). Starch-galactomannan interactions: Functionality and rheological aspects. *Food Chemistry, 55*(3), 259-264.

Takada, Y., Sato, T., & Teramoto, A. (1991). Dynamics of Stiff-Chain Polymers in Isotropic Solution .2. Viscosity of Aqueous-Solutions of Xanthan, a Rigid Double-Helical Polysaccharide. *Macromolecules, 24*(23), 6215-6219.

Tako, M., Teruya, T., Tamaki, Y., & Ohkawa, K. (2010). Co-gelation mechanism of xanthan and galactomannan. *Colloid and Polymer Science, 288*(10-11), 1161-1166.

Tattiyakul, J., & Rao, M. A. (2000). Rheological behavior of cross-linked waxy maize starch dispersions during and after heating. *Carbohydrate Polymers, 43*(3), 215-222.

Tecante, A., & Doublier, J. L. (1999). Steady flow and viscoelastic behavior of crosslinked waxy corn starch-kappa-carrageenan pastes and gels. *Carbohydrate Polymers, 40*(3), 221-231.

Temsiripong, T., Pongsawatmanit, R., Ikeda, S., & Nishinari, K. (2005). Influence of xyloglucan on gelatinization and retrogradation of tapioca starch. *Food Hydrocolloids, 19*(6), 1054-1063.

Tester, R. F., Karkalas, J., & Qi, X. (2004). Starch - composition, fine structure and architecture. *Journal of Cereal Science, 39*(2), 151-165.

Tester, R. F., & Sommerville, M. D. (2003). The effects of non-starch polysaccharides on the extent of gelatinisation, swelling and alpha-amylase hydrolysis of maize and wheat starches. *Food Hydrocolloids, 17*(1), 41-54.

Tharanathan, R. N. (2005). Starch-value addition by modification. *Critical Reviews in Food Science and Nutrition, 45*(5), 371-384.

Thygesen, L. G., Blennow, A., & Engelsen, S. B. (2003). The effects of amylose and starch phosphate on starch gel retrogradation studied by low-field H-1 NMR relaxometry. *Starch-Starke, 55*(6), 241-249.

Tromp, R. H., van de Velde, F., van Riel, J., & Paques, M. (2001). Confocal scanning light microscopy (CSLM) on mixtures of gelatine and polysaccharides. *Food Research International, 34*(10), 931-938.

Tsai, M. L., Li, C. F., & Lii, C. Y. (1997). Effects of granular structures on the pasting behaviors of starches. *Cereal Chemistry, 74*(6), 750-757.

Van Nevel, S., Hennebel, T., De Beuf, K., Du Laing, G., Verstraete, W., & Boon, N. (2012). Transparent exopolymer particle removal in different drinking water production centers. *Water Research, 46*(11), 3603-3611.

Viturawong, Y., Achayuthakan, P., & Suphantharika, M. (2008). Gelatinization and rheological properties of rice starch/xanthan mixtures: Effects of molecular weight of xanthan and different salts. *Food Chemistry, 111*(1), 106-114.

Walls, H. J., Caines, S. B., Sanchez, A. M., & Khan, S. A. (2003). Yield stress and wall slip phenomena in colloidal silica gels. *Journal of Rheology, 47*(4), 847-868.

Walstra, P. (2003). *Physical Chemistry of Foods*. Marcel Dekker, Inc.

Wang, B., Wang, L. J., Li, D., Ozkan, N., Li, S. J., & Mao, Z. H. (2009). Rheological properties of waxy maize starch and xanthan gum mixtures in the presence of sucrose. *Carbohydrate Polymers, 77*(3), 472-481.

Weber, F. H., Clerici, M. T. P. S., Collares-Queiroz, F. P., & Chang, Y. K. (2009). Interaction of Guar and Xanthan Gums with Starch in the Gels Obtained from Normal, Waxy and High-amylose Corn Starches. *Starch-Starke, 61*(1), 28-34.

Wei, Q. R., Ai, H., & Gu, Z. W. (2011). Matrix polyelectrolyte capsules based on polysaccharide/MnCO3 hybrid microparticle templates. *Colloids and Surfaces B-Biointerfaces, 85*(1), 63-72.

Wyatt, N. B., Gunther, C. M., & Liberatore, M. W. (2011). Increasing viscosity in entangled polyelectrolyte solutions by the addition of salt. *Polymer, 52*(11), 2437-2444.

Wyatt, N. B., & Liberatore, M. W. (2009). Rheology and Viscosity Scaling of the Polyelectrolyte Xanthan Gum. *Journal of Applied Polymer Science, 114*(6), 4076-4084.

Wyatt, N. B., & Liberatore, M. W. (2010). The effect of counterion size and valency on the increase in viscosity in polyelectrolyte solutions. *Soft Matter, 6*(14), 3346-3352.

Yoo, D., Kim, C., & Yoo, B. (2005). Steady and dynamic shear rheology of rice starch-galactomannan mixtures. *Starch-Starke, 57*(7), 310-318.

Yoshimura, M., Takaya, T., & Nishinari, K. (1996). Effects of konjac-glucomannan on the gelatinization and retrogradation of corn starch as determined by rheology and differential scanning calorimetry. *Journal of Agricultural and Food Chemistry, 44*(10), 2970-2976.

Yoshimura, M., Takaya, T., & Nishinari, K. (1999). Effects of xyloglucan on the gelatinization and retrogradation of corn starch as studied by rheology and differential scanning calorimetry. *Food Hydrocolloids, 13*(2), 101-111.

Zhang, G. Q., & Hirasaki, G. J. (2003). CPMG relaxation by diffusion with constant magnetic field gradient in a restricted geometry: numerical simulation and application. *Journal of Magnetic Resonance, 163*(1), 81-91.

Zhang, Y. J., & Cremer, P. S. (2006). Interactions between macromolecules and ions: the Hofmeister series. *Current Opinion in Chemical Biology, 10*(6), 658-663.

Zhu, W. X., Gayin, J., Chatel, F., Dewettinck, K., & Van der Meeren, P. (2009). Influence of electrolytes on the heat-induced swelling of aqueous dispersions of native wheat starch granules. *Food Hydrocolloids, 23*(8), 2204-2211.

CURRICULUM VITAE

Bart Heyman werd geboren te Ninove op 28 januari 1984 en behaalde in 2002 het diploma Hoger Secundair Onderwijs, richting Latijn-Wiskunde aan het Sint-Aloysiuscollege te Ninove. In juli 2007 behaalde hij met grote onderscheiding het diploma van Bio-ingenieur Scheikunde aan de Universiteit Gent. Sinds september 2007 is hij verbonden aan het Laboratorium voor Levensmiddelentechnologie en –proceskunde. Aanvankelijk was hij actief als wetenschappelijk medewerker op het Flanders' FOOD project rond fysico-chemische stabiliteit van complexe levensmiddelen. In oktober 2009 startte hij een doctoraatsonderzoek gefinancierd door het Bijzonder Onderzoeksfonds (BOF) van de Universiteit Gent. Hij participeerde eveneens in de dienstverlening- en onderwijsactiviteiten van de vakgroep. Zo verzorgde hij onder meer de praktische oefeningen en begeleidde hij verscheidene binnen- en buitenlandse thesisstudenten. Zijn onderzoek heeft geleid tot meerdere publicaties in peer-reviewed wetenschappelijke tijdschriften en hij verzorgde meerdere voordrachten en posters op nationale en internationale congressen.

Peer reviewed Publications (A1)

- **Heyman, B.**, Van Bockstaele, F., Van de Walle, D., Dewettinck, K. (2013). Long-term stability of waxy maize starch/xanthan gum mixtures prepared at a temperature within the gelatinization range. Food Research International (submitted).
- **Heyman, B.**, De Vos, W., Van der Meeren, P., Dewettinck, K. (2013). Gums tuning the rheological properties of modified maize starch pastes: differences between guar and xanthan. Food Hydrocolloids (submitted).
- **Heyman, B.**, De Vos, W., Depypere, F., Van der Meeren, P., Dewettinck, K. (2013). Guar and xanthan gum differentially affect shear induced breakdown of native waxy maize starch. Food Hydrocolloids (in press). *http://dx.doi.org/10.1016/j.foodhyd.2013.07.011*.
- Fredrick, E., **Heyman, B**., Moens, K., Fischer, S., Verwijlen, T., Moldenaers, P., Van der Meeren, P., Dewettinck, K. (2013). Monoacylglycerols in dairy recombined cream: II. The effect on partial coalescence and whipping properties. Food Research International 51(2), 936-945. *http://dx.doi.org/10.1016/j.foodres.2013.02.006.*
- Fredrick, E., Moens, K., **Heyman, B**., Fischer, S., Van der Meeren, P., Dewettinck, K. (2013). Monoacylglycerols in dairy recombined creams. I. Effect on milk fat crystallization.

Food Research International 51(2), 892-898. *http://dx.doi.org/10.1016/j.foodres.2013.02.007.*

- **Heyman, B.**, De Hertogh, D., Van der Meeren, P., Depypere, F., Dewettinck, K. (2013). Influence of xanthan transition on the rheological properties of waxy starches. Carbohydrate Polymers 96 (2), 568-577. *http://dx.doi.org/10.1016/j.carbpol.2012.10.077.*
- **Heyman, B**., Depypere, F., Van der Meeren, P., Dewettinck, K. (2013). Processing of waxy starch/xanthan gum mixtures within the gelatinization temperature range. Carbohydrate Polymers 96 (2), 560-567. *http://dx.doi.org/10.1016/j.carbpol.2012.10.076.*
- Le, T., Sabatino, P., **Heyman, B**., Kasinos, M., Dinh, H., Dewettinck, K., Martins, J., Van der Meeren, P. (2011). Improved heat stability by whey protein-surfactant interaction. Food Hydrocolloids 25(4), 594-603. *http://dx.doi.org/10.1016/j.foodhyd.2010.07.012.*
- **Heyman, B**., Depypere, F., Delbaere, C., Dewettinck, K. (2010). Effects of non-starch hydrocolloids on the physicochemical properties and stability of a commercial bechamel sauce. Journal of Food Engineering 99 (2), 115-120. *http://dx.doi.org/10.1016/j.jfoodeng.2010.02.005.*

Presentations at international conferences

- **Heyman, B.**, Van der Meeren, P., Depypere, F., Dewettinck, K. Influence of processing conditions on the functionality of waxy maize starch/xanthan gum systems. 11th International Hydrocolloids Conference, Purdue University, USA, 14-18 May 2012.
- **Heyman, B.**, De Hertogh, D., De Vos, W., Van der Meeren, P., Depypere, F., Dewettinck, K. Influence of xanthan transition on the rheological properties of waxy starch systems systems. 11th International Hydrocolloids Conference, Purdue University, USA, 14-18 May 2012.
- **Heyman, B.**, Delbaere, C., Depypere, F., Dewettinck, K. Effect of hydrocolloids on the rheological properties and stability of a béchamel sauce. 5th International Symposium on Food Rheology and Structure, ETH Zürich, Switzerland, 15-18 June 2009 (poster).
- Dhooge, M., **Heyman, B.**, Depypere, F., Dewettinck, K. Fat replacement in salad dressing: a mixture design approach. EFFOST First European Food Congress, Ljubljana, Slovenië, 4-9 november 2008.
- **Heyman, B.**, Dhooge, M., Delbaere, C., Depypere, F., Dewettinck, K. The effect of hydrocolloids on the physicochemical stability of a béchamel sauce. EFFOST First European Food Congress, Ljubljana, Slovenia, 4-9 November 2008.

Seminar Lectures

- **Intrafood 12: ‘Hydrocolloids in Sauces: Choose Wisely’,** Kortrijk, 13 September 2012
- **Flanders’ FOOD: ‘Gelling and Thickening Agents: Theory and Application’,** Module 3: Workshop Food Rheology, 2 February 2012
- **Flanders’ FOOD: ‘Gelling and Thickening Agents: Theory and Application’,** Module 3: Food Thickeners, 17 January 2012

encumbered forever by desire and ambition
there's a hunger still unsatisfied
our weary eyes still stray to the horizon
though down this road we've been so many times

High Hopes – Pink Floyd